SCUOLA DI DOTTORATO

UNIVERSITÀ DEGLI STUDI DI MILANO-BICOCCA

PhD program in Material Science and Nanotechnology

Cycle *XXIX* - Industrial Curriculum

Lignin-based elastomeric composites for sustainable tyre technology

Davide Barana

Tutor: *Prof. Marco Emilio Orlandi*

Co-tutor: *Dott. Luca Castellani*

Supervisor: *Prof. Gianfranco Pacchioni*

Coordinator: *Prof. Gian Paolo Brivio*

March 2017

Table of contents

CHAPTER 1 - Synopsis

The research dealt with the valorization of low-value lignocellulosic substrates, investigating the possibility to produce elastomeric materials from renewable resources. The motivation for the research arises from the global challenges that are connected to the indiscriminate exploitation of the fossil resources. The tyre market is incredibly large, with a worldwide production of billions of tyres every year. However, the technology is still relying heavily on materials that are generated from fossil, intrinsically non-renewable resources. The dependence from the fossil raw materials is generating a growing concern, in relation to the volatility of the prices, to the negative effects on the environment, and ultimately to the prospective depletion of the resources. The problems are intensified by the raising global demand, fostered by the growing economies. In this scenario, policy makers, commercial partners and final users are pressing tyre manufactures, advocating a fast progress towards greener technologies. The main challenge is to produce sustainable counterparts for products that have been evolving over decades, reaching high technological standards. In the last fifteen years, the research for more sustainable materials, producible from renewable resources saw a flourishing commitment. One relevant outcome is that the first bioplastics are being employed in commercial applications. Now the endeavor is gradually involving also the field of elastomeric materials and many researchers are focusing on the development of solutions from alternative resources. Lignocellulosic biomasses are the most abundantly available raw material on the Earth, and their exploitation is going to have a pivotal role in the transition to a biobased economy. Nevertheless, their full exploitation is a major challenge and the valorization of some constituents, as lignin, is limiting the commercial actualization of the new generation biorefineries. Lignin is a complex biopolymer and its heterogeneity is hindering the development of suitable applications. Nevertheless, the alluring properties of lignin are gathering increasing attentions. The work that is presented in this thesis was developed from the initial attempt to generate new renewable materials for elastomeric applications. The research activities begun assessing the possibility to cogenerate different materials from lignocellulosic side-products through an integrated biorefinery process. Afterwards they focused on the development of lignin based materials, investigating the relationships between the structure of lignin and the properties of lignin/rubber composites. Subsequently different approaches were explored based on the gained knowledge, all aimed at the improvement of the lignin/rubber composites materials, striving to make them more suitable for tyre manufacturing. The general organization of the investigation was based on a detailed characterization of the products, which involved a

wide array of techniques. The characterized products were then tested in model compounds with natural rubber to assess the properties conferred to the elastomeric composites (mainly mechanical and thermal properties). The observed behavior was then correlated to specific features of the tentative materials. Finally, the products were modified with the aim to exalt their favorable characteristics.

The thesis is outlined in the following way: chapter two offers a general introduction regarding the problems connected to the indiscriminate use of the fossil resources, deals with the importance of the transition toward a biobased economy and the pivotal role of lignocellulosic biomasses. Follows a rather detailed discussion concerning the main characteristics of lignocellulosic materials, their major components, and the extractive technologies. Chapter three presents an overview of the fundamental body of knowledge that is relevant for tyre technology. In chapter four the main characterization techniques that were used are briefly described along with the experimental procedures. Chapter five focuses on the biorefinery processing of two lignocellulosic side-products, rice husk and *Arundo donax,* and the consequent simultaneously recovery of three products: lignin, cellulose nanocrystals, and silica with high purity and reasonable yields. Successively a modification of the biorefinery process that led to the production of a fourth material, a tentative lignin-silica biofiller, is also introduced. Chapter six provides the results of a more in depth investigation of the lignin-silica filler. In chapter seven the relationship between the structure of several lignins and their behavior in the composites with natural rubber is studied. Chapter eight is dedicated to lignin modification and to the properties of modified lignin/natural rubber systems.

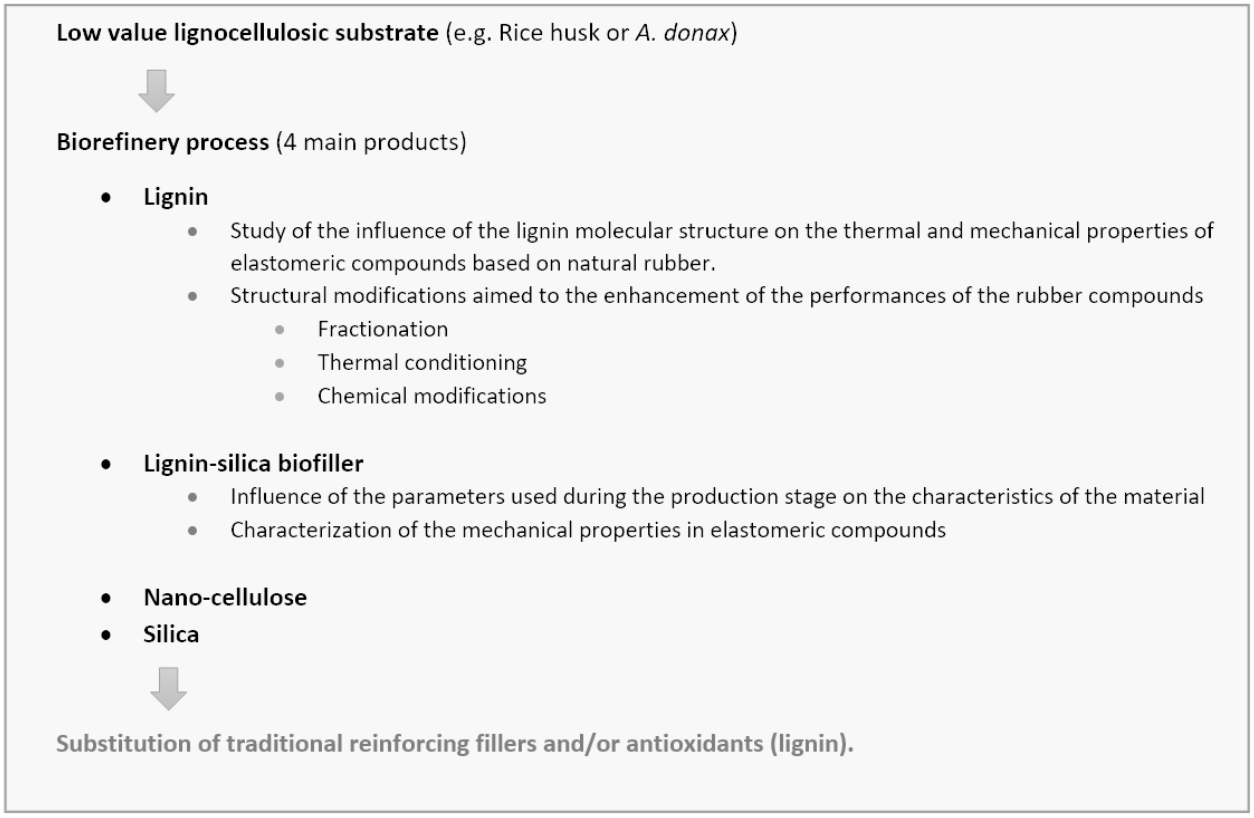

Figure 1 – Schematic outline showing the connection between the different topics.

CAP 2 - Materials from renewable resources: transition toward a sustainable economy

The study of the natural world, through observation and experimentation, and the ensuing exercise of the gained knowledge for practical purposes always played a crucial role along the history of humankind. [1] Deeply embedded amongst the scientific disciplines, material science was a main player in many aspects of development. The availability of materials with specific characteristics, in fact, is decisive for the success of any technology and, on the other side, breakthroughs in the field of materials often led to important advancements that ultimately resulted in a whirlwind of new technological applications. The perfect example is the advent of synthetic materials, which spurred a revolution in mass production that deeply impacted the economic models of the 20th century and widely influenced our contemporary lifestyle, providing a plethora of technological tools otherwise precluded to a large portion of the population. Currently our society relies heavily on the production of materials and chemicals from fossil feedstocks, however the weight of the wild exploitation of non-renewable resources is turning unbearable as environmental, economic, and political constraints become tighter. The demand for sustainable, greener materials is increasing rapidly, however, matching or improving the performances of the actual materials while engineering new solutions using exclusively renewable resources and cost-effective processes is anything but a straightforward endeavour.

2.1 Fossil vs Renewable: a brief history

Advancements in technology were always deeply influenced by the capability of humankind to master different materials; from the production of rudimental tools with coarse stones to the recently gained ability to manipulate the matter at the molecular level that ultimately opened the doors to the contemporary, flourishing field of nanotechnology. The ability to shape artefacts with different materials played a crucial role from the beginning of human history, influencing the behaviour of our ancestors and the way that primordial societies were organized. The actual importance of materials is also reflected in the names used to identify some prehistoric periods in the field of archaeology, such as: Palaeolithic, Neolithic, Bronze Age, Iron Age and Pottery period. During the ages our ancestors learned how to produce more sophisticated tools. From stone, wood, bones and ivory we moved to different metals and along with hides we learnt to produce fabrics and clothes from natural fibres such as wool, cotton and silk. Largely naturally available woods and stones were extensively used to build first shelters and infrastructures. Moving into history

different civilizations improved the expertise in the field of metallurgy and started to cast items from metals and alloys. During the following periods metals held a dominant position in the field of materials engineering. From Hellenic and roman periods, through the middle ages manufacturing techniques improved. And finally, during 17th and 18th century, when chemistry definitely emerged as an independent discipline, freed from the mysticism of alchemy, progresses in iron and steel ultimately resulted in the industrial revolution that transformed the agrarian economy of Britain in the first industrialized civilization.[2] In this time frame the economy switched for the first time from renewable to fossil resources on a large scale. Coal was found to be more cost effective and practical then wood and its demand raised quickly, stimulated by the diffusion of the steam engine, the steel industry, the cotton mills, the coal powered gas lamps and the development of national railways.[3] By the end of the 19th century the uncontrolled exploitation of coal caused the first known environmental problems of anthropogenic origin. Over late 19th century and early 20th century a second escalation of industrial developments spread across western Europe and the United States of America. Recent studies on global warming date back to this period the beginning of human influence on whether on a global scale.[4] Along with the introduction of modern organizational methods and diffusion of electrification and mass production, during this period, industries began to exploit many different natural and synthetic resources: lighter metals, new alloys, synthetic products such as plastics, as well as new energy sources.[5] The first industrially relevant materials produced by polymer science appeared in the form of chemically modified natural macromolecules: cellulose acetate from the esterification of cellulose, Linoleum from linseed oil and vulcanized rubber as a result of sulphur crosslinking of natural polyisoprene.[6] Afterwards the production of polymers from fossil resources boomed as the exploitation of petrol provided a seamless flow of low coast raw chemicals and fuels, boosting the economy and the development of new materials. From then on fossil-based thermoplastics, thermosetting and elastomers dominated the markets until the end of the 20th century and beyond. At the beginning of the 21th century the environmental performance of the materials started to play a more relevant role promoted by the increasing awareness towards the environmental problems.[7] Different factors began to align, paving the way towards the comeback of materials produced from renewable resources. The demand for greener products from the consumers, the growing awareness and concern regarding pollution and fast global warming among world leaders, altogether with the volatility of the fossil feedstocks prices due to the growing global demand, the political instability of the main producing countries and the approaching depletion of the resources, started to push R&d efforts toward greener, sustainable solutions. Thus, by the second decade of the 21th century, a first wave of renewable materials, able to substitute polyolefins in a wide array of applications, entered mass production.

Fossil resources

Since the appearance of our modern ancestors, human activities relied mainly on renewable, bio-based, organic materials. The use of mineral sources was limited to small volumes and most of the products, such as those made of metals and glasses, were recyclable since they could have been re-forged into different shapes. Therefore, for a very long time, corresponding roughly to the 99% of the total existence of the humankind, societies were intrinsically sustainable and the human impact on the equilibriums of the planet was negligible. The existence of fossil resources is known since millennia, but their use was confined to occasional wood replacement for heating and cooking. This paradigm changed at the dawn of industrial revolution, when Britain switched from a self-sustaining organic economy to a mineral resource depleting economy.[8] With the invention of the steam engine, for the first time in history, humanity was relieved from manual labour in some heavy productive activities. The introduction of machines also brought a sweeping increases in production capacity that would affect all basic human needs, including food production, medicine, housing, and clothing.[9] The technological advancements transformed the entire industry within a few decades, as a result the quality and quantity of the goods produced increased rapidly and among the major consequences there was a sensible increment of the population growing rate.[10] Ultimately all this events that characterized the progress of the society during the first industrialization were literally fuelled by the exploitation of coal. Still, at that time, fossil resources were only used for energetic purposes, while technology was relying on long-established materials.

Historical impact of the petrochemical boom

In the second half of the 19th century the development of well drilling techniques, pipelines and refining systems, together with the invention of the internal combustion engine prepared the way for the extensive exploitation of crude oil that deeply characterized the 20th century. One of the first commercial applications of a product distilled from crude oil was the use of kerosene in oil lamps. The new, cheaper, fuel rapidly pushed whale oil off the shelves creating a new market for crude oil,[11] probably saving endangered species from extinction as the multi-million dollar whaling industry partially plummeted[12]. Afterwards, throughout the 20th century petrol assumed an increasingly pivotal role in the economy of industrialized countries culminating in the actual situation where nearly every production process is related or dependant from crude oil. During the first half of the 20th century the increasing demand for petrol in the U.S. drove large investments towards its production and the economy quickly become bound to the availability of the fossil resource. At the beginning of the 1950s the internal production couldn't front the growing demand and the U.S. become a major importer of crude oil, nonetheless the availability of petrol at a low and steady price on the global market was assured by the exporting countries and economies of the western countries could

continue to prosper. With the first crisis of 1973 the circumstances changed and since then sharp rises in oil prices periodically occurred mainly due to political instability in key producing countries. The largest amount of petrol is used to produce fuels for the transportation sector followed by the energy production for the industries and the furniture of electricity and heat for commercial activities and residential units.[13] Only a relatively small fraction of the crude oil is used for the production of chemical products,[14] however their impact of the contemporary society is comparable to that of fuels and energy production. In fact, since the first decades of the 20th chemists made fundamental discoveries in the field of macromolecules and found the first pathways to produce synthetic polymers. The first completely synthetic thermoplastic, Bakelite, was quickly followed by many other plastics and the shortage of natural rubber during war times also lead to the development of synthetic alternatives to sustain the production of elastomeric products.[15] Over the years a growing number of synthetic polymers was invented: polyolefins, vinyl polymers, diene polymers, polyesters, polyamides, polyurethanes, epoxy polymers, silicone polymers and phenolic polymers.[16] The optimization of the production processes led soon to the development of synthetic materials with improved and adaptable characteristics, the growing reliability of this materials, along with their specific and desirable properties favoured their diffusion in a very broad range of applications. They were quickly employed in many fields, in fact due to their relatively low cost, ease of processing and the desirable chemical, mechanical and thermal properties synthetic polymers produced from petrol are now extensively used by automotive, aerospace, medical, building and packaging industries and to produce a countless variety of costumer goods. Typical examples of petrol based products are reported in table 1. Ultimately, by the end of the 20th century any industrialized economy was heavily relying on fossil resources to produce fuels, energy and commodities. The large availability of relatively inexpensive crude oil on the markets supported thriving economies over several decades and, together with mass production, granted access to mass consumption of material goods to a larger portion of the growing global population.

Solvents	Diesel fuel	Motor Oil	Bearing Grease	Denture Adhesive	Linoleum	Ice Cube Trays	Synthetic Rubber
Ink	Floor Wax	Ballpoint Pens	Football Cleats	Speakers	Plastic Wood	Electric Blankets	Glycerin
Upholstery	Sweaters	Boats	Insecticides	Tennis Rackets	Rubber Cement	Fishing Boots	Dice
Bicycle Tires	Sports Car Bodies	Nail Polish	Fishing lures	Nylon Rope	Candles	Trash Bags	House Paint
Dresses	Tires	Golf Bags	Perfumes	Water Pipes	Hand Lotion	Roller Skates	Surf Boards
Cassettes	Dishwasher parts	Tool Boxes	Shoe Polish	Shampoo	Wheels	Paint Rollers	Shower Curtains
Motorcycle Helmet	Caulking	Petroleum Jelly	Transparent Tape	Guitar Strings	Luggage	Aspirin	Safety Glasses
CD Player	Faucet Washers	Antiseptics	Clothesline	Antifreeze	Football Helmets	Awnings	Eyeglasses
Curtains	Food Preservatives	Basketballs	Soap	Clothes	Toothbrushes	Ice Chests	Footballs
Vitamin Capsules	Antihistamines	Purses	Shoes	Combs	CD's & DVD's	Paint Brushes	Detergents
Dashboards	Cortisone	Deodorant	Footballs	Vaporizers	Balloons	Sun Glasses	Tents
Putty	Dyes	Panty Hose	Refrigerant	Heart Valves	Crayons	Parachutes	Telephones
Percolators	Life Jackets	Rubbing Alcohol	Linings	Enamel	Pillows	Dishes	Cameras
Skis	TV Cabinets	Shag Rugs	Electrician's Tape	Anesthetics	Artificial Turf	Artificial limbs	Bandages
Tool Racks	Car Battery Cases	Epoxy	Paint	Dentures	Model Cars	Folding Doors	Hair Curlers
Mops	Slacks	Insect Repellent	Oil Filters	Cold cream	Movie film	Soft Contact lenses	Drinking Cups
Umbrellas	Yarn	Fertilizers	Hair Coloring	Fan Belts	Car Enamel	Shaving Cream	Ammonia
Roofing	Toilet Seats	Fishing Rods	Lipstick	Refrigerators	Golf Balls	Toothpaste	Gasoline

Table 1 - a partial list of products mass produced from petrol at the turn of the 21st century (reproduced from reference).[17]

Issues connected with the mass exploitation of fossil resources

For thousands of years the impact of the human presence on environment was negligible due to the intrinsically sustainable lifestyle and the limited extent of the global population. However, with the beginning of the Industrial Revolution, a global economy started to emerge and the world population began to increase rapidly fostered by the new technological means, the improvements in agriculture and the diffusion of better sanitation standards[4]. This lead to migration of people and to the exploration and the subsequent exploitation of the virgin lands. At the beginning of the 18th century only Europe and partially Asia were relatively densely populated, while large parts of the world were substantially uninhabited. Nowadays the situation completely changed and most of the lands are under some form of human influence. Thus, large parts of the natural land were converted into agricultural land to face the increasing demand of food. This led to several issues: environmental damage, pollution and loss of biodiversity.[18]

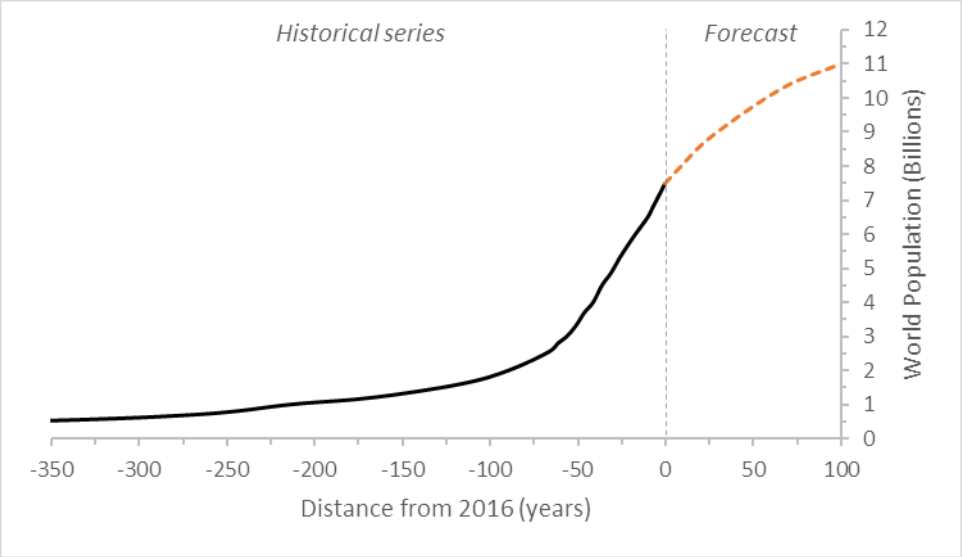

Figure 2 - Human population, historical series and plausible forecast.[9,19,20]

Alongside the greater demand for food the steep increase in population and the growth of the economies of developed and developing countries also promoted an upsurge of the global demand for fuels, energy and basically any kind of commercial products. In this scenario, all the issues connected to an economical model based on the exploitation of non-renewable resources escalate quickly and their solution becomes a priority on the agenda of the leaders around the globe. The main issues can be resumed in three points:

1. Depletion of the resources
2. Economic viability
3. Environmental concerns

Fossil resources are generated from renewable organic matter of biological origin, nevertheless the process of transformation takes millions of years and they can be classified as non-renewable for practical reasons. Hence their amount is limited and their availability in the future is essentially determined by the extension of the natural reservoirs and the consumption rate. To put depletion into prospective we can consider the case of petroleum, the quintessential fossil resource. The typical production profile of a single oil field can be divided in three phases; a graphical representation is reported in figure 3. Initially production is rising early until the peak (or a short plateau) where the rate of production is maximum. When the peak is reached, one quarter to one half of the total recoverable oil has been extracted. The rate of production at the plateau depends by the size of the infrastructure, usually selected upon considerations on the price of oil in the future. Eventually production starts to drop under the influence of physical constraints and a long period of decline begins (production tail). [21]

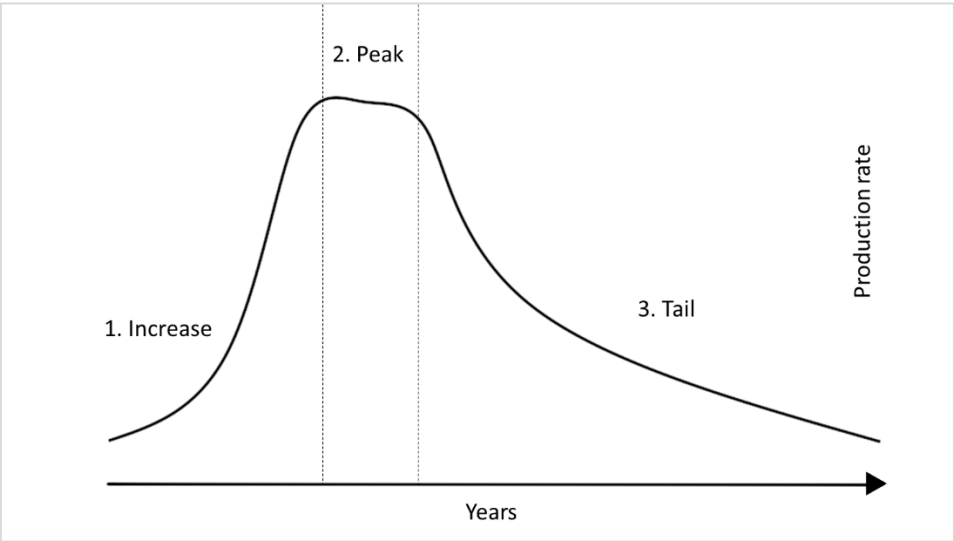

Figure 3 - Typical production profile for a single oil field

In a region, the decline of a production field can be compensated by new discoveries, however most of the oil is found in a relatively small number of large fields that are discovered earlier and the peak of discoveries usually precedes the peak of production by several years. At the global level, it is likely that the production peak of 'conventional oils' is passed within the first or second decade of the 21st century, while the peak of 'all-oils' is expected around 2020.[21,22] The estimation is subject to the large uncertainty in the underlying data, particularly regarding the extension of Middle East and Former Soviet Union reserves for conventional oil.[21] Anyway it is rather clear that reaching the maximum production rate is a matter of few years and that global production is probably going to see a decline within the next decades. In addition, it has also to be considered that the exploitation of non-conventional oil fields implies a higher cost and a larger consumption

of water, adding more concern on the second and third points, i.e. economic and environmental concerns.

The economic issues arise from the fact that the global demand of crude oil is rising due to the transition of developing countries (e.g. China) from agricultural to modern industrial economies,[23] while the worldwide availability is essentially granted and controlled by a limited number of countries (14 in 2016) reunited in the Organization of the Petroleum Exporting Countries (OPEC).[24] It is worth noticing that 64% of the global petroleum reserves are estimated to be located in the Middle East.[13] Starting from the 1970s the depletion of the oil fields in the U.S. and geopolitical instability in the regions of main producers caused periodical instabilities in the price of oil.[13,23] In importing countries the availability of the crude oil and the volatility of its price have a strong impact on the price of the derived commodities as it affects the production cost due to the changes in the prices of raw materials, transportation and energy supply, resulting in noticeable consequences for the final consumer.[25]

In the 20th century the growth in population, GDP and global materials use started to influence the environment on a planetary scale. The growing industrial metabolism can be identified as one of the major drivers for this change.[26] The impact of humanity on the environment was found to be so profound that a new geological epoch named Anthropocene was proposed. The new epoch that should begin in the 1950s,[27] in concomitance with the great acceleration of the influence of human activity on the Earth systems,[28,29] and was recommended by a Working Group on the Anthropocene (WGA) to the International Geological Congress on 29 August 2016.[30] There are several outstanding facts supporting the institution of the Anthropocene, among which: the increase in the animal extinction rates, the raise of carbon dioxide level in the atmosphere (from ~280 ppm before the industrial revolution to ~310 ppm in 1950 and ~400 ppm of present time) along with other greenhouse gasses leading to global warming, the virtually ubiquitous presence of microplastics due to the introduction of plastic wastes in the waterways, the increase in nitrogen and phosphorous in the soils caused by the diffused consumption of fertilizers, and the appearance of a permanent layer of airborne particulates in sediment and glacial ice such as black carbon produced by fossil resources burning processes.[28,29,31] The general concern about global warming is rapidly increasing and some fundamental, well-established facts are now widely accepted by policy makers: the concentration of greenhouse gases (GHG) in the Earth's atmosphere is directly linked to the average global temperature on Earth, their concentration has been rising steadily since the industrial revolution and the burning of fossil resources is the main cause.[32] Those shared scientific understandings promoted actions and cooperation among a large number of countries. From the first world climate conference held in 1979 several international meetings took place and led to the adoption of Kyoto protocol in 1997, the first agreement setting binding emission reductions targets, and the Paris agreement of 2015, where it was declared the objective of contain the global temperature rise within this century, with the limit of 2 degrees Celsius above pre-industrial levels.[33] The main purpose of the agreement is to limit global warming in order to avoid potentially catastrophic events,

as a decline in the production of major crops, an excessive rise of the sea levels,[32] and a major decrease in the pH of the oceans.[34] On the other hand, effective measures against global warming could bring also benefits for air quality and human health, since actions to reduce GHG emissions often reduce co-emitted air pollutants.[35] Other environmental problems caused by the use of fossil feedstock are connected to manufacturing sector. Plastics, for instance, due to their outstanding characteristics and cost effectiveness are broadly used, in fact they represent the major output of the chemical industry with a production rate of 3×10^8 tons per year. However, their indiscriminate use is connected with a number of environmental hazards, including waste accumulation and significant contributions to greenhouse emissions.[36] Recently, the issue of the microplastics is emerging, an additional source of environmental concern connected to mass production of synthetic polymers. Microplastics are small particles (< 5mm) made of synthetic polymers that are now found worldwide, generated by the careless disposal of waste items. Microplastics are categorized as primary and secondary. Primary microplastics are intentionally produced in small size. Secondary microplastics result from the fragmentation of larger items under the effect of different causes. Such particles are stable in the marine conditions and are potentially toxic for organisms. Microparticles can also end up in the soil and remain for many years. Additionally, microparticles can act as vectors for toxic substances that can be present in the original product or that have been adsorbed later. Added concern is rising as microparticles can be picked up by different organisms, entering in the food chain. Different studies have already found microparticles in food products.[37–39] The main sources of primary microplastics are personal care products, raw materials for plastics production, paints, blasting abrasive and rubber granulate. Secondary microparticles are released from tyres, paints, building materials and consumer goods. The contribution of tyres to the total release of both primary and secondary microplastics is particularly relevant.[39]

Renewable resources

The political efforts to protect the environment from the negative anthropogenic influences are mainly focused on the reduction of the GHG emissions. In industrialized countries the larger contribution to is attributable to fossil fuels for transportation and energy production.[40] As a result, starting from the late 20st century, there is a growing effort directed toward the development of carbon neutral technologies. The main strategies pursued involve the production of energy from renewable resources and the development of sustainable technologies. In the energy sector many alternatives are being considered and developed: solar, photovoltaic, hydropower, wind, wave, tidal, geothermal and biomasses.[41] In the transport sector, viable strategies on short to long term seem to be the replacement of conventional fuels with biofuels produced from biomasses[42] and the implementation of solutions based on alternative energy carriers. For instance switching to hydrogen[43] and electric[44] vehicles. Nevertheless, the production of commodity chemicals and

materials cannot be postponed or treated separately from the production of fuels since they are both deeply rooted into the actual refinery scheme of crude oil and are subject to the same main concerns. Biobased chemicals and materials might be conveniently produced from fractions of the biomasses not suitable to yield biofuels and hence adding further value to the biomass, enhancing the economic sustainability. Additionally, commodities produced from renewable resources could also result more environmental friendly by design and favor the disposal of the products at the end of their life cycle, reducing the issues linked to the accumulation of persistent wastes.

Transition to a biobased economy

The transition from a fossil-based economy toward a bio-based economy has been advocated by policy-makers, still most of the productive activities are currently based on conventional production schemes. The transition started but the progression is slow and this is attributable to the complexity of the interactions between industry, technology, science, markets, and policy.[45] Even though in the initial phase, the transition toward a sustainable economy seems to be a global trend, beneficial for different reasons. In first place the transition to an economy based on renewable resources would limit the dependence from fossil feedstocks, potentially addressing the major issues previously exposed: deployment of the natural resources, cost of the raw materials end environmental concerns. Secondly switching to biomasses is going to reduce the dependency from few exporting countries and could provide different options for the promotion of regional and rural development.[46] In fact the presence of biomasses is more ubiquitous around the globe and countries could invest on different vegetal species in order to cope with local conditions and productive needs. Overall the resources would be redistributed in a fairer way, as graphically represented in figure 4.

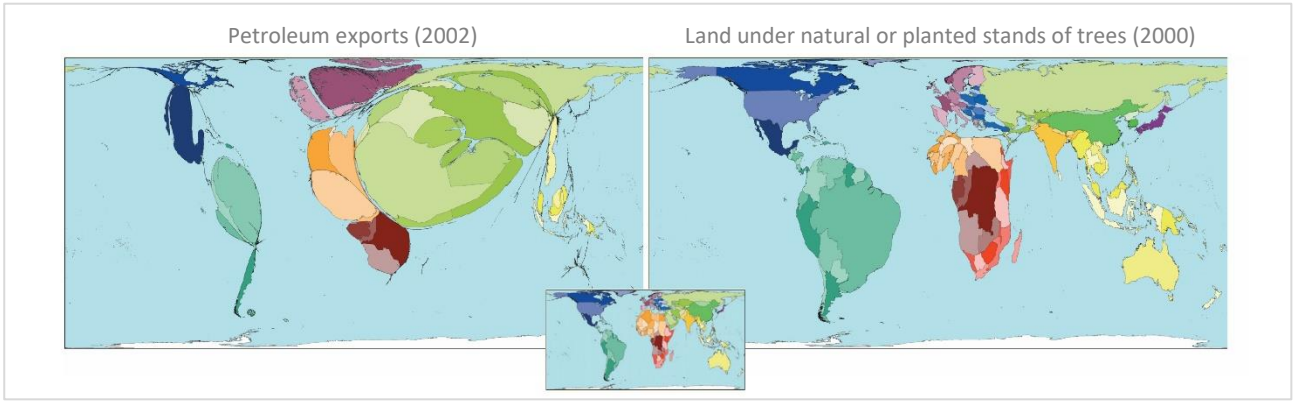

Figure 4 - Density equalizing cartograms. (Redesigned with permission from reference[47]).

A massive exploitation of the biomasses can reduce the dependence from crude oil but on the other hand can lead to new problems and challenges. Biomass is an abundant and carbon neutral resource. However, the effective production of substantial amounts of biomass is still connected to the availability of land and water. Furthermore, the production of feedstocks for biofuels, biochemicals and biomaterials can potentially enter in competition with the production of food crops, determining a dangerous rise in the food prices.

Biomass as a feedstock

Fossil resources are regarded as carbon positive, since when they burn they release carbon that was stocked and not available in the atmosphere. Biomass, on the other hand, is considered carbon neutral, since the same amount of carbon dioxide that is eventually released after combustion was recently captured during the growing phase of the biomass. While growing, in fact, plants convert the energy provided by the sun in chemical energy through the photosynthesis, directly withdrawing carbon dioxide from the atmosphere. Energy is stored in carbohydrates as $6\ CO_2 + 6\ H_2O \rightarrow C_6H_{12}O_6 + 6\ O_2$.[48] Even though biomasses are intrinsically carbon neutral, the complete life cycle of the products generated from the renewable resources usually is still carbon positives as energy is also consumed during harvesting and processing. The capture efficiency of solar radiation is ~1% for most of vegetal species, nevertheless every year 10^{11} tons of carbon are converted in biomass,[34] while the world primary energy consumption reached $1{,}3 \times 10^9$ tons of petroleum equivalents in 2015.[49] These numbers might seem appealing, but the large-scale utilization of biomasses must be carefully evaluated. To produce enough resources to compensate the huge amount of fossil resources that we are currently consuming more land needs to be cultivated and more intensively, at the expenses of forest areas that play a central role in the equilibrium of the ecosystems. In addition, intensive industrial cultivating techniques use large amounts of water, not always locally available, along with fertilizers and pesticides that can degrade the quality of soil and water.[50] Furthermore production of biofuels from food crops already generated a noticeable level of concern as they compete with the production of the same crops for food, increasing the demand and inflating their price. On the contrary, a large amount of biomass is already produced as a waste, including residues from the agricultural and forestry activities, food, and municipal solid waste. Also invasive plants that grow on marginal land, not suitable for agriculture could be periodically harvested and used as a source of biomass.[34] The final verdict regarding the feasibility of mass production of fuels from biomasses is still unanswered as the need a very large amount of renewable feedstock at steady supply rates constitutes a major drawback and is also very difficult to make exhaustive life cycle assessments. The situation might be different for chemicals and materials. If we considering how petroleum is used it is possible to see that a very large amount is incinerated rather quickly to produce heat, electricity and to power transports. Only smaller fractions are used to produce chemicals and materials.[51] In this prospective the production of chemicals and materials from biomasses seems much more reasonable than that of energy

and fuels. Similar considerations can be done if we consider as an example the situation in the U.S. in 2007. Here the breakdown of the oil usage is a bit different than the global situation, anyway the ratio between the amount of crude oil used for energy and fuel and the amount used to make chemicals is comparable. In this specific case the materials are not present in the breakdown of petroleum usage since in the U.S. the primary source to produce synthetic materials is natural gas.[52] Observing the data reported in figure 5 it is possible to notice that while 70% of the crude oil is used to produce fuels, only 3% is converted into chemicals. At the same time the value-added worth (value including capital and labor costs) of the final products is comparable.[14] The possibility to generate a large value using only a fraction of the raw material is an interesting economic point at the advantage of the production of chemicals from biomasses. A similar argument can be used also to support the production of materials from biomass as their added-value, usually lower than that of fine chemicals, is consistently higher than that of fuels.[46] Additionally, if the materials are produced with a fraction of the biomass that is not suitable to produce chemicals there will be another favorable effect as the two processes would help each other to be profitable, maximizing the yield of the renewable raw materials. Life cycle assessment on the production of bio-based materials gave partially positive results, a literature review performed in 2012 led to the result that one metric ton of bio-based materials saves, relative to conventional materials, 55 ± 34 gigajoules of primary energy and 3 ± 1 tons of carbon dioxide equivalents of greenhouse gases. Still, potential side effects such as loss of biodiversity, soil carbon depletion, soil erosion and deforestation are a serious treats associated with the exploitation of biomasses and must be taken as well into consideration.[50]

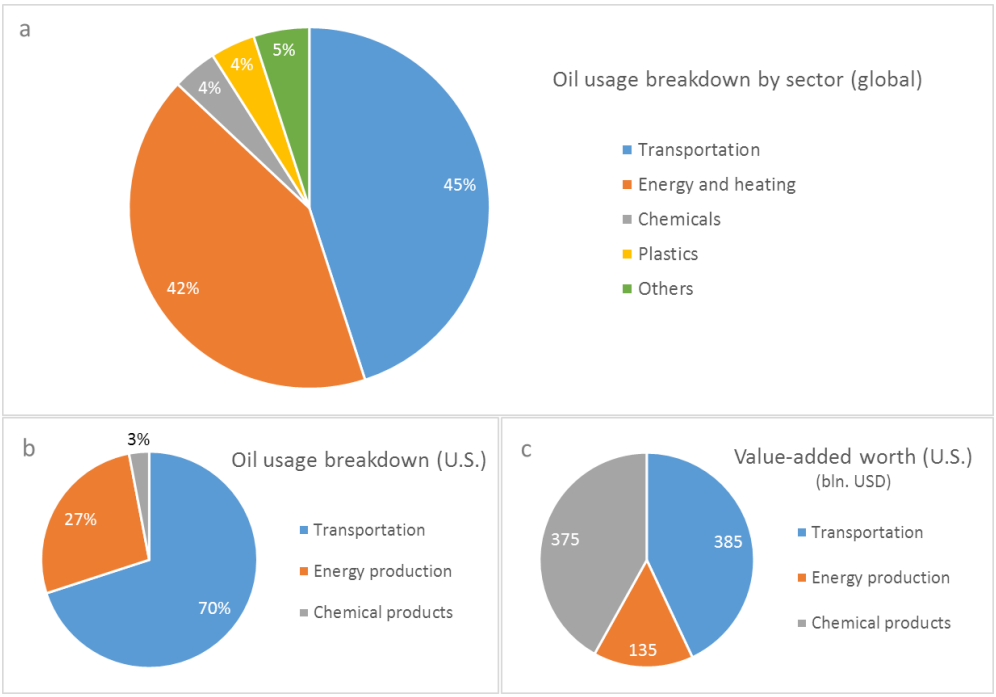

Figure 5 - Crude oil usage breakdown by sector, globally and in the U.S. (a, b) and value-added worth for U.S. (c).[14,51]

Green chemistry and sustainable materials

During 20th century the chemical industry supported virtually every productive sector in fulfilling the fast-increasing material needs of the global society, largely contributing to the ensuing improvement of life quality. Nevertheless, the disruptive attitude towards the environment associated with the generation of hazardous wastes and the strong dependence from fossil resources started to generate a growing criticism. At the turn of the 21st century a higher attention threshold in the global opinion towards environment and human health along with the tighter constrains faced by the 20th century development fashion helped to redirect political and scientific efforts, to find more sustainable economic models and technical solutions.[53] Since the late 1990s there was a growing interest in green (or sustainable) chemistry. A fast-growing field which fundamental objective is to meet environmental and economic goals simultaneously. Green chemistry aims to be benign "by design", eliminating the use and the generation of harmful substances and achieving sustainability at the molecular level. The guiding framework for the design of new chemical products is summarized in the twelve principles of green chemistry:[54,55]

The twelve principles of green chemistry

1. Prevention
   It is better to prevent waste than to treat or clean up waste after it has been created.
2. Atom Economy
   Synthetic methods should be designed to maximize the incorporation of all materials used in the process into the final product.
3. Less Hazardous Chemical Syntheses
   Wherever practicable, synthetic methods should be designed to use and generate substances that possess little or no toxicity to human health and the environment.
4. Designing Safer Chemicals
   Chemical products should be designed to affect their desired function while minimizing their toxicity.
5. Safer Solvents and Auxiliaries
   The use of auxiliary substances (e.g., solvents, separation agents, etc.) should be made unnecessary wherever possible and innocuous when used.
6. Design for Energy Efficiency
   Energy requirements of chemical processes should be recognized for their environmental and economic impacts and should be minimized. If possible, synthetic methods should be conducted at ambient temperature and pressure.
7. Use of Renewable Feedstocks
   A raw material or feedstock should be renewable rather than depleting whenever technically and economically practicable.
8. Reduce Derivatives
   Unnecessary derivatization (use of blocking groups, protection/ deprotection, temporary modification of physical/chemical processes) should be minimized or avoided if possible, because such steps require additional reagents and can generate waste.
9. Catalysis
   Catalytic reagents (as selective as possible) are superior to stoichiometric reagents.
10. Design for Degradation
    Chemical products should be designed so that at the end of their function they break down into innocuous degradation products and do not persist in the environment.
11. Real-time analysis for Pollution Prevention
    Analytical methodologies need to be further developed to allow for real-time, in-process monitoring and control prior to the formation of hazardous substances.
12. Inherently Safer Chemistry for Accident Prevention
    Substances and the form of a substance used in a chemical process should be chosen to minimize the potential for chemical accidents, including releases, explosions, and fires.

The Green Chemistry approach has already proven to be successful in all industry sectors. From aerospace, automobile, cosmetic, electronics, energy, household products, pharmaceutical, to agriculture.[54] The road to a completely sustainable industrial development withholds many challenges, but the shift to the new approach brings also a variety of opportunities. The most successful companies, in fact, are those who managed to exploit the economic, legislative and public image advantages provided by the sustainable way.[56] The basic principles of green chemistry are rapidly crossing the borders, diffusing into the interdisciplinary fields. In the last few years the quest for sustainability started to greatly influence the main research directions also in the fields of materials science and nanotechnology.[57,58] The new biodegradable and bio-based polymers will be produced from yearly renewable feedstocks and biomasses and will help to create a new range of eco-efficient products.[57] Polymer science is going back to its roots, in fact, the first large scale commercial products were based on natural polymers and oligomers, such as cellulose, linseed oil and natural rubber and their chemical modifications, cellulose-esters, Linoleum and vulcanized natural rubber.[6] Many are demanding a reconciliation with the environment, to find a new, sustainable development model, but at the same time we all want to maintain the improvements brought about by the technological evolution that deeply changed our lifestyles over the last hundred years. The challenge is to meet the technical properties of the fossil-based materials that dominated the scene during the 20th century, enabling the development of countless new applications, thanks to their large availability, low cost, straightforward processability and the outstanding characteristics of the final items. In figure 6 a tentative timeline, representing a selection of relevant materials used by humanity during its historical course is reported. It is interesting how on a logarithmic scale synthetic materials from non-renewable resources are confined in a well-defined temporal gap. At some point in history, a rapid disconnection from the past can be spotted, as the relationship with the environment, rapidly and deeply changed. On the other side, it is possible to see a certain symmetry in the plot and it seems that since the last 10-15 year we are already transitioning towards a new equilibrium. The first generation of greener technological solutions is already becoming a reality and new materials produced from renewables are moving from the laboratories to pilot and mass production scales. A virtuous process started, but it must be carried on and expanded to new market sectors. Many scientific and technological challenges lie ahead, but also countless new, exciting possibilities.

Figure 6 - *Humankind timeline based on a selection of technological materials.*[59–80]

2.2 Lignocellulosic biomass

As illustrated in the previous section, biomasses are going to be the resource of choice for the eco-friendly materials of the 21st century. Biomass is a general term that host a wide array of different substances. Biomasses can be of animal or vegetal origin, but while the first could have some, limited, relevance in the energetic sector only the latter is suitable to produce material goods, due to unrivalled abundancy and usable chemical composition. Biomasses can be retrieved from a lot of different sources. Large amounts are already generated as collateral products by the agricultural and forestry industries, others are produced as waste from urban activities, ultimately, they can also be produced from ad hoc cultivations. The most abundant constituent of biomass is lignocellulose, it accounts for half of the plant matter generated by the photosynthetic process,[34] with a yearly supply of ~200 billion metric tons worldwide.[48] Lignocellulose is a natural occurring composite material, its main constituents are three natural polymers: cellulose, lignin and hemicellulose. In the native biomass, they are deeply permeated and chemically bound to each other. Together they form a rigid material that in plants form the main constituent of the cell wall, adding physical resistance and chemical recalcitrance to the structure. Relative abundances and structural features of the three biopolymers depend by the botanical source. An average composition for the main typologies of lignocellulosic materials are presented in table 2. A schematic representation of the composite structure of a lignocellulosic material found in plants cell walls is presented in figure 7.

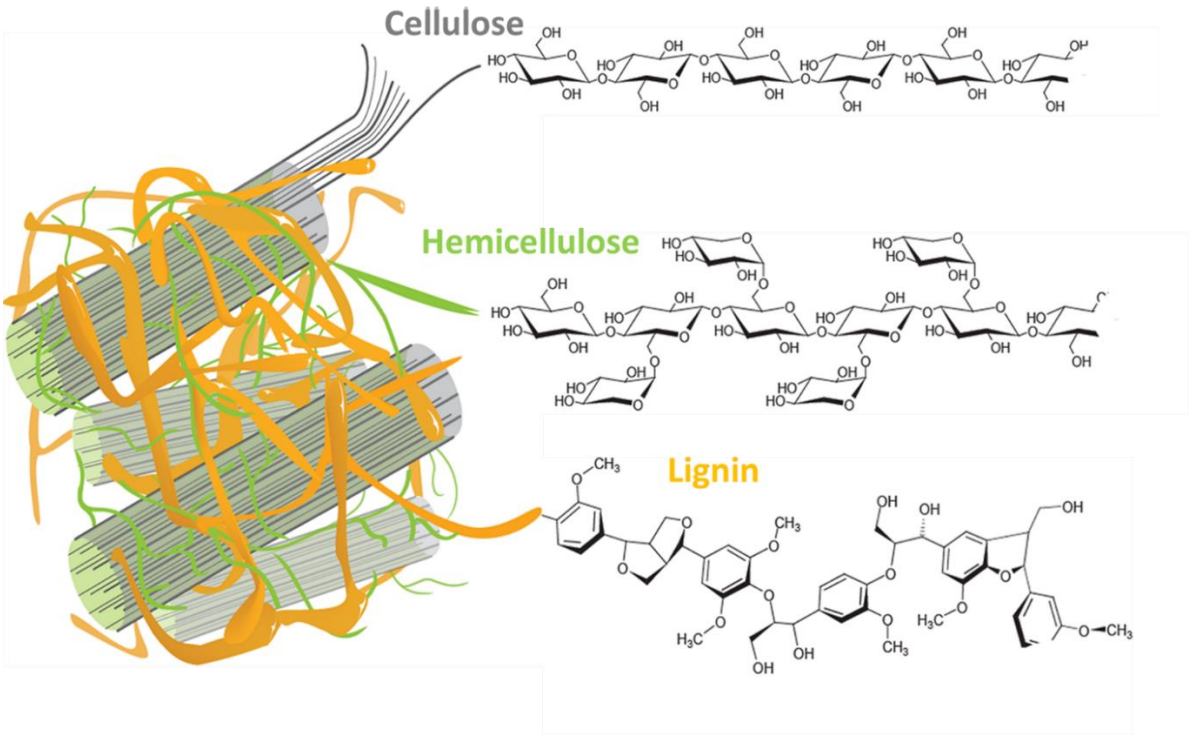

Figure 7 - Graphical representation of lignocellulose composite material found in plants cell wall. (reproduced from reference).[81]

Source	Cellulose	Hemicellulose	Lignin
Hardwood	40-55	24-40	18-25
Softwood	45-50	25-35	25-35
Herbaceous	25-40	25-50	10-30

Table 2 – Composition ranges in lignocellulosic materials from different sources (%).[82]

Lignocellulosic biomasses relevant for industrial applications are commonly divided into three main categories: hardwood softwood and herbaceous. Hardwood and softwood refer to woody plants characterized by a strong stem such as trees. Are classified as hardwoods the woody plants belonging to angiosperms. Angiosperms, also called flowering plants, have seeds that are enclosed within an ovary (usually a fruit), they usually have a seasonal life cycle and have flat leaves. Woody plants belonging to gymnosperms are classified as softwoods, they have naked seeds found on scales, leaves or as cones. As a general rule softwoods are evergreen and have needle-like leaves.[83] The categorization of trees into hardwood and softwood is because angiosperms usually have a hard and durable wood, while gymnosperms a soft and workable wood. This is generally true, but there are exceptions, as yew trees are softwood with a relatively hard wood while balsa wood is one of the most malleable woods and is from a hardwood specie.[84] Herbaceous plants, sometimes referred to as grasses, are those with a flexible stem. Their leaves and stems die down to soil level at the end of every growing season. Herbaceous plants can be annual, biennial or perennial. Annual herbaceous die every year, the next season new plants grow from the seeds. In biennial and perennial herbaceous plants only the stems and leaves die at the end of growing season but parts of the plant survive and grow again the next year.[85]

Figure 8 - Artistic representation of Hardwood, Softwood and Herbaceous plants.

Cellulose

Cellulose is a linear syndiotactic high molecular weight homopolymer composed of anhydro-D-glucose (D-anhydroglucopyranose) units, linked by β-1,4-glycosidic bonds. Every glucose unit is corkscrewed 180° with respect to its neighbors, hence the effective repeating unit is the dimer of glucose, cellobiose. The two ends of the chains are not equivalent, on one side there is a chemically reducing functionality (hemiacetal), on the other end a non-reducing functionality (aliphatic hydroxyl). Glucopyranose rings adopt a $^4C_1$ chair conformation, with the hydroxyl groups aligned along the equatorial plane of the rings and the hydrogens in axial position. The β conformation with hydroxyl groups aligned on the molecular plane make the chain to extend in a linear fashion. The supramolecular, hierarchical, organization of cellulose is strongly influenced by the abundancy of laterally protruding hydroxyl groups. In fact, the linear chains can easily interact forming a dense network of intramolecular and intermolecular hydrogen bonds. Thus, cellulose tents to organize into densely packed, crystalline domains surrounded by less ordered, semi-crystalline and amorphous regions. Based on the source, extraction process and eventual modifications cellulose can arrange in different, up to six, crystalline structures characterized by a different pattern of hydrogen bonding. On the other hand, native cellulose is may only be found in three crystalline allomorphs, cellulose Iα, cellulose Iβ, and para-crystalline cellulose. The average degree of polymerization of native cellulose can space from 500 to 15000 glucose units according to the specific botanical source, making cellulose one of the longest bio-macromolecules in nature.[86–89] In higher plants, cellulose is synthesized during the formation of primary and secondary cell wall at the plasma membrane by rosette transmembrane complexes. The complexes are presumably constituted of 36 individual cellulose synthase (CESA) proteins, arranged into six subunits. Hence, cellulose primary fibrils are thought to be formed by 36 glucan chains. The deposition of the chains is highly ordered and is probably guided by the cortical microtubules.[89]

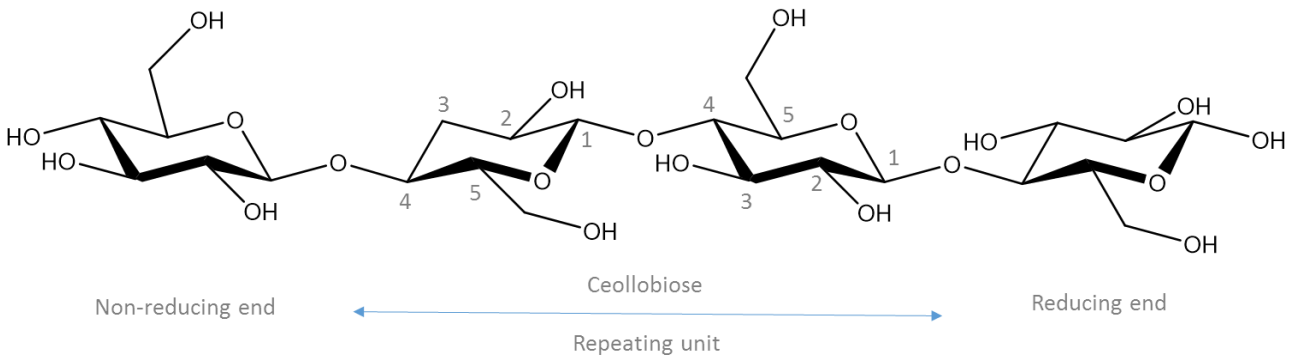

Figure 9 - Chemical structure of cellulose (redrawn from reference).[87]

Cellulose is the most abundant renewable organic material produced in the biosphere, having an annual production that is estimated to be over 7.5×10^{10} tons.[87] It is mainly found in plants where, due to its fibrillar nature, exerts a structural function forming a composite substrate in association with other natural polymers (lignin, hemicellulose and pectin). Cellulose is also bio-synthetized by other living systems such as marine organism (tunicates), algae, fungi and bacteria. Because of its large availability, intrinsic renewability and desirable qualities cellulose has already been exploited at industrial scale to produce paper and textiles (cotton). Materials produced from the chemical modifications of cellulose have been synthetized and largely used more than one century ago. Celluloid, a composite of cellulose nitrate and camphor, was the first thermoplastic. Semi-synthetic films (cellophane) and fibers (rayon) were prepared through the viscose process.[90] Recently cellulose is receiving a high deal of attention due to the full recognition of its intrinsic qualities. Cellulose properties are well-established at macroscopic and molecular level, nonetheless cellulose is organized in a hierarchical way, with the polymeric chains arranged in crystalline domains at the nanoscale. The growing interest for renewable materials and nanotechnology revamped the research on cellulose, especially on cellulose nanocrystals (or nanowhiskers). In fact, thanks to their outstanding properties, they are promising candidates for a wide range of high-tech applications, such as the production of bio-materials, nanocomposites and smart materials.[86,87,91–93]

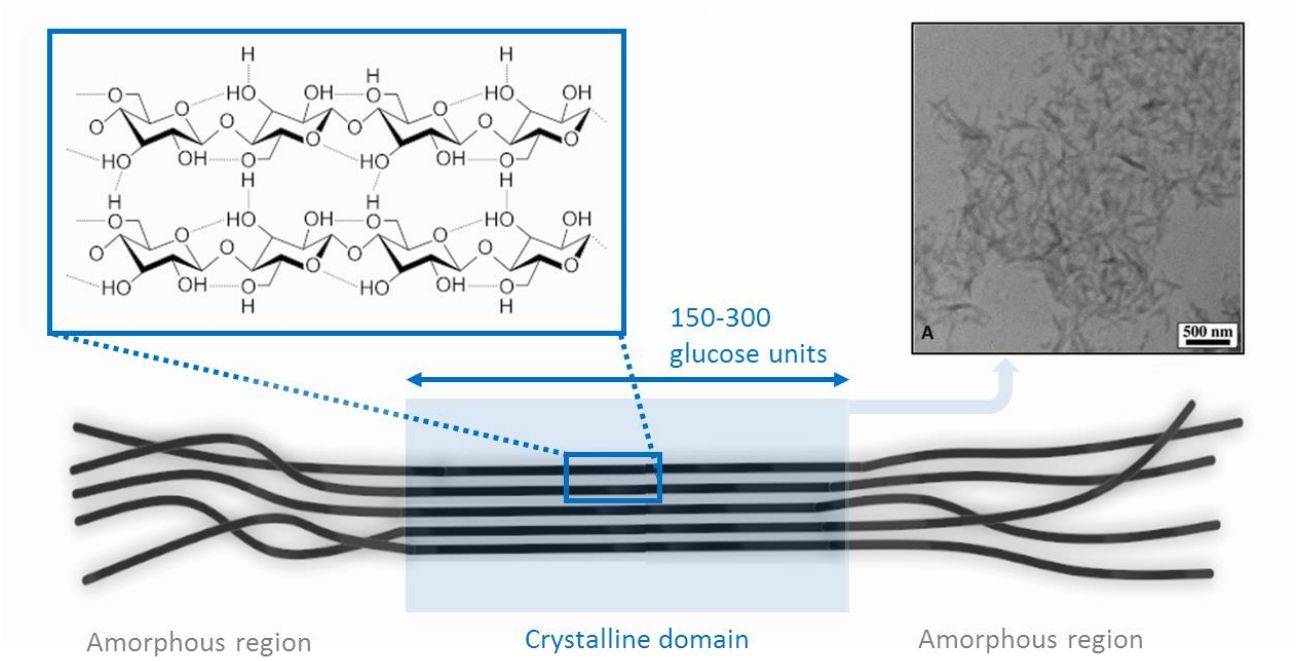

Figure 10 - Schematic representation of cellulose hydrogen bond connectivity, formation of crystalline domains and TEM microscopy of cellulose nanocrystals isolated by acid hydrolysis from filter paper whatman #1.

Hemicellulose

The structure of hemicellulose is less regular than that of cellulose. The type and the abundance of the building units, as well as the interconnectivity is different among hemicelluloses from different sources. Hemicelluloses can be described as heterogenous polysaccharides composed of different monomeric units. They are composed by pentose sugars, xylose and arabinose, hexose sugars, mannose, glucose and galactose, and some sugar acids residues, as 4-O-methyl glucuronic acid and galacturonic acid. Usually the degree of polymerization of hemicelluloses is lower than that of cellulose and some hemicelluloses can exhibit a branched structure. Frequency and composition of the branches depend from the botanical origin. Hemicelluloses from hardwoods and herbaceous plants, such as agricultural by-products, are mainly composed of xylans, whereas those from softwoods contain mainly glucommannans.[94,95] Xylans are polysaccharides with a backbone composed of β-D-xylopyranose units connected by 1-4 bonds (as glucose in cellulose). The backbone can be linear or ramified with monomeric or oligomeric side chains and may contain arabinose, glucuronic acid or its 4-O-methyl ether, and acetic, ferulic, and p-coumaric acids. Xylans can hence be divided in linear homo-xylans, arabinoxylans, glucuronoxylans, and glucuronoarabinoxylans. Xylans are almost as ubiquitous as cellulose and may play a critical role in the stabilization of the cell walls, forming an array of covalent and non-covalent interactions.[96] Due to the highly heterogeneous structure of hemicelluloses their industrial utilization can be problematic. Nonetheless by constituting a substantial fraction of the biomass their conversion in profitable products is a key objective. The main strategy concerning the valorization of hemicellulose are the conversion in fermentable sugars and the production of valuable chemicals.

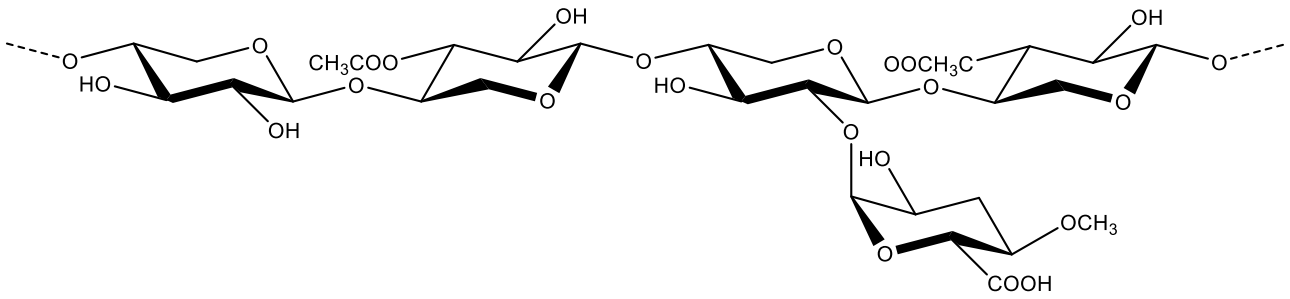

Figure 11 - Partial molecular structure of a glucuronoxylan (redrawn from reference).[94]

Lignin

Alongside the polysaccharidic fractions lignin represents a major constituent of biomass. In the lignocellulosic material lignin acts as a sealant, enhancing mechanical, chemical and biological resistances of the composite. Lignin is a heterogeneous, branched, three-dimensional, amorphous polymer constituted by phenyl propane units characterized by a different degree of substitution. The relative amount between the different monomeric units, their connective patterns and the size of the macromolecule are highly affected by the botanical source of the lignin, as well as by the isolation process used to recover the biopolymer.

Biosynthesis

The fundamental precursor of lignin is the amino acid phenylalanine (Phe). Through the general phenylpropanoid and monolignol-specific pathways phenylalanine is converted into the three hydroxycinnamyl alcohols also called monolignols. Comparative genomics studies indicate that the complete biosynthetic pathway first appeared in moss but was absent from green algae, hence it is believed that lignin was an evolutionary response related to the new structural needs of the first terrestrial plants.[97] The monolignols are stored and transported inside the cells as monolignol glucosides (glycosylation occurs on phenolic hydroxyl), since the free species are relatively toxic, unstable compounds and do not accumulate to high levels within living plants.

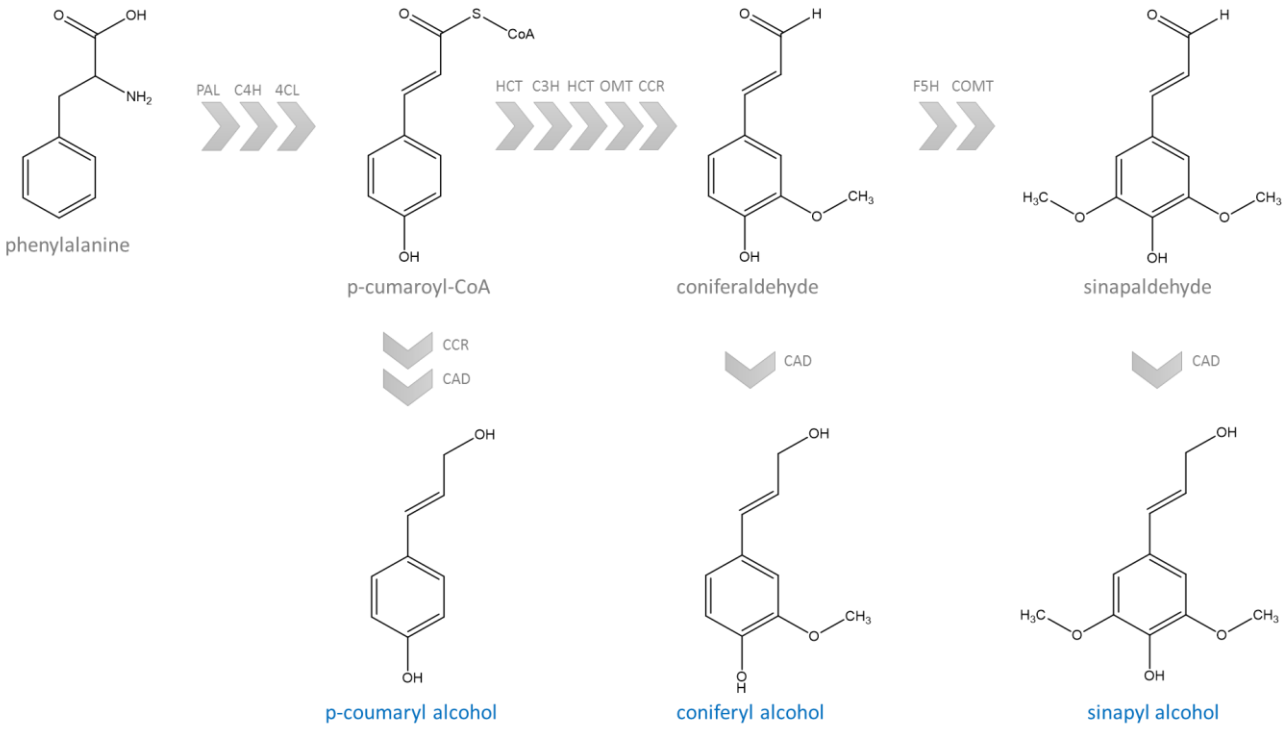

Figure 12 - The main biosynthetic route from phenylamine to the monolignols (redrawn from reference).[97]

After the cleavage of the glycosidic bond the monolignols are oxidized by cell wall laccase and peroxidase, the synthesis of lignin then proceeds through a mechanism of free radical polymerization via radical coupling of the activated (dehydrogenated) monolignols.[98,99]

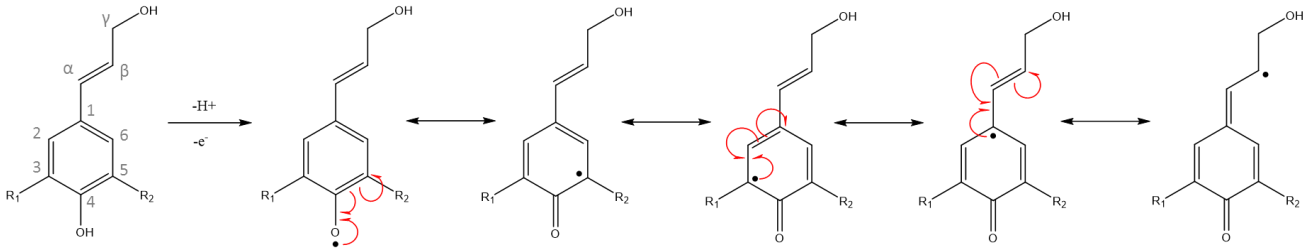

Figure 13 - Formation of a resonance stabilized radical on the phenylpropanoid structure of monolignols. (p-coumaril R_1=R_2=H ; coniferyl R_1=H R_2=OMe ; sinapyl R_1=R_2=OMe)

When the monolignols have been activated by the enzymes they can react with each other. The dimerization reaction between two monolignols is the first step of the lignification process is.[100] The most frequent bond that is formed is β-O-4, while the formation of 5-5' and 4-O-5 bonds between two monolignols does not occur in a significant way.[101] The initial coupling of monolignols in lignin synthesis is a two steps reaction itself. The first step is the radical coupling, in the second step the adduct can undergo tautomerization or nucleophilic addition of water to regain aromaticity. A computational quantum mechanical modelling (DFT) of the enthalpies of coupling concluded that β-O-4 linkage is most thermodynamically favorable, β-β' linkage and the β-5 linkage at unsubstituted sites are also strongly favorable, whereas the 4-O-5 and 5-5' couplings are clearly less favorable.[100]

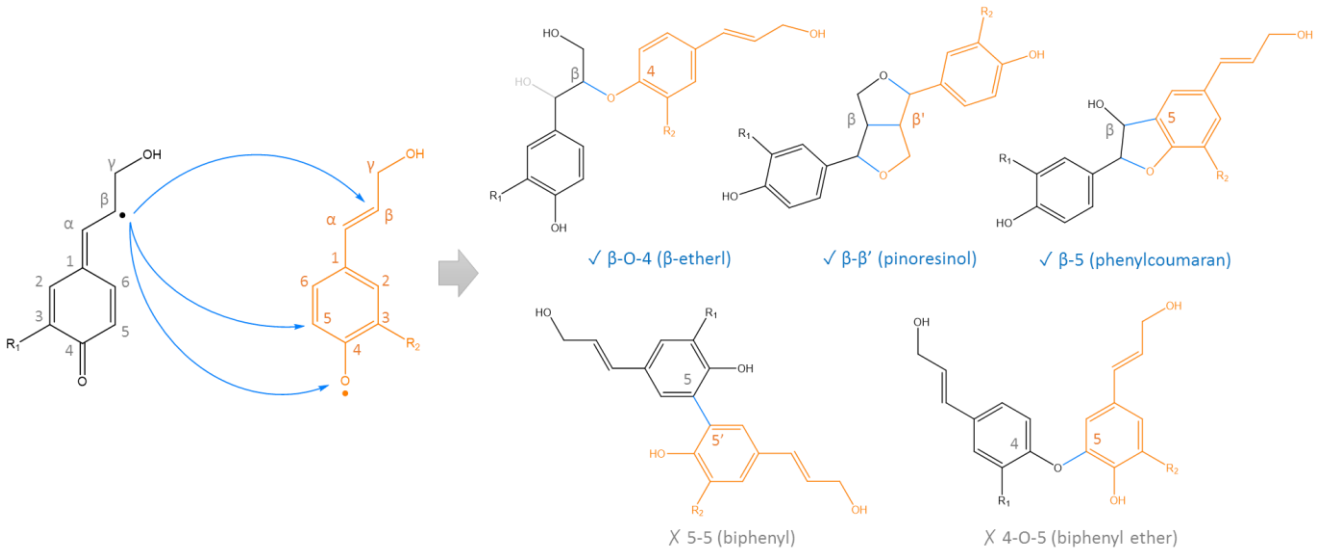

Figure 14 - Dimer formation by coupling reaction of two monolignols (redrawn from reference).[101]

Coupling between pre-formed lignin oligomers, on the other hand can yield 4–O–5 and 5–5' linkages. The second (main) step of the lignification process is the "end-wise" coupling of new monolignols to the forming macromolecule. For every additional coupling two radicals are consumed, hence radicals are thought to be reformed on the growing polymer by radical transfer from monolignols or other intermediaries as p-Coumarates that form less stable radicals.[101] The relative amount (frequency) of the various units obtained during the "end-wise" growth is different from that produced during the dimerization step. During progressive chain extension, in fact, there is no place for the formation of β-β' bonds and the reaction with monolignols yields prevalently β-O-4 and β-5 connections, whereas reactions with other growing segments can result in 5-5' and 4-O-5 linkages. It is worth noticing that for di-substituted phenols (as in sinapyl alcohol) the only possible outcome is a β-O-4 ether bond. Also for this reason the latter is the most frequent linkage found in lignins.

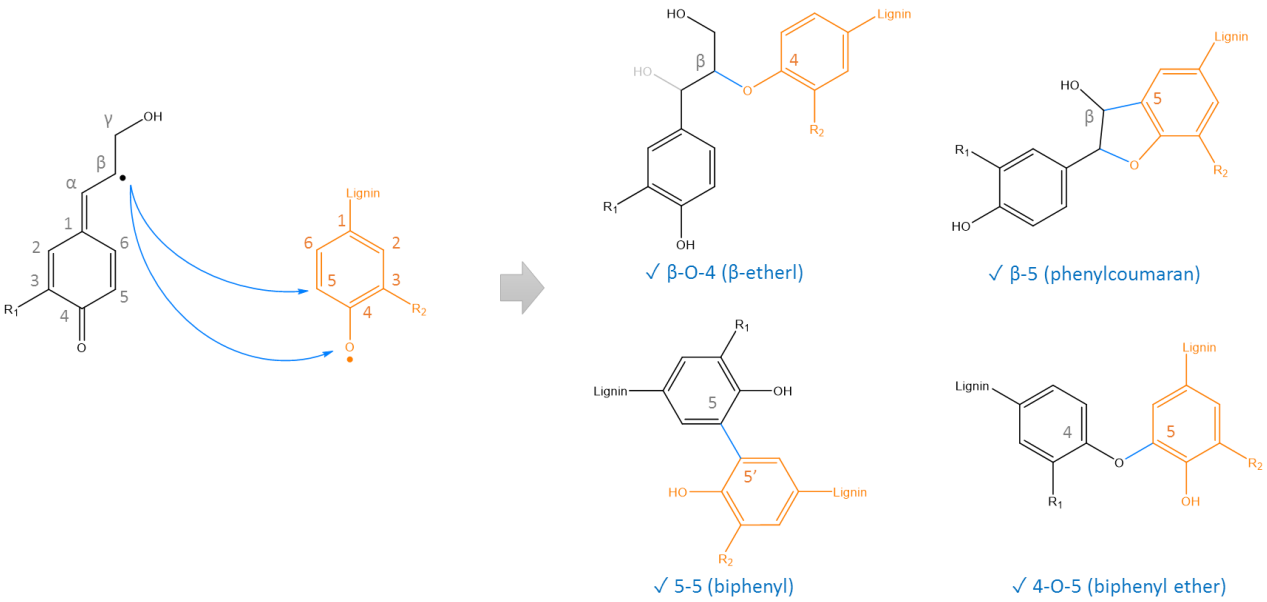

Figure 15 – Coupling of monolignols and oligomers to the growing chain (redrawn form reference).[101]

While the production of monolignols is under strict biosynthetic control, the lignification process is thought to be driven by the chemistry of radical coupling. The major fact supporting this hypothesis is that lignin is racemic, whereas enzymes are generally believed to be highly regio and stereo selective catalysts, in fact most of the natural compounds are produced in a pure enantiomeric form.[102] Nonetheless the connectivity pattern of lignin-like polymers synthetized in vitro bulk polymerization from lignin precursor is appreciably different from that of natural occurring lignins and there is evidence that it is influenced by the supplying rate of monolignols.[101] As already mentioned, the frequency of linking types is influenced by the degree of

substitution of the aromatic ring, in fact the positions 3 and 5 are increasingly hindered in coniferyl and sinapyl alcohols and this accounts for the extensive presence of β-O-4 bonds. It's also been experimentally observed that an excess of p-coumaryl alcohol leads to the formation of lignins with a lower molecular weight. This behavior was rationalized using computational simulations, indeed it was found that unsubstituted phenolic units are less effective to undergo radical polymerization due to the lesser electron density on the unmethoxylated phenolic oxygen, hence it was confirmed that their presence at the molecular terminals can hinder further chain growth.[103] Additionally in some lignins a prevalence of *erythro* or threo-forms of β-O-4 structures was observed. Also in this case the structure of lignin is believed to be influenced by the relative abundance of available monolignols. In fact a positive correlation was found between the ratio of coniferyl/sinapyl units and the ratio of *erythro/threo* structures.[104] Eventually the lignification process leads to the formation of a complex three-dimensional molecular architecture. In the final structure the C9 units derived from each specific monolignol can still be recognized. In the polymerized lignin, the units resulting from **p-Coumaryl**, **coniferyl** and **sinapyl** alcohol are named p-**hydroxyphenyl** (**H**), **guaiacyl** (**G**) and **siryngil** (**S**) respectively. Plausible molecular fragments of hardwood and softwood lignins are reproduced in figure 16 and 17.

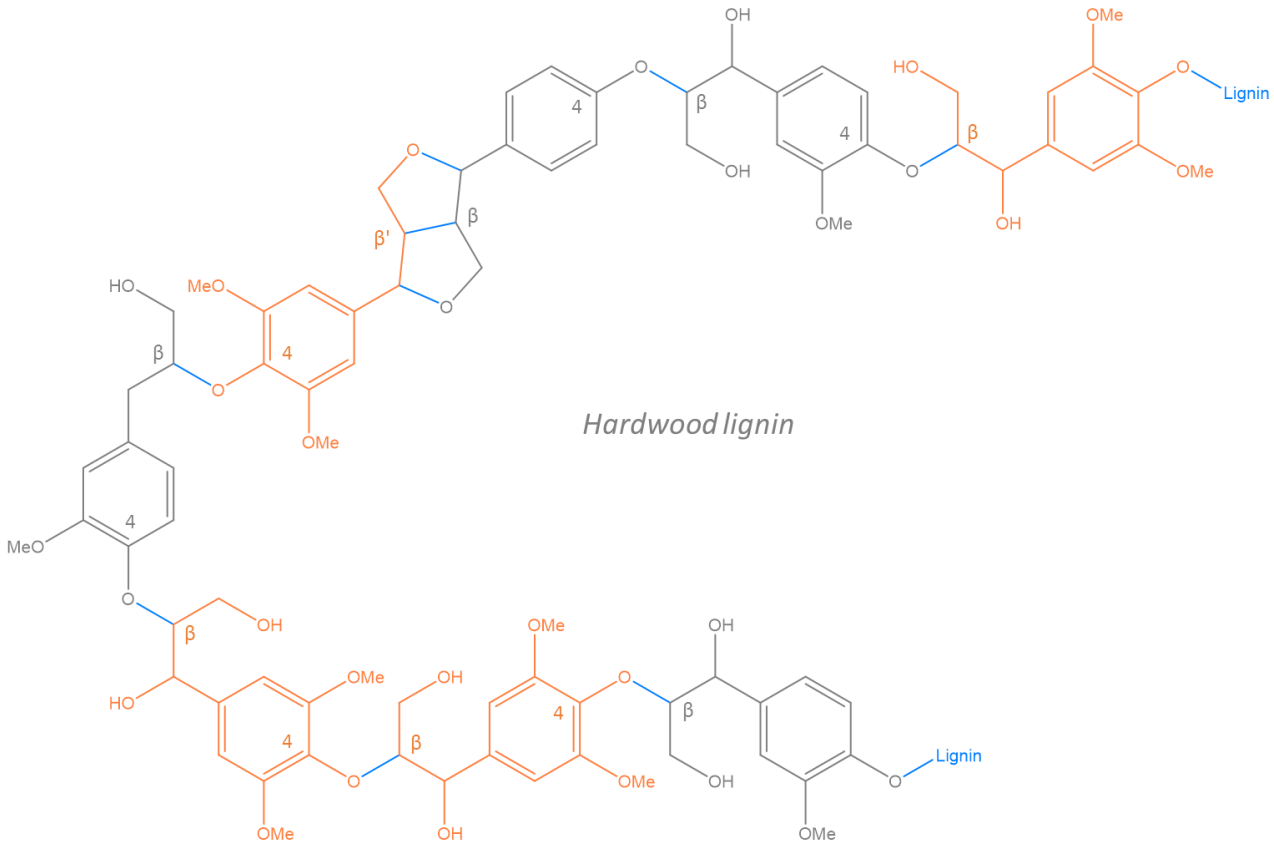

Figure 16 – Hypothetical partial structure of a hardwood lignin, guaiacyl (G) units are in grey siringyl units (S) in orange, intermonomer bonds are highlighted in light blue (redrawn form reference).[105]

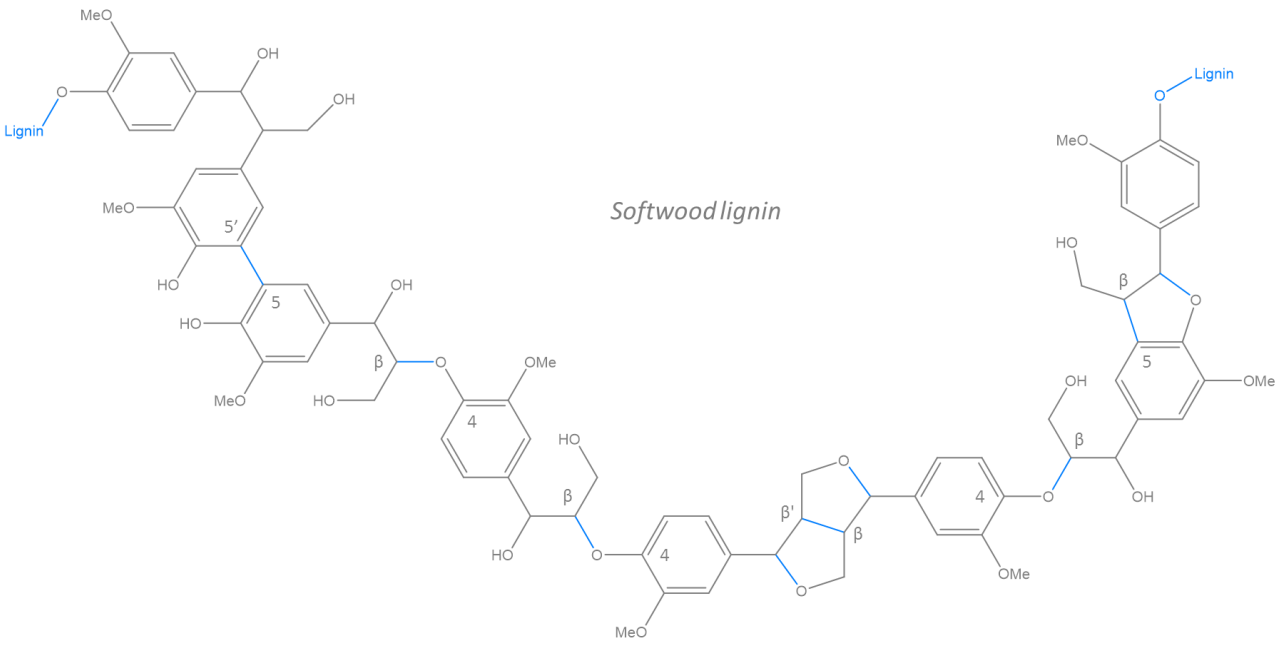

Figure 17 - Hypothetical partial structure of a softwood lignin, guaiacyl (G) units are in grey, intermonomer bonds are highlighted in light blue (redrawn form reference[105]).

Botanical sources

As seen in the previous section the relative amount of different monolignols that are available during the lignification process and by the effective supply rate affect the final structure of lignin. Lignin's architecture varies among species, between different parts of the plant, with the aging of the plant and is also affected by environmental conditions. In general, lignins from hardwoods (gymnosperms) are rich in both G and S units while H units are present only in traces, softwood lignins are composed almost exclusively of G units, with low levels of H unit, finally lignins from herbaceous plants have comparable amounts of G and S units and present a higher content of H units compared to lignins of woody plants.[106,107] As demonstrated also by experimental results on the synthesis of lignin models[105] the availability of different ratio between G and S units during the lignification process exerts a strong influence also on the connectivity patterns. The predominant linkage is β-O-4 in any lignin and accounts for roughly 50% of the total bonds. In hardwood lignins, due to the increased amount of S units the dominating linkages are β-O-4, whereas β–5 and 5-5' bonds are hindered by the presence of S units and thus β–β' occur more frequency. In softwood lignin, as a result of the dominance of G units, β–5 and 5-5' linkages occur more frequently at the expenses of the other intermonomeric connections. Herbaceous lignin contain all three monomers in appreciable amounts and their structure resemble more that of hardwoods.[108]

Linkage type	Softwood	Hardwood	Units frequency	Softwood	Hardwood	Herbaceous
β-O-4	50	60	H	9	4	17
α-O-4	5	7	G	91	33	49
β-5	10	6	S	0	63	34
5-5'	10	5				
4-O-5	4	7				
Other bonds	21	15				

Table 3 – Typical proportions between linkages and monomeric units in different lignins (as %).[109,110]

Another property of lignin that is affected by the degree of methoxylation on the constituting units is the extent of crosslinking in the three-dimensional network. In fact lignin with more methoxy functional groups (i.e. more S units) have less tendency to form branched or crosslinked structures.[111] Hardwoods form more linear chains, with a lower frequency of crosslinks. On the other hand, softwood lignins are more branched as G units are susceptible to further radical coupling reactions in position 5, enhancing the potential connectivity. Two of the possible structures responsible for branching in lignins are reported in figure 18. A dibenzodioxin on the left and a G unit engaged in three intermonomeric bonds on the right. In softwood lignin, the amount of dibenzodioxocins was found to be 3.7/100 C9 units, hence in this type of lignins around the 11% of the C9 units are engaged in such structures.[112]

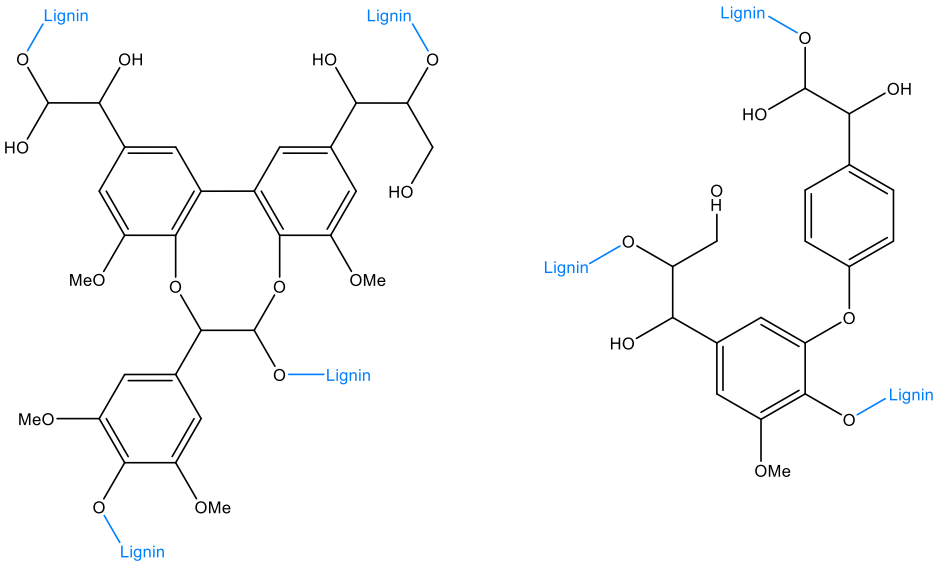

Figure 18 – Two examples of structures accountable for ramifications in lignin.

Lignin carbohydrate complexes (LCC)

In the complex structure of a lignocellulosic materials lignin acts as a matrix, enveloping cellulose, and hemicellulose. In any composite material, good compatibility between the different components plays an important role as it affects the mechanical properties. Due to its richness in functional groups lignin can form non-covalent interactions with carbohydrates. For instance, lignin can form hydrogen bonds due to the large availability of aliphatic and aromatic hydroxyls. Nonetheless it is thought that lignin is also chemically bound to carbohydrates,[108] especially hemicellulose at some extent. The covalent interaction is supposed to exist in the form of ester and ether linkages, some examples are featured in figure 19.

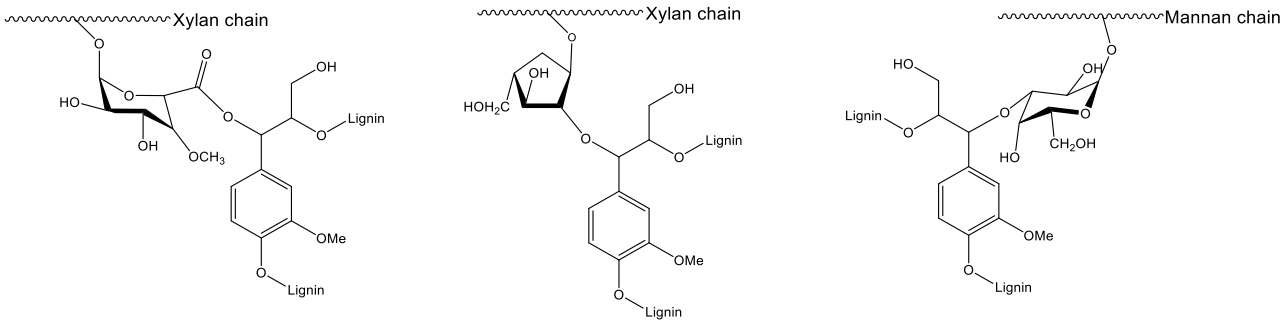

Figure 19 - Examples of ester and ether covalent bonds between lignin and hemicelluloses (redrawn from reference).[113]

Isolation process (technical lignins)

In the complex structure of lignocellulosic materials cellulose, hemicellulose and lignin are embedded into each other at molecular level and are interconnected by a myriad of physical and chemical interactions. To be exploited, the three major components must be separated. For this reason a fractionation pretreatment plays a key role in the processing of lignocellulosic substrates and is a mandatory step for most of the applications.[114] Pretreatments can be done with different techniques, in agreement with the type of feedstock and the desired product. They can rely on mechanical, chemical and biological strategies. Some successful techniques are: mechanical comminution, pyrolysis, steam explosion, ammonia explosion, CO_2 explosion, ozonolysis, acid/alkaline hydrolysis, organosolv and biodegradation.[115] There are also industrial processes, based on different technologies, that have been used since years to separate the main components of lignocellulosic materials. Historically wood have been largely exploited by the paper industry where the desired product was cellulose and lignin was considered as a by-product. More recently there is a growing interest towards a more holistic approach, summarized in the concept of biorefinery. In this idea, the full range of biomass components should be valorized by conversion into suitable products. In any case the separation of lignin from the polysaccharides is key step in any technology. At present, there are different

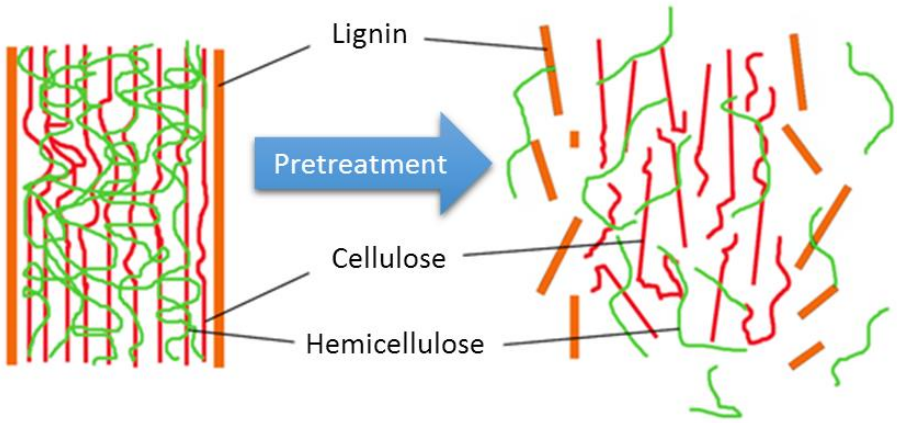

Figure 20 - Effect of the pretreatment on a lignocellulosic substrate (redrawn from reference).[114]

processes that are used on an industrial scale to achieve this separation. Lignins resulting from those processes are substantially different from the native lignin present in intact plants. In fact, in the delignification process some ether and ester bonds are cleaved and the resulting lignins differs in molecular weight and functional groups distributions, in relation with the conditions of the process. The fragmented lignins recovered after the delignification are often characterized by a variable amount of impurities. These modified, impure lignins produced on a large scale by means of industrial processes are referred to as technical lignins. The main processes can be divided in two groups, sulfur-based and sulfur-free. **Kraft lignins** are originated from the sulphate process extensively used by pulp and paper industries and they constitute roughly the 85% of the world lignin production.[116] In the cooking conditions, some bonds, mainly the abundant β-O-aryls, are cleaved and the molecular fragments get readily solubilized in the alkaline environment. Due to the cleavage of etheric bonds Kraft lignins usually present a higher amount of phenolic hydroxyl groups. Because of the oxidative conditions of the cooking, Kraft lignins tent to react forming more condensed structures and to incorporate sulfur. The recovered lignins generally have a sulfur content in the 1-2 % range. At the end of the cooking phase lignin is precipitated from the dark solution called black liquor by the addition of a diluted solution of sulfuric acid and recovered. Kraft lignin made during papermaking is predominately burnt in as it's use as a cheap fuel is an integral part of the paper and board manufacturing process. Thus, less than 2% of the available lignin is isolated and sold. It is estimated that around 6 x 10^5 tons of Kraft lignin are produced on a yearly basis. **Lignosulfonate** are by products of the sulfite process. During the cooking in the presence of HSO_3^- and SO_3^{2-} ions lignin is sulfonated and the resulting product is a water-soluble polyelectrolyte. The degree of sulfonation is ~0.5 per phenylpropanoid unit. Lignosulfonates are recovered in the salt form and their reactivity is related to the countercation: $NH_4^+ > Na^+ > Mg^{2+} > Ca_2^+$. About 5 x 10^5 metric tons of lignin are commercialized every year. Compared to sulfur lignins, sulfur-free lignins are highly fragmented but their structure is closer to that of the native lignin. **Soda or alkaline** pulping is used

more extensively to extract lignin from annual crops. Due to the absence of sulfur during the cooking soda lignin are usually purer and they can be used for applications where a high sulfur content would be an issue. Soda lignin can present also high silicate and nitrogen contents. The extraction medium used to obtain **organosolv lignins** is a mixture of solvents (acetic/formic/organic peroxide acids, ethanol) and water. As a trend organosolv lignins are more hydrophobic, have a lower molecular weight and a higher purity than other technical lignins. As a result organosolv lignins usually have a higher value.[106,116]

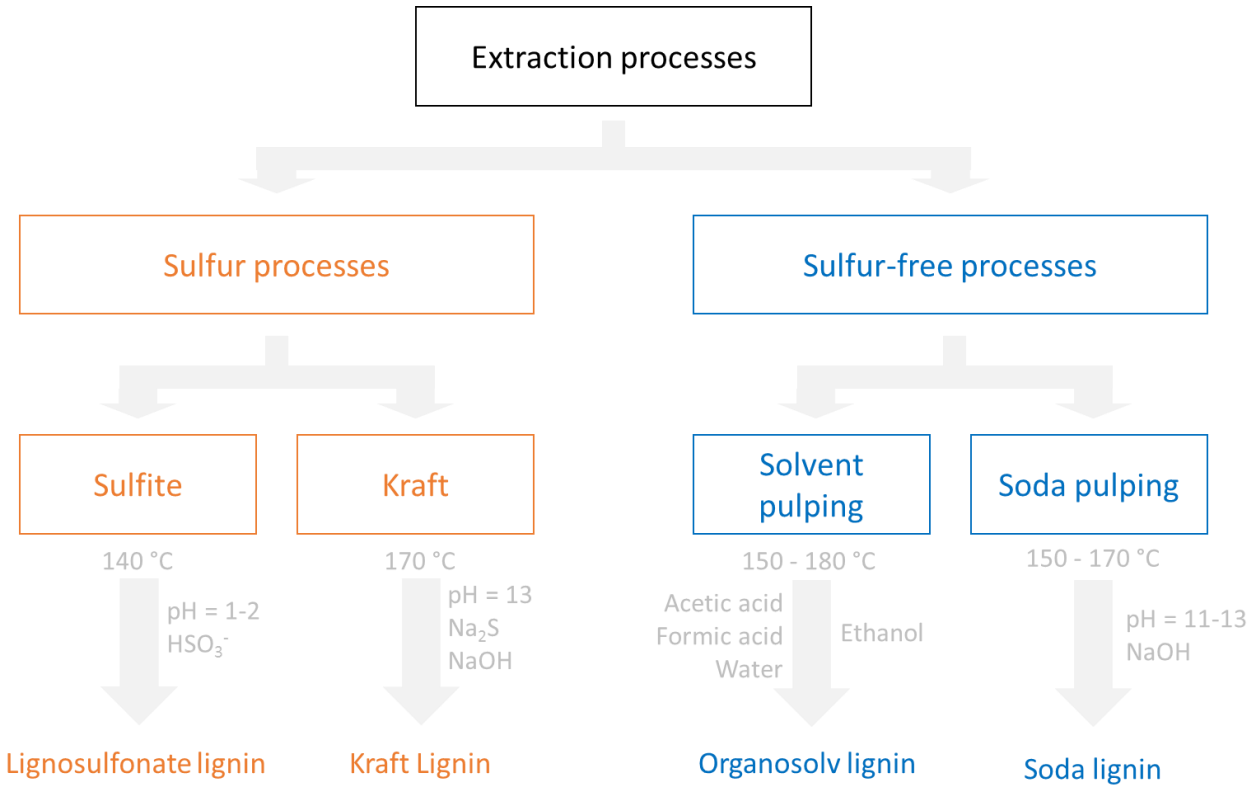

Figure 21 - Industrial processes for the production of technical lignins (redrawn from reference).[106]

Minor components

In biomasses, beside cellulose, hemicellulose and lignin there are other components that in some cases can have a noteworthy influence on the material and its processability. The three biopolymers combined are always the dominant fraction in lignocellulosic materials, accounting for at least ~70% of the total dry weight of the biomass. Alongside there are other, usually smaller, organic compounds labelled extractives and a mineral fraction, the ashes, constituted by different metal oxides. In woody materials extractives and ashes are present in relatively limited amounts, in fact extractives can be accountable for 2-7% of the dry mass while the ashes for 1% or less. In herbaceous plants the situation can be different. In this case extractives span from a minimum value of 4% to a maximum of 25%. The presence of ashes can also greatly differ from one specie to the other and their contribution to the total composition of the biomass falls in the broad 2% - 17% range.[117] **Extractives** can be constituted by different classes of compounds, such as alkanes, fatty alcohols, fatty acids, free and conjugated sterols, terpenoids, triglycerides and waxes. Even if present in low amounts, this compounds have a more lipophilic character, their presence can be critical for some processes and must be taken into account.[118] Additionally in the cell wall there are other organic substances, like starch, pectin and proteins. **Ashes** represent the solid residue obtained when biomass is incinerated. Ashes can be composed of different metal oxides such as: SiO_2, Al_2O_3, Na_2O, K_2O, MgO and CaO.[119]

Applications of lignin

Lignin possess promising features that look good on paper and has a high applicative potential. It represents the most abundant renewable, carbon neutral, source of aromatic species. Its unique aromatic backbone is decorated with different functional groups, enabling many possibilities regarding modifications and tailoring of the properties. However, the complexity of the molecular structure, the recalcitrance towards physical, chemical, and/or biological treatments, the variability of the properties in relation with the botanical source and the extractive processes, and the overall low grade of purity of technical lignins represent a barrier to lignin's applicability. Finally, the effective utilization of lignin is critical for the accelerated development and deployment of the advanced cellulosic biorefinery.[99] Currently lignin, predominantly as lignosulphonates, is used as a binding and dispersing agent in different industries.[120] Technical lignin produced by the paper industry has traditionally been utilized as a stabilizer for plastics and rubber, phenolic resins, dispersants, automotive brakes and wood panel products and for the research is ongoing regarding the production of aromatic chemicals, carbon fibers and thermoplastics from various lignins.[121]

2.3 Biorefinery

The concept of the biorefinery arise from a straightforward idea. To use biomasses as multipurpose feedstocks to produce fuels, chemicals and other bio-products. Biorefineries should operate to some extent in analogy to today's petroleum refineries, which produce multiple fuels and chemicals from a fossil feedstock. Biorefineries integrate environment- and resource-friendly technologies in a fully integrated system for the conversion of renewable and carbon neutral biomasses to produce fuels, power, heat, and value-added chemicals from biomass. The main steps of the refining process consist in the separation of the carbohydrates from the lignin followed by a controlled depolymerization. The product are fermentable sugars and other small molecules that can be converted in lignocellulosic ethanol, chemicals or other biobased products. In this scenario, lignin is often considered a less valuable product, with the not so profitable option to be used as a fuel for energy production. Nevertheless, multi-product biorefineries would be more economically convenient. Economic analysis based on product revenues suggests that co-utilization of lignocellulose components would increase the net margin up to six-fold.[48] Hence any application able to valorize lignin would be particularly beneficial for the whole process and a key player for economic feasibility of the lignocellulosic biorefinery.

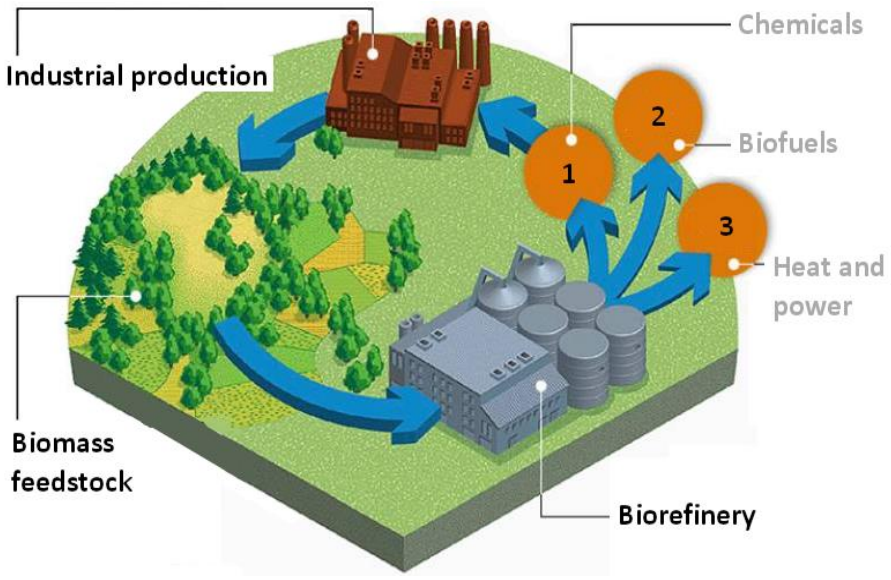

Figure 22 - The sustainable cycle in the biorefinery concept (modified form reference).[122]

The idea of biorefinery started to take relevance at the end of the 1990s, over the years it evolved in the so-called phase III biorefineries.[123] In phase I biorefineries a fixed product such as ethanol, biodiesel or biogas is produced from food feedstocks (grain, seeds, sugar, starch, vegetable oil or animal fats) using conventional technologies, resulting in an overall rather stiff process. Phase II biorefineries are still based on food crops

(grain or sugar) but they can deliver a wider range of products: biodegradable plastics, such as poly-3-hydroxybutyrate, sugar and ethanol are an example. Phase III biorefinery can use a more flexible mix of biomasses (especially lignocellulosic) to produce a variety of chemicals, fuels and intermediates or end-products.[123] The most recent biorefinery scheme is going to use a broad range of feedstocks that can be provided by different sectors: agriculture (dedicated crops and residues), forestry, industries (process residues and leftovers) and households (municipal solid waste and wastewaters), aquaculture (algae and seaweeds). To improve flexibility the raw materials can be converted with different techniques such as mechanical, thermochemical, biochemical and chemical processes. Regarding the otputs of the process it is possible to do a parallel with traditional refineries. Petrochemical industry processes crude oil into naphtha, gasoline, kerosene, gas oil and residues. Afterwards ethylene, propylene, C4-olefins and BTX (aromatics) are produced from naphtha and used to produce almost the totality of bulk chemicals. In principle, all oil refinery platform chemicals can be also derived from biomass, nonetheless this wouldn't be economically competitive. The best way to produce chemicals from lignocellulosic feedstock will take advantage of the abundancy of cellulose and hemicellulose. From carbohydrates is possible to obtain sugars via hydrolysis and afterwards build a small pull of fundamental chemicals via chemical or biological conversion of the sugars. Main outputs of latest generation biorefineries can be conveniently chategorized by their application, energy or material needs. Biofuels can be gases, liquids or solid (hydrogen, methane, bioethanol, biodiesel, pellets, lignin etc.). Non-fuels can be chemicals (fine, bulk, fertilizers etc.), materials (bioplastics, paper, resins etc.), food and animal feeds.[124] Once more the key for the profitability of biorefineries seems to lie in the cogeneration of different products. The production of large quantities of cheap (but eco-friendlier) fuels might be achieved only if high value biobased chemicals can be cogenerated by the process.[125] Anyway, large scale development of this kind of biorefineries is going to produce incredibly high volumes of lignin, as it is the second most abundant biopolymer after cellulose. Now, there is a shortage of applications capable to add considerable value to lignin and take advantage of the large availability. In fact, technical challenges related to the low purity of technical lignins and their intrinsically heterogeneous nature still limit the effective exploitability of potential applications. At the light of this facts it seems clear how important it would be to develop new ways to use lignin, taking advantage of its alluring characteristics.

References

(1) Shane Ross. Important Events in Human History http://www2.esm.vt.edu/~sdross/text/humanhistory.html (accessed Jul 15, 2016).

(2) Ferguson, C. Historical Introduction to the Development of Material Science and Engineering as a Teaching Discipline.

(3) Robert Wilde. Coal in the Industrial Revolution http://europeanhistory.about.com/od/industryandagriculture/fl/Coal-in-the-Industrial-Revolution.htm.

(4) American Institute of Physics. The Discovery of Global Warming https://www.aip.org/history/climate/timeline.htm.

(5) The Editors of Encyclopædia Britannica. Industrial Revolution https://www.britannica.com/event/Industrial-Revolution.

(6) Gandini, A. The irruption of polymers from renewable resources on the scene of macromolecular science and technology. *Green Chem.* **2011**, *13* (5), 1061.

(7) Patel, M.; Marscheider-, F.; Schleich, J.; Hüsing, B. *Techno-economic Feasibility of Large-scale Production of Bio-based Polymers in Europe*; 2005.

(8) Clark, G.; Jacks, D. Coal and the industrial revolution, I700-I869. *European Review of Economic History*. 2007, pp 39–72.

(9) Eric McLamb. The Ecological Impact of the Industrial Revolution http://www.ecology.com/2011/09/18/ecological-impact-industrial-revolution/.

(10) Galor, O. The demographic transition: causes and consequences.

(11) George E. Totten. A timeline of highlights from the histories of ASTM COMMITTEE D02 and the petroleum industry. http://www.astm.org/COMMIT/D02/to1899_index.html (accessed Nov 3, 2016).

(12) Meghan E. Marrero and Stuart Thornton. Big Fish: A Brief History of Whaling http://nationalgeographic.org/news/big-fish-history-whaling/.

(13) Hejny, S.; Nielsen, J. Past , Present , & Future of Petroleum. **2003**.

(14) FitzPatrick, M.; Champagne, P.; Cunningham, M. F.; Whitney, R. A. A biorefinery processing perspective: Treatment of lignocellulosic materials for the production of value-added products. *Bioresour. Technol.* **2010**, *101* (23), 8915–8922.

(15) Alan J. Rocke. chemistry - Chemistry and society | Britannica.com https://www.britannica.com/science/chemistry/Chemistry-and-society.

(16) Dorel Feldman and Alla Barbalata. *Synthetic Polymers: Technology, Properties, Applications.*; Chapman & Hall: London, 2000.

(17) A partial list of products made from petroleum http://www.ranken-energy.com/products from petroleum.htm.

(18) Goldewijk, K. K. Three centuries of global population growth: A spatial referenced population (density) database for 1700-2000. *Popul. Environ.* **2005**, *26* (4), 343–367.

(19) Rosenberg, M. Current World Population and World Population Growth Since the Year One http://geography.about.com/od/obtainpopulationdata/a/worldpopulation.htm.

(20) Kremer, M. Population Growth and Technological Change: One Million B.C. to 1990. *Q. J. Econ.* **1993**, *108* (3), 681–716.

(21) Introduction, P. O. *Introduction to peak oil*; 2007.

(22) Bardi, U. Peak oil: The four stages of a new idea. *Energy* **2009**, *34* (3), 323–326.

(23) Hamilton, J. D. Historical Oil Shocks. **2011**.

(24) OPEC : Member Countries http://www.opec.org/opec_web/en/about_us/25.htm (accessed Nov 5, 2016).

(25) Regnier, E. Oil and energy price volatility. *Energy Econ.* **2007**, *29* (3), 405–427.

(26) Krausmann, F.; Gingrich, S.; Eisenmenger, N.; Erb, K. H.; Haberl, H.; Fischer-Kowalski, M. Growth in global materials use, GDP and population during the 20th century. *Ecol. Econ.* **2009**, *68* (10), 2696–2705.

(27) Lewis, S. L.; Maslin, M. A. Defining the Anthropocene. *Nature* **2015**, *519* (7542), 171–180.

(28) Steffen, W.; Broadgate, W.; Deutsch, L.; Gaffney, O.; Ludwig, C. The trajectory of the Anthropocene: The Great Acceleration. *Anthr. Rev.* **2015**, *2* (1), 81–98.

(29) The Anthropocene epoch: scientists declare dawn of human-influenced age | Science | The Guardian https://www.theguardian.com/environment/2016/aug/29/declare-anthropocene-epoch-experts-urge-geological-congress-human-impact-earth (accessed Nov 6, 2016).

(30) Anthropocene https://en.wikipedia.org/wiki/Anthropocene (accessed Nov 6, 2016).

(31) Steffen, W.; Crutzen, P. J.; McNeill, J. R. The Anthropocene: Are Humans Now Overwhelming the Great Forces of Nature. *AMBIO A J. Hum. Environ.* **2007**, *36* (8), 614–621.

(32) Climate Science and the Basis of the Convention http://unfccc.int/essential_background/the_science/items/6064.php (accessed Nov 6, 2016).

(33) Background on the UNFCCC: The international response to climate change http://unfccc.int/essential_background/items/6031.php (accessed Nov 6, 2016).

(34) Abbasi, T.; Abbasi, S. A. Biomass energy and the environmental impacts associated with its production and utilization. *Renew. Sustain. Energy Rev.* **2010**, *14* (3), 919–937.

(35) J. Jason West, Steven J. Smith, Raquel A. Silva, Vaishali Naik, Yuqiang Zhang, Zachariah Adelman, Meridith M. Fry, Susan Anenberg, L. W. H. & J.-F. L. Co-benefits of mitigating global greenhouse gas emissions for future air quality and human health.

(36) Meier, M. Sustainable polymers: reduced environmental impact, renewable raw materials and catalysis. *Green Chem.* **2014**, *16* (4), 1672.

(37) Andrady, A. L. Microplastics in the marine environment. *Mar. Pollut. Bull.* **2011**, *62* (8), 1596–1605.

(38) Cole, M.; Lindeque, P.; Halsband, C.; Galloway, T. S. Microplastics as contaminants in the marine environment: A review. *Mar. Pollut. Bull.* **2011**, *62* (12), 2588–2597.

(39) Lassen, Carsten; Hansen, Steffen Foss; Magnusson, Kerstin; Hartmann, N. B. . R. J.; Pernille; Nielsen, Torkel Gissel; Brinch, A. *Microplastics: Occurrence , effects and sources of releases in the environment in Denmark*; Copenaghen, 2015.

(40) Rafaj, P.; Amann, M.; Siri, J.; Wuester, H. Changes in European greenhouse gas and air pollutant emissions 1960–2010: decomposition of determining factors. *Clim. Change* **2014**, *124* (3), 477–504.

(41) John Twidell, T. W. *Renewable Energy Resources*, Third.; Routledge, 2015.

(42) Christensen, C. H.; Rass-Hansen, J.; Marsden, C. C.; Taarning, E.; Egeblad, K. The renewable chemicals industry. *ChemSusChem* **2008**, *1* (4), 283–289.

(43) Muradov, N. Z.; Veziroğlu, T. N. “Green” path from fossil-based to hydrogen economy: An overview of carbon-neutral technologies. *Int. J. Hydrogen Energy* **2008**, *33* (23), 6804–6839.

(44) van Vliet, O.; Brouwer, A. S.; Kuramochi, T.; van den Broek, M.; Faaij, A. Energy use, cost and CO2 emissions of electric cars. *J. Power Sources* **2011**, *196* (4), 2298–2310.

(45) Vandermeulen, V.; Van der Steen, M.; Stevens, C. V.; Van Huylenbroeck, G. Industry expectations regarding the transition toward a biobased economy. *Biofuels, Bioprod. Biorefining* **2012**, *6* (4), 453–464.

(46) Langeveld, J. W. A. *The Biobased Economy*; 2010.

(47) SASI group (Sheffield) and Mark Newman (Michigan). Density equalizing cartograms of petrol exports vs. forest areas. www.worldmapper.org (accessed Jun 15, 2016).

(48) Zhang, Y. H. P. Reviving the carbohydrate economy via multi-product lignocellulose biorefineries. *J. Ind. Microbiol. Biotechnol.* **2008**, *35* (5), 367–375.

(49) *BP Statistical Review of World Energy June 2015*.

(50) Weiss, M.; Haufe, J.; Carus, M.; Brandão, M.; Bringezu, S.; Hermann, B.; Patel, M. K. A Review of the Environmental Impacts of Biobased Materials. *J. Ind. Ecol.* **2012**, *16* (SUPPL.1).

(51) British Plastic Federation: Oil Consumption http://www.bpf.co.uk/Press/Oil_Consumption.aspx (accessed Nov 7, 2016).

(52) U.S. Energy Information Administration (EIA) http://www.eia.gov/tools/faqs/faq.cfm?id=34&t=6 (accessed Nov 7, 2016).

(53) Clark, J. H. Green chemistry for the second generation biorefinery—sustainable chemical manufacturing based on biomass. *J. Chem. Technol. Biotechnol.* **2007**, *82* (7), 603–609.

(54) Anastas, P.; Eghbali, N. Green Chemistry: Principles and Practice. *Chem. Soc. Rev.* **2010**, *39* (1), 301–312.

(55) 12 Principles of Green Chemistry - American Chemical Society https://www.acs.org/content/acs/en/greenchemistry/what-is-green-chemistry/principles/12-principles-of-green-chemistry.html (accessed Nov 8, 2016).

(56) Clark, J. H. Green chemistry : challenges and opportunities. **1999**, No. February, 1–8.

(57) Mohanty, A. K.; Misra, M.; Drzal, L. T. Sustainable Bio-Composites from Renewable Resources: Opportunities and Challenges in the Green Materials World. *J. Polym. Environ.* **2002**, *10* (1/2), 19–26.

(58) Murphy, C. J. Sustainability as an emerging design criterion in nanoparticle synthesis and applications. *J. Mater. Chem.* **2008**, *18* (19), 2173.

(59) Shane Ross. Important Events in Human History http://www2.esm.vt.edu/~sdross/text/humanhistory.html.

(60) Chris Woodford. Technology timeline http://www.explainthatstuff.com/timeline.html.

(61) Technology Timeline: 1752 - 1990 http://www.pbs.org/wgbh/amex/telephone/timeline/timeline_text.html (accessed Jul 26, 2016).

(62) by Chris Woodford. History of invention: A science and technology timeline http://www.explainthatstuff.com/timeline.html (accessed Nov 10, 2016).

(63) American Experience. Technology Timeline 1752-1990 http://www.pbs.org/wgbh/amex/telephone/timeline/timeline_text.html.

(64) John Pickrell. Timeline: Human Evolution https://www.newscientist.com/article/dn9989-timeline-human-evolution/ (accessed Nov 4, 2016).

(65) Technology Timeline http://www.datesandevents.org/events-timelines/12-technology-timeline.htm (accessed Nov 4, 2016).

(66) Ramani Narayan. A Case Study on commercializing Starch-based biodegradable plastics https://msu.edu/~narayan/commercializingstarchplastics.htm (accessed Nov 4, 2016).

(67) Ferguson, C. Historical Introduction to the Development of Material Science and Engineering as a Teaching Discipline.

(68) Sustainable Plastics | DuPont USA http://www.dupont.com/products-and-services/plastics-polymers-resins/bio-based-polymers/articles/renewable-biopolymers.html (accessed Nov 4, 2016).

(69) Seb Egerton-Read. A New Way To Make Plastic http://circulatenews.org/2015/09/a-new-way-to-make-plastic/ (accessed Nov 4, 2016).

(70) Toray Industries, I. Production of Fully Renewable, Biobased Polyethylene Terephthalate (PET) Polymer http://www.toray.com/news/rd/nr110627.html (accessed Nov 4, 2016).

(71) Gibney, E. The super materials that could trump graphene. *Nature* **2015**, *522* (7556), 274–276.

(72) Wood, J. The top ten advances in materials science. *Mater. Today* **2008**, *11* (1), 40–45.

(73) DuPont Tate & Lyle Bio Products. New Investment to Meet the Growing Demand for Biomaterials http://www.duponttateandlyle.com/news_050410 (accessed Nov 4, 2016).

(74) The bioplastic market http://www.bio-plastics.org/en/information--knowledge-a-market-know-how/basics/the-bioplastics-market-an-overview (accessed Nov 4, 2011).

(75) TECNARO GmbH - Arboform http://www.tecnaro.de/english/arboform.htm?section=arboform (accessed Nov 4, 2011).

(76) Dobrzański, L. A. Significance of materials science for the future development of societies. *J. Mater. Process. Technol.* **2006**, *175* (1–3), 133–148.

(77) Plan, L. L. Man and Materials through History. 9–12.

(78) Systems, E. Chapter 1 Introduction. 1–12.

(79) Ashby, M. Materials–a brief history. *Philos. Mag. Lett.* **2008**, *88* (9–10), 749–755.

(80) Northwest, P. Introduction to Materials Science and Technology What is Materials Science ? 1–15.

(81) Boerjan, W. Bioenergy and bioaromatics: lignin http://www.psb.ugent.be/bio-energy/313-lignin.

(82) Shahzadi, T.; Mehmood, S.; Irshad, M.; Anwar, Z.; Afroz, A.; Zeeshan, N.; Rashid, U.; Sughra, K. Advances in lignocellulosic biotechnology: A brief review on lignocellulosic biomass and cellulases. *Adv. Biosci. Biotechnol.* **2014**, *5* (3), 246–251.

(83) Angiosperms vs Gymnosperms - Difference and Comparison http://www.diffen.com/difference/Angiosperms_vs_Gymnosperms.

(84) Hardwood vs Softwood - Difference and Comparison http://www.diffen.com/difference/Hardwood_vs_Softwood.

(85) Herbaceous VS Woody Plants - PLANT KINGDOM http://sbi3uiplantkingdom.weebly.com/week-12/herbaceous-vs-woody-plants.

(86) Qiu, X.; Hu, S. "Smart" materials based on cellulose: A review of the preparations, properties, and applications. *Materials (Basel).* **2013**, *6* (3), 738–781.

(87) Klemm, D.; Kramer, F.; Moritz, S.; Lindstr??m, T.; Ankerfors, M.; Gray, D.; Dorris, A.; Habibi, Y.; Lucia, L. a; Rojas, O. J. Cellulose Nanocrystals : Chemistry , Self-Assembly , and Applications. *Angew. Chemie - Int. Ed.* **2009**, *50* (24), 5438–5466.

(88) Hallac, B. B.; Ragauskas, A. J. Analyzing cellulose degree of polymerization and its relevancy to cellulosic ethanol. *Biofuels, Bioprod. Biorefining* **2011**, *5* (2), 215–225.

(89) Mutwil, M.; Debolt, S.; Persson, S. Cellulose synthesis: a complex complex. *Curr. Opin. Plant Biol.* **2008**, *11* (3), 252–257.

(90) Rose, M.; Palkovits, R. Cellulose-Based Sustainable Polymers: State of the Art and Future Trends. *Macromol. Rapid Commun.* **2011**, *32* (17), 1299–1311.

(91) Siqueira, G.; Bras, J.; Dufresne, A. Cellulosic bionanocomposites: A review of preparation, properties and applications. *Polymers (Basel).* **2010**, *2* (4), 728–765.

(92) Moon, R. J.; Martini, A.; Nairn, J.; Simonsen, J.; Youngblood, J. *Cellulose nanomaterials review: structure, properties and nanocomposites*; 2011; Vol. 40.

(93) Kalia, S.; Dufresne, A.; Cherian, B. M.; Kaith, B. S.; Avérous, L.; Njuguna, J.; Nassiopoulos, E. Cellulose-based bio- and nanocomposites: A review. *Int. J. Polym. Sci.* **2011**, *2011*.

(94) Mamman, A. S.; Lee, J.-M.; Kim, Y.-C.; Hwang, I. T.; Park, N.-J.; Hwang, Y. K.; Chang, J.-S.; Hwang, J.-S. Furfural: Hemicellulose/xylosederived biochemical. *Biofuels, Bioprod. Biorefining* **2008**, *2* (5), 438–454.

(95) Gao, X.; Kumar, R.; Wyman, C. E. Fast hemicellulose quantification via a simple one-step acid hydrolysis. *Biotechnol. Bioeng.* **2014**, *111* (6), 1088–1096.

(96) Saha, B. C. Hemicellulose bioconversion. *J. Ind. Microbiol. Biotechnol.* **2003**, *30* (5), 279–291.

(97) Vanholme, R.; Demedts, B.; Morreel, K.; Ralph, J.; Boerjan, W. Lignin biosynthesis and structure. *Plant Physiol.* **2010**, *153* (3), 895–905.

(98) Whetten, R.; Sederoff, R. Lignin Biosynthesis. *Plant Cell* **1995**, *7* (7), 1001–1013.

(99) Ragauskas, A. J.; Beckham, G. T.; Biddy, M. J.; Chandra, R.; Chen, F.; Davis, M. F.; Davison, B. H.; Dixon, R. a; Gilna, P.; Keller, M.; et al. Lignin valorization: improving lignin processing in the biorefinery. *Science* **2014**, *344* (6185), 1246843.

(100) Sangha, A. K.; Parks, J. M.; Standaert, R. F.; Ziebell, A.; Davis, M. F.; Smith, J. C. Radical Coupling Reactions in Lignin Synthesis: A DFT study. *J. Phys. Chem. B* **2012**, 120404161010005.

(101) Boerjan, W.; Ralph, J.; Baucher, M. L IGNIN B IOSYNTHESIS. *Annu. Rev. Plant Biol.* **2003**, *54* (1), 519–546.

(102) Finefield, J. M.; Sherman, D. H.; Kreitman, M.; Williams, R. M. Enantiomeric natural products: occurrence and biogenesis. *Angew. Chem. Int. Ed. Engl.* **2012**, *51* (20), 4802–4836.

(103) Sangha, A. K.; Davison, B. H.; Standaert, R. F.; Davis, M. F.; Smith, J. C.; Parks, J. M. Chemical factors that control lignin polymerization ESI. *J. Phys. Chem. B* **2014**, *118* (1), 164–170.

(104) Akiyama, T.; Goto, H.; Nawawi, D. S.; Syafii, W.; Matsumoto, Y.; Meshitsuka, G. Erythro/threo ratio of β-O-4-structures as an important structural characteristic of lignin. Part 4: Variation in the erythro/threo ratio in softwood and hardwood lignins and its relation to syringyl/guaiacyl ratio. *Holzforschung* **2005**, *59* (3), 276–281.

(105) Lancefield, C. S.; Westwood, N. J. The synthesis and analysis of advanced lignin model polymers. *Green Chem.* **2015**, *17* (11), 4980–4990.

(106) Laurichesse, S.; Avérous, L. Chemical modification of lignins: Towards biobased polymers. *Prog. Polym. Sci.* **2014**, *39* (7), 1266–1290.

(107) Calvo-Flores, F. G.; Dobado, J. A. Lignin as renewable raw material. *ChemSusChem* **2010**, *3* (11), 1227–1235.

(108) Buranov, A. U.; Mazza, G. Lignin in straw of herbaceous crops. *Ind. Crops Prod.* **2008**, *28* (3), 237–259.

(109) Adler, E. Lignin chemistry-past, present and future. *Wood Sci. Technol.* **1977**, *11* (3), 169–218.

(110) Monteil-Rivera, F.; Phuong, M.; Ye, M.; Halasz, A.; Hawari, J. Isolation and characterization of herbaceous lignins for applications in biomaterials. *Ind. Crops Prod.* **2013**, *41*, 356–364.

(111) Ratnaweera, D. R.; Saha, D.; Pingali, S. V.; Labbé, N.; Naskar, A. K.; Dadmun, M. The impact of lignin source on its self-assembly in solution. *RSC Adv.* **2015**, *5* (82), 67258–67266.

(112) Ris, V. I. A. K.; Ia, Z. H. X.; Un, Y. U. S.; Alus, E. R. P. Abundance and Reactivity of Dibenzodioxocins in Softwood Lignin. **2002**, 658–666.

(113) Wang, D.; Class, W. C. *Basic Lignin Chemistry Lignin*.

(114) Mosier, N.; Wyman, C.; Dale, B.; Elander, R.; Lee, Y. Y.; Holtzapple, M.; Ladisch, M. Features of promising technologies for pretreatment of lignocellulosic biomass. *Bioresour. Technol.* **2005**, *96* (6), 673–686.

(115) Sun, Y.; Cheng, J. Hydrolysis of lignocellulosic materials for ethanol production : a review q. *Bioresour. Technol.* **2002**, *83* (1), 1–11.

(116) Vishtal, A. G.; Kraslawski, A. CHALLENGES IN INDUSTRIAL APPLICATIONS OF TECHNICAL LIGNINS. *BioResources* **2011**, *6* (3), 3547–3568.

(117) Zhao, X.; Zhang, L.; Liu, D. Biomass recalcitrance. Part I: the chemical compositions and physical structures affecting the enzymatic hydrolysis of lignocellulose. *Biofuels, Bioprod. Biorefining* **2012**, *6* (4), 465–482.

(118) Marques, G.; del Río, J. C.; Gutiérrez, A. Lipophilic extractives from several nonwoody lignocellulosic crops (flax, hemp, sisal, abaca) and their fate during alkaline pulping and TCF/ECF bleaching. *Bioresour. Technol.* **2010**, *101* (1), 260–267.

(119) Barana, D.; Salanti, A.; Orlandi, M.; Ali, D. S.; Zoia, L. Biorefinery process for the simultaneous recovery of lignin, hemicelluloses, cellulose nanocrystals and silica from rice husk and Arundo donax. *Ind. Crops Prod.* **2016**, *86*.

(120) Zakzeski, J.; Bruijnincx, P. C. A.; Jongerius, A. L.; Weckhuysen, B. M. The Catalytic Valorization of Ligning for the Production of Renewable Chemicals. *Chem. Rev.* **2010**, *110*, 3552–3599.

(121) Kim, J.-Y.; Hwang, H.; Oh, S.; Kim, Y.-S.; Kim, U.-J.; Choi, J. W. Investigation of structural modification and thermal characteristics of lignin after heat treatment. *Int. J. Biol. Macromol.* **2014**, *66*, 57–65.

(122) Biernat, K.; Grzelak, P. L. Biorefinery Systems as an Element of Sustainable Development. In *Biofuels - Status and Perspective*; InTech, 2015.

(123) Kamm, B.; Kamm, M. Principles of biorefineries. *Appl. Microbiol. Biotechnol.* **2004**, *64* (2), 137–145.

(124) Cherubini, F. The biorefinery concept: Using biomass instead of oil for producing energy and chemicals. *Energy Convers. Manag.* **2010**, *51* (7), 1412–1421.

(125) Bozell, J. J.; Petersen, G. R. Technology development for the production of biobased products from biorefinery carbohydrates—the US Department of Energy's "Top 10" revisited. *Green Chem.* **2010**, *12* (4), 539.

CAP 3 - Tyre technology

The first pneumatic tyre was patented in 1845 by Robert Thomson. Unfortunately, durability was a major issue and the market was still dominated by solid rubber tyres. The popularity of the air-filled tyres started to raise at the end of the 19th century, when another Scotsman, John Boyd Dunlop, patented a pneumatic tyre for the most popular vehicle of the time, the bicycle. Afterwards, with the introduction of tyres reinforced with rubberized fabric cords embedded in the structure known as bias-ply tyres, pneumatic tyres generated a larger interested and began to make their way into the market. The next evolution was the introduction of steel belted radial tyres in the 1948. In these tyres a steel fabric reinforces the rubber along with nylon, rayon, or polyester fibers. Michelin developed radial cords to outperform cross-ply tire designs with reduced tire temperature, lesser rolling resistance and greater longevity. At that time, Michelin in France, Bridgestone in Japan, Pirelli in Italy, and Continental in Germany became powerful radial tire manufacturers. In the U.S., the introduction of radial tyres was firstly delayed since they were more expensive. After several years radial tyres proved their superiority in durability and gas mileage and finally, in consequence of the growing demand, also the American manufacturer Goodyear introduced radial technology in its products.[1–3] In 1974 Pirelli invented the "wide radial tyre" with reduced height of the sidewalls, capable to withstand the growing power available on cars.[4] The following evolutions of radial technology represent the foundation of contemporary standard design for essentially all automotive tyres. Nowadays tyres are extensively used by an incredibly large number of vehicles: automobiles, trucks, buses, tractors, industrial vehicles, bicycles, motor bicycles, wheel chairs, airplanes, and more. In 2015 it was evaluated that more than three billion tyres were produced.[5] The market is expanding rapidly and by 2020 the global pneumatic tyre market is expected to generate a revenue of approximately $290 billion.[6] Independently from the diverse evolutions that the transportation sector will possibly embrace in the future; traditional fuels, biofuels, hydrogen, methane or electric engines, tyres are still going to be an essential component for the vast majority of the vehicles. Due to increasing automobile production, especially in the Asia-Pacific region, the augmented demand of tyres is pushing producers towards the development of more sustainable solutions, to cope with the extremely high demand of raw materials, the environmental impact of the manufacturing process, the release of environmentally persistent microparticles during the use of the tyres, and the issues related to the disposal of growing amounts of exhausted products. In fact, a gradual introduction of stricter laws, regarding the various environmental aspects on which companies may impact (atmospheric emissions, waste generation, impacts on soil, water use, etc.) is expected to occur.[7] In this

scenario, leading manufacturers are declaring their will to act. The mission is to reduce CO_2 emissions and value natural resources, to create balance between operations and the environment through technical innovation and business model innovation.[8]

Figure 23 - Tyre graveyard in Kuwait with more than 7 million tyres (reproduced from reference).[9]

3.1 Structure and components

Over the years, the structure of tyres greatly evolved resulting in the complex, highly engineered product that it is today. A radial tyre for passenger cars, for instance, is composed by several elements fused together. Many different rubber compounds are used to fulfil specific roles within the tyre. Their characteristics are finely tuned blending different rubbers with specific amounts and qualities of vulcanizing agents, fillers, protective substances, and processing aids. These rubbery parts are held together by a network of steel wires and synthetic fabrics that help to reinforce the structure and to improve the mechanical properties. The main components of a passenger car tyre are the thread, the sidewalls, and the beads. The tread is the part in contact with the ground and is responsible for good traction and low rolling resistance. For this reason, the rubber compounds in the treat may greatly differ from that in the sidewalls that should be stiffer. Sidewalls must support the thread and maintain the shape of the tyre under the effect of different forces. The beads are constituted by strong steel wirings covered by different types of rubber compounds and their role is to keep the tyre in position on the rim.[3] Specific layers are added to improve adhesion between different structural components such as rubber compounds and fabrics. Other elements can be inserted to confer

desired properties. For instance, to maintain the inner pressure over time a layer called inner liner with enhanced gas barrier effect is added. On modern tyres, additional elements are also introduced to produce self-sealing or self-supporting tyres. These two strategies are the most exploited for run-on-flat technologies.

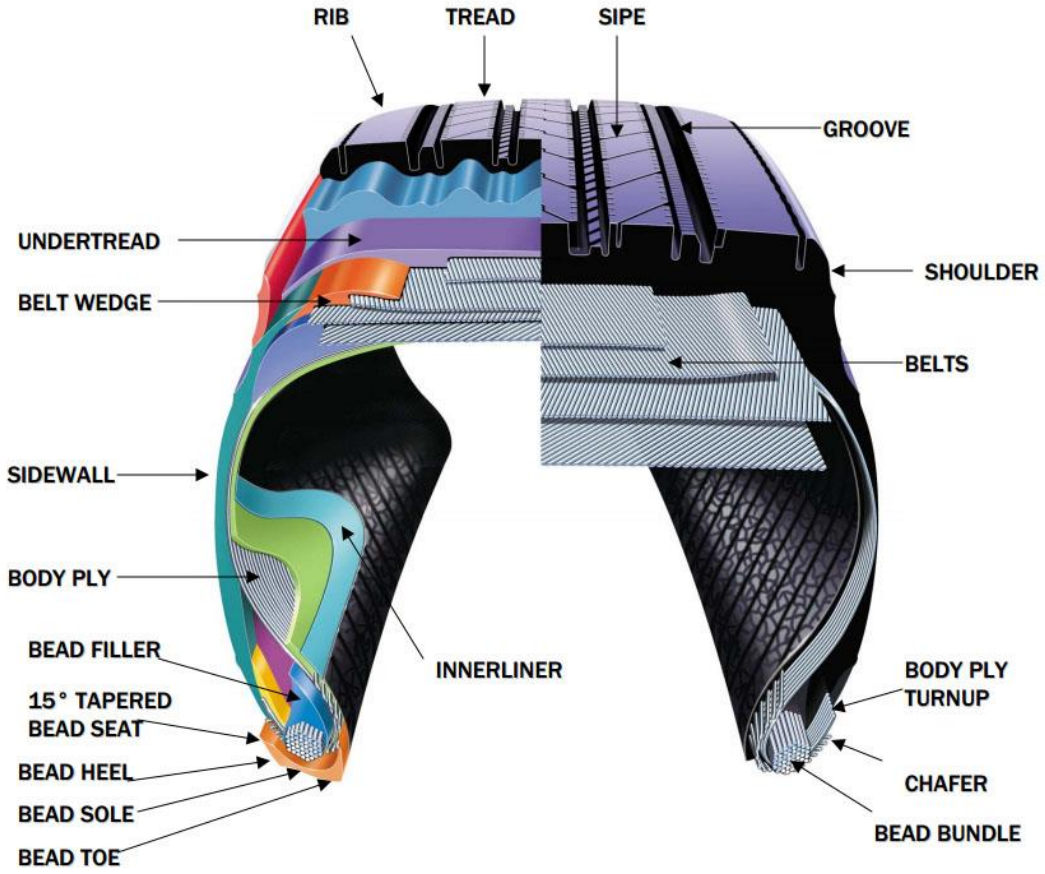

Figure 24 – Insight in the structure of a radial tyre (reproduced from reference).[10]

3.2 Materials

As highlighted in the previous section different components in the tyre must possess specific properties to exert their function. The compound in the thread is optimized to reduce rolling resistance and to resist abrasion while still providing excellent grip on different surfaces and in a wide range of temperatures. The blends in the sidewall must confer enhanced flex resistance and protection from the environmental stresses. Compounds in the inner liner shall minimize air loss, and so on. Thus, multiple rubber compounds with specific formulations are used to generate the required attributes for every component. Due to the demanding specifications that are often required, a broad assortment of raw materials is used to produce compounds with the desired properties and every company has its secret formulations. Over 200 raw materials can be used to make up the final composition of a tyre.[11] Nevertheless, it is possible to divide the ingredients in few main groups based on their function. The most abundant fraction comprises the polymers

that constitute the matrix of the compounds, many different kind of synthetic rubber and few different natural rubbers can be used. The vulcanizing agents are accountable for the crosslinking of the polymeric matrix and regulate the speed at which it occurs. The reinforcing fillers are largely employed to dramatically improve the mechanical properties of the final compounds. Resins can be used to promote adhesion between chords and rubber and to increase reinforcement. Furthermore, many different chemicals are used to confer enhanced stability (antioxidants, antiozonants etc.) and improved processability (plasticizers). An average composition of tyres used in different application areas is reported in table 4. It must be noted that the compositions are based on the data available in 2006. More recently there is a tendency of building tyres with higher loads of silica to reduce rolling resistance. Ultimately it is esteemed that more than 50% of the raw materials used to manufacture a tyre are from fossil origin,[12] and that on average approximately 26,5 litres of crude oil are used to make one item: 19 for raw materials and 7,5 for energy.[13]

Ingredients	Passenger tyres	Lorry tyres	OTR* tyres
Rubbers	47 %	45 %	47 %
Carbon black	21,5 %	22 %	22 %
Metal	16,5 %	25 %	12 %
Textiles	5,5 %	-	10 %
Zinc Oxide	1 %	2 %	2 %
Sulphur	1 %	1 %	1 %
Additives	7,5 %	5 %	6 %

**Off The Road*

Table 4 - Average composition of tires for different applications (data from 2006, reproduced from reference).[12]

Polymers

Elastomers are polymer that can regain their original shape after being deformed. Elastomers that are useful for practical applications typically are constituted by linear and flexible chains characterized by a high average molecular weight. Furthermore, to be useful for an application, the polymers must possess a glass transition temperature lower than the range of working temperatures. In fact, to have macroscopic rubber-like properties the molecules of the material must be able to move, reaching the conformation of maximum entropy. The second requirement to have an elastomeric material is the presence of links between the chains to avoid the slippage of the chains, introducing a sort of "memory" of the previous configuration in the material. The connections between the chains can be of physical or chemical nature. If the two conditions are met the material can show macroscopic elastomeric properties. At the molecular level when a tensional force is applied to the specimen the chains will be stretched and will align in the direction of the force and the system will lose entropy. Due to the presence of the links the chains cannot slide and cannot recover the configuration of higher entropy when the external force is kept. When the force is finally released the system spontaneously evolve towards the equilibrium (maximum entropy) that corresponds to the initial situation.[14]

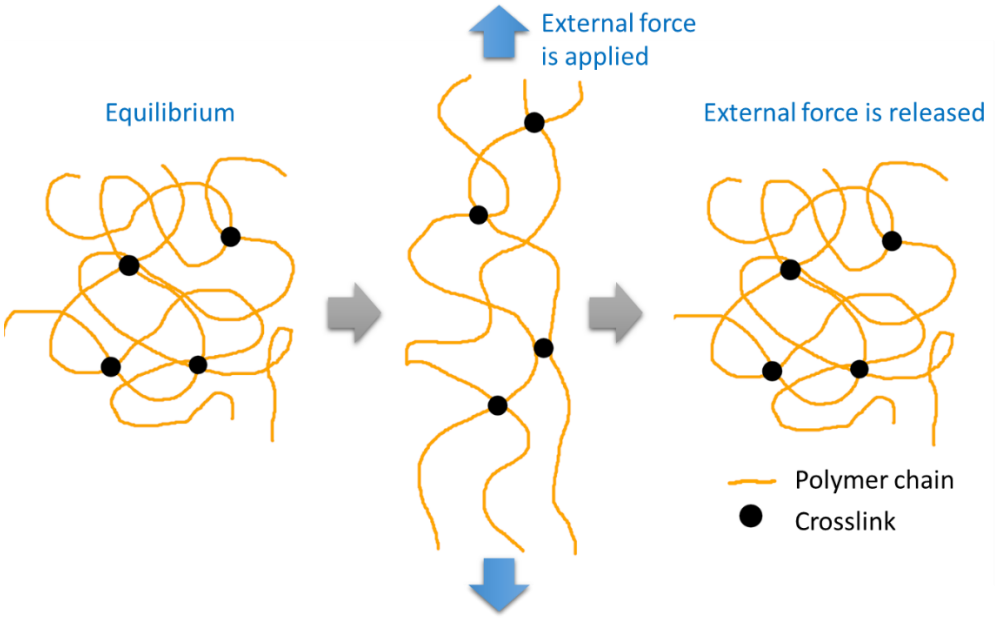

Figure 25 - Evolution of a crosslinked macromolecular (elastomeric) system when a tensile stress is applied.

The first known elastomeric material was natural rubber obtained from the latex extracted from the rubber tree (*Hevea brasiliensis*). The existence of natural rubber is known to Europeans since the end of the 18th century.[15] The use of natural rubber to produce commercial goods dates back to the 19th century, nevertheless the applicability was very limited until the discovery of vulcanization in 1839.[16] The development of synthetic counterparts of natural rubber started in Germany at the turn of the 20th century in association with the increased production of tyres for motor vehicles, while the mass production of pneumatic tyres and other goods from synthetic rubbers took off during the world wars, to overcome the deficiency of natural rubber supplies. Nowadays up to 30 different kinds of rubber are used in the formulations of elastomeric compounds for tyre manufacturing.[17] Roughly 60% of the rubber used in the tire industry is synthetic rubber, produced from petroleum-derived hydrocarbons, although natural rubber is still used and accounts for 40% of the total rubber consumption.[11]

Natural rubber

At the molecular level, natural rubber (NR) is constituted of linear polymeric chains mainly composed of cis-1,4-polyisoprene. On one end the chains end with the 1,1-dimethylallyl group followed by few isoprene repeating units in trans configuration (chains of *Hevea* rubber for instance have two trans units), the terminal group on the other side of the chain can be a primary alcohol or a fatty acid ester. Natural rubber possesses a high average molecular weight (Mn = 10^5-10^6 g/mol), the distribution is broad and bimodal, with a polydispersity index (Mw/Mn) that falls in the 2-10 range.[18] Glass transition (T_g) occurs at around 200 K.[19]

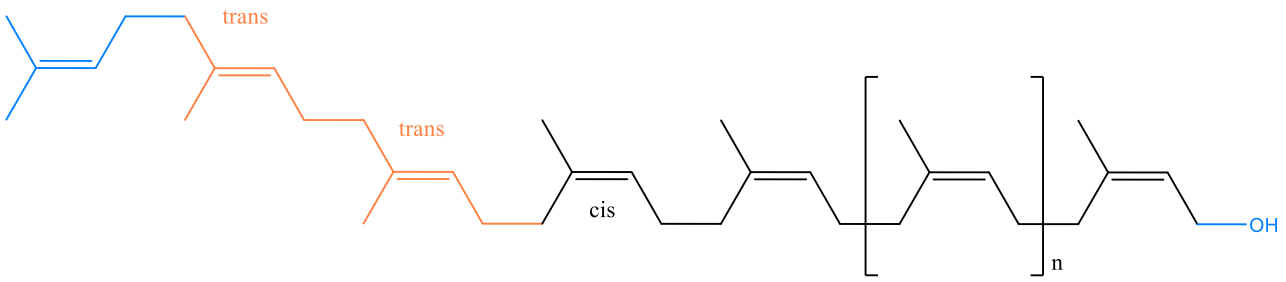

Figure 26 - Molecular structure of natural polyisoprene.

Natural rubber is found in form of a stable aqueous emulsion (latex) in many plants (up to 2500 species[18]). However, for commercial purposes, natural rubber is obtained almost exclusively from the rubber tree (*Hevea brasiliensis*), even though alternatives as Guayule (*P. argentatum*), Russian dandelion (*Taraxacum kok-saghyz*) and Canadian goldenrod (*S. canadensis*) are being explored in consequence to the general shift towards renewables and the expansion of the demand for rubber.[20] The natural rubber latex (NRL) is a colloidal system and is constituted by micrometric natural rubber particles dispersed in an aqueous medium. The spherical particles of natural rubber are stabilized by the presence of proteins, phospholipids and other lipidic substances that are adsorbed on the particles forming a thin ~10nm layer. The solid fraction of natural rubber latex usually accounts for 30-40% in weight. Up to 36% can be natural rubber, the remaining fraction consists of lipids (~3%) proteins (1-1,5%), sugars and soluble salts of calcium, magnesium, potassium, and copper. Freshly tapped NRL is neutral but it is not stable when exposed to air for long periods. In fact, proteins from latex particles have isoelectric points ranging from pH 4.0 to 4.6 and the exposition to air promotes acidification and the consequent coagulation of the rubber. Commercial NRL is stabilized by the addition of ammonia which hinders the proliferation of microorganisms and preserves an alkaline environment.[15,21–23] Natural rubber shows outstanding overall properties that cannot be matched by synthetic analogues. This is attributed to its characteristic microstructure: in fact, the biological control over the living polymerization leads to 100% cis conformation, high molecular weight, defined molecular weight distributions and to the presence of specific terminal chemical groups and proteins. Recent works also correlated the enhanced properties of natural rubber to the presence of divalent ions as Ca^{2+} that could promote ionic crosslinking between the chains by bridging two carboxylate groups.[24] Another phenomenon that contributes to the high performances of natural rubber is its capability to undergo strain induced crystallization (SIC). Under a uniaxial stress the chains of the natural polymer tent to align along the axis of the deformation forming nanometric crystalline domains that behave like fillers formed in-situ, creating additional physical crosslinking points, that reinforce the material.[25]

Synthetic rubbers

Over the 20th century many types of synthetic rubbers produced from fossil feedstocks have been developed. They were firstly designed as a replacement for natural rubber to answer to the increased request for elastomeric materials and to reduce costs. In second place the proliferation of elastomeric polymers also resulted in the expansion of the range of properties, leading to the development of rubbers for special applications. Tyres manufacturing is accountable for ~70% of world consumption of synthetic rubbers,[26] rubbers extensively used for tyre applications are styrene-butadiene (SBR) and butadiene rubber (BR). SBR is a copolymer of styrene and 1,3- butadiene, on industrial scale is synthetized with two methods: emulsion (E-SBR) and solution (S-SBR). In both products monomers are randomly arranged in the chain and there is a styrene unit every six or seven butadiene units, resulting in a butadiene to styrene proportions in weight of about 3:1. Regarding the microstructure, butadiene units can be found in the chain as cis, trans and vinylic, with the trans configuration occurring more frequently. SBR has more irregular chains than NR and the polymer is completely amorphous. When compared to NR, SBR vulcanizates have lower resilience, fatigue resistance and resistance to tearing and cut growth, however they possess enhanced resistance towards abrasion, thermal aging, and mechanical cleavage of the chains. Today commercial polybutadienes (BR) are made exclusively by solution polymerization processes employing organometallic catalysts capable of controlled microstructure, yielding high selectivity for cis (90-98%) and narrow molecular weight distributions. Polybutadiene is usually used in blends with natural rubber due to the useful balance of physical properties. [15,27–29]

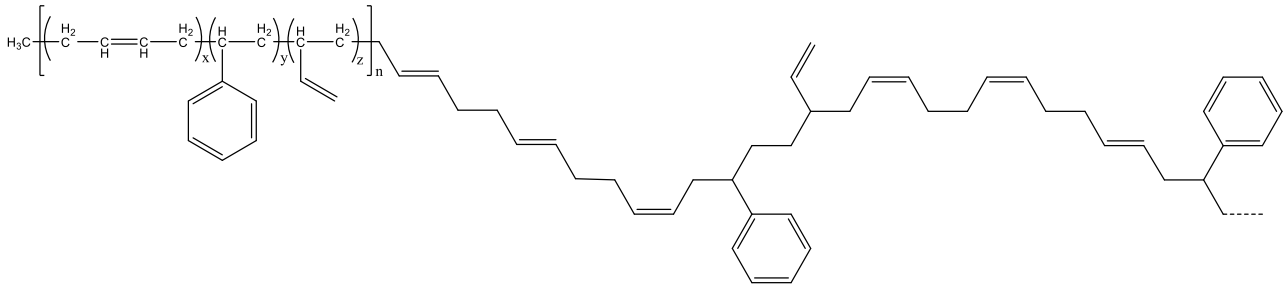

Figure 27 - Representation of the molecular structure of Styrene-Butadiene Rubber (SBR).

Vulcanization

Ingredients	PHR
Sulphur	0.5-4
Accelerator(s)	0.5-2
Zinc Oxide	2-10
Fatty acid	1-4

Table 5 – Common amounts of vulcanizers for accelerated Sulphur vulcanization (from reference).[29]

Vulcanization is the key process that unlocked the possibility to employ rubber in many useful applications. Without additional crosslinking, conventional rubbers don't possess very good mechanical properties and cannot be used for purposes where outstanding mechanical properties are required as for the manufacturing of tyres. After vulcanization, the elastomer's chains are chemically bound in a three-dimensional network. Thus, the plasticity of the material is reduced and the elasticity is enhanced. Other properties that play a crucial role on the performances, as tensile strength, dynamic modulus, hysteresis, and abrasion resistance are also dramatically improved. In addition, the dimensional stability of the rubber is also greatly enhanced by vulcanization and when the crosslinking is complete it is no longer possible to solubilize or reshape the rubber items. Industrially the crosslinking of rubbers is achieved using two types of vulcanizations: sulphur and peroxide based, with the first one being the most widely used. Sulphur vulcanization is a complex process that involves different reactive species and the crosslinking reaction consists in several subsequent steps. Even though a large amount of detailed insight has been brought to light, the exhaustive comprehension of the vulcanization process has not been accomplished yet. In **accelerated sulphur vulcanization**, beside soluble sulphur, at least one type of accelerator and one system activator generated by the interaction of zinc oxide and a fatty acid are always present. Additionally, the start of the crosslinking can also be controlled adding premature vulcanization inhibitors. Accelerators are organic compounds based on different general structures: they can be classified into benzothiazoles, benzothiazolesulfenamides, dithiocarbamantes and secondary amines. Accelerators interact with soluble sulphur to form Ac-S_x-Ac structures (Ac = structure derived from the accelerator) that can later interact with rubber yielding rubber-S_x-Ac that can further evolve in the final rubber-S_x-rubber crosslinks. Activators are inorganic species that can form adducts with accelerators and increase their efficiency. When accelerators are used during vulcanization, crosslinking efficiencies and crosslinking rates are improved. In presence of activators there is an increased rate in the formation of early rubber-S_x-Ac precursors, a decrease in the rate of formation of crosslinks and a higher number of crosslinks at the end of curing. In figure 28 there is a schematic representation of the fundamental steps that occur during sulphenamide-accelerated sulphur vulcanization in the presence of Zinc oxide as activator. The schematic representation also gives justification for the fact that when activators are employed the number of crosslinks is higher and the length of sulphur bridges is reduced. The final properties of the vulcanizates can be modulated changing the absolute and relative amounts of the vulcanizers. Increasing both sulphur and accelerator leads to a higher crosslinking density that is associated with stiffer compounds. The ratio between sulphur and accelerator, on the other hand, influences the average length of sulphur crosslinks, the number of rubber-S_x-Ac pendent groups, and the extent of intramolecular crosslinking. Conventional vulcanization systems use high level of sulphur and

low levels of accelerators, the result is that most of the crosslinks consists in polysulphidic chains. Efficient systems, on the contrary, are characterized by lower amounts of sulphur and greater amounts of accelerators and at optimum vulcanization time they produce mainly monosulsulphidic crosslinks and much less chain modification.[27,29–34]

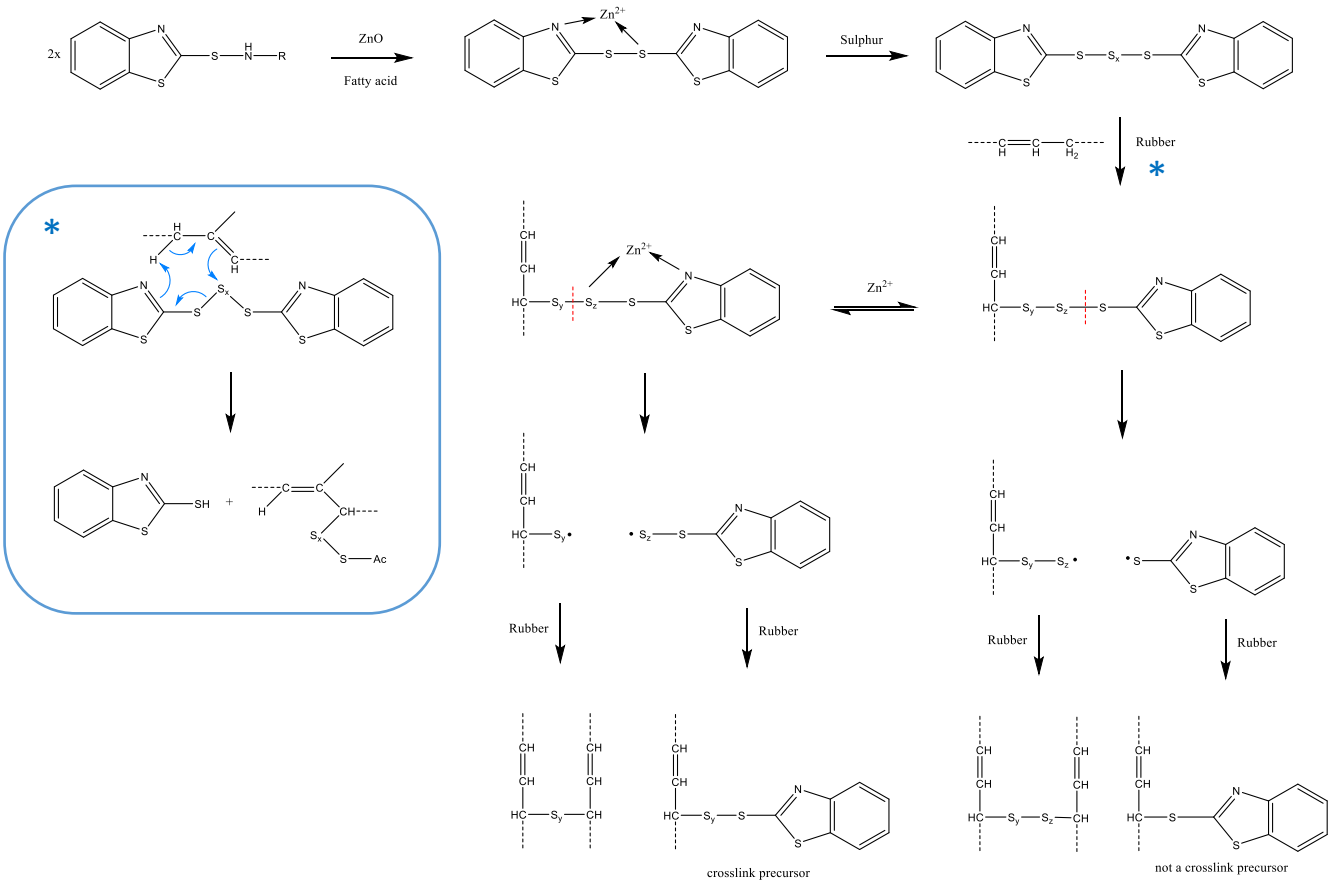

Figure 28 - Schematic pathway for Sulphur vulcanization with a generic benzothiazole accelerator and zinc oxide.

Peroxide-induced vulcanization begins with the decomposition of the peroxide to give free radicals. The free radicals can interact with the rubber chains following two mechanisms: abstraction of a hydrogen in allylic position or addition to a double bond. For isoprene rubber, the abstraction route predominates. The radical on the polymer chain can then couple with another radical or react with a double bond of a neighbouring chain. The result is always a crosslinking of the two chains by the formation of a new C-C bond. In the second case the radical survives and can still react forming additional crosslinks. A polymeric radical can also decompose to give a vinyl group and a new polymeric radical, resulting in a chain scission. The efficiency of the vulcanization depends on the ratio between the two reaction pathways and is affected by the polymer. In SBR for instance double bonds are less hindered than in NR and the coupling of two radicals occurs less often, hence efficiency of peroxide vulcanization is higher when SBR is used.[29,35]

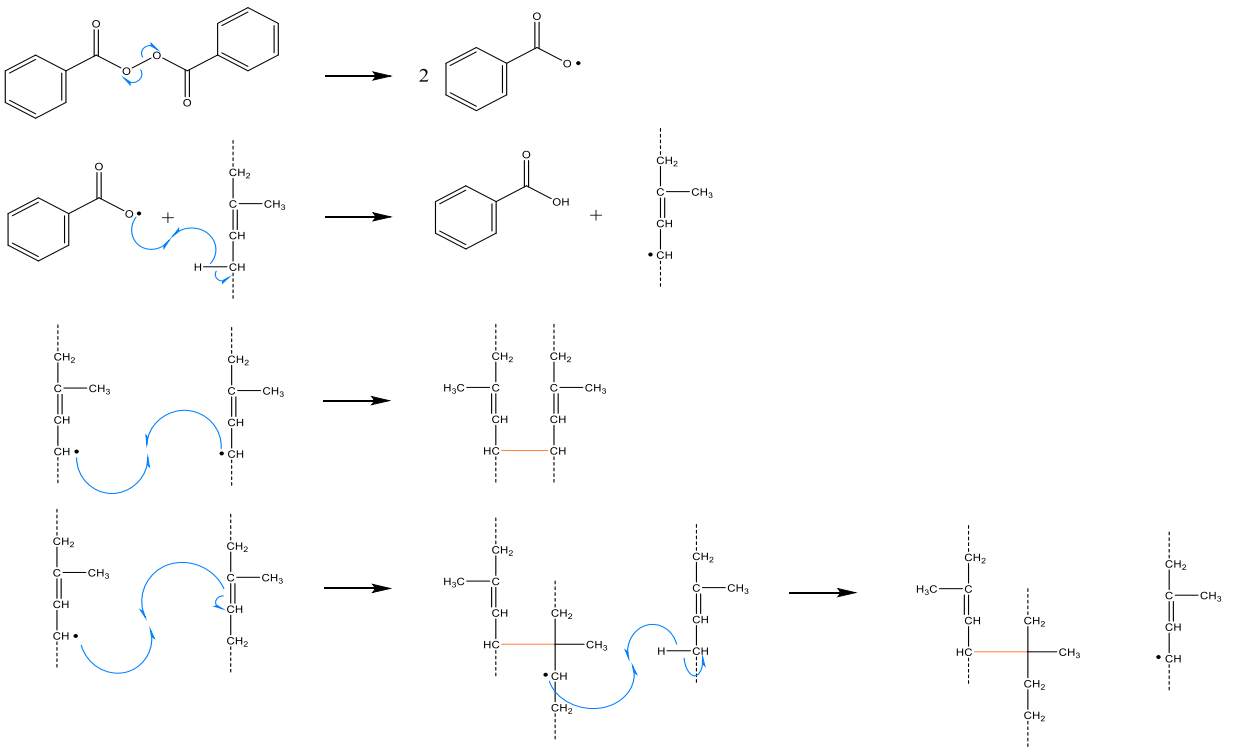

Figure 29 - Vulcanization mechanism of polyisoprene with dicumyl peroxide: an example of peroxide curing.

Fillers

Fillers are used in rubber compounding to reduce the cost or to improve the properties, the former are inert fillers and the latter reinforcing fillers. To enhance the properties of the elastomeric materials, at least one reinforcing filler is usually present in the compound. Reinforcing fillers are made of particles that present at least one dimension in the nanometric domain whether they are: nano-particles (3 dimensions in nano-scale), nanofibres (2 dimensions) and nano-plates (one dimension). The addiction of reinforcing fillers improves some intensive properties of the rubber compounds, such as: hardness, tensile strength, viscosity, compression set, abrasion resistance and elongation at break. This leads to the possibility to build tyres with superior mechanical performances. Furthermore, their use could also provide additional interesting features to the final product as lower rolling resistance, wear resistance, and heat buildup. The capability to protect the rubber from degrading agents like heat, light and chemicals is also an important characteristic. Some fillers can also improve the impermeability to gases promoting a barrier effect that results in augmented pressure retention in tyres. The reinforcing mechanism is complex with some differences from one filler to another. Nonetheless there are some main characteristic that are essential to achieve reinforcement. One very important feature is the particle size, this is probably the parameter that most influences reinforcement, for reinforcing fillers it can range from 10 nm up to 500 nm. The interactions between the filler and the polymer chains are also very important; the macromolecules can be adsorbed on the surface of the filler's

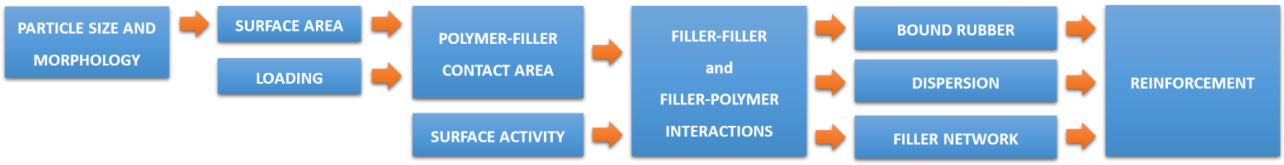

Figure 30 - Interconnections between fundamental properties of fillers and their reinforcing capability

particles by means of Van der Waals forces or can be grafted through chemical reactions with the functional groups present on the surface (chemisorption). A fraction of the matrix can also be mechanically locked on the filler's surface. Greater adhesion between rubber and filler particles leads to a higher reinforcement, and again particle size plays a key role since smaller particles and/or nanostructured particles result in higher surface areas and thus greater contact area and adhesion. There is an immobilized layer of rubber around filler's particles, the fraction of the polymer locked on the surface of the filler is called bound rubber, its amount depends from the surface activity and is related to the reinforcing capability. A portion of the polymeric matrix can also be completely interlocked in the voids between the filler particles. This fraction, called occluded rubber, is shielded from deformation, and increases the effective fraction of the filler. The final properties of the compound are also influenced by filler-filler interactions that can be dispersive, polar or hydrogen bonds. Above percolation threshold filler particles are all connected in a three-dimensional network. Several theories and models have been proposed to explain the complex behavior of filled elastomers: increase in viscosity (hydrodynamic theory), breakdown of the filler aggregate structure (Payne effect), presence of local strains higher than the applied (strain amplification), weak and strong linkages, slippage of the molecular chains under strain and redistribution of the stress (slippage at interface), connection of the filler's particles by common rubber polymer's chains and redistribution of the stress (Bueche model). However, it is not possible to fully explain the behavior of filled elastomers using a single model as reinforcement effect affects many different properties and depends from polymer properties, filler

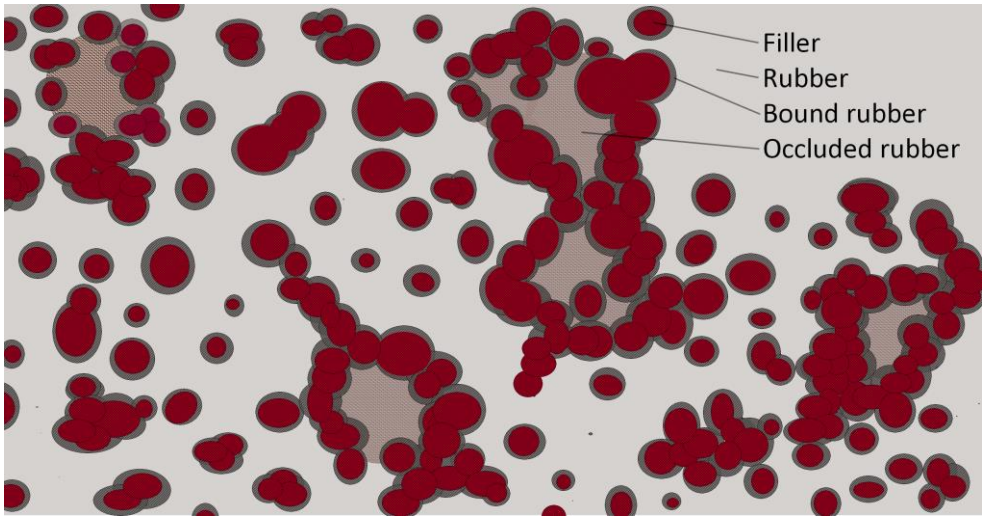

Figure 31 - Schematic representation of filler particles dispersed in an elastomeric matrix

properties and processing. The term reinforcement itself is not well defined but it usually refers to a noticeable increase in one or more properties of the elastomeric compounds, as tensile strength, tear resistance, abrasion resistance and modulus.[36–46]

Conventional reinforcing fillers that are currently extensively used in the manufacturing of tyres are carbon black and silica. Carbon black is the quintessential reinforcing filler, its history runs parallel to that of tyre technology and the use in rubber compounds has been widely investigated starting from 1960s. Carbon black is constituted of almost pure elemental carbon arranged in imperfect graphitic layers that are stacked to form spherical primary nanoparticles. The surface of the particles is rough and is decorated with several functional groups as phenols, carboxylic acids, ketones, quinones and lactones. A huge amount of carbon black is produced on yearly base (8 x 10^6 metric tons[47]) and the majority is used for tyre manufacturing. The industrial processes used to produce the filler used on a large scale are two: furnace black process and thermal black process. The most relevant is the furnace process, heavy aromatic oils in vapor phase are partially pyrolyzed under precisely controlled conditions to produce microscopic particles. The key characteristics of the particles as size, structure and surface activity can be modified altering the parameters of the process. The result is that countless grades of commercial carbon blacks are available. Different grades are commonly identified using ASTM nomenclature. The nomenclature format consists in a letter followed from 3 digits; the letters N or S stand for normal and slow curing respectively, the first digit is related to particle size as resumed in table 6, second and third digits are assigned by ASTM committee and higher numbers are usually assigned to blacks with high structure. For instance carbon black N375 has a surface area of roughly 90 m^2/g, an avarage diameter of primary particles in the range of 23-30 nm and high structure. Figure 32 displays the four principal archetypes of carbon blacks.[41,42,48–51]

ASTM 1st digit	Particle size (nm)	Surface area (m^2/g)
9	201-500	0-10
8	101-200	11-20
7	61-100	21-32
6	49-60	33-39
5	40-48	40-49
4	31-39	50-69
3	26-30	70-99
2	20-25	100-120
1	11-19	121-150
0	1-10	>150

Table 6 - ASTM nomenclature for carbon blacks

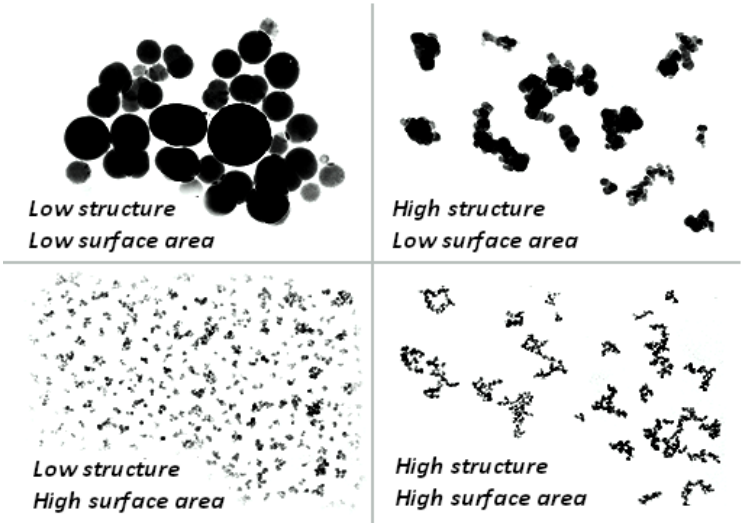

Figure 32 - Different types of carbon blacks (reproduced from reference[82]).

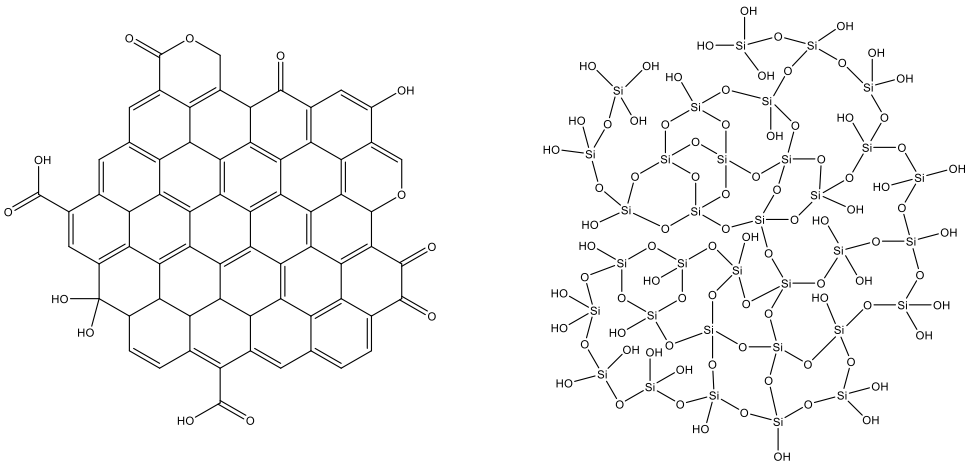

Figure 33 – Drafts depicting the chemical nature of carbon black and amorphous silica particles.

Silica started to be used as reinforcing filler alongside with carbon black in the 1990s. The main advantage brought by the inorganic filler is the possibility to build tyres with reduced rolling resistance (up to 20%), increasing the fuel efficiency of vehicles. The disadvantages are the higher cost and the low compatibility of silica particles with the elastomers. Precipitated silica is produced from the controlled neutralization of a diluted solution of sodium silicate, fumed or pyrogenic silica is prepared from flame pyrolysis. The resulting inorganic filler is composed of nanometric primary particles (few nanometers) that are fused together forming larger aggregates (100-500nm) characterized by a high structure. Aggregates can interact between themselves forming larger agglomerates (up to several microns). Silicas usually exhibit large surface areas (50-400 m^2/g). While carbon black has naturally a good affinity for rubber, the surface of silica particles is covered with polar hydroxyl groups (silanols), this leads to the instauration of strong filler-filler interactions and weak filler-polymer interactions. To achieve good dispersion, limit flocculation, and improve the adhesion to the polymeric matrix, silicas must be modified with specific coupling agents. The most used coupling agent is bis[3-(triethoxysilyl)propyl] tetrasulfide (TESPT). The organosilane is composed by a part that can react with the Si-OH groups on the surface of the filler and a part capable to improve compatibility with the hydrophobic backbones of the polymers and provide a strong adhesion through the formation of covalent bonds during vulcanization. [52–60]

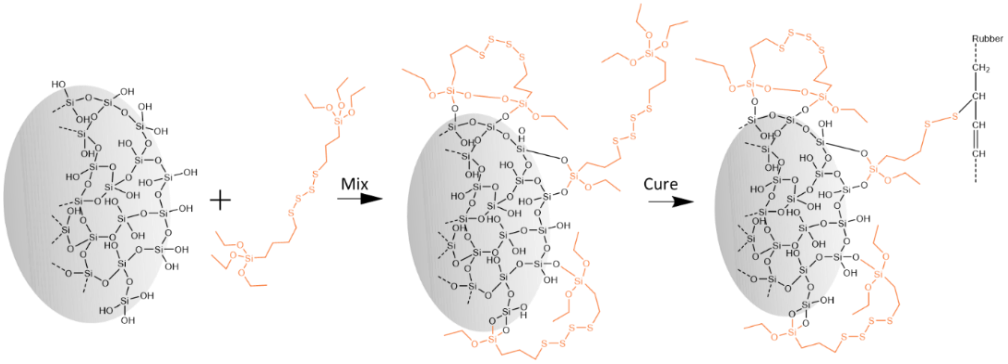

Figure 34 - Functionalization of the surface of silica particles with a organosilane coupling agent (TESPT).

Up to the present date a big effort has been made to develop new fillers that could match and even go beyond carbon black and silica, to develop new or significantly improved products. The focus is on new nanomaterials capable to further enhance mechanical properties and barrier effect. Compounds reinforced with Polyhedral Oligomeric Silsesquioxanes (POSS) and Silica/Allumina nano-oxides showed lower hysteresis at high temperatures favoring lower rolling resistance. High aspect-ratio nanofillers (ie: only one or two dimension at nanoscale) like Carbon Nano Fibers (CNF), Carbon Nano Tubes (CNT), Polymeric Nanofibers, Graphenes (delaminated Graphite), Clays and Zirconium Phosphates have a lower percolation threshold and can provide superior mechanical properties. [61,62]

While there has always been a great attention towards new fillers, with outstanding characteristics and their capability to improve the properties of the elastomeric materials, recently there is also a growing interest towards the development of fillers produced from renewable resources that could reduce the ecological footprint associated with tyre manufacturing. Besides being inherently more environmentally friendly than carbon black due to their carbon neutrality, fillers produced from biomasses may also possess other interesting characteristics. They are often largely available, low cost, safe to handle, biodegradable or easier to dispose, and have a reduced specific gravity. In recent years, there was an evident upsurge in the number of works connected to this topic. In the field of elastomeric materials, different renewable products were tested as potential fillers. Some examples are: cellulose, cellulose nanocrystals, starch nanocrystals, chitin nanowhiskers, bamboo fibers, rice husk fibers, rice husk ashes, lignin, biochars, pollens, and soy flour. [63–72]

Stabilizers

Organic polymers are susceptible to the phenomenon of aging. In fact, several external agents as oxygen, ozone, light, heat, mechanical stress, and the presence of metal ions can degrade the polymers compromising the properties of the products. Unsaturated elastomers are particularly susceptible to heat because the energy required to break π-bonds in the C=C linkages to form active radicals is relatively low. For this reason, the use of anti-degradants to protect rubbers against oxygen and ozone is fundamental, to maintain the initial properties and to prevent the embrittlement of the products. There are different types of inhibitors, they protect polymers from degradation through different mechanisms, the main categories are: *free radical chain stoppers, peroxide decomposers, light absorber, metal deactivators, and inhibitor regenerators*. Common primary antioxidants are secondary amine and hindered phenols. They exert the antioxidant activity mainly scavenging free radicals, halting the propagation steps in the oxidation mechanism. A schematic overview on the oxidation mechanism of the elastomeric hydrocarbons and the protective mechanism of common antioxidant is proposed in figure 35. Conventional antidegradants for rubbers such as 6PPD (N-(1,3-dimethylbutyl)-N'-phenyl-p-phenylenediamine) and TMQ (1,2-dihydro-2,2,4-trimethyl-quinoline) provide good protection against oxygen, ozone and fatigue. The main drawbacks are the limited duration over time

and toxicity. In fact, due to their low molecular weight, commercial antioxidants, can migrate through rubber compounds and possess significant volatility and leachability. Additionally, waxes (microcrystalline and paraffin) are introduced in the compounds as they form a physical barrier on the surface of the tyres against ozone. [29,73–77]

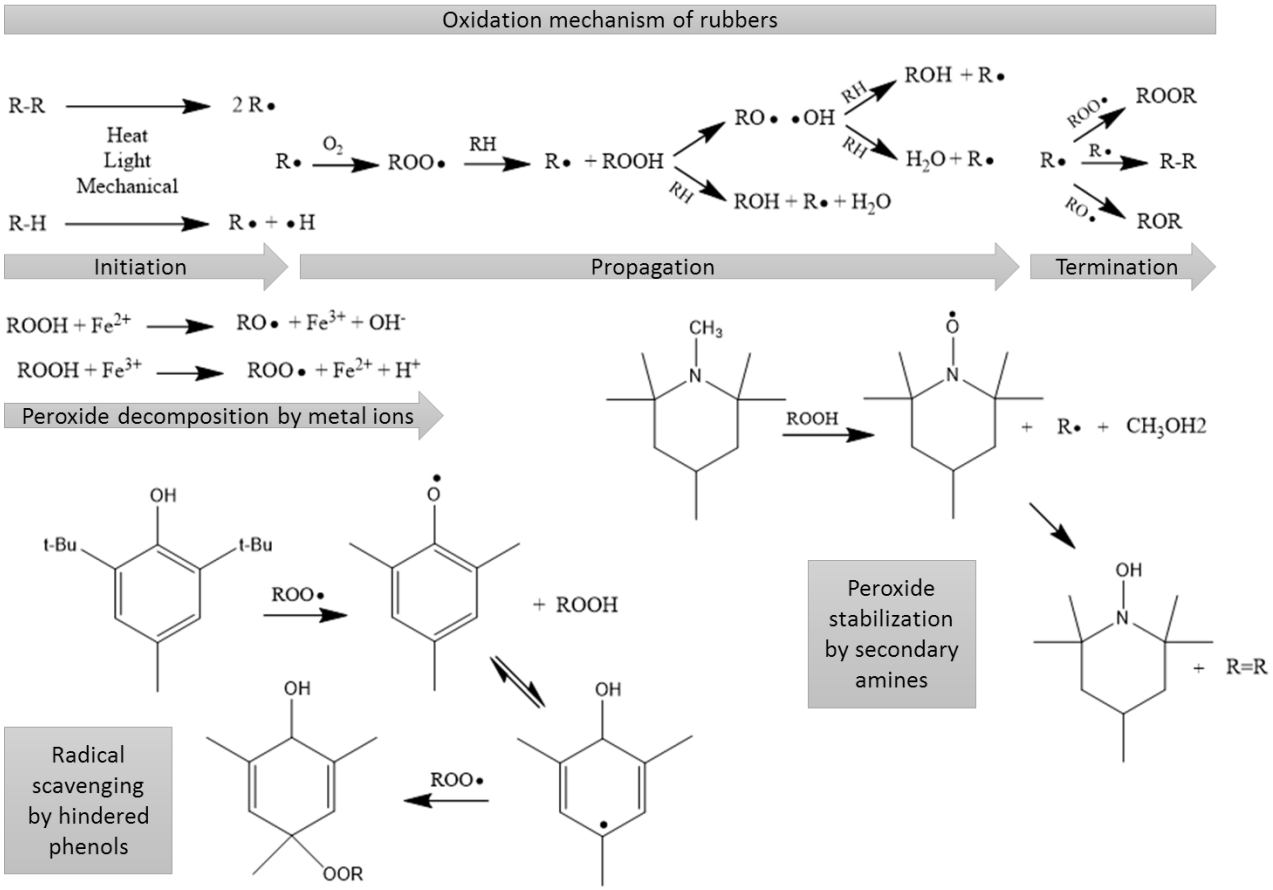

Figure 35 - Oxidation mechanism and protecting mechanism of common antioxidants (adapted from reference).[78]

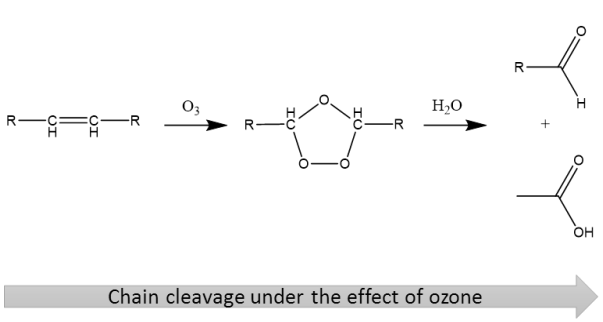

Figure 36 - Degradation mechanism in presence of ozone.

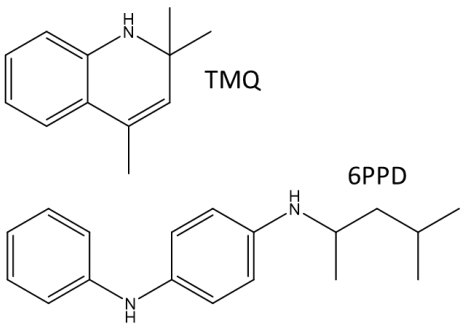

Figure 37 - Stabilizers used in tyre manufacturing.

Other components

Polymers, fillers, vulcanizers and stabilizers represent the fundamental components of the rubber blends used in the tyre manufacturing. In industrial production, many other minor components are added to the blends to achieve the required specifications. Processing oils and plasticizers are added to improve the flexibility and hence the processability of the rubber compounds. Aromatic oils have been used in tyre industries over many years but concerns related to the toxicity of polycyclic aromatic hydrocarbons (PAHs) and consecutive legislative constrains promoted the employment of natural vegetable oils as eco-friendly substitutes. Resins (petroleum, phenolic, etc.) are also added to improve processability, reinforcement or the tackiness between the other components. [29,79–81]

References

(1) Modern Tire Technology Basics | Digital Trends http://www.digitaltrends.com/cars/modern-tire-technology-basics/.

(2) John Thomson. WHAT WE SHOULD KNOW ABOUT TIRES: A Historical Background http://www.jags.org/TechInfo/2001/05May01/tires/historyoftires.htm.

(3) Robert C. Miller. How tire is made - material, history, used, processing, parts, components, composition, steps, product http://www.madehow.com/Volume-1/Tire.html.

(4) Pirelli http://www.companieshistory.com/pirelli/.

(5) Rubber World Magazine. *Global Demand For Tires To Reach 3.3 Billion Units In 2015*.

(6) Allied Market Research. *World Pneumatic Tire- Market Opportunities and Forecasts, 2014-2020*; 2015.

(7) *Pirelli 2015 annual report*.

(8) *Bridgestone Group Environmental Report 2015*.

(9) Being a Garbage Collector is The Best Job Ever – Medium https://medium.com/@emmabarkerjones/being-a-garbage-collector-is-the-best-job-ever-cc65ec4aa42d#.3xtvxg7lt.

(10) Tire Safety, Labelling, Buying, Manufacture & Ratings Database http://www.utires.com/blog/tire-safety-plus-database/.

(11) An unknow object: the tire - Materials | Michelin The tire digest http://thetiredigest.michelin.com/an-unknown-object-the-tire-materials.

(12) Evans, R. The Composition of a Tyre: Typical Components Creating markets for recycled resources. **2006**.

(13) Rubber Faqs | Rubber Manufacturers Association https://rma.org/about-rma/rubber-faqs.

(14) M. Guaita, F. Ciardelli, La Mantia, E. P. *Fondamenti di scienza dei polimeri*, Edizioni N.; 2006.

(15) Niyogi, U. K. Natural and Synthetic Rubber. *Introd. to Fibre Sci. Rubber Technol.* **2007**.

(16) Treloar, L. R. G. The Elasticity and Related Properties of Rubbers. *Rubber Chem. Technol.* **1974**, *47* (7), 625–696.

(17) How Tyres are made https://www.goodyear.eu/en_gb/consumer/learn/how-tires-are-made.html.

(18) Puskas, J. E.; Gautriaud, E.; Deffieux, A.; Kennedy, J. P. Natural rubber biosynthesis—A living carbocationic polymerization? *Prog. Polym. Sci.* **2006**, *31* (6), 533–548.

(19) Glass, T. H. E. The glass transition temperature of natural rubber. **1985**, 929–941.

(20) van Beilen, J. B.; Poirier, Y. Establishment of new crops for the production of natural rubber. *Trends Biotechnol.* **2007**, *25* (11), 522–529.

(21) Ho, C. C.; Kondo, T.; Muramatsu, N.; Ohshima, H. Surface Structure of Natural Rubber Latex Particles from Electrophoretic Mobility Data. *J. Colloid Interface Sci.* **1996**, *178* (2), 442.

(22) Sansatsadeekul, J.; Sakdapipanich, J. Origin of colloidal behavior of natural rubber particle. ? 14–16.

(23) Sansatsadeekul, J.; Sakdapipanich, J.; Rojruthai, P. Characterization of associated proteins and phospholipids in natural rubber latex. *J. Biosci. Bioeng.* **2011**, *111* (6), 628–634.

(24) Rippel, M. M.; Galembeck, F. Nanostructures and adhesion in natural rubber: new era for a classic. *J. Braz. Chem. Soc.* **2009**, *20* (6), 1024–1030.

(25) Zhang, H.; Scholz, A. K.; Merckel, Y.; Brieu, M.; Berghezan, D.; Kramer, E. J.; Creton, C. Strain induced nanocavitation and crystallization in natural rubber probed by real time small and wide angle X-ray scattering. *J. Polym. Sci. Part B Polym. Phys.* **2013**, *51* (15), 1125–1138.

(26) Vehicle and tyre http://www.therubbereconomist.com/The_Rubber_Economist/Vehicle_and_tyre.html.

(27) Introduction, O.; Rubber, E. P.; Rubber, N.; Rubber, B.; Nitrile, H.; Rubber, B. Rubber technology. 1–20.

(28) Morton, M. *Rubber Technology*; 2010.

(29) Tobergte, D. R.; Curtis, S. *Science and Technology of RUBBER (3rd edition)*; James E., M., Burak, E., Frederick R., E., Eds.;

Elsevier, 2013; Vol. 53.

(30) Of, C. Sulfur Vulcanization of Natural Rubber for Benzothiazole Accelerated Formulations : 592–693.

(31) Kumar, C. S. S. R.; Nijasure, A. M. Vulcanization of rubber. *Resonance* **1997**, *2* (4), 55–59.

(32) Coran, A. Y. Chemistry of the vulcanization and protection of elastomers: A review of the achievements. *J. Appl. Polym. Sci.* **2003**, *87* (1 SPEC.), 24–30.

(33) González, L.; Rodríguez, A.; Valentin, J. L.; Marcos-Fernández, A.; Posadas, P. Conventional and efficient crosslinking of natural rubber effect of heterogeneities on the physical properties. *KGK Kautschuk Gummi Kunststoffe* **2005**, *58* (12), 638–643.

(34) Heideman, G.; Datta, R. N.; Noordermeer, J. W. M.; Baarle, B. van. Influence of zinc oxide during different stages of sulfur vulcanization. Elucidated by model compound studies. *J. Appl. Polym. Sci.* **2005**, *95* (6), 1388–1404.

(35) PEROXIDE VULCANIZATION | RUBBER COMPOUNDING BASICS https://rubbertech.wordpress.com/2013/07/26/peroxide-vulcanisation/.

(36) Scotti, R.; Wahba, L.; Crippa, M.; D'Arienzo, M.; Donetti, R.; Santo, N.; Morazzoni, F. Rubber–silica nanocomposites obtained by in situ sol–gel method: particle shape influence on the filler–filler and filler–rubber interactions. *Soft Matter* **2012**, *8*, 2131.

(37) Wang, M.-J. Effect of Polymer-Filler and Filler-Filler Interactions on Dynamic Properties of Filled Vulcanizates. *Rubber Chem. Technol.* **1998**, *71* (3), 520–589.

(38) Edwards, D. C. Polymer-filler interactions in rubber reinforcement. *J. Mater. Sci.* **1990**, *25* (10), 4175–4185.

(39) Wang, M. the Role of Filler Networking in. **1998**, 430–448.

(40) Guth, E. Theory of filler reinforcement. *Journal of Applied Physics*. 1945, pp 20–25.

(41) Fröhlich, J.; Niedermeier, W.; Luginsland, H. D. The effect of filler-filler and filler-elastomer interaction on rubber reinforcement. *Compos. Part A Appl. Sci. Manuf.* **2005**, *36* (4), 449–460.

(42) Leblanc, J. L. Rubber-filler interactions and rheological properties in filled compounds. *Prog. Polym. Sci.* **2002**, *27* (4), 627–687.

(43) Niedermeier, W.; Fro, J. Reinforcement Mechanism in the Rubber Matrix by Active Fillers. **2002**, No. 7.

(44) Effect of Filler Concentration on the Physico- Mechanical. **2011**, No. JANUARY.

(45) Zhang, Y.; Ge, S.; Tang, B.; Koga, T.; Rafailovich, M. H.; Sokolov, J. C.; Peiffer, D. G.; Li, Z.; Dias, A. J.; McElrath, K. O.; et al. Effect of carbon black and silica fillers in elastomer blends. *Macromolecules* **2001**, *34* (20), 7056–7065.

(46) Wolff, S.; Wang, M.-J.; Omnès, B.; Thuillier, S.; Pilvin, P.; Grohens, Y.; Gillet, S. Carbon Black Filler Reinforcement of Elastomers. *Carbon Black Sci. Technol.* **2008**, *39* (October), 460.

(47) General Information, What is Carbon Black? - International Carbon Black Association - ICBA http://www.carbon-black.org/index.php/what-is-carbon-black.

(48) Li, Z. H.; Zhang, J.; Chen, S. J. Effects of carbon blacks with various structures on vulcanization and reinforcement of filled ethylene-propylene-diene rubber. *Express Polym. Lett.* **2008**, *2* (10), 695–704.

(49) Crump, E. L. Economic Impact Analysis For the Proposed Carbon Black Manufacturing NESHAP. **2000**, No. May, 1–14.

(50) Wolff, S. Chemical Aspects of Rubber Reinforcement by Fillers. *Rubber Chemistry and Technology*. 1996, pp 325–346.

(51) Manager, D. T. N. RUBBER GRADE CARBON BLACKS http://www.continentalcarbon.com/pdfs/What_Is_Carbon_Black.pdf (accessed Dec 8, 2016).

(52) Dierkes, W. K. *Economic mixing of silica-rubber compounds*; 2005.

(53) Cassagnau, P. Melt rheology of organoclay and fumed silica nanocomposites. *Polymer (Guildf).* **2008**, *49* (9), 2183–2196.

(54) Park, S. J.; Cho, K. S. Filler-elastomer interactions: Influence of silane coupling agent on crosslink density and thermal stability of silica/rubber composites. *J. Colloid Interface Sci.* **2003**, *267* (1), 86–91.

(55) Brinke, JW. *Silica Reinforced Tyre Rubbers*; 2002.

(56) Mihara, S, Datta, RN, Noordermeer, JWM. Flocculation in Silica Reinforced Rubber Compounds. *Rubber Chem. Technol.*

2009, *82* (5), 524–540.

(57) Robertson, C. G.; Lin, C. J.; Bogoslovov, R. B.; Rackaitis, M.; Sadhukhan, P.; Quinn, J. D.; Roland, C. M. Flocculation, Reinforcement, and Glass Transition Effects in Silica-Filled Styrene-Butadiene Rubber. *Rubber Chem. Technol.* **2011**, *84* (4), 507–519.

(58) Cichomski, E.; Blume, A.; Dierkes, W. K.; Noordermeer, J. W. M.; Tolpekina, T. V.; Schultz, S. Influence of silica-polymer bond microstructure on tire-performance indicators. *KGK Kautschuk Gummi Kunststoffe* **2015**, *68* (4), 38–45.

(59) Vilmin, F.; Bottero, I.; Travert, A.; Malicki, N.; Gaboriaud, F.; Trivella, A.; Thibault-Starzyk, F. Reactivity of bis[3-(triethoxysilyl)propyl] tetrasulfide (TESPT) silane coupling agent over hydrated silica: Operando IR spectroscopy and chemometrics study. *J. Phys. Chem. C* **2014**, *118* (8), 4056–4071.

(60) Cichomski, E. *Silica-Silane Reinforced Passenger Car Tire Treads*; 2015.

(61) Stöckelhuber, K. W.; Das, A.; Jurk, R.; Heinrich, G. Contribution of physico-chemical properties of interfaces on dispersibility, adhesion and flocculation of filler particles in rubber. *Polymer (Guildf).* **2010**, *51* (9), 1954–1963.

(62) Zhang, P.; Morris, M.; Doshi, D. Materials Development for Lowering Rolling Resistance of Tires. *Rubber Chem. Technol.* **2016**, *89* (1), 79–116.

(63) Martins, A. F.; Visconte, L. L. Y.; Nunes, R. C. R. Evaluation of natural rubber and cellulose II compositions by curing and mechanical properties. *KGK-Kautschuk und Gummi Kunststoffe* **2002**, *55* (12), 637–641.

(64) Siqueira, G.; Tapin-Lingua, S.; Bras, J.; da Silva Perez, D.; Dufresne, A. Mechanical properties of natural rubber nanocomposites reinforced with cellulosic nanoparticles obtained from combined mechanical shearing, and enzymatic and acid hydrolysis of sisal fibers. *Cellulose* **2011**, *18* (1), 57–65.

(65) Molina-boisseau, S.; Dufresne, A. Mechanical Properties of Waxy Maize Starch Nanocrystal Reinforced Natural Rubber. **2005**, 9161–9170.

(66) Gopalan Nair, K.; Dufresne, A. Crab shell chitin whisker reinforced natural rubber nanocomposites. 1. Processing and swelling behavior. *Biomacromolecules* **2003**, *4* (3), 657–665.

(67) Sengupta, R.; Chakraborty, S.; Bandyopadhyay, S.; Dasgupta, S.; Mukhopadhyay, R.; Auddy, K.; Deuri, a S.; Siqueira, G.; Abdillahi, H.; Bras, J.; et al. Modified and unmodified multiwalled carbon nanotubes in high performance solution-styrene-butadiene and butadiene rubber blends. *Compos. Sci. Technol.* **2008**, *47* (2), 21–25.

(68) Gopalan Nair, K.; Dufresne, A.; Andrews, E. H.; Ismail, H.; Nordin, R.; Noor, A. M.; Molina-boisseau, S.; Dufresne, A.; Ramorino, G.; Bignotti, F.; et al. Application of sulphur-free lignins as a filler for elastomers: Effect of hexamethylenetetramine treatment. *Adv. Mater. Res.* **2006**, *410* (2), 90–93.

(69) Jiang, C.; He, H.; Jiang, H.; Ma, L.; Jia, D. M. Nano-lignin filled natural rubber composites: Preparation and characterization. *Express Polym. Lett.* **2013**, *7* (5), 480–493.

(70) Peterson, S. C. Evaluating corn starch and corn stover biochar as renewable filler in carboxylated styrene– butadiene rubber composites. *J. Elastomers Plast. 44* (1), 43–54.

(71) Fadiran, O. O.; Meredith, J. C. Surface treated pollen performance as a renewable reinforcing filler for poly(vinyl acetate). *J. Mater. Chem. A* **2014**, *2* (40), 17031–17040.

(72) Thakur, V. K.; Grewell, D.; Thunga, M.; Kessler, M. R. Novel Composites from Eco-Friendly Soy Flour/SBS Triblock Copolymer. *Macromol. Mater. Eng.* **2014**, *299* (8), 953–958.

(73) Nicolaas Maria Huntink. *Durability of rubber products*; Twente University Press, 2003.

(74) Nocil Limited. *Antioxidants & Antidegradants*.

(75) Narathichat, M.; Sahakaro, K.; Nakason, C. Assessment degradation of natural rubber by moving die processability test and FTIR spectroscopy. *J. Appl. Polym. Sci.* **2010**, *115* (3), 1702–1709.

(76) Wik, A.; Dave, G. Environmental labeling of car tires—toxicity to Daphnia magna can be used as a screening method. *Chemosphere* **2005**, *58* (5), 645–651.

(77) Wik, A. Toxic components leaching from tire rubber. *Bull. Environ. Contam. Toxicol.* **2007**, *79* (1), 114–119.

(78) Huntink, N. M.; Datta, R. N. Durability of rubber products. *KGK Kautschuk, Gummi, Kunststoffe* **2003**, *56* (6).

(79) Dasgupta, S.; Agrawal, S. L.; Bandyopadhyay, S.; Mukhopadhyay, R.; Malkani, R. K.; Ameta, S. C. Eco-friendly processing oils: A new tool to achieve the improved mileage in tyre tread. *Polym. Test.* **2009**, *28* (3), 251–263.

(80) Dasgupta, S.; Agrawal, S. L.; Bandyopadhyay, S.; Chakraborty, S.; Mukhopadhyay, R.; Malkani, R. K.; Ameta, S. C. Characterization of eco-friendly processing aids for rubber compound. *Polym. Test.* **2007**, *26* (4), 489–500.

(81) Achary, P. S.; Ramaswamy, R. Reactive compatibilization of a nitrile rubber/phenolic resin blend: Effect on adhesive and composite properties. *J. Appl. Polym. Sci.* **1998**, *69* (6), 1187–1201.

(82) Dispersion | Cabot Corporation http://www.cabotcorp.com/solutions/applications/industrial-rubber-products/dispersion.

CHAPTER 4 - Materials preparations and characterizations

The characterization techniques and the experimental procedures that played more than a marginal role in this work are fully described in this chapter. The analytic techniques are listed first, followed by a section dedicated to solubility modelling. The last two sections are dedicated to the preparation of rubber composites and their characterizations, respectively. In the following chapters, only a short description will be proposed in the experimental, while the details are only reported in this chapter to avoid redundancy.

4.1 Analytical techniques

In this section the main analytical techniques used during the experimental work are briefly introduced and are followed by the detailed operational procedures and the technical specifications of the equipment.

^{31}P-NMR spectroscopy

This powerful quantitative technique was employed for the structural characterization of lignin. Lignin is analysable with ^{31}P-NMR only after chemical reaction with a phosphitylating agent, as illustrated in figure 38. After modification, through ^{31}P-NMR it is possible to recognize the different hydroxyl groups that are present in the structure of lignins (aliphatic, carboxyl and phenolic),[1] to discriminate between the units derived from the three monolignols: p-hydroxyl (H), guaiacyl (G), and syringyl (S), and also to recognize units with carbon substituents at the C5 position.[2] The quantification is made integrating the peaks in the characteristic regions of the spectra as summarized in table 7. However, due to signal overlapping it might not be possible to discriminate between syringyl phenolics and C5 substituted guaiacyl phenolics. Another factor that must be taken into consideration is that the phosphitylation does not selectively occur on lignin and the hydroxyl groups of residual carbohydrates or other impurities are quantified as well.

Sample preparation

Accurately weighed lignin samples (30 mg) were dissolved in a pyridine-deuterated chloroform solution (1.6:1 v/v mL, 800 L) containing 1 mg/mL of chromium-(III) acetylacetonate (Cr(acac)3). Then 100 L of an e-HNDI solution (121.5 mM, CDCl3/pyridine 4.5:0.5) was added, along with 100 L of 2-chloro-4,4,5,5-tetramethyl-1,3,2-dioxaphospholane as the derivatizing agent, to quantify the amount of different hydroxyl groups.

Equipment and setup

^{31}P-NMR spectra were recorded on 800 L samples on a Bruker Avance 500 MHz instrument. The ^{31}P-NMR data reported are the average of three experiments. The maximum standard deviation was 2 × 10−2mmol g−1, while the maximum standard error was 1 × 10−2mmol g^{-1}.

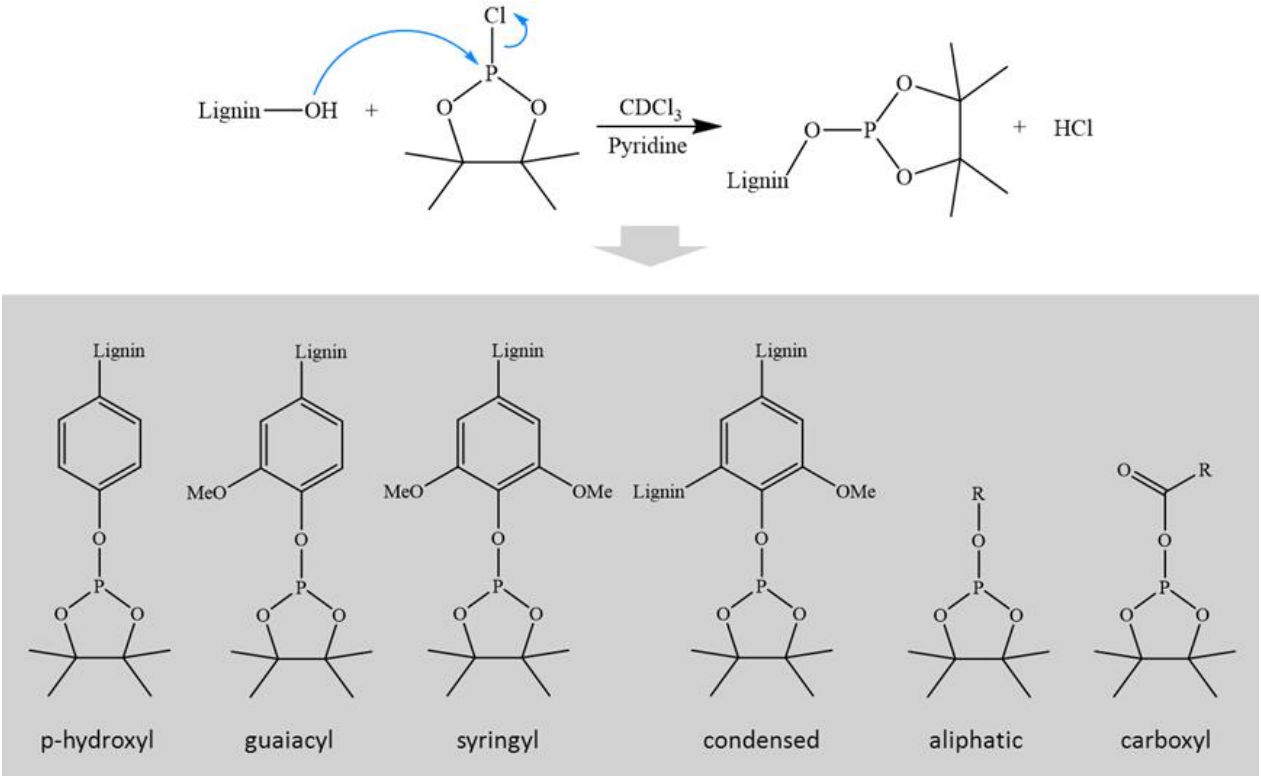

Figure 38 - modification of lignin for quantitative 31P-NMR spectroscopy (redrawn and adapted from reference).[2]

Structure	δ (ppm)
Aliphatic OH	145.4–150.0
Phenolic OH	137.6–144.0
Condensed (C5 substituted)	140.0–144.5
β–5	~143.5
Syringyl	~142.7
4–O–5	~142.3
5–5	~141.2
Guaiacyl	139.0–140.2
Catechol	~138.9
p–hydroxyphenyl	~137.8
Carboxylic acid OH	133.6–136.0

Table 7 - Typical chemical shifts and integration regions for lignin in n a ^{31}P-NMR (reproduced from reference).[2]

2D-HSQC NMR - *Heteronuclear Single Quantum Correlation Nuclear Magnetic Resonance*

Two-dimensional NMR spectra can provide greater information about a molecule than one-dimensional NMR spectra and are especially helpful in determining the structure of a complex molecules. It is particularly useful with irregular polymers, like lignin, which structures are too complicated to be rationalized with one-dimensional NMR techniques. The molecular structures with the relative cross-peak assignments obtained from literature can be found in figure 39 and table 9 respectively.

Preparation

2D-HSQC spectra were run in DMSO-d_6 on acetylated samples to avoid the fractionation of the material before NMR analysis and to increase both solubility and chemical shift dispersion of the side chain units.

Equipment and setup

The inverse detected ^{1}H-^{13}C correlation spectra (HSQC) were measured on a Varian Mercury 400 MHz instrument at 308 K. The spectral width was set at 5 kHz in F2 and 25 kHz in F1. Altogether 128 transients in 256 time increments were collected. The polarization transfer delay was set at the assumed coupling of 140 Hz and a relaxation delay of 2 s was used. The spectra were processed using $\pi/2$ shifted squared sinebell functions in both dimensions before Fourier transformation.

^{29}Si-NMR CP/MAS spectroscopy

In silicon glasses, the tetrahedral silicon atoms are labelled according to the number (n) of shared bridging oxygens; the general nomenclature of a general specie is Q^n, where $0 \leq n \leq 4$. ^{29}Si solid state NMR can be used to identify the predominant structures in amorphous silica.[3]

Structure	Label	Chemical shift (ppm)
$(HO)_2Si(OSi)_2$	Q2	-87 to -91
$(HO)Si(OSi)_3$	Q3	-94 to -100
$Si(OSi)_4$	Q4	-107 to -109

Table 8 – Indicative chemical shifts for silicon atoms with different structures in silica glasses.[4]

Equipment and setup

The analyses were performed using a MSL300 Bruker instrument and the following specifications: MAS at 9 KHz, contact time 5 ms, recycle delay 2 s, 3000-5000 scans.

Label	δC/δH	Assignments
Cβ	53.2/3.80	Cβ–Hβ in phenylcoumaran (β-5′) substructures (C)
Bβ	53.6/3.06	Cβ–Hβ in resinol (β-β′) substructures (B)
Aγ	59.65/3.61 and 3.27	Cγ–Hγ in β-O-4′ substructures (A)
Dβ	59.77/2.78	Cβ–Hβ in spirodienone (β-1′) substructures (D)
Iγ	61.3/4.09	Cγ–Hγ in cinnamyl alcohol end-groups (I)
A′γ/A″γ	62.7/3.83–4.30	Cγ–Hγ in γ-acylated β-O-4′ substructures (A′/A″)
I′γ	64.0/4.79	Cγ–Hγ in γ-acylated cinnamyl alcohol end-groups (I′)
Bγ	71.1/3.82 and 4.19	Cγ–Hγ in resinol (β-β′) substructures (B)
Aα(S)	71.4/4.86	Cα–Hα in β-O-4′ substructures linked to a S unit (erythro) (A)
Eα	79.2/5.52	Cα–Hα in α,β-diaryl ether substructures (E)
Dα	81.0/5.01	Cα–Hα in spirodienone (β-1′) substructures (D)
A′β(G)	81.0/4.49	Cβ–Hβ in γ-acylated β-O-4′ substructures linked to a G unit (A′)
Aβ(G) and A′β(S)	83.4/4.31	Cβ–Hβ in β-O-4′ substructures linked to a G unit (A) and in γ-acylated β-O-4′ substructures linked to a S unit (A′)
Dα′	84.65/4.67	Cα′–Hα′ in spirodienone (β-1′) substructures (D)
Bα	84.8/4.66	Cα–Hα in resinol (β-β′) substructures (B)
Aβ(S)	85.9/4.12	Cβ–Hβ in β-O-4′ substructures linked to a S unit (erythro) (A)
Cα	86.6/5.47	Cα–Hα in phenylcoumaran (β-5′) substructures (C)
T8	94.4/6.64	C8–H8 in tricin (T)
T6	98.9/6.28	C6–H6 in tricin (T)
S2,6	103.7/6.71	C2,6–H2,6 in etherified syringyl units (S)
T′2,6	103.9/7.30	C2′,6′–H2′,6′ in tricin (T)
T3	104.7/7.03	C3–H3 in tricin (T)
S′2,6	106.7/7.28	C2,6–H2,6 in Cα-oxidized (Cα═O) phenolic syringyl units (S′)
G2	110.7/6.98	C2–H2 in guaiacyl units (G)
FA2	111.0/7.32	C2–H2 in ferulate (FA)
J2(G)	112.24/7.25	C2–H2 in cinnamyl aldehyde end-groups (J)
PCAβ and FAβ	113.5/6.27	Cβ-Hβ in p-coumarate (PCA) and ferulate (FA)
G5	114.9/6.72 and 6.94	C5–H5 in guaiacyl units (G)
PCA3,5	115.5/6.77	C3,5–H3,5 in p-coumarate (PCA)
G6	118.7/6.77	C6–H6 in guaiacyl units (G)
J6(G)	122.3/7.10	C6–H6 in cinnamyl aldehyde end-groups (J)
FA6	123.1/7.15	C6–H6 in ferulate (FA)
H2,6	127.8/7.22	C2,6–H2,6 in p-hydroxyphenyl units (H)
PCA2,6	129.9/7.46	C2,6–H2,6 in p-coumarate (PCA)
PCAα and FAα	144.7/7.45	Cα–Hα in p-coumarate (PCA) and ferulate (FA)
Polysaccharides		
X5	63.2/3.26 and 3.95	C5–H5 in β-d-xylopyranoside
X2	72.9/3.14	C2–H2 in β-d-xylopyranoside
X′2	73.0/4.49	C2–H2 in 2-O-Ac-β-d-xylopyranoside
X3	74.1/3.32	C3–H3 in β-d-xylopyranoside
X′3	74.7/4.79	C3–H3 in 3-O-Ac-β-d-xylopyranoside
X4	75.6/3.63	C4–H4 in β-d-xylopyranoside

Table 9 – 2D-HSQC NMR cross-peak assignments for Arundo donax lignin (reproduced from reference).[5]

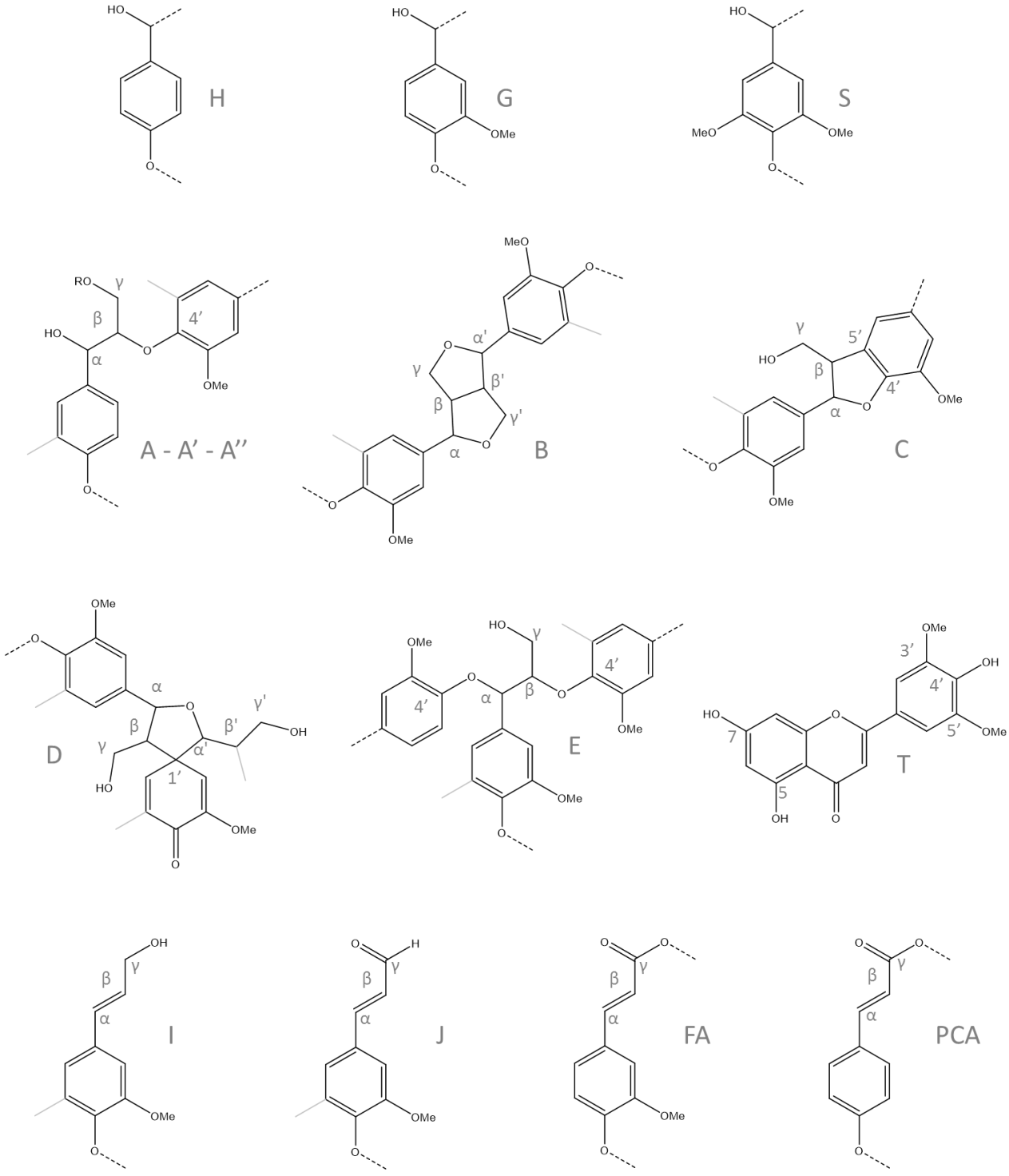

Figure 39 – Molecular structures relative to the assignments reported in table 9 (redrawn from reference) [5]

FT-IR (ATR) – *Fourier Transform Infrared Spectroscopy (Attenuated Total Reflectance)*

FT-IR spectroscopy is a versatile technique that can provide useful information regarding different characteristics of the lignocellulosic biomasses and their components. The absorption spectra are determined by the structure of the compounds, but also reflect the presence of contaminants. IR spectroscopy was used to characterize several materials obtained from renewable feedstock and to investigate their modifications. In table 10 it is possible to find the characteristic absorption bands for the principal products studied in this thesis and the relative assignments obtained from the available literature.

Equipment and setup

The analyses were performed with a Nicolet iS10 spectrometer (Thermo Scientific) equipped with an iTR Smart device (total scan 32, range 4000–800 cm^{-1}, resolution 1 cm^{-1}).

Band Position (cm^{-1})	Vibration	Assignment
	Lignin	
3350-3420	ν OH	Aliphatic + Phenolic OH
2934-2938	ν_{as} CH	CH2 + CH3
2840-2846	ν_{s} CH	(O)CH3
1700-1737	ν C=O	Unconjugated C=O and COOH
1635-1682	ν C=O	Conjugated C=O
1595-1600	ν CC	Aromatic Skeleton
1502-1513	ν CC	Aromatic Skeleton
1453-1465	δ CH	Asymm CH2 + CH3
1440	δ OH	In plane bending
1426-1428	ν CH	Aromatic + in plane CH
1370	δ_{ip} OH + δ CH	Phenols + CH3
1319-1330	ν CO	CO of Syringil units
1252-1265	ν CO	CO of Guayacil units
1226	N CC, CO, C=O	
1215	ν (Ar)CO(H) + ν (Ar)CO(Ar)	Phenols + Aromatic Ethers
1147-1151	δ_{ip} (Ar)CH	CH of G units
1114-1116	δ_{ip} (Ar)CH	CH of S units
1078	ν CO(H)	Secondary aliphatic OH
1024	ν CO(H)	Primary aliphatic OH
850	δ_{op} (Ar)CH	CH bonds of G
827-832	δ_{op} (Ar)CH	CH bonds of S
	Cellulose	
3330-3360	ν OH	Free and hydrogen bond OH
~2900	ν CH	
1640	δ H2O	adsorbed H2O
1420-1430	δ_{as} CH	in CH_2
1374	δ_{s} CH	
1318	δ CH	CH_2 wagging

1201	δ OH	
1159-1174	ν_{as} COC	bridge
1105-1112	ν_{as} CC	In-phase ring vibration
1059-1070	ν CO	Skeletal vibration
1049	ν COC	pyranose ring skeletal vibration
910	ν COC	glycosidic bond
897-899	ν_{as} CC	Out-phase ring vibration
	Hemicellulose (Xylans)	
3300-3400	ν OH	
2976	ν_{as} CH_3	in xylopyranose rings of the main xylan chain
2930	ν_{as} CH_2	
2870	ν_s CH_2	
2839	ν_s CH_3	
1645	δ H_2O	adsorbed H_2O
1477	δ CH	CH_2
1312-1381	δ CH + δ OH	
1125-1171	ν CC + ν COC	
1047-1106	ν CO + ν CC + ring	
1044	δ OH	bending in C-OH
1000-1026	ν CC + ν CO	in C-OH
985	ν CO + δ OH + ring	
897-904	δ CH + ring	in C1-H1
856		furanoid ring
	Silica	
3690	ν OH	free OH
3200-3400	ν OH	hydrogen bonded OH
1630-1640	δ H_2O	adsorbed H2O
1000-1130	ν_s SiO	in Si-O-Si
850-960	ν SiO	in Si-OH
805	ν_{as} SiO	in Si-O-Si

Table 10 - IR correlation chart for the main components of lignocellulosic materials (data rationalized from references[6–25]).

DLS – *Dynamic Light Scattering*

The DLS was used to analyze the average particle size of lignin extracted from rice husk in aqueous solutions at different pH values.

SEC/GPC - Size Exclusion Chromatography / *Gel Permeation Chromatography*

This technique is largely used for the characterization of macromolecules and hence in polymer science. Molecules characterized by different hydrodynamic volumes, which are correlated to the molecular weight, are differentiated on the basis of their ability to permeate through a porous material. The output is the distribution of chain sizes, or the molecular weight distribution. While for synthetic polymers the molecular weight distribution is determined by the conditions of the polymerization, the molecular weight distribution of lignin is highly affected by the botanical source, by the extraction process, by eventual purification steps, and by thermal treatments. To describe the distribution of a polymer usually at least two average molecular weights are used: the number molecular weight $M_n = \frac{\sum N_i \cdot M_i}{\sum N_i}$ where N_i indicates the number of moles of molecules having a molecular weight of M_i and the mass average molecular weight $M_w = \frac{\sum N_i \cdot M_i^2}{\sum N_i \cdot M_i}$. The ratio between the two determines the index of polydispersity $PDI = \frac{M_w}{M_n}$, a measure of how narrow a distribution is. The degree of polymerization, finally, is the average number of monomeric units contained in a molecule and is obtained dividing the Mn by the molecular weight of the repeating unit $DP_n = \frac{M_n}{MW}$.

One of the potential problems with GPC analysis is that the absolute values of the average molecular weights can be overestimated because of self-aggregation as observed in comparative analysis, where the results of the GPC gave higher degree of polymerization than end-groups titration.[26]

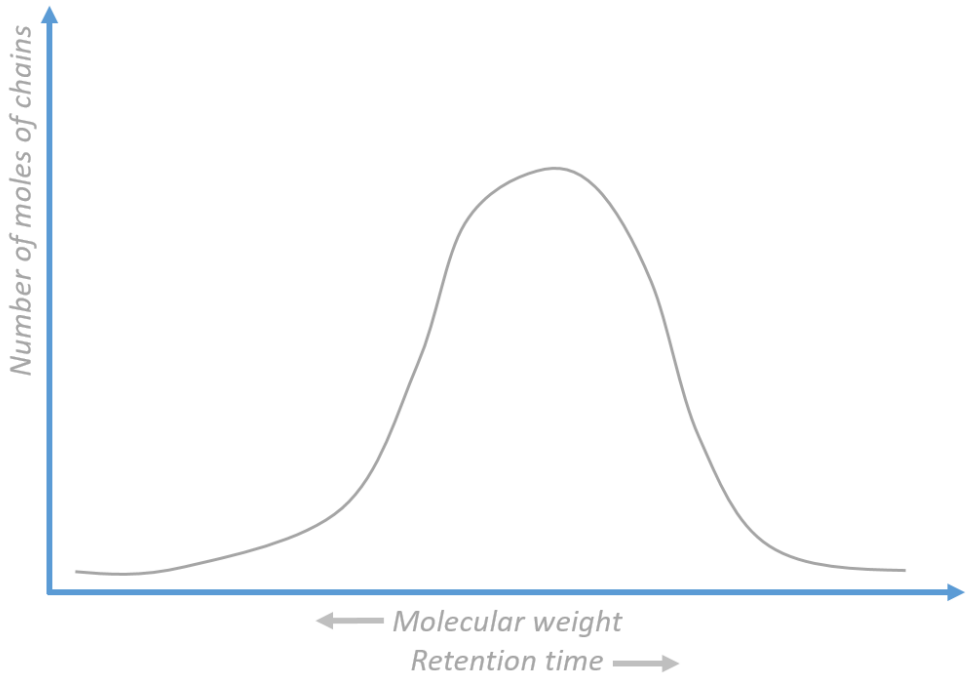

Figure 40- Typical GPC chromatogram obtained for a continuous distribution of molecular weights.

Gel permeation chromatography was used to investigate the molecular weight distributions of acetylated lignin specimens.

Sample preparation

Lignocellulosic material acetylation in IL - The acetylation reaction was carried out in 1-allyl-3-methylimidazolium chloride - [amim]Cl, following the procedure described elsewhere.[27]

Hemicellulose benzoylation in IL - The benzoylation reaction was carried out in 1-allyl-3-methylimidazolium chloride - [amim]Cl, according to the method described elsewhere.[27]

Lignin acetylation - A total of 60 mg of extracted lignin was acetylated in a pyridine-acetic anhydride solution (1:1 v/v, 4 mL) and kept overnight at 40 °C. After stripping with ethanol, toluene, and chloroform (25 mL × 3 each solvent), the sample was dried in vacuum. The acetylated lignin was solubilized in THF for GPC analysis.

Equipment and setup

Gel permeation chromatography analyses were performed on a Waters 600 E liquid chromatography connected to a HP1040 ultraviolet detector set at 280 nm. The injection port was a Rheodyne loop valve equipped with a 20 L loop. The GP-column system was composed by an Agilent PL gel 5 μm, 500 Å, and an Agilent PL gel 5 μm, 104 Å. The sol-vent used was tetrahydrofuran (Fluka 99.8%). Polymer standards of polystyrene from Polymer Laboratories were used for calibration.

Alkaline Size Exclusion Chromatography

The molar mass distribution of unmodified lignins was analysed by alkaline SEC using a TSK gel Toyopearl HW-55F column, 0.5 M NaOH as eluent, UV detection at 280 nm and calibration with sodium-polystyrene sulfonates, according to the procedure as described in the reference.[28]

TGA - Thermogravimetric Analysis

In TGA a small sample of the material under investigation is placed in a chamber where the atmosphere can be controlled, usually with air, oxygen, or nitrogen. The sample can be heated at different rates or analysed at isothermal conditions. The weight loss is recorded and can be plotted as a function of temperature or time. TGA is used to assess the release of adsorbed substances, volatiles and the thermal decomposition.

Equipment and setup

The analyses were performed with a Mettler Toledo TGA 1 instrument.

DSC - *Differential Scanning Calorimetry*

Oxygen Induction time

The analysis was performed with a Metler Toledo 822 DSC instrument to quantify the thermal stabilization provided by lignin to NR. Air-dried coagulated natural rubber and masterbatches containing lignin at different concentrations were dried in an oven at 35 °C under vacuum for 12 h. Afterward, a 3-mg sample was accurately weighted and placed in an aluminum pan. The sample was heated to 170 °C at 15 °C/min under nitrogen atmosphere, it was then kept at 170 °C for 2 min to equilibrate at isothermal condition, and finally the oxygen stream was opened and the induction time recorded at the onset of the exothermal peak.

Electron Microscopies

The electron microscopies were used for the characterization of the tentative fillers, especially to investigate particle size and morphology. In second place, they provided an effective method for the analysis of the dispersion in rubber compounds.

SEM – *Scanning Electron Microscopy*

Equipment and setup

Scanning Electron Microscopy (SEM) were performed in high vacuum conditions by a Tescan Vega TS5136XM, equipped with an energy dispersion electronic microprobe EDAX Genesis 4000 XMS Imaging 60 SEM (accelerating voltage, 20 kV; current, 190 pA; working distance,23 mm; spot size, 250 nm) and a Field Emission Scanning Electron Microscope FESEM ULTRA PLUS Zeiss (INLENS modality, accelerating voltage 10KV).

TEM – *Transmission Electron Microscopy*

Trasmission electron microscopy was used to investigate the size and the morphology of cellulose nanocrystals prepared from rice husk.

Preparation

10 μL of nanocrystals suspension were dropped onto a 300 mesh copper grids. After 5 minutes the solution was gently removed. Samples were counterstained for 5 min with a saturated solution of uranyl acetate, washed with MilliQ water to eliminate excess uranyl acetate, and allowed to dry.

Equipment and setup

TEM analyses were performed on a Zeiss LEO 912ab Energy Filtering TEM operating at 120 kV, and images were collected using a CCD-BM/1Ksystem. Digital images were taken at a magnification of 15k and 30k.

Nitrogen Physiosorption Isotherms (BET/BJH)

The surface area and the pore size distribution can be obtained experimentally exploiting the correlation between the multilayer nitrogen adsorption and the relative pressures measured in the adsorption isotherms (usually at measured at 77 K). The isotherms are built increasing the nitrogen pressure in several steps inside the closed chamber and leaving each time the sample to equilibrate, to calculate the adsorbed amount. The BET (Brunauer, Emmet, and Teller) theory allows to calculate the total specific surface area of materials from the adsorption data. With the BJH (Barrett, Joyner, and Halenda) method it is possible to determine the pore size distributions from experimental isotherms. Finally, with the t-Plot, also the external surface area and micropore volume of microporous materials can be obtained from the adsorptions. Porous solid materials are classified by IUPAC in relation to the predominant pore sizes. Microporous when pores are smaller than 2.0 nm, mesopores when pores diameter is between 2.0 and 50.0 nm, macroporous materials when pore sizes exceeds 50.0 nm.[29] Adsorption isotherms are also classified by IUPAC since the they are connected to porosity of the adsorbents materials that can be: microporous (type I), nonporous or macroporous (types II, III, and VI), or mesoporous (types IV and V). The approximative general shapes of the six isotherms are rendered in figure 41.

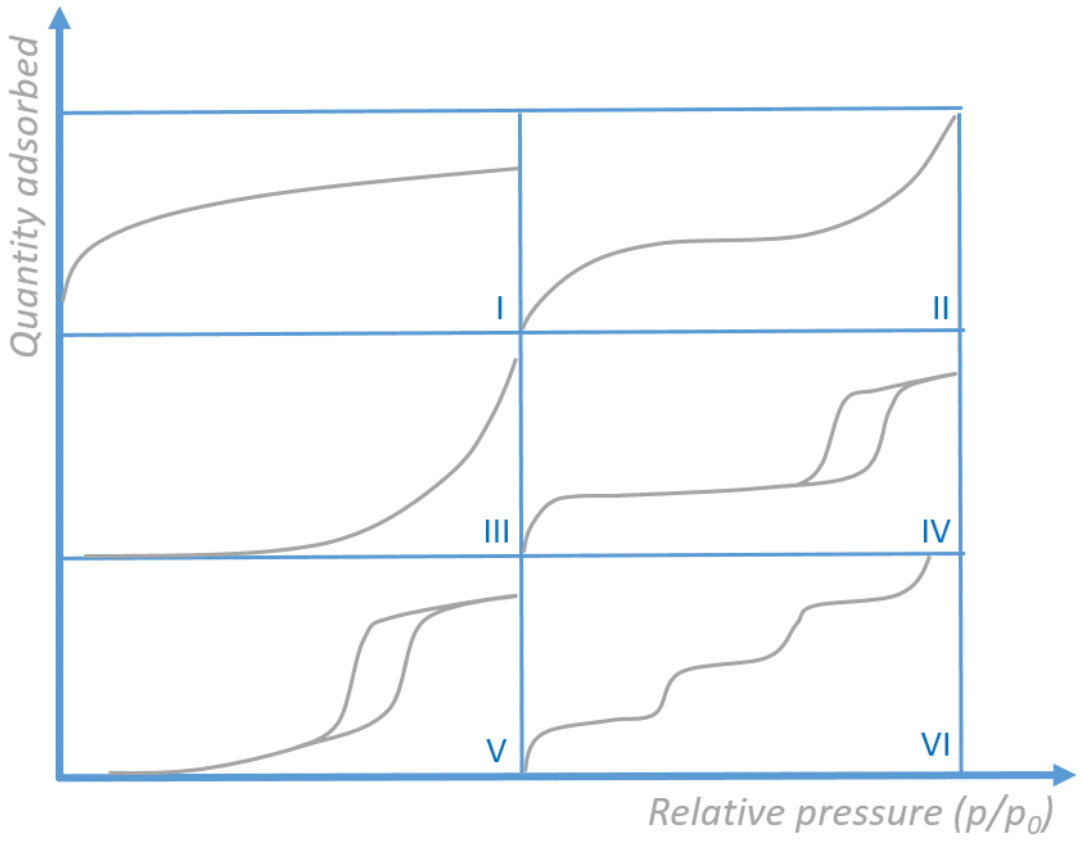

Figure 41 - IUPAC classification of adsorption isotherms (sorption and desorption, redrawn from reference).[29]

4.2 Solubility modelling

Solubility parameters

The Hansen solubility parameters are widely used by the paint and coatings industry to select suitable solvents.[30] However also additives for polymers, like fillers, can be characterized by Hansen solubility parameters, like polymers. [31] The solubility parameters are based on the cohesive energy density (CED). The cohesive energy (CE) is the energy needed to break the molecules of a liquid into gas (enthalpy of vaporization), and reflect the various contributions to the cohesion of substance. The cohesive energy is related to the latent heat of vaporization (ΔH_V): CE = $\Delta H_V - RT$. The cohesive energy density of a substance is the cohesive energy divided by the molar volume of the substance (CED = CE/V_m, where V_m is the molar volume). The total solubility parameter, or Hildebrand solubility parameter (δ) is the square root of CED (δ^2=CED) or:

$$\delta = \sqrt{\frac{\Delta H_V - RT}{Vm}}$$

The basic principle of the solubility parameter is that "like dissolves like", as it is empirically observed that substances are usually miscible when the difference between their solubility parameters is small, but is not always true. With Hansen Solubility Parameters, the total parameter (δ) is broken into three components: δ_D, δ_P and δ_H representing dispersion, polar and hydrogen-bonding contributions. The relationship between Hildebrand and Hansen parameter is the following: $\delta^2 = \delta_D^2 + \delta_P^2 + \delta_H^2$. The division of δ into its HSP components has improved its success in solvent selection and in related applications. The affinity of two substances (1 and 2) can be measured through the HSP distance: $R_a^2 = 4(\delta_{D1}-\delta_{D2})^2 + (\delta_{P1}-\delta_{P2})^2 + (\delta_{H1}-\delta_{H2})^2$, if the relative energy difference RED = R_a/R_o is > 1 two substance will probably not mix, if RED < 1 the two substances will mix, when RED = 1 there is partial miscibility. R_o is the radius of the sphere that contains all the good solvents for the substance in the Hansen space. Hansen parameters can be linked to the regular solution theory:

In the Flory–Huggins solution theory the Gibbs free energy change ($\Delta G_m = \Delta H_m - T\Delta S_m$) for mixing a polymer (1) with a solvent (2) is described by the equation $\Delta G_m = RT[n_1 \ln \phi_1 + n_2 \ln \phi_2 + n_1\phi_2\chi_{12}]$, where n and ϕ are the numbers of moles and the volume fractions. The interaction parameter χ_{12} depends on the nature of both the solvent and the solute and it is specific for every couple of materials. The Flory-Huggins interaction parameter can be expressed:

$$\chi_{12} = \frac{v_s}{RT}(\delta_1 - \delta_2)^2 = \frac{v_s}{RT}[(\delta_{D1} - \delta_{D2})^2 + (\delta_{P1} - \delta_{P2})^2 + (\delta_{H1} - \delta_{H2})^2]$$

where $v_s$is the solvent molar volume.[32–36]

Prediction of Hansen Solubility Parameters with a group-contribution method

The Group-Contribution method of Stefanis and Panayiotou was used to evaluate the values of the Hansen Solubility Parameters (HSP) for lignin and its modifications. The model was first proposed in 2008,[37] and was updated in 2012.[33] The method supports a large variety of characteristic chemical groups, allowing the prediction of Hansen solubility parameters for a broad series of organic compounds, including those having complex multi-ring, heterocyclic, and aromatic structures, as lignin. The basic molecular structure of organic is described as the sum of the different functional groups. Limiting the method to the first order groups, each property is then calculated from the molecular structure through the basic equation:

$$f(x) = \Sigma_i N_i C_i$$

where C_i is the contribution of the first-order group of type *i* that appears N_i times in the molecular structure of the compound. *f(x)* is a single equation of the property, *x*, and is selected after a thorough study of the physicochemical and thermodynamic behaviour of the property. The determination of the group contributions is done by regression analysis, using the polynomial equation that fitted the experimental of δ at best. The model is applicable to organic compounds with three or more carbon atoms, excluding the atom of the characteristic group (e.g., –COOH or –CHO). The equations for the estimation of Hansen solubility parameters are the following:

$$\delta_d = \left(\sum_i N_i C_i + \sum_j M_j D_j + 959.11 \right)^{0.4126} \quad \text{MPa}^{(1/2)}$$

$$\delta_p = \left(\sum_i N_i C_i + \sum_j M_j D_j + 7.6134 \right) \quad (\text{MPa})^{(1/2)}$$

$$\delta_{hb} = \left(\sum_i N_i C_i + \sum_j M_j D_j + 7.7003 \right) \quad (\text{MPa})^{(1/2)}$$

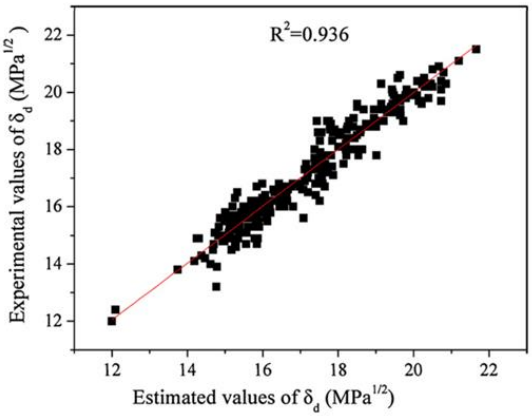

Figure 42 - Correlation between estimated and experimental values of dispersion partial solubility parameter δ^d for 347 compounds (reproduced from reference).[33]

The values of C_i are tabulated and are available for a large number of functional groups. The method is proven to work well with organic compounds with more than three carbon atoms as well as with polymer. However, lignin is not a regular polymer and it is not possible to accurately describe the structure through a repeating unit. At this point, to be able to calculate HSP for lignin an approximation was made assuming that lignin is the product of the polymerization of a G monomeric unit as proposed by Boeriu et al.[38] This approximation is going to make absolute values less reliable, even if rather in line with values already reported in literature,

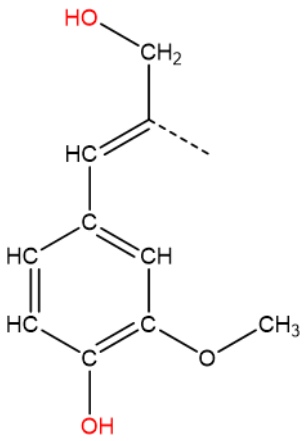

Figure 43 - Repeating unit (C9) used to calculate the Hansen solubility parameters of softwood lignin.

however the main objective is to evaluate the relative differences in the HSP between the starting lignin and its chemical modifications, and since solubility modelling considers only the difference between solute and solvent, these model errors will largely cancel each other out as already pointed out in other works.[32] The values were calculated also for polyisoprene to represent natural rubber.

Polyisoprene					
Group		-CH3	CH2=C<	-CH2-	CH<
Occurence		1	1	1	1
Contribution		-123,01	-126,15	1,82	82,94
δd	15,7				
Group		-CH3	CH2=C<	-CH2-	CH<
Occurence		1	1	1	1
Contribution		-1,6444	-2,017	-0,3141	0,6051
δp	4,2				
Group		-CH3	CH2=C<	-CH2-	CH<
Occurence		1	1	1	1
Contribution		-0,7458	-1,1783	-0,3877	-0,2064
δh	5,2				
δ Total	17,1				

Table 11 - Predictions of the Hansen solubility parameters for polyisoprene.

The total solubility parameter (δ = 17.1) is in sufficient agreement with the values reported in literature that falls in the range 17.5 – 18.2,[39,40] even if slightly underestimated. The calculations for the prediction of the Hansen solubility parameters of lignin, based on the structure of the repeating unit (C9) schematized in figure 43 are reported in table 11. However, in the simplified structure the concentration of hydroxyls groups is overestimated and doesn't represent well the actual concentration of the different functionalities that are

C9 unit (G)								
Group		AC	ACH	ACOH	CH3O	CH=CH	CH2	OH
Occurence		2	3	1	1	1	1	1
Parameter		98,84	29,87	58,52	-68,07	28,65	1,82	-29,97
δd	18,5							
Group		AC	ACH	ACOH	CH3O	CH=CH	CH2	OH
Occurence		2	3	1	1	1	2	1
Parameter		0,7661	-0,5771	1,052	0,0089	-0,5037	-0,3141	1,0587
δp	8,4							
Group		AC	ACH	ACOH	CH3O	CH=CH	CH2	OH
Occurence		2	3	1	1	1	2	1
Parameter		-0,1553	-0,3554	6,9757	0,2676	-0,1253	-0,3877	7,3609
δh	20,0							
δ Total	28,5							

Table 12 - Predictions of the Hansen solubility parameters for the C9 repeating unit of lignin.

actually present in lignin. To obtain more accurate predictions of HSP, the number of chemical functionalities was corrected using the real concentrations obtained through the characterization of the softwood Kraft lignin with ^{31}P-NMR spectroscopy and sulfur content that are reported in chapter 6.

C9 unit (G) corrected with groups from 31P-NMR										
Group		AC	ACH	ACOH	CH3O	CH=C<	CH2	OH	COOH	SH
Occurence		2,38	2,63	0,86	1	1	1	0,4	0,11	0,12
Parameter		98,84	29,87	58,52	-68,07	62,48	1,82	-29,97	-38,16	190
δd	19,4									
Group		AC	ACH	ACOH	CH3O	CH=C<	CH2	OH	COOH	SH
Occurence		2,38	2,63	0,86	1	1	1	0,4	0,11	0,12
Parameter		0,7661	-0,5771	1,052	0,0089	-1,1018	-0,3141	1,0587	0,7153	1,8229
δp	8,1									
Group		AC	ACH	ACOH	CH3O	CH=C<	CH2	OH	COOH	SH
Occurence		2,38	2,63	0,86	1	1	1	0,4	0,11	0,12
Parameter		-0,1553	-0,3554	6,9757	0,2676	-1,7171	-0,3877	7,3609	3,8422	4,9279
δh	14,5									
δ Total	25,6									

Table 13 - Predictions of the Hansen solubility parameters for the repeating unit of lignin with correction on the number of chemical groups per C9 unit based on empirical data.

The HSP for chemically modified lignin were calculated based on this scheme, supposing that the reaction affected every hydroxyl group.

4.3 Rubber compounding

This section describes the main procedures that were used to prepare rubber model compounds.

Materials

For rubber compounding the following products were used. Stabilized natural rubber latex (NR) 60% solid content (Latex trade center), Natural rubber Sir20 (Astlett), soluble sulfur (Zolfoindustria), zinc oxide (Zincol ossidi), stearic acid (Sogis), and N-cyclohexyl-2-benzothiazole sulfenamide - CBS (Zolfoindustria), carbon black N375 (Birla), and silica Ultrasil VN3 (Evonik).

Equipment and setup

The rubber compounds were prepared on two scales. With a small-sized Brabender mixer with an internal chamber of 50 mL and a fill factor of 0,9 and a medium-sized Haake mixer with an internal chamber of 250 mL and a fill factor of 0,8.

Compounding

Rubber compounds were prepared incorporating several ingredients (fillers, vulcanizers and antioxidants) in different rubbers using internal chamber mixers and open two-roll mixers, according to the following procedures and the formulations reported in the relative chapters.

Procedure 1. Temperature was set at 60 °C and rotor speed at 70 rpm. At first, rubber was gradually introduced in the mixer. After 3 min, dicumyl peroxide was added and mixed with the rubber for 5 min. After the mixing the rubber compounds were passed three times through a two-roll mill at 40 °C for further homogenization.

Procedure 2. Rubber compounds were prepared adding the vulcanizing agents to neat natural rubber or NR/lignin masterbatches with the internal chamber mixer. Rubber was kneaded at 60 °C and 70 rpm. After 3 min, stearic acid, zinc oxide, accelerator (CBS), and sulfur were added and mixed with the rubber composites for 5 min. At the end of the mixing, the rubber compounds were passed three times through a two-roll mill at 40 °C for further homogenization.

Procedure 3

	Time (min)	Temp (°C)	Action
step 1	0	50	Load rubber or masterbatch
	3	50	Add fillers and silane
	5	50 -> 135	Raise temp
	6.5	140	Temp reached
	8.5	135-145	Dump
step 2	0	50	Load compound from step 1
	3	50	Add antioxidants and vulcanizers
	8	50	Dump

Rotor speed was held constant at 70 RPM. At the end of the mixing, the rubber compounds were passed three times through a two-roll mill at 40 °C for further homogenization.

Procedure 4

	Time (min)	RPM	Temp (°C)	Action
step 1	0	50	60	Load rubber or masterbatch
	3	50	60	Load fillers
	5	50	60	Load Stearic Acid and Zinc Oxide
	7	50	60	Antioxidants
	12	50	60	Dump
step 2	0	40	40	Load compound from step 1
	3	40	40	Load Sulfur and Accelerator
	8	40	40	Dump

At the end of both steps, the rubber compounds were passed three times through a two-roll mill at 40 °C for further homogenization.

Coprecipitation: lignin/NR masterbatches

To prepare NR/lignin masterbatches, the proper amount of lignin, according to the desired final concentration (e.g. 15 PHR = 13%), was added to a 0.1 M NaOH aqueous solution (15 mL per gram of lignin) and the pH was adjusted to 13 using 10 wt % NaOH. After being stirred for 1 h, the solution was gently poured in beaker containing 83.4 g of 60 wt % natural rubber latex. The emulsion obtained was kept under stirring for one additional hour and finally 10 wt % sulfuric acid was progressively added to obtain complete coagulation, evaluated by visual inspection. The coagulated rubber was reduced in thin layers using a rubber two-roll mixer and then washed with excess of water, until pH 6 was reached. The thin layers of rubber/lignin composites were left air drying sheltered from light until constant weight was reached. References of coagulated natural rubber (neat natural rubber) were prepared in the same manner in absence of lignin. The procedure is illustrated in figure 44.

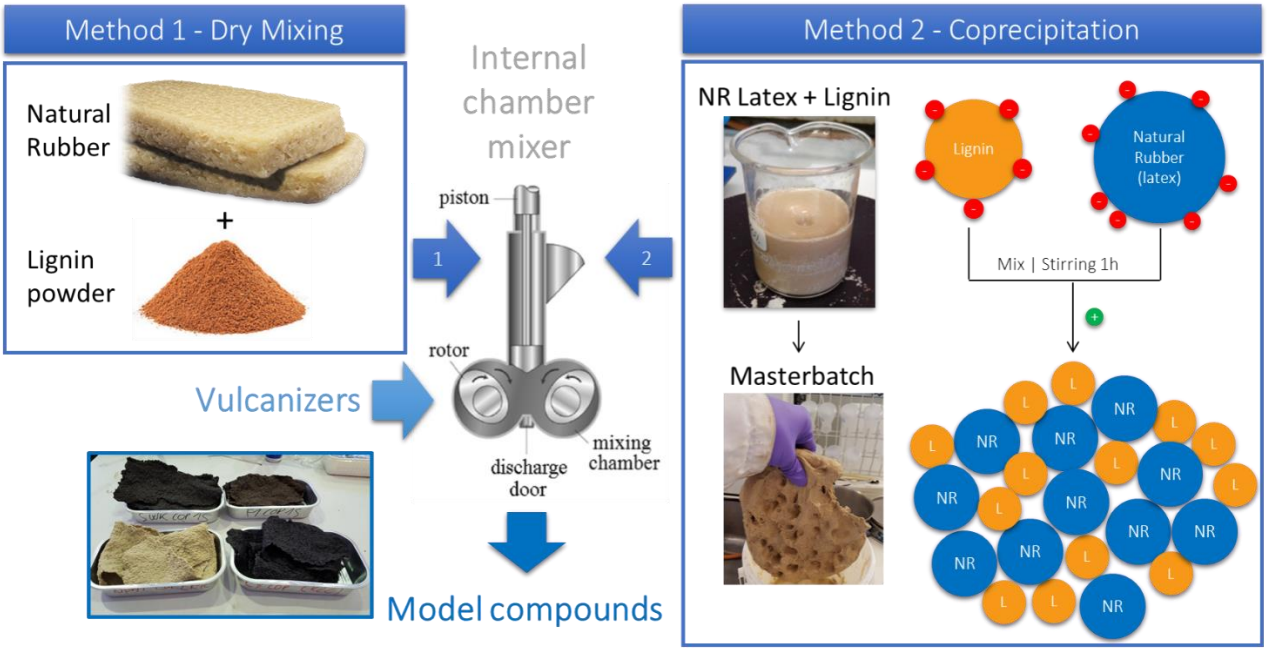

Figure 44 – Preparation of lignin/rubber model compounds with the two methods: 1 – Dry mixing, 2 – Coprecipitation.

4.4 Characterization of rubber compounds

Vulcanization

The evolution of the crosslinking in the rubber compounds during vulcanization can be monitored using different rheometers, commonly the mooney viscometer, the MDR (Moving Die Rheometer) or the RPA (Rubber Process Analyzer). The rheometer measures the change in the torque that is required to apply a periodical (small) deformation. The torque is plotted against the time to obtain the vulcanization curve at a certain temperature. From the curve, it is possible to obtain useful data. ML and MH indicate the minimum and the maximum torque respectively. The difference, (MH – ML) is a function of the extension of crosslinking, but is also influenced by other factors as, for instance, filler flocculation. The scorch or induction time indicates the beginning of the crosslinking that is evidenced by the ramping up of torque. This parameter is important for the processing because after the start of the crosslinking the items cannot be reshaped. Scorch time is often identified with Ts2, the time from beginning of the test to the time the torque has increases 2 units above ML value. T90 (or t_{90}) is the time required for the torque to reach 90% of the maximum achievable torque and is referred to as optimum cure time.[41] Reversion is the loss of crosslinking caused by thermal aging. It is more severe in synthetic and natural polyisoprene rubbers due to the increased presence of polysulfidic crosslinks that are more heat-labile.[42]

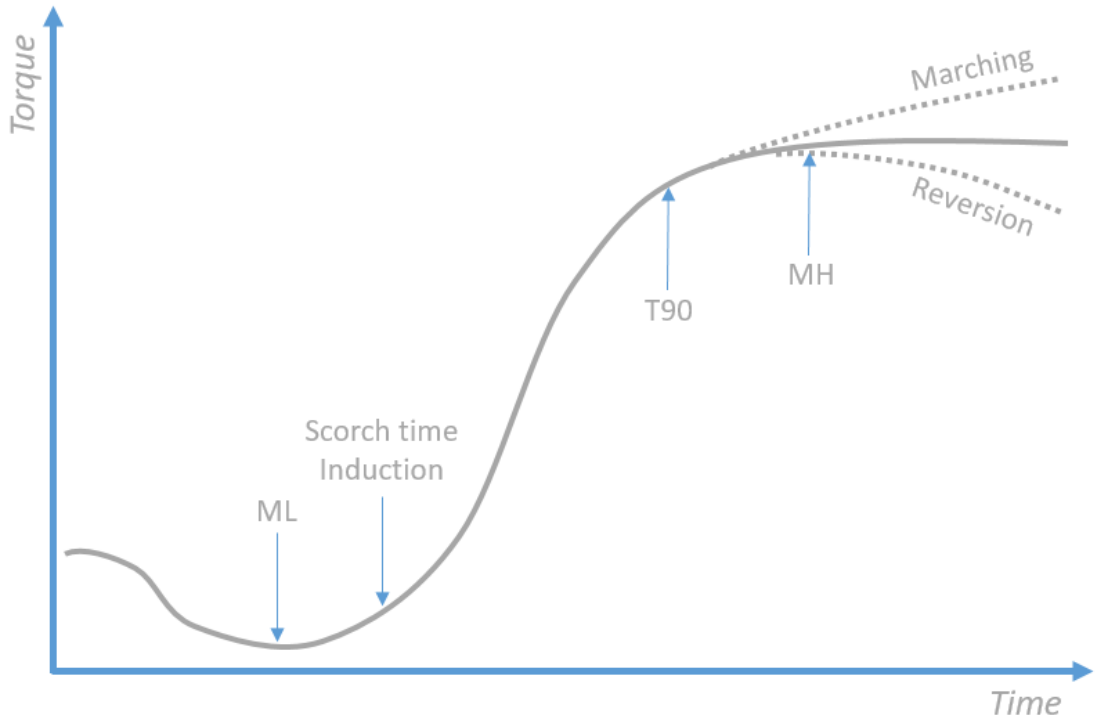

Figure 45 - Typical vulcanization curve obtainable with different rehometers.

Tensile properties

Stress-strain curves are the common output of a tensile test of the mechanical properties. In this kind of tests a dumbbell (or ring) shaped specimen is elongated increasing the strain at a constant rate. This simple analysis can provide a general understanding of the macroscopic mechanical properties of elastomeric materials. The stiffness of the material is defined as the stress (σ) that must be applied to elongate the specimen at a certain strain (ε) and is defined by the (tensile) elastic modulus: $E(\sigma) = \sigma/\varepsilon$. The curves of the elastomers are not linear and the modulus is a function of the elongation. Other important properties are the properties at failure. The (ultimate) tensile strength is the capacity of a material to withstand loads and is the force per unit area (MPa or psi) required to break a material. Ultimate elongation or elongation at break represents the capacity of a material to deform before cracking. It is defined as the increase in length (%) that occurs before it breaks. The toughness is the ability of a material to absorb energy, is the amount of energy per unit volume that a material can absorb before failing. Toughness can be determined by integrating the stress-strain curve: $\frac{energy}{volume} = \int_{\varepsilon_0}^{\varepsilon_b} \sigma \, d\varepsilon$. The reinforcement of elastomers with active fillers is usually associated to an enhancement of stiffness and ultimate tensile strength that can be detected in tensile test. In rubber technology sometimes is also used a reinforcement index that is defined as modulus at 300% strain divided by modulus at 100% strain.[43]

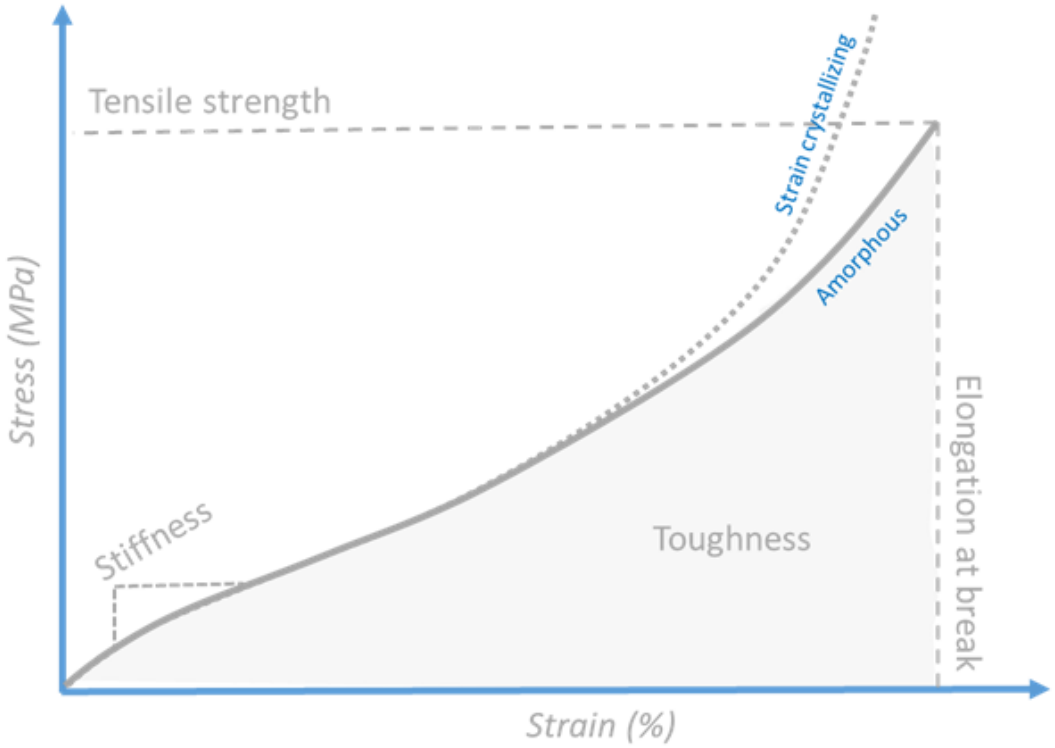

Figure 46 - General shape of the stress-strain curve for elastomeric specimens.

Preparation

After mixing, rubber compounds were left to rest at room temperature for 24 h. Subsequently, they were reduced into 8 mm thick sheets using a two-roll mill and vulcanized in a hydraulic press at 151 °C or 170 °C, pressure 4.3 bar for 10-30 minutes. Five dumbbell shaped test specimens were die-cut for each compound sheet and their thickness was accurately measured. Stress–strain curves were recorded as the samples were progressively strained. The tensile stress was recorded at Dynamic mechanical properties 10, 50, 100, and 300% elongation; tensile strength (ultimate tensile stress) and elongation at break (ultimate elongation) were also recorded.

Equipment and setup

Tensile stress/strain analyses were performed using a Zwick/Roell tensile testing machine, the parameters of the measurement were set in compliance with ISO 37 and UNI 6065 standards. The data reported in tables are the mean of 5 analyses, plotted curves are relative to the median sample.

DMA / RPA - *Dynamic Mechanical Analysis / Rubber Processing Analyzer*

The analysis of the dynamic mechanical properties of elastomers can provide useful additional information that are complementary to the insight obtained with static techniques. In oscillatory tests a specimen is deformed under dynamic conditions, with the imposed strain γ following a periodic law:

$$\gamma = \gamma_0 \sin \omega t$$

Where γ_0 is the maximum deformation and $\omega = 2\pi\nu$ is the frequency (in rad/s). The resulting stress is also sinusoidal and has the same frequency. For elastic materials, the stress is in phase with the strain ($\sigma_0 = \gamma_0 G$), on the contrary, for viscous materials, stress and strain are out of phase by 90° ($\sigma_0 = \eta\dot{\gamma}$; where $\dot{\gamma} = \frac{\partial\gamma}{\partial t}$ and η = viscosity). Elastomers are viscoelastic materials; the stress is out of phase with the strain with an angle δ (0° > δ > 90°). The stress for a viscoelastic material is:

$$\sigma = \sigma_0 \sin(\omega t + \delta) = \sigma_0(\sin\delta\cos\omega t + \cos\delta\sin\omega t)$$

The relationship between stress and strain can be defined by two components: one in phase with deformation that represents the stored energy (elastic or storage modulus G') and one out of phase by 90° representing the energy dissipated as heat (viscous or loss modulus G'').

$$\sigma = \gamma_0(G'\sin\omega t + G''\cos\omega t)$$

Where $G' = \frac{\sigma_0}{\gamma_0}\cos\delta$; $G'' = \frac{\sigma_0}{\gamma_0}\sin\delta$; $\frac{G''}{G'} = \tan\delta$ and $G^* = G' + iG''$.[44]

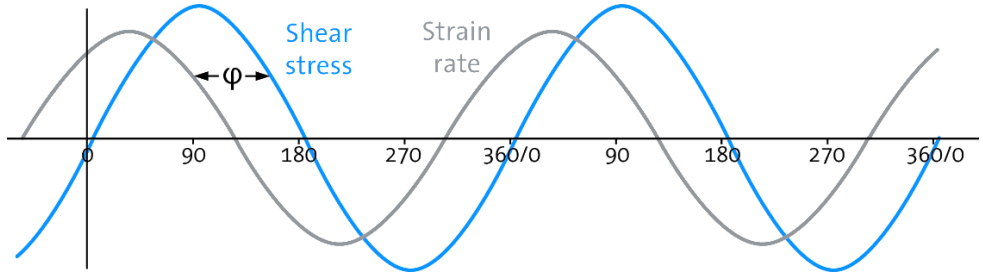

Figure 47 - Dynamic viscoelastic modulus G is obtained as a function of strain frequency (ω) (reproduced from reference[45]).*

The analysis of the complex modulus (G*), storage modulus (G'), loss modulus (G'') and the dumping factor (tan δ) can give a deeper insight into the reinforcing mechanism of filled elastomers.[46] The samples can be analyzed with common instruments suitable for dynamic testing, however on elastomeric materials is often used the Rubber Process Analyzer (RPA), a dynamic mechanical rheological tester especially designed for rubber blends and filled rubbers. The relationship between several characteristics of traditional fillers (e.g.

loading, particle size, surface area, structure and surface activity), like silica and especially carbon black, and the dynamic properties of the composite materials has been studied by several authors and a conspicuous amount of literature is available.[43,46–54] The addition of fillers to rubber compounds has a strong impact on the static and dynamic behavior of rubber samples. The behavior of the complex shear modulus vs. dynamic deformation of filled elastomers is often idealized as the result of four main contributions: three are strain independent and one is strain dependent (figure 48). The *polymer network* (1) corresponds to the modulus of the unfilled elastomer and depends by the characteristics of the polymer and is influenced by vulcanization (crosslink density). The *hydrodynamic effect*s (2) is the effect of strain amplification due to the presence of undeformable colloidal spherical particles (filler) as predicted by the Einstein-Guth-Gold expression: $\frac{\eta}{\eta_0} = \frac{G}{G_0} = 1 + 2.5\varphi + 14.1\,\varphi^2$; where η_0 and G_0 are the viscosity and the shear modulus of the unfilled elastomer respectively, and φ is the filler fraction. The *in-rubber structure* (3) is a combination of the structure assumed by the filler in the polymeric matrix and the strength of filler-polymer interactions. It is a measure of the bound and occluded rubber, it affects reinforcement because the rubber that is shielded from deformations increases the effective concentration of the filler. *Filler network* (4) represents the sum of all the filler-filler interactions. The contribution of the filler network to the modulus decreases at higher deformations, the behavior is attributed to the breakdown of filler agglomerates and is known as Payne effect. The model is built upon decades of experiments with carbon black (CB). However, most considerations are based on general principles and can be successfully extended to other fillers (like silicas), even if there might be some differences.

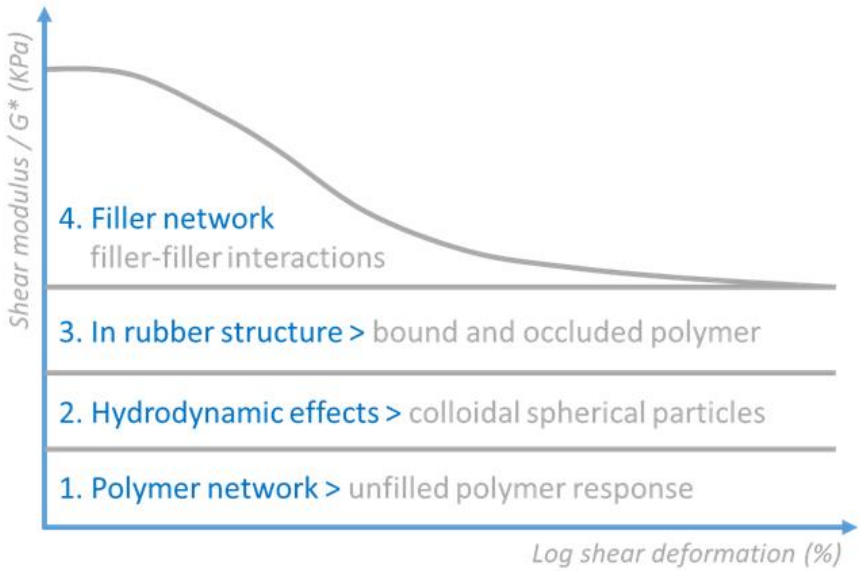

Figure 48 - Strain dependent and independent contributions to the idealized complex modulus of filled elastomers.

Unfilled rubber should display no Payne effect and G* should be strain independent. Payne effect increases with **filler concentration (loading)** and during vulcanization because of fillers **flocculation**. Payne effects is reduced with longer mixing times because they promote better **dispersions**. Tan δ decreases with filler loadings in the green (un-vulcanized) compounds at low to medium strains, then increases fast at high strain when the filler-network breaks down. After vulcanization, the polymer is more elastic and has almost no hysteresis. In vulcanized specimens tan δ increases with filler concentration, the hysteresis is associated with the breakdown of the filler-network. The higher the **surface area** (SA) the higher the Payne effect. On the contrary, the modulus at high deformations (G_∞) is unaffected by SA. This is because high surface areas usually correspond to small **particle size**, when particle size decreases, interaggregate distance decreases, and networking increases. With high **structure** fillers, the modulus is enhanced at all strains, while Payne effect is not significantly affected. When the **surface activity** of the filler is lowered (graphitized CB or non-compatibilized silica), filler-polymer interactions are hindered, thus the modulus is increased at low strains (more filler-filler interactions) and decreases at high strains. Regarding silica, there are some differences that deserve to be noted. The filler network of silica is stronger due to hydrogen bonding (vs. van der Waals bonding of carbon black) and breaks down at higher strain amplitudes and a wider range. Functionalization of silica with coupling agents decreases the modulus at low strains, and enhance the modulus at high strain. As a result, Payne-effect is greatly diminished.

Procedure

A sample of around 5.5 grams was cut from the rubber compounds and placed between two thin Mylar films measuring 4x4 cm. Afterwards the sample covered on both sides by the polymeric films was manually placed in the measurement pod of the RPA.

Instrument

The tests were performed with a RPA 2000 Alpha Technologies rubber process analyzer. Alternatively, when it was not possible to use RPA, dynamic properties of rubber compounds were recorded using a ARES-G2 TA instruments rotational rheometer.

Density

To know the density of the fillers is important for rubber compounding, as it is needed to calculate the total volume occupied by the compounds and the weight of the ingredients in relation to the volume of the internal chamber mixer and the fill factor. In addition, filler with lower densities are considered a technological advantage as they can help to reduce the total weight of tyres, increasing the efficiency. The density was measured on few grams of well dried powder materials, with a Micromeritics Accupy C 1330 helium pycnometer, the results are the average of five measurements.

Swelling measurements (bound rubber and crosslink density)

The bound rubber can be evaluated measuring the rubber that can be extracted by a good solvent on green compounds. Roughly 500 mg of each rubber compound were immersed in an excess of toluene (25 mL) for one week and toluene was replaced twice. Afterwards the samples were left to air dry for three days under the fume hood and were finished in oven under vacuum at 35 °C for few hours. The bound rubber (BR) was calculated according to the equation:[55]

$$BR = 100\,\frac{W_{fg} - W_t\left(\frac{m_f}{m_f + m_r}\right)}{W_t\left(\frac{m_r}{m_f + m_r}\right)}$$

where W_{fg} the weight of filler and gel, W_t the weight of the sample, m_f the fraction of filler in the compound, m_r the fraction of rubber in the compound. The crosslinking density of the vulcanized compounds was also determined by solvent-swelling measurements with toluene. About 500 mg of the vulcanized samples were placed in an excess of toluene (25 mL) and were left to reach equilibrium (3 days at RT). Afterwards the samples were removed from the solvent, lightly tapped with paper and quickly weighted. The crosslinking density (CD) was determined applying the Flory–Rhener equation:[56–58]

$$CD = \frac{-[\ln(1 - V_R) + V_R + \chi V_R^2]}{\rho_R V_0\left(V_R^{\frac{1}{3}} - \frac{V_R^2}{2}\right)}$$

Where ρ_ρ is the density of rubber (0,92 g/cm^3), V_0 is the molar volume of the solvent (106,3 cm^3/mol for toluene), V_R is the volume fraction of rubber in the swollen material, and χ is the the Flory-Huggins polymer-solvent interaction term (0,36).

References

(1) Faix, O.; Argyropoulos, D. S.; Robert, D.; Neirinck, V. Determination of Hydroxyl Groups in Lignins Evaluation of ^{1}H-, ^{13}C-, ^{31}P-NMR, FTIR and Wet Chemical Methods. *Holzforschung* **1994**, *48* (5), 387–394.

(2) Pu, Y.; Cao, S.; Ragauskas, A. J.; Ragauskas, A. J.; Williams, C. K.; Davison, B. H.; Britovsek, G.; Cairney, J.; Eckert, C. A.; Frederick, W. J.; et al. Application of quantitative 31P NMR in biomass lignin and biofuel precursors characterization. *Energy Environ. Sci.* **2011**, *4* (9), 3154.

(3) Stebbins, J. F. Identification of multiple structural species in silicate glasses by 29Si NMR. *Nature* **1987**, *330* (6147), 465–467.

(4) Maciel, G. E.; Sindorf, D. W. Silicon-29 NMR study of the surface of silica gel by cross polarization and magic-angle spinning. *J. Am. Chem. Soc.* **1980**, *102* (25), 7606–7607.

(5) You, T.-T.; Mao, J.-Z.; Yuan, T.-Q.; Wen, J.-L.; Xu, F. Structural Elucidation of the Lignins from Stems and Foliage of Arundo donax Linn. *J. Agric. Food Chem.* **2013**, *61* (22), 5361–5370.

(6) Tejado, A.; Peña, C.; Labidi, J.; Echeverria, J. M.; Mondragon, I. Physico-chemical characterization of lignins from different sources for use in phenol-formaldehyde resin synthesis. *Bioresource Technology*. 2007, pp 1655–1663.

(7) You, T. T.; Zhang, L. M.; Zhou, S. K.; Xu, F. Structural elucidation of lignin-carbohydrate complex (LCC) preparations and lignin from Arundo donax Linn. *Ind. Crops Prod.* **2015**, *71*, 65–74.

(8) Kline, L. M.; Hayes, D. G.; Womac, A. R.; Labbe, N. SIMPLIFIED DETERMINATION OF LIGNIN CONTENT IN HARD AND SOFT WOODS VIA UV-SPECTROPHOTOMETRIC ANALYSIS OF BIOMASS DISSOLVED IN IONIC LIQUIDS. *BioResources* **2010**, *5* (3), 1366–1383.

(9) You, T.-T.; Mao, J.-Z.; Yuan, T.-Q.; Wen, J.-L.; Xu, F. Structural Elucidation of the Lignins from Stems and Foliage of Arundo donax Linn. *J. Agric. Food Chem.* **2013**, *61* (22), 5361–5370.

(10) Lisperguer, J.; Perez, P.; Urizar, S. Structure and thermal properties of lignins: Characterization by infrared spectroscopy and differential scanning calorimetry. *J. Chil. Chem. Soc.* **2009**, *54* (4), 460–463.

(11) Frigerio, P.; Zoia, L.; Orlandi, M.; Hanel, T.; Castellani, L. Application of sulphur-free lignins as a filler for elastomers: Effect of hexamethylenetetramine treatment. *BioResources* **2014**, *9* (1), 1387–1400.

(12) Rosa, S. M. L.; Rehman, N.; de Miranda, M. I. G.; Nachtigall, S. M. B.; Bica, C. I. D. Chlorine-free extraction of cellulose from rice husk and whisker isolation. *Carbohydr. Polym.* **2012**, *87* (2), 1131–1138.

(13) Kačuráková, M.; Capek, P.; Sasinková, V.; Wellner, N.; Ebringerová, A. FT-IR study of plant cell wall model compounds: pectic polysaccharides and hemicelluloses. *Carbohydr. Polym.* **2000**, *43* (2), 195–203.

(14) James, J.; Rao, M. S. Silica from rice husk through thermal decomposition. *Thermochim. Acta* **1986**, *97*, 329–336.

(15) Liou, T.-H. Preparation and characterization of nano-structured silica from rice husk. *Mater. Sci. Eng. A* **2004**, *364* (1), 313–323.

(16) Buslov, D. K.; Kaputski, F. N.; Sushko, N. I.; Torgashev, V. I.; Solov'eva, L. V.; Tsarenkov, V. M.; Zubets, O. V.; Larchenko, L. V. Infrared spectroscopic analysis of the structure of xylans. *J. Appl. Spectrosc.* **2009**, *76* (6), 801–805.

(17) Peng, F.; Bian, J.; Peng, P.; Guan, Y.; Xu, F.; Sun, R.-C. FRACTIONAL SEPARATION AND STRUCTURAL FEATURES OF HEMICELLULOSES FROM SWEET SORGHUM LEAVES. *BioResources* **2012**, *7* (4), 4744–4759.

(18) Olsson, A.-M.; Salmén, L. The association of water to cellulose and hemicellulose in paper examined by FTIR spectroscopy. *Carbohydr. Res.* **2004**, *339* (4), 813–818.

(19) Yang, H.; Yan, R.; Chen, H.; Lee, D. H.; Zheng, C. Characteristics of hemicellulose, cellulose and lignin pyrolysis. **2007**.

(20) Kačuráková, M.; Wellner, N.; Ebringerová, A.; Hromádková, Z.; Wilson, R. .; Belton, P. . Characterisation of xylan-type polysaccharides and associated cell wall components by FT-IR and FT-Raman spectroscopies. *Food Hydrocoll.* **1999**, *13* (1), 35–41.

(21) Pandey, K. K. A study of chemical structure of soft and hardwood and wood polymers by FTIR spectroscopy. *J. Appl. Polym. Sci.* **1999**, *71* (12), 1969–1975.

(22) Kačuráková, M.; Belton, P. S.; Wilson, R. H.; Hirsch, J.; Ebringerová, A. Hydration properties of xylan-type structures: an FTIR study of xylooligosaccharides. *J. Sci. Food Agric.* **1998**, *77* (1), 38–44.

(23) Eduardo da Silva, A.; Rodrigues Marcelino, H.; Christine Salgado Gomes, M.; Eleamen Oliveira, E.; Nagashima Jr, T.; Sócrates Tabosa Egito, E. Xylan, a Promising Hemicellulose for Pharmaceutical Use.

(24) Launer, P. J. Infrared analysis of organosilicon compounds: spectra-structure correlations. *Silicone Compd. Regist. Rev.* **1987**, *100*.

(25) Lupoi, J. S.; Singh, S.; Parthasarathi, R.; Simmons, B. A.; Henry, R. J. Recent innovations in analytical methods for the qualitative and quantitative assessment of lignin. *Renew. Sustain. Energy Rev.* **2015**, *49*, 871–906.

(26) Crestini, C.; Melone, F.; Sette, M.; Saladino, R. Milled Wood Lignin: A Linear Oligomer. *Biomacromolecules* **2011**, *12* (11), 3928–3935.

(27) Salanti, A.; Zoia, L.; Tolppa, E.-L.; Orlandi, M. Chromatographic Detection of Lignin–Carbohydrate Complexes in Annual Plants by Derivatization in Ionic Liquid. *Biomacromolecules* **2012**, *13* (2), 445–454.

(28) Gosselink, R. J. A.; van Dam, J. E. G.; de Jong, E.; Scott, E. L.; Sanders, J. P. M.; Li, J.; Gellerstedt, G. Fractionation, analysis, and PCA modeling of properties of four technical lignins for prediction of their application potential in binders. *Holzforschung* **2010**, *64* (2), 193–200.

(29) ALOthman, Z.; A., Z. A Review: Fundamental Aspects of Silicate Mesoporous Materials. *Materials (Basel).* **2012**, *5* (12), 2874–2902.

(30) Lindvig, T.; Michelsen, M. L.; Kontogeorgis, G. M. A Flory-Huggins model based on the Hansen solubility parameters. *Fluid Phase Equilib.* **2002**, *203* (1–2), 247–260.

(31) Hansen, C. M. Polymer additives and solubility parameters. *Prog. Org. Coatings* **2004**, *51* (2), 109–112.

(32) and, W. T.; Wool*, R. P. Lignin Esters for Use in Unsaturated Thermosets: Lignin Modification and Solubility Modeling. **2005**.

(33) Stefanis, E.; Panayiotou, C. A new expanded solubility parameter approach. *Int. J. Pharm.* **2012**, *426* (1–2), 29–43.

(34) Flory, P. J. Thermodynamics of High Polymer Solutions. *J. Chem. Phys.* **1942**, *10* (1), 51–61.

(35) Burke, J. Solubility Parameters: Theory and Application. **1984**.

(36) HSP Basics | Hansen Solubility Parameters http://www.hansen-solubility.com/HSP-science/basics.php (accessed Jan 5, 2017).

(37) Stefanis, E.; Panayiotou, C. Prediction of hansen solubility parameters with a new group-contribution method. *Int. J. Thermophys.* **2008**, *29* (2), 568–585.

(38) Boeriu, C. G.; Fiţigău, F. I.; Gosselink, R. J. A.; Frissen, A. E.; Stoutjesdijk, J.; Peter, F. Fractionation of five technical lignins by selective extraction in green solvents and characterisation of isolated fractions. *Ind. Crops Prod.* **2014**, *62*, 481–490.

(39) Zellers, E. T.; Anna, D. H.; Sulewski, R.; Wei, X. Improved methods for the determination of Hansen's solubility parameters and the estimation of solvent uptake for lightly crosslinked polymers. *J. Appl. Polym. Sci.* **1996**, *62* (12), 2081–2096.

(40) Hansen, C. M. *Hansen Solubility Parameters: A User's Handbook*, Second.; Group, T. & F., Ed.; 2000.

(41) Khimi, S. R.; Pickering, K. L. A New Method to Predict Optimum Cure Time of Rubber Compound Using Dynamic Mechanical Analysis. **2014**, *40008*, 1–6.

(42) Tobergte, D. R.; Curtis, S. *Science and Technology of RUBBER (3rd edition)*; James E., M., Burak, E., Frederick R., E., Eds.; Elsevier, 2013; Vol. 53.

(43) Fröhlich, J.; Niedermeier, W.; Luginsland, H. D. The effect of filler-filler and filler-elastomer interaction on rubber reinforcement. *Compos. Part A Appl. Sci. Manuf.* **2005**, *36* (4), 449–460.

(44) M. Guaita, F. Ciardelli, La Mantia, E. P. *Fondamenti di scienza dei polimeri*, Edizioni N.; 2006.

(45) Scientific Instrumentation - Biolin Scientific http://www.biolinscientific.com/ (accessed Dec 17, 2016).

(46) Niedermeier, W.; Fro, J. Reinforcement Mechanism in the Rubber Matrix by Active Fillers. **2002**, No. 7.

(47) Meier, J. G.; Klüppel, M.; Gopalan Nair, K.; Dufresne, A.; Andrews, E. H.; Ismail, H.; Nordin, R.; Noor, A. M.; Molina-boisseau, S.; Dufresne, A.; et al. Carbon black networking in elastomers monitored by dynamic mechanical and dielectric spectroscopy. *Compos. Sci. Technol.* **2005**, *221* (5), 565–569.

(48) Robertson, C. G.; Lin, C. J.; Bogoslovov, R. B.; Rackaitis, M.; Sadhukhan, P.; Quinn, J. D.; Roland, C. M. Flocculation, Reinforcement, and Glass Transition Effects in Silica-Filled Styrene-Butadiene Rubber. *Rubber Chem. Technol.* **2011**, *84* (4), 507–519.

(49) Cassagnau, P. Melt rheology of organoclay and fumed silica nanocomposites. *Polymer (Guildf).* **2008**, *49* (9), 2183–2196.

(50) Cassagnau, P. Payne effect and shear elasticity of silica-filled polymers in concentrated solutions and in molten state. *Polymer (Guildf).* **2003**, *44* (8), 2455–2462.

(51) Chazeau, L.; Brown, J. D.; Yanyo, L. C.; Sternstein, S. S. Modulus recovery kinetics end other insights into the Payne effect for filled elastomers. *Polym. Compos.* **2000**, *21* (2), 202–222.

(52) Lion, a.; Kardelky, C.; Haupt, P.; Of, E.; Of, N. on the Frequency and Amplitude Dependence of the Payne Effect : Theory and Experiments. *Rubber Chem. Technol.* **2003**, *76* (2), 533–547.

(53) Ramier, J.; Gauthier, C.; Chazeau, L.; Stelandre, L.; Guy, L. Payne effect in silica-filled styrene–butadiene rubber: Influence of surface treatment. *J. Polym. Sci. Part B Polym. Phys.* **2007**, *45* (3), 286–298.

(54) Leblanc, J. L. Rubber-filler interactions and rheological properties in filled compounds. *Prog. Polym. Sci.* **2002**, *27* (4), 627–687.

(55) Choi, S.-S. Influence of storage time and temperature and silane coupling agent on bound rubber formation in filled styrene–butadiene rubber compounds. *Polym. Test.* **2002**, *21* (2), 201–208.

(56) Joseph, R.; George, K. E.; Francis, D. J.; Thomast, K. T. Polymer-Solvent Interaction Parameter for NR / SBR and NR / BR Blends. *Int. J. Polym. Mater.* **1987**, *12*, 29–34.

(57) El-Sabbagh, S. H.; Yehia, A. A. Detection of Crosslink Density by Different Methods for Natural Rubber Blended with SBR and NBR. *Egypt. J. Solids* **2007**, No. 302.

(58) Arroyo, M.; López-Manchado, M. .; Herrero, B. Organo-montmorillonite as substitute of carbon black in natural rubber compounds. *Polymer (Guildf).* **2003**, *44* (8), 2447–2453.

CAP 5 - Production of sustainable materials form lignocellulosic biomasses through an integrated biorefinery process and assessment of their applicability in elastomeric composites

The growing request for more eco-friendly materials is promoting the research of alternatives to products derived from fossil feedstocks. Lignocellulosic biomasses are expected to play a major role in the transition towards a biobased economy due to their large annual availability, low-cost, carbon neutrality and composition. The concept of producing materials from renewable lignocellulosic biomasses is compelling, however, to be exploited, lignocellulosic biomasses must be fractionated into their main components. The technological challenge is to setup a process that is environmentally and economically sustainable. In this study two lignocellulosic feedstocks were selected and fractionated to produce several bio-commodities through an integrated biorefinery process characterized by a low environmental impact. Afterwards the products were tested in composites with natural rubber to assess the potential for the manufacturing of greener elastomeric composites.

5.1 Selection of the lignocellulosic feedstocks

The selected lignocellulosic feedstocks are rice husk (RH) and *Arundo donax (*AD). Rice husk is a nice example of lignocellulosic biomass that could represent a viable source of sustainable products. Rice husk or rice hull is the protecting cover of rice grains. Rice is a major agricultural product cultivated all around the world, its annual production is expected to reach 7,5 x 10^8 tonnes in 2016.[1] Rice husk accounts for 20% of the weight of the rice harvested, hence about 1,5 x 10^8 tons of the lignocellulosic by-product are produced every year. Besides being already collected rice husk has another advantage, in fact it is naturally shaped in small pieces (few millimetres) and can be immediately processed avoiding additional energy-consuming mechanical pre-treatments. The utilization of rice husk is also strongly advocated to pose a solution to the disposal problem and to reduce the cost of waste management. Many uses have been proposed taking into account the organic components of RH (energy, activated carbon, fertilizers, animal feed, bioethanol) or the substantial content of inorganic matter (low-cost biological source of silica).[2] However, the high content of ashes usually hinders the exploitation of the organic fractions while the recovery of SiO_2 is achieved through the incineration of the organic fraction. The simultaneous recovery of several components and their conversion in high value-

added products may represent a more effective strategy for the valorisation of this agricultural side-product. *Arundo donax,* also known as giant cane, is a perennial herbaceous plant characterized by a high degree of adaptability and high biomass productivity. It can be cultivated in marginal lands, not suitable for food crops, in a wide range of soil types and climatic conditions.[3] Differently from rice husk, *Arundo donax* doesn't possess a considerable inorganic fraction, hence the valorisation strategy must be centred on the conversion of cellulose, hemicellulose and lignin in valuable products.

5.2 Materials

Rice husk and *Arundo donax* were kindly provided by a local farm. All reagents and solvents (ACS grade) were purchased from Sigma-Aldrich and used as received without further purification.

5.3 Composition of rice husk and *Arundo donax*

The initial compositions of rice husk (RH) and *Arundo donax* (AD) were characterized evaluating the relative abundance of polysaccharides, lignin, and ashes.

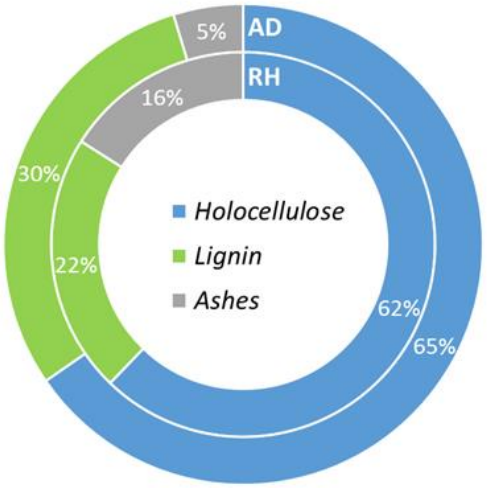

Figure 49 - Composition of RH and AD

Experimental

The **holocellulose content** (total polysaccharides) was evaluated using the following equation: [100% - (lignin content + ash content)]. The **lignin content** was measured with the methodology reported by Yeh et al.[4] According to the method 100 mg of oven-dried material were left in 2 mL of 72% H_2SO_4 at room temperature for 2 h. Afterwards the H_2SO_4 solution was diluted with demineralized water to 3% concentration and heated at 121 °C and 2 atm for 1 h. Vacuum assisted filtration was used to recover the acid-insoluble lignin that was then dried and accurately weighted. After dilution with 100 ml of demineralized water, the concentration of the acid-soluble lignin was calculated from the UV absorbance at 205 nm using an extinction coefficient of 110 (AU L)/(g cm). The total amount of lignin is obtained as the sum of the acid-insoluble lignin (Klason lignin) and acid soluble lignin minus the acid insoluble ash content. The **ash content** (minerals) was determined gravimetrically after the incineration of the organic fractions. Small samples of RH and AD were rinsed with demineralized water and exsiccated in oven overnight. Hundred milligrams of accurately dried samples were put in tared, well desiccated porcelain crucibles and placed in a muffle furnace set at 550°C for 3 hours. The residual solids were left to cool off in a desiccator for 10 minutes and finally weighted. The results are the average of three analyses (±1.0%) and are concisely reported in figure 49.

Results and discussion

Arundo donax was found to be characterized by 65.4% holocellulose, 29.9% lignin and 4.7% ashes, whereas rice husk was composed by 62.2% holocellulose, 21.8% lignin and 16.0% ashes. The composition of Arundo donax is in good agreement with recent literature[5] [63.5% holocellulose, 19.2% lignin and 4.2% ashes] except the value of lignin that was found to be somewhat higher. The discrepancy can be explained by the fact that lignin content vary within stems, foliage, nodes and internodes[6] and is also affected by the stage of maturity of the plant.[7] Nevertheless the presence of a higher amount of lignin, above 28%, was already reported.[8] Relative amounts of rice husk constituents were found to be in line with the compositions proposed by previous studies.[9]

5.4 Fractionation process

The biorefinery processes for *Arundo donax* (AD) and rice husk (RH) share a similar design, especially in the first steps. Nevertheless, there are few substantial differences introduced to better adapt the process to the peculiar compositions of the two lignocellulosic substrates. The specific procedures are highlighted and discussed in the following sections. An overview of the processes is offered for AD and RH in figure 50 and 51.

Experimental

Acidic Leaching – Ten grams of the air-dried lignocellulosic starting material were crushed in a blender for 5 min and sieved to exclude particles bigger than 1 mm. After the grinding the materials were soaked in 200 ml of 0.1 M HCl and kept at 100 °C for 2 h under magnetic stirring. The solids were recovered by Buchner filtration, washed with 20 ml of fresh water and air dried overnight. The filtrate was collected for successive processing.

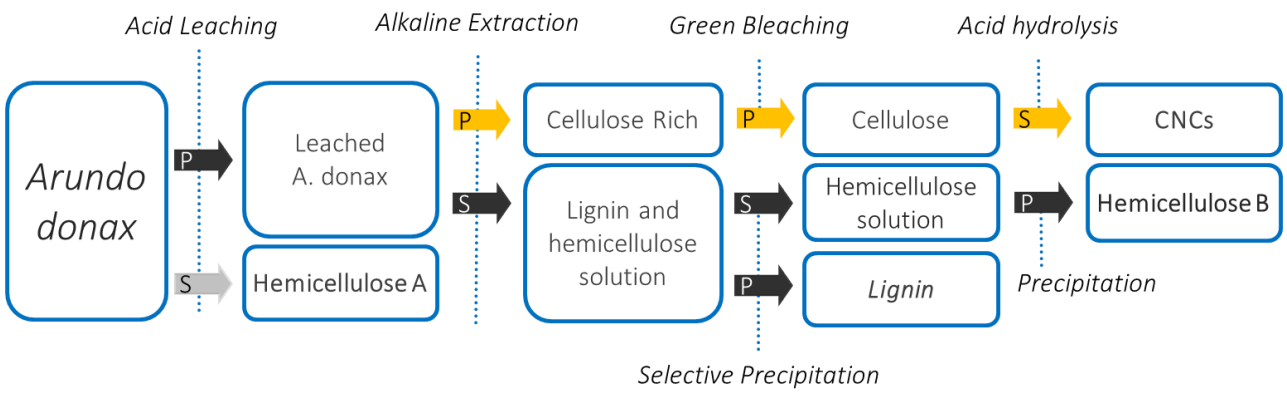

Figure 50 - Flow diagram for the biorefinery processing of AD (P = precipitate, S = supernatant).

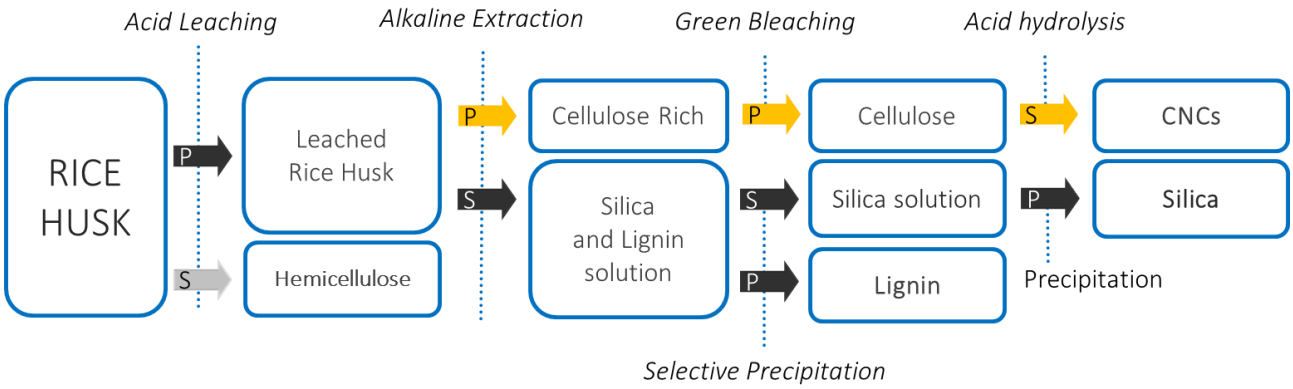

Figure 51 - Flow diagram for the biorefinery processing of RH (P = precipitate, S = supernatant).

Alkaline extraction – Both untreated starting materials (references) and leached samples were treated with 200 mL of 0.1 M NaOH for a specific period (1 or 2 h) at 100 °C under magnetic stirring. The cellulose rich insoluble material, was separated by filtration from the solubilized fractions and washed with 20 mL of a 0.1 M NaOH aqueous solution. The filtrate was acidified with 5 M HCl until pH 1 to promote the precipitation of lignin. The brown sediment was recovered by centrifugation (3500 g, 10 min), washed with deionized water, and freeze-dried. The aqueous supernatant was also collected and briefly stored for successive processing.

Recovery of Hemicellulose (Hemicellulose A for AD) – The filtrate collected at the end of the leaching step was reduced in volume under vacuum and poured into a ten-fold volume of ethanol (absolute alcohol, 99.8%) and cooled at 4°C for 24 h to precipitate the polysaccharides. The white precipitate, named Hemicellulose A, was recovered by centrifugation (3500 g, 10 min) and air dried.

Recovery of Hemicellulose B (AD only) – The aqueous supernatant separated from lignin at the end of the alkaline extraction was reduced in volume by rotavapor and poured into a ten-fold volume of ethanol to precipitate hemicelluloses. After 24h at 4 °C, the precipitated matter named Hemicellulose B, was recovered by means of centrifugation (3500g, 10 min) and air dried.

Silica recovery (RH only) – The aqueous supernatant collected during lignin precipitation was transferred in a round bottom flask, then the pH was adjusted to 4 slowly adding a 0.5 M NaOH solution while under magnetic stirring. Afterwards the solution was heated to 90 °C for 4h to precipitate the silica. The precipitated white powder was purified with 3 centrifugation cycles (3500g, 10 min) to remove the water-soluble salts resulting from the neutralization. The recovered silica was finally oven dried at 100 °C overnight.

Totally chlorine free bleaching – The procedure is an adaptation of a published method optimized for the delignification of aspen wood.[10] Five grams of cellulose-rich solids were treated with 150 mL of bleaching solution for 4 hours at 100 °C under vigorous stirring. The water based bleaching solution contains acetic acid (25 wt%), hydrogen peroxide (4 wt%) and sulfuric acid (2 wt%). At the end of the treatment the bleached

samples were recovered by filtration (Büchner), washed with cold demineralized water and finally oven dried at 60 °C overnight.

Cellulose acidic hydrolysis and nanocrystal isolation – Cellulose nanocrystals (CNCs) were obtained hydrolysing the amorphous components of the of the bleached cellulose-rich materials. The depolimerization was achieved soaking the bleached cellulose-rich substrates in an ice-cold solution of concentrated sulphuric acid (60 wt% - 9 mL x g of cellulose) for 30 minutes and then raising the temperature at 55 °C for 60-120 minutes under vigorous stirring. The reaction was quenched pouring the solution in a large amount of cold water (10 mL x mL of acidic solution) and stirred for 10 min. The white sediment was purified by repeated cycles of centrifugation (3200 g for 15 min) and re-suspension. After every centrifugation round, the supernatant was discarded and the solid residue was re-suspended in distilled water through 5 minutes of ultrasonication. After several cycles, when the pH approached neutrality (>4) a turbid supernatant was obtained. At this point the cellulose nanocrystals were further purified with dialysis against distilled water until the suspension reached a pH of 5–6 was. To calculate the yield, 10 mL of the suspension containing the CNCs were dried in oven at 100 °C until the solid reached constant weight.

Acidolytic lignin isolation (reference lignin) – To recover the acidolytic lignin the fibres were hydrolysed with concentrated sulphuric acid in compliance with the methodology reported in reference.[11]

The experimental procedures used to the characterize the products are described in chapter 4: Materials preparations and characterizations > 4.1 Analytical techniques.

Results and discussion

The first step of the process is the pre-treatment of the lignocellulosic biomasses with a rather diluted acidic solution. Recently, it was demonstrated the superior efficiency of a combined acidic-alkaline treatments in increasing the digestibility of cellulose for bio-ethanol production.[12–16] To assess the impact of the acid pre-treatment, the quality of the products was assessed with several characterization techniques and compared with the references obtained with the sole alkaline treatment (all performed at 100 °C) and the lignin obtained through the acidolytic method. The results relative to the yields, the purity degrees, and the quantification of the functional groups of the recovered lignin are reported in table 15. The purity was assessed with the Klason method, while the yields were calculated with respect to the initial lignin content reported in section 5.3. The lignins isolated exclusively with the alkaline treatments resulted heavily contaminated with high levels of hydrolysable fibres (cleaved during the Klason assessment). The extension of the treatment resulted in a moderate increase in both yield and purity. The degree of purity is also reflected in the results of FTIR and 31P-NMR analysis. The lignins recovered with the sole alkaline treatment presented a fraction that was insoluble in analytical solvent, incomplete lignin solubilisation is often related

Arundo donax	NaOH (1h)	NaOH (2h)	HCl (2h) + NaOH (2h)	Acidolytic
Purity (%)	45	55	90	95
Lignin Yield (%)	43	53	45	48
31P-NMR (mmol · g^{-1})				
Aliphatic -OH	1.48*	1.68*	3.45	4.35
S-OH + Cond.	0.02*	0.18*	0.48	0.32
G-OH	0.17*	0.23*	0.67	0.61
H-OH	0.02*	0.07*	0.22	0.53
-COOH	0.27*	0.28*	0.78	0.15

* Incomplete solubility.

Table 14 - Purity, yield and functional groups of AD lignin samples obtained with different extraction methods.

Rice husk	NaOH (4h) *	HCl (2h) + NaOH (2h)	Acidolytic
Purity (%)	78	95	90
Lignin Yield (%)	29	46	51
31P-NMR (mmol g-1)			
Aliphatic -OH	3.71	3.32	3.03
S-OH + Cond.	0.13	0.36	0.23
G-OH	0.38	0.59	0.65
H-OH	0.14	0.50	0.65
-COOH	0.59	0.88	0.23
GPC (g/mol)			
Mp	4500	3900	5100
Mn	13600	8800	10200
Mw	115000	32500	41000
PD	8.4	3.7	4.0

*data from reference[17]

Table 15 - Purity, yield, functional groups concentration and average molecular weights of RH lignin samples obtained with different extraction methods.

to the presence of polysaccharide impurities. The amount of free phenolic moieties increased to some extent with longer extraction times. The substantial amount of polysaccharides is also detectable in the results of the FT-IR analysis (figure 52 and 53). The lignins obtained with NaOH-1h and NaOH-2h extractions display a characteristic peak in the 1100–1000 cm^{-1} range attributable to the C-O stretching vibration typical of polysaccharides. The effect of the combined acidic-alkaline treatment (0.1 M HCl, 100 °C, 2 h + 0.1M NaOH, 100 °C, 2 h) is clearly recognisable in the results presented in table 14 and 15. The introduction of the acid pre-treatment, influenced significantly the degree of purity that increased from 55% to 90% for AD and from 78% to 95% for RH. The high levels of purity and the yields obtained with the combined process resemble those of the acidolytic lignin. In the process of isolation of the acidolytic lignin carbohydrates are hydrolysed, hence virtually all the organic matter present in the sample is lignin. The FT-IR analysis (Figure 52 and 53) of

the lignins obtained with the combined acid + alkaline extraction, reflects the increase in purity. The spectra are very similar to the spectra of the acidolytic reference and the peak related to C-O stretching vibrations resulted largely resized. 31-P-NMR analysis revealed a general increase in both aliphatic and phenolic groups. This trend can be attributed to the enhanced solubility into the analytical solvent and the hydrolysis of ester-type lignin-carbohydrate complexes. On the ensemble, the NMR values align to the values observed for the reference, except for the concentrations of carboxyl moieties that are much higher. The molecular weight distributions of the lignins extracted with the several methods were also analysed (GPC) after chemical modification (acetylation in ionic liquid) to ensure the complete solubilisation in the solvent of choice (THF). In figure 54 are reported the chromatograms acquired for the different lignin samples extracted from *Arundo donax*. The chromatographic system is equipped with a UV detector that was set at 280 nm. The instrumental response of carbohydrates is negligible at this wavelength and only molecules containing aromatic or unsaturated moieties are detectable. However, high molecular weights are attributable to carbohydrates, this could be a hint of a presence of Lignin Carbohydrate Complexes (LCC). In fact, the presence of hemicellulose connect to aromatic compounds (phenolic compounds and/or lignin) in *Arundo donax* is already reported.[18] For this reasons, the high molecular weights, exceeding 100.000 g · mol^{-1}, can be attributed to hemicelluloses linked to phenolic compounds. The solid line (Ref AD acetylated) is relative to the starting, unrefined, acetylated lignocellulosic material. While the molecular weights distribution of the unfractionated material is unimodal the curves relative to the lignins extracted with the alkaline treatments reveal bi- or multi-modal distributions. This phenomenon can be attributed to the partial hydrolysis of the lignin-carbohydrate complexes, and is compatible with the partial release of lignin, characterized by lower molecular weights. Nevertheless, a fraction of lignin is clearly still connected to the carbohydrates. This trend seems to be clearly time dependent, in fact, when the alkaline extraction is protracted (from 1 to 2 h), there is a change in the chromatographic peaks, and the peak attributable to the "free" lignin (around 10.000 g · mol^{-1}) becomes predominant. When the alkaline extraction is combined with the acid leaching the average molecular drops and the distribution is unimodal (apart from the small peaks associable to the presence of oligomers). The peak associated to lignin-carbohydrate complexes completely disappears, and the chromatogram corresponds to the reference acidolytic lignin. This trend of the molecular weight distributions, in combination with the result of the spectroscopic characterization, gives a strong evidence that the double treatment (HCl + NaOH) is much more effective in cleaving the LCCs and that hemicellulose that is normally extracted during the alkaline treatment, is whether extracted during the acid leaching or is still extracted during the alkaline treatment but is efficiently separated from lignin. Overall, the analyses collected indicated that, in the starting material, a certain amount of polysaccharides are covalently bonded with lignin and that a combined acidic-alkaline treatment improves the degradation of LCCs resulting in the isolation of a pure lignin fraction. Considering the positive results obtained for *Arundo donax*, the combined acidic-alkaline treatment was also applied for the fractionation of rice husk. The data relative to lignin yield,

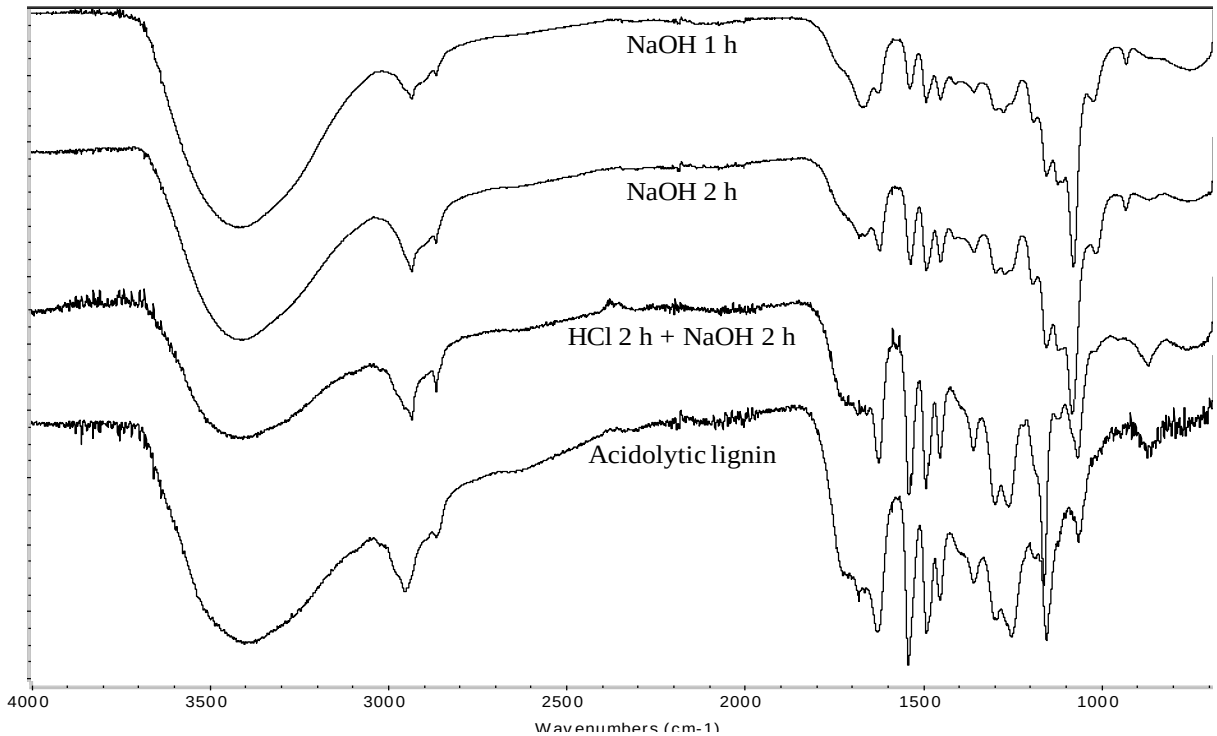

*Figure 52 - FT-IR spectra of **Arundo donax** lignin samples recovered with different extraction methods.*

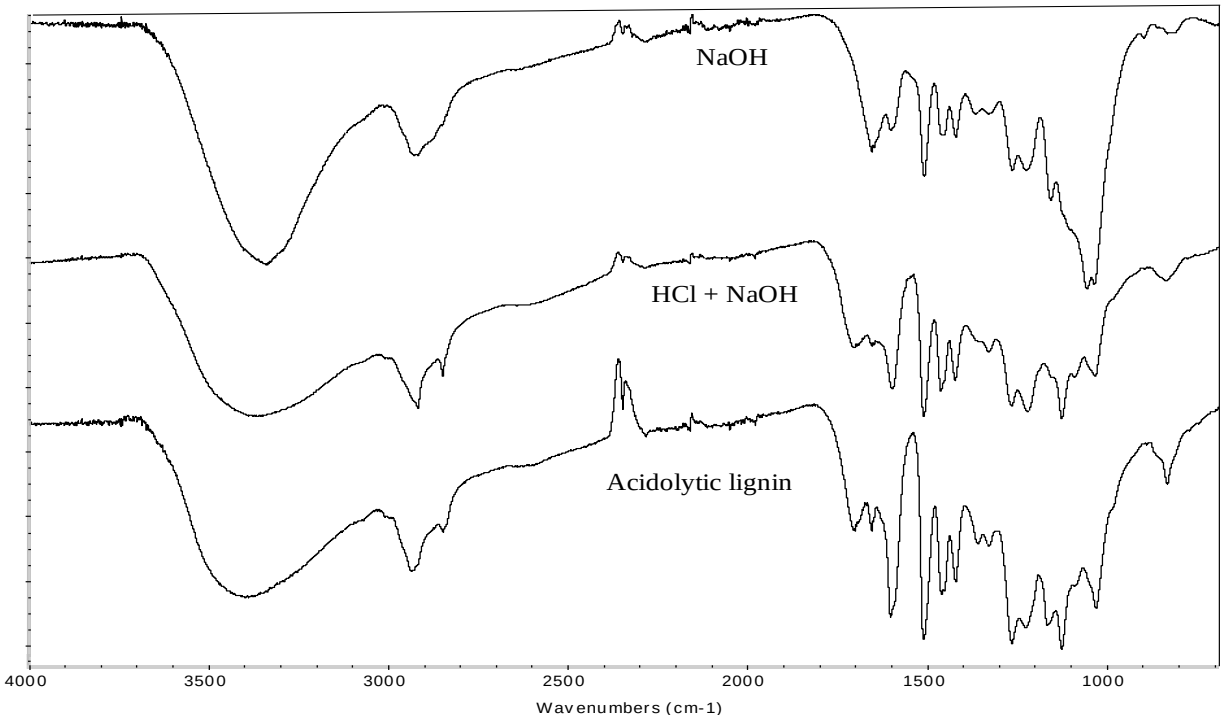

*Figure 53 - FT-IR spectra of **rice husk** lignin samples recovered with different extraction methods.*

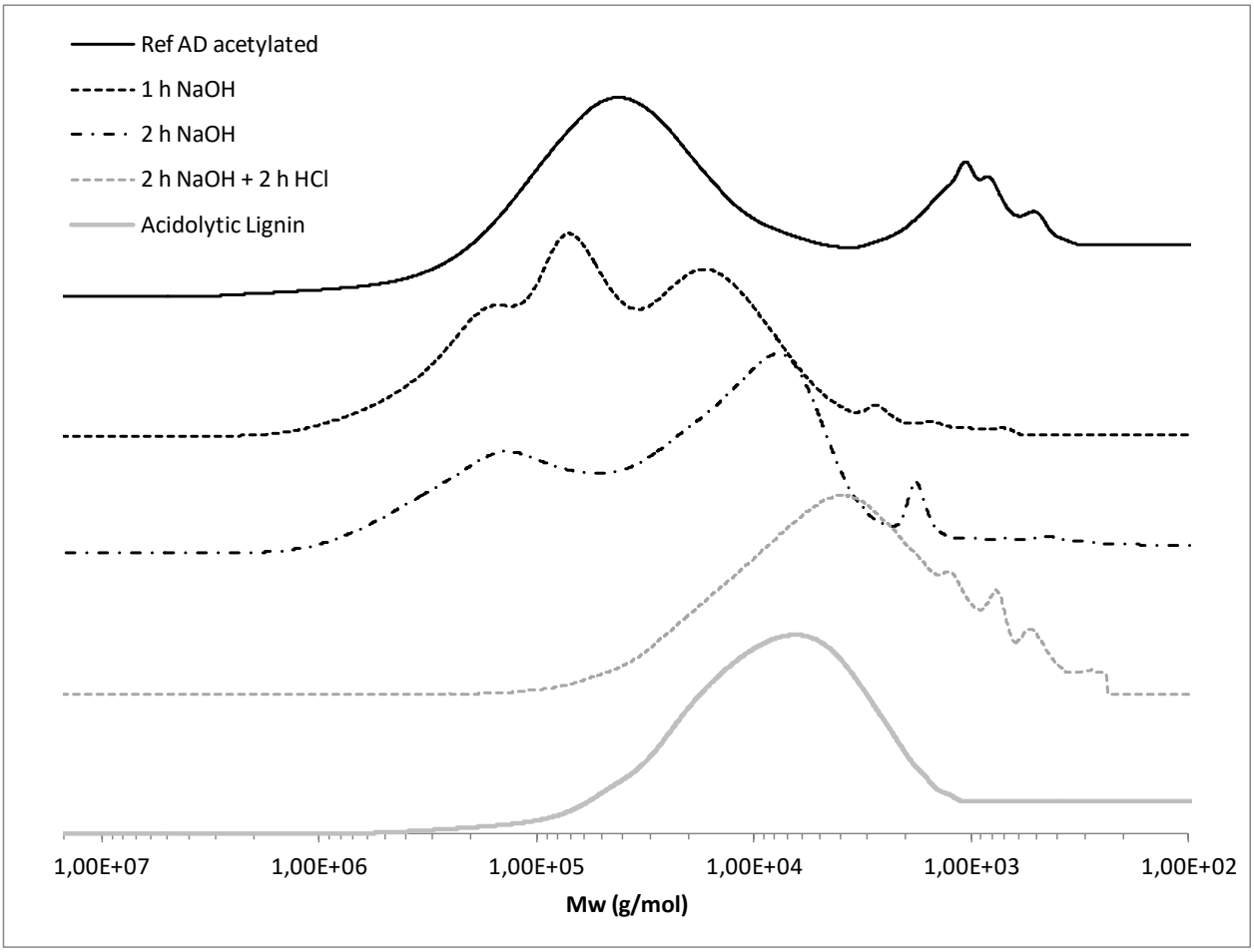

*Figure 54 - Molecular weight distributions (GPC) for acetylated of **Arundo donax** samples.*

purity, labile hydroxyls distribution, and average molecular weight indexes are compared with the same results obtained by Salanti et al. (2010),[17] where the authors optimized the lignin extraction using the alkaline treatment. Acidolytic lignin is also reported as a reference. The optimized alkaline treatment utilizes harsher reaction conditions (NaOH concentration from 0,1M up to 0,3M and extraction time 4h, up from 2h), nonetheless purity and yield are lower. There is a solid evidence that the acidic leaching treatment followed by alkaline extraction enhanced the degradation of the lignin-carbohydrates and consequently also the yield and the purity of lignin. To gain a greater insight regarding the molecular structure of the lignins isolated with the biorefinery process, both AD and RH products were subjected to 2D-HSQC NMR analysis. The spectra and the identified molecular structures are summarized in figure 55. The assignments were based on the chemical shift data available in literature.[6,17,18] A correlation table with the chemical shifts (δ_C/δ_H) used for the cross-peak assignments is reported in the experimental section (Chapter 4 > Section 4.1 > 2D-HSQC NMR). For both rice husk and *Arundo donax* lignins the cross-peaks are clearly divided in two clusters: the aliphatic-oxygenated region (δ_C/δ_H 50–90/2.5–6.0) and the aromatic region (δ_C/δ_H 90–160/6.0–8.0). In the former region it is possible to identify the major types of intermonomeric linkages: arylglycerol-β-arylether (β-O-4),

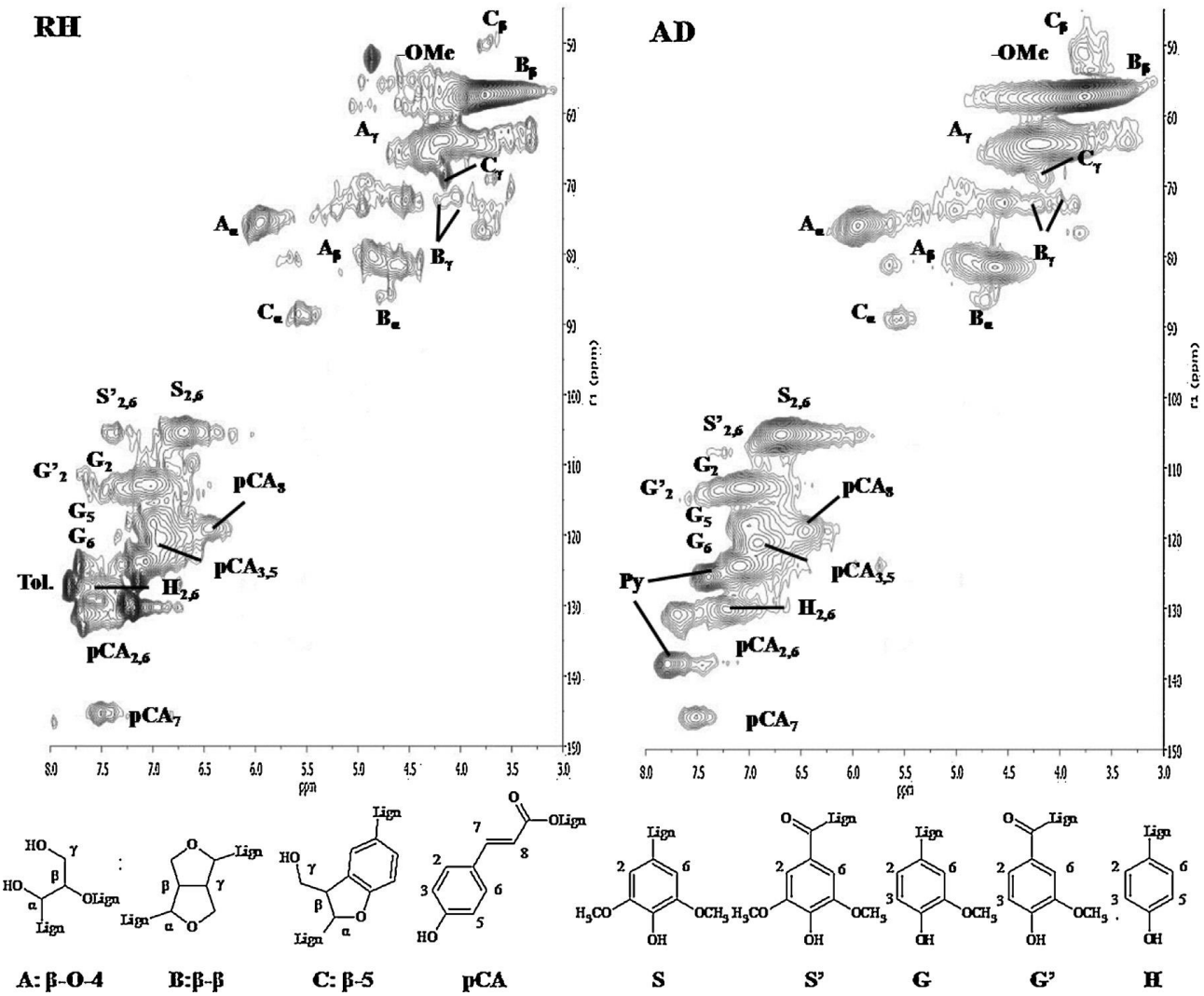

Figure 55 - 2D-HSQC NMR spectra of acetylated RH and AD lignin samples, showing the aliphatic side chain (α, β, γ) for the main lignin intermonomeric bonds (A: β-O-4, B β-β,C: β-5*) and the aromatic region (S syringyl, S' syringyl oxidized, G guaiacyl, G' guaiacyl oxidized, H p-coumaryl, pCA p-cumarate ester). Residual solvents: Py (pyridine), Tol (toluene).*

phenylcoumaran (β-5) and pinoresinol (β-β). There is a significant cross-peak attributable to the methoxy groups. It is also worth noticing that the spectra relative to the lignin of AD is completely free from any signal associable with the presence of polysaccharides. The RH spectra shows few peaks that might reveal the presence of carbohydrates (around δ_C/δ_H - 75/3.75), but the intensity is noticeably low. This is in good agreement with the hypothesis based on the results of the previous characterizations: LCCs are efficiently cleaved in in the combined extraction process and lignins possess a high degree of purity. In the aromatic area, as expected, cross-peaks reveal syringyl, guaiacyl and p-coumaryl units but also the presence of p-coumarates, that are involved in the lignification process and are particularly abundant in herbaceous plants. The biorefinery process was found successful in recovering a large fraction of the initial lignin present in the starting materials (roughly 45%). It was demonstrated that the extracted lignins possessed a high degree of

purity (90% and 95% for AD and RH respectively). Finally, the investigation of the molecular structure (NMR e GPC) confirmed that the process is not too harsh and that the molecular structure of lignins are preserved. This data are encouraging, in fact, high purity and the retention of specific chemical moieties (eg. phenolic-OH) are considered crucial for the utilization of lignins in a range of valuable applications as reported in literature by several authors.[17,19–22]

Experimental evidence supports the fact that in the first steps of the processing an appreciable amount of the connections between lignin and carbohydrates are cleaved. As a result, also a fraction of the hemicelluloses are extracted from the biomass. During the processing of *Arundo donax, a* portion of the hemicelluloses is solubilized during the acid leaching, and a second fraction is released in the successive step, the alkaline extraction. The analysis of the two fractions (Hemicellulose A and B) was performed via IR spectroscopy. The technique doesn't grant a deep characterization in terms of molecular structure and composition, however the main target of the investigation was to explore the possibility to potentially recover a sizable amount of hemicellulose, along with the other main constituents of the starting materials; and a thorough characterization lies outside the focus of this work. Nevertheless, the infrared spectra of hemicelluloses A and B (figure 56) feature the typical peaks of xylans in the 1200-1000 cm^{-1} range that is dominated by ring vibrations overlapped with stretching vibrations of (C–OH) side groups and the (C–O–C) glycosidic bond vibration.[23] Fraction B seemed to be partly contaminated with a certain amount of cellulose that is probably also solubilized during the alkaline treatment. The analysis of the molecular weight distributions supports the hypothesis (on benzoylated samples - GPC). The distribution of hemicellulose A is centred around 20.000 g/mol, while the chromatogram of fraction B was shifted towards higher molecular weights and presents a tail associable to the presence of heavy macromolecules consistent with cellulose.

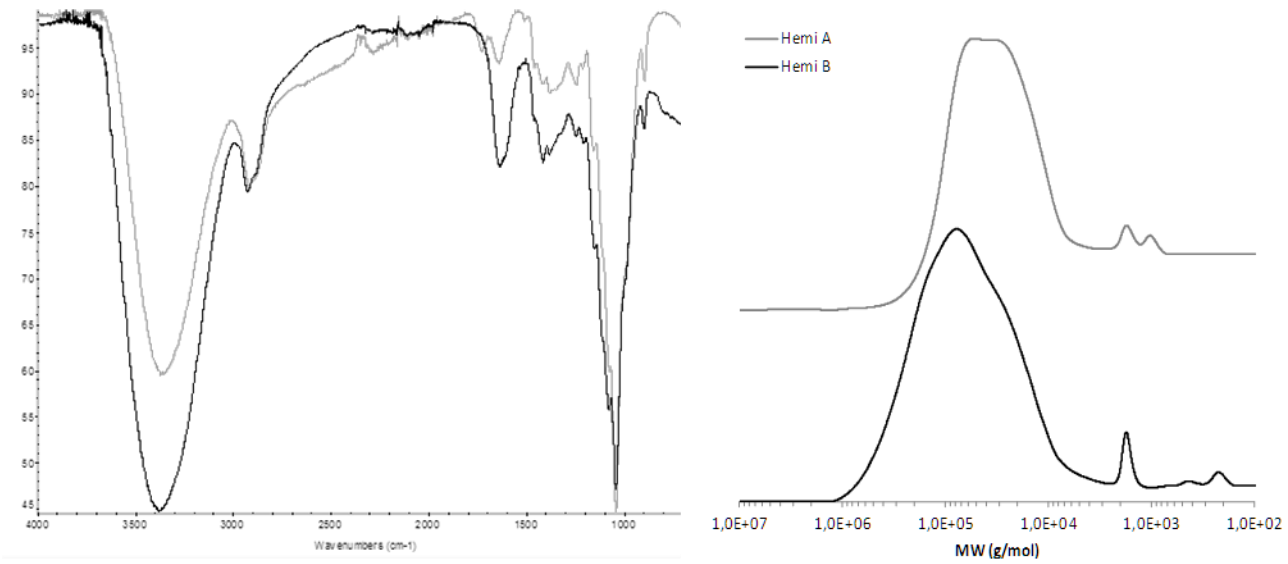

Figure 56 - FT-IR (<-) and GPC (->) characterization of Hemicelluloses (fraction A and B) from AD.

Ultimately, the recovered solid was white in colour and the characteristic peaks of lignin corresponding to the aromatic skeleton vibrations were not identifiable in the spectra. When the aqueous supernatant recovered at the end of the leaching step was treated with the antisolvent only a modest amount of hemicellulose was recovered (450mg from RH vs. 7g from AD). The lower concentration of hemicelluloses in the starting material cannot account alone for the considerable difference but it is likely that such discrepancy is related to structural differences in the complex molecular architectures of rice husk and *Arundo donax.* In fact, in terms of yield, 7 g of hemicellulose A and 8 g of fraction B ware recovered from 100 g of *Arundo donax.* Assuming a hemicellulose content in *Arundo donax* of about 28% w/w, approximately 55% of the original hemicellulose was recovered. For rice husk the simultaneous recovery of hemicellulose seems to be extremely hindered with an overall yield that falls to 2%.

Rice husk is indeed a peculiar lignocellulosic material, in fact, it retains a remarkable amount of inorganic matter, largely constituted by silicon dioxide. This component could serve as an additional source of valuable products, hence a procedure addressed to its recovery was included in the biorefinery scheme. The silica was precipitated and purified from the supernatant recovered after lignin coagulation, with the methodology reported in the experimental section. The siliceous powder was characterized via scanning electron microscopy (SEM) and the detailed composition of the inorganic solid was investigated with EDX analyses.

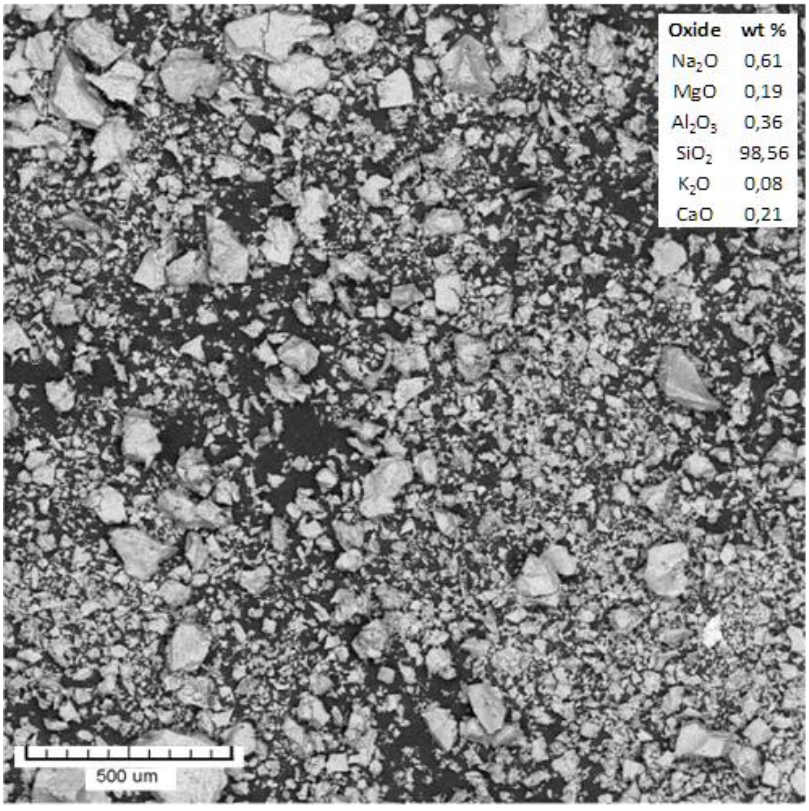

Figure 57 – SEM image of the amorphous particles recovered from RH and results of EDX analysis.

As visible in figure 57, the particles didn't exhibit a defined shape but displayed a coarse morphology. EDX analysis not only confirmed the presence of silicon dioxide, but also revealed that the mineral product is characterized by a high purity, in fact, silica accounted for the 98.5% of the material. The remaining part included different metal oxides, prevalently oxides of Sodium, Aluminium, Calcium, and Magnesium. Infrared spectroscopy (figure 57), demonstrated that the silica recovered through the biorefinery process retained a certain degree of hydroxylation of the surface, on the other hand, most of the silanols are lost when silica is recovered incinerating the organic matter, in fact dihydroxylation is promoted at temperatures higher than 190 °C.[24] Retaining the hydroxyls on the surface of silica particles is important for many applications. The presence of superficial silanols is also particularly important in tyre technology, in fact, the compatibilization of silica with rubber is based on the superficial modification of silica by chemical reaction between the coupling agents and the silanols.[25,26] Eventually, from 100 g of rice husk it was possible to recover 14 g of ashes. The initial amount of ashes was 16 g; hence the process yield is 88%. SiO_2 accounts for the 96% of the inorganic fraction in the starting material and for the 98,5% of the recovered fraction. The efficiency related to the selective recovery of silica exceeds 90%.

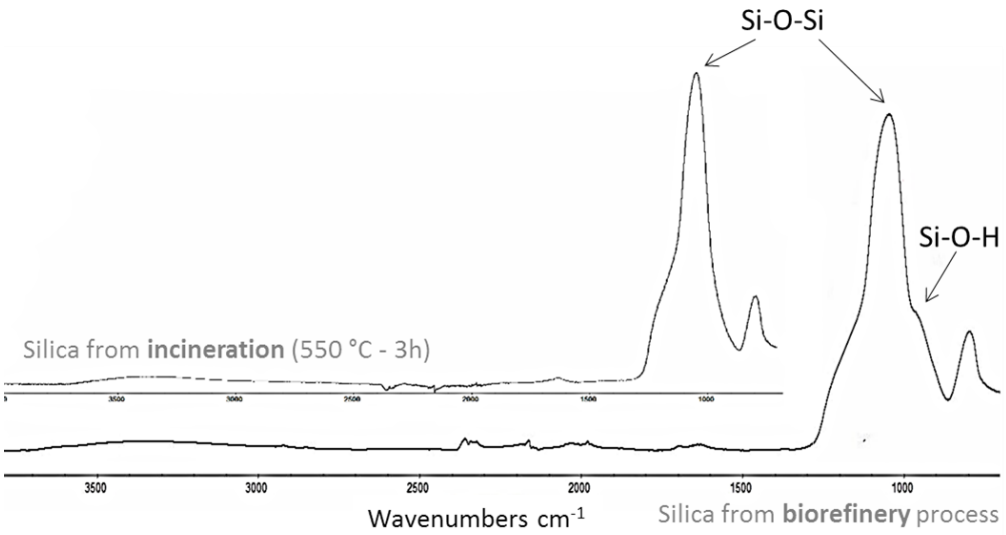

Figure 58 - FT-IR spectra of RH silica recovered through incineration (top) and via biorefinery process (bottom).

The extraction of lignin, hemicellulose, ashes, and water soluble extractives by the acid/alkaline combined method produced a solid material characterized by a high content of cellulose, hence denominated cellulose rich material. The cellulose rich material recovered at the end of the alkaline extraction still contained a substantial part of the starting materials: accounting for 47% of the initial weight of RH and 53% of the initial weight of AD. This fraction rich in cellulose was then further purified by means of a TCF (totally chlorine free) bleaching treatment to remove residual lignin. The bleaching produced extremely white materials essentially composed by pure cellulose. It was possible to recover about 63% of the cellulose initially present in the RH

and 61% of the cellulose content of AD. After bleaching, the white cellulose rich materials were treated with concentrated sulfuric acid, to pursue the valorisation strategy aimed at the production of cellulose nanocrystals (CNCs). The hydrolysis step produced a 0.8 wt% suspension containing 12 g of CNCs in the case of RH, yet a 0.5 wt% suspension containing 11 g of CNCs was obtained from AD. In the first trials, necessary to optimize the isolation procedure for the nanocrystals, the presence of CNCs was confirmed by the observation of the distinctive texture of the suspension under polarized light source. The morphology of cellulose nanocrystals produced in the final experiments was entirely characterized through electron microscopy (TEM). The images confirmed the expected organization for the crystalline domain of cellulose.

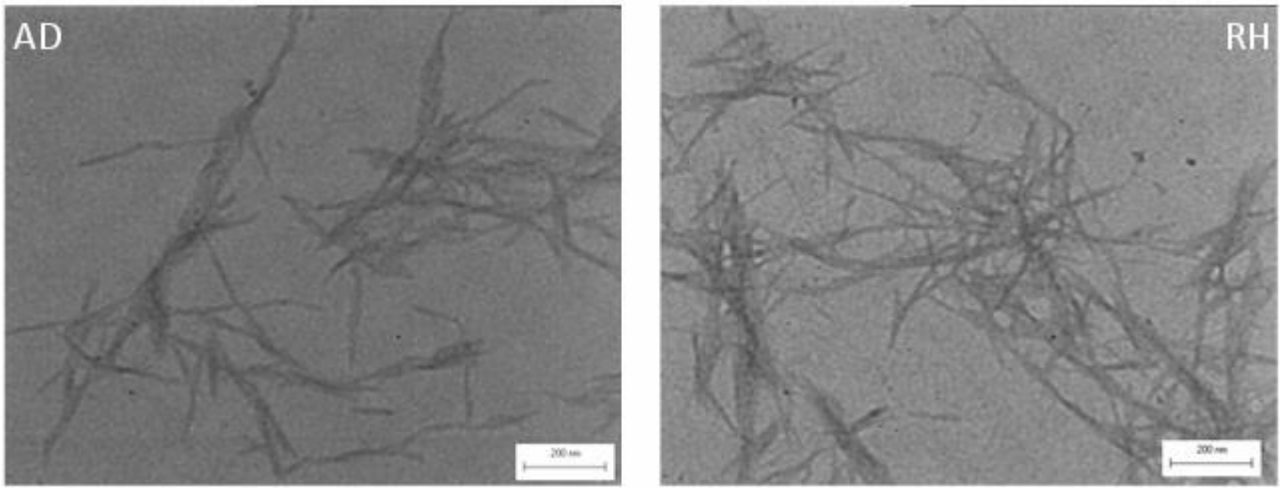

Figure 59- TEM microscopies relative to cellulose nanocrystals isolated from Arundo donax (<-) and rice husk (->).

For both AD and RH, the crystallites presented a rod-like structure characterized by a certain degree of aggregation that could result from the drying phase. The single nanocrystals are supposed to have a high aspects ratio with the principal dimension falling in the range of few hundreds of nanometres and the secondary dimensions displaying a much smaller magnitude, in the range of the tens of nanometres. The isolation of cellulose nano-whiskers from rice husk was recently reported by few authors,[27,28] whereas cellulose nanocrystals were successfully isolated from *Arundo donax* for the first time.

5.5 Process overview

With the proposed process, it was possible to simultaneously recover several components from both of the selected lignocellulosic bioresources, rice husk and *Arundo donax*. Table 16 gives an overview on the efficiency of the process, summarizing the specific yields, based on the initial amount of every distinct component, and the overall yields calculated on 100 g of starting material. In terms of mass balance, it was possible to refine the investigated bio-masses with an overall yield that approaches value of 40%. This result

might not seem outstanding; however, it can be considered satisfactory if the quality of the products and the relatively mild conditions are taken into consideration. Roughly one third of the cellulose initially present was effectively converted in cellulose nanocrystals, hence providing a great added value to the products. It should also be noted that in the pristine feedstocks only two thirds of the cellulose is ordered in crystalline forms,[27] therefore half of the crystalline cellulose was successfully transmuted. A large amount of the amorphous cellulose and part of the crystalline cellulose were hydrolysed during the refining process, mainly in the acid hydrolysis step used to retrieve the nanocrystals. A minor fraction was discarded during the purification of cellulose nanocrystals (centrifugations). The discarded fraction consists in a partially hydrolysed substrate, not much valuable if compared to the nanocrystals, technically its simultaneous recovery is possible but it might not be convincing from the economic perspective. Regarding hemicelluloses, about 55% of the xylans initially present in *Arundo donax* were recovered. A small fraction may remain soluble after the addition of the anti-solvent and could be recovered with other techniques. For both RH and AD, it is probable that most of the hemicellulose that was not recovered remained bound to cellulose, consequently we believe that it was degraded during bleaching and acid hydrolysis steps. Similarly, roughly half of the starting lignin content in both biomasses was successfully extracted during the alkaline treatment and recovered. A small amount of lignin might have gotten cleaved in the form of small soluble fragments during different steps of the process. However, it is likely that the preponderant part of the unrecovered fraction remained trapped into the cellulose rich substrate and subsequently it was degraded in the bleaching process. From rice husk, it was also possible to recover silicon dioxide. This fraction is particularly interesting as it enables the possibility to use the biomass as an eco-friendly and economically viable raw material to produce silica. Rice husk is already exploited to produce silica, also for tyre manufacturing,[29] However, the state of the art of the technology involves the combustion of the organic fractions, hence roughly 84% of the material is forcedly converted in energy to produce the ashes. The possibility to obtain different materials from the same feedstock is alluring for many reasons: to produce materials with new and unique characteristics, to minimize the environmental impact, and to maximize the economic viability through the production of several products characterized by an added value that can help to obtain an economically feasible process. It is also worth to remark that the

	Rice Husk			Arundo donax		
	Starting	*Specific yield*	*Overall yield*	*Starting*	*Specific yield*	*Overall yield*
Cellulose (NC)	40*	30	12	35*	31	11
Hemicellulose	21*	-	-	28*	55	15
Lignin	22	46	10	29	45	13
Ashes	16	90	14	4	-	-
Total			**36**			**39**

*estimated from common values for RH and AD reported in literature.[18,30]

Table 16 - Initial compositions and yields for the biorefinery processes of RH and AD (g x 100g of starting material).

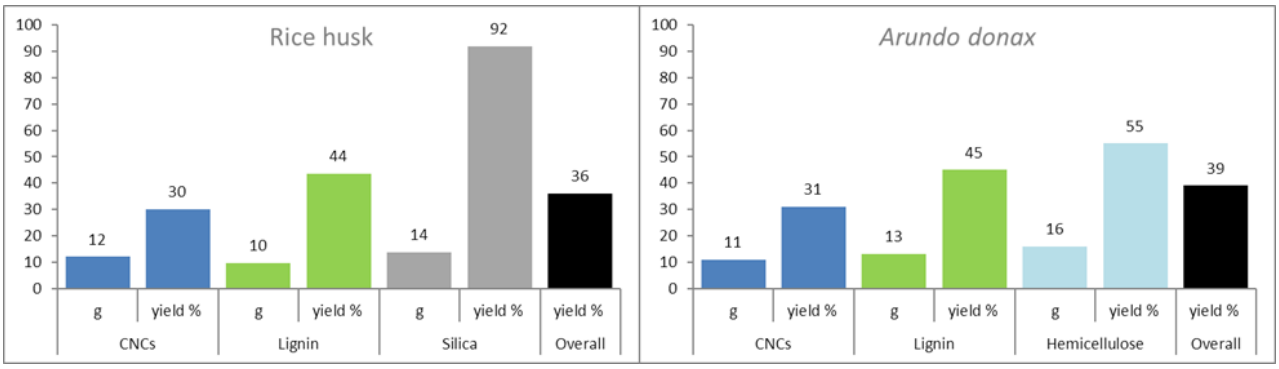

Figure 60 – Specific yields and grams of products obtainable with the proposed biorefinery processes starting from hundred grams of rice husk and Arundo donax (values are approximated to the closest integer, ±1%).

process enables to recover silica in high yields and purities, respectively 96 and 98,5%. Silica is also already solubilized in the process and the precipitation can be modified to obtain silicas with specific properties. It is also important to mention that peculiar characteristics and purity of all the isolated fractions play a pivotal role when the objective is to confer high added value to the recovered products. Hence, the safeguard of the structural integrity and the high purities might have a higher priority than a boost in the yield. A harsher treatments can improve the yields (up to 70%) as previously reported,[31] but it can also compromise the recovery of highly valuable products, for instance disrupting the crystalline domains of cellulose, hindering the production of nanocrystals. Referring specifically to the processing of rice husk, at the best of our knowledge, this is the first time that a process able to valorise three major components at the same time is reported. Furthermore, the yields of silica and cellulose nanocrystals are appealing while the lower efficiency of the process towards the refinement of lignin is compensated by lignin purity. The importance of lignin purity is largely recognised. Nowadays the refinement of technical lignins, in analogy to what happens for crude oil, is considered unavoidable in order to actualize the full potential of the biopolymer.[32]

5.6 Alternative products from the biorefinery processing of rice husk: Lignin-Silica Material

In a second instance, the biorefinery processing of rice husk was modified. A coprecipitation step was introduced, replacing the selective precipitation that, in the original process, brought to the recovery of lignin and silica as two separated products. A deeper investigation of the material obtained with the simultaneous coprecipitation of lignin and silica is proposed in the next chapter. In chapter six the influence of different parameters of the coprecipitation on the characteristics of the material, as well as a broader analysis of the material and its properties in rubber compounds are discussed. Here, only the essential features that are functional to the discussion of the results, proposed in the following section (5.8), are reported.

Experimental

Lignin-Silica Material preparation – The filtrate recovered from the alkaline extraction step of the biorefinery process was transferred into a three-neck 500 mL round-bottom flask. The solution was slowly acidified with 2 M sulphuric acid until pH 4. The flask was equipped with a condenser and placed in an oil bath set at 95 °C. After 6 hours under vigorous mechanical stirring, the reaction was stopped and the round-bottom flask was left to cool at room temperature. The product was then recovered by centrifugation (3500g, 5 min). The lightly brown but transparent supernatant was replaced with demineralized water and the precipitated brown slurry was re-suspended and centrifugated again for other four times to remove the salts produced during the acidification. After the final centrifugation, the clear supernatant was discarded while the thick slurry containing the product was transferred in a Petri dish and freeze-dried.

Purification – 500 mg of the lignin-silica material (LSM) were dispersed in 50 mL of demineralized water; the suspension was then put in a dialysis tubing (Sigma Aldrich, 33mm, 14000 Da) and dialyzed against demineralized water for 5 days. The content of the tubing was recovered in a tared Petri dish, air dried overnight and finally exsiccated in the oven at 105 °C for 10 minutes.

Separation of lignin and silica – different strategies were used to evaluate the possibility to extract lignin from the material. In preliminary trials, two small tranches of roughly 50 mg of the lignin-silica material were placed in 20 mL vials, one containing 10 mL of acetone, and the other one 10 mL of 1,4-dioxane. The vials were vortexed at maximum speed for 30 seconds and set to rest for one day. The results of the experiments were evaluated by visual inspection. In a second experiment, 50 mg of LSM were transferred in a vial with 10 mL of 1,4-dioxane. The vial was capped and immersed in an ultrasonic bath for 30 minutes. Afterwards the solid residue was recovered via vacuum assisted filtration and the solids were washed on the filter with 5 mL of the same solvent for 3 times. The precipitate was transferred in a watch glass and dried in oven at 40 °C. Ultimately, a dry sample of the brownish powder was analysed with ATR FT-IR.

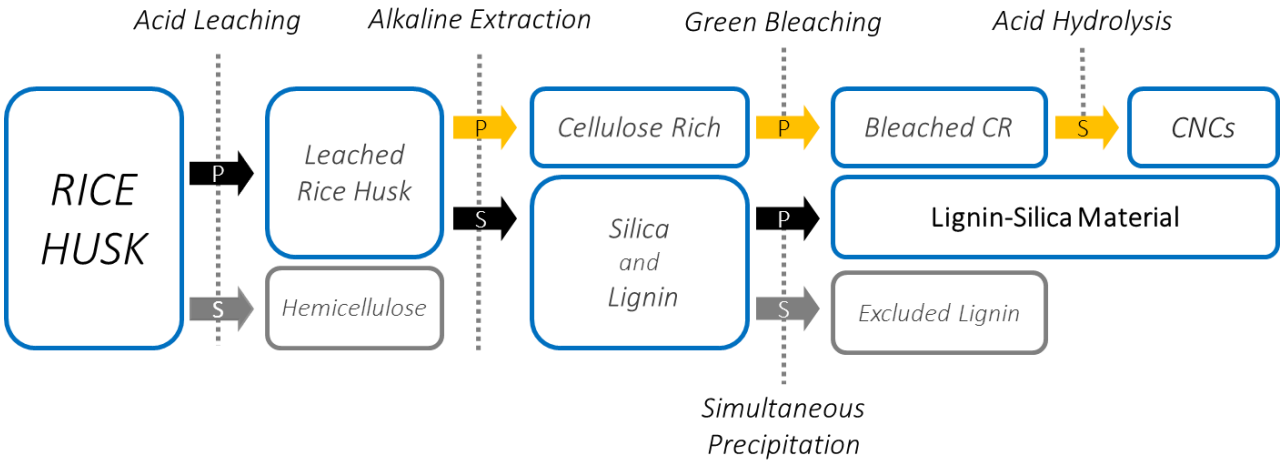

Figure 61 - Flow diagram for the alternative biorefinery processing of RH (P = precipitate, S = supernatant).

Results and discussion

The recovered material was found free from salts, in fact after 5 days of dialysis against demineralized water the weight was found to be constant. The overall yield of the process was slightly lower if compared with the overall yield of the biorefinery process of rice husk reported in the previous sections. Probably a small amount of soluble fragments was lost during the purification of the silica-lignin material, however the difference in yield was found to be rather small. After freeze-drying a light brown fine powder was recovered. A quick evaluation of the product was made using different techniques. A small sample was analysed with IR spectroscopy, and the spectra was evaluated in comparison with the spectra of silica and lignin extracted from rice husk (figure 63). The spectra of the lignin-silica material (SLM) presents the distinctive signals of both silica (1000-1100 cm^{-1}) and lignin (1300-1700 cm^{-1}). The relative amount between organic and inorganic fraction was assessed thermogravimetrically, exposing a well dried sample at a temperature of 600 °C in air for three hours. The material was found to be composed by 52% of silica and 48% of lignin. A completely white powder was recovered at the end of the experiment and the IR spectra was compatible with that of the silica recovered from rice husk. The specific surface area (BET) of the material was determined on the pristine material and after calcination (550 °C for 3 hours).

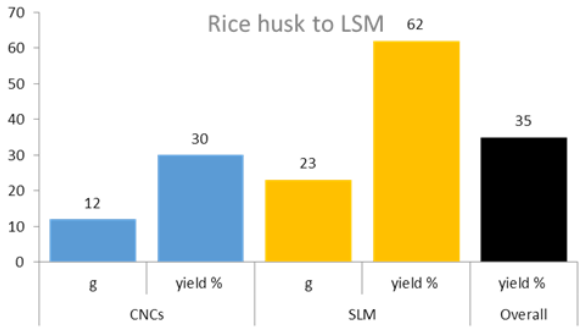

Figure 62 - Specific yields and grams of products obtainable with the alternative biorefinery processes from 100 grams of rice husk.

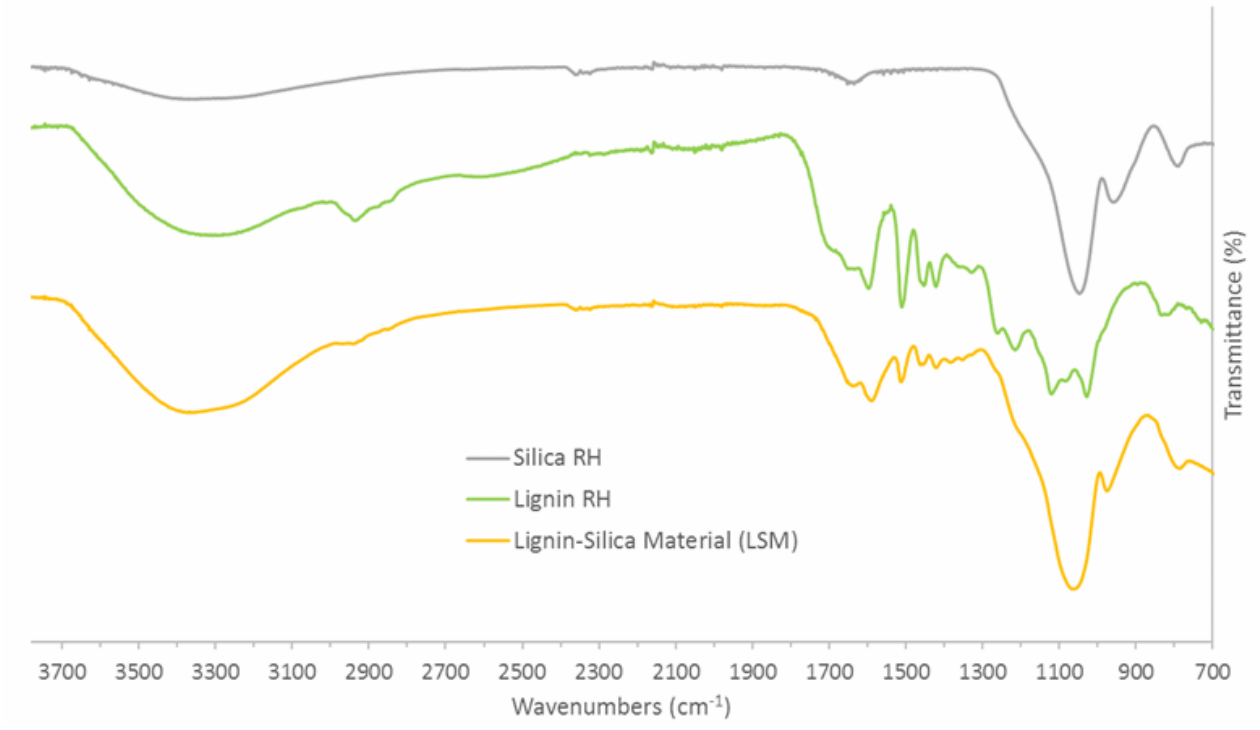

Figure 63 - FT-IR spectra of silica, lignin and silica-lignin material obtained from the biorefinery of rice husk.

The surface area was found to be of 268 m^2/g for pristine LSM and was enhanced to 442 m^2/g with the thermal treatment. The values are compatible with the values of activated silica produced from rice husk by incineration (63 - 321 m^2/g) having a particle size distribution in the range of 150-450 nm.[33] The removal of lignin through calcination determined a sharp increase of the surface area (+63%). This could be associated with a templating effect of lignin on silica, ongoing at the microscopic level during the preparation of the material. Other details regarding the nature of the material were obtained with the separation tests described in the experimental. In the small trials with acetone and 1,4-dioxane it was not possible to separate lignin and silica. In fact, after 24 hours the brown suspension produced with the vortex settled to the bottom of the vials leaving a completely colourless and transparent supernatant. It must be noted that when a physical blend prepared mixing silica and lignin in a mortar was treated in the same way, it was possible to solubilize lignin and, using an excess of solvent, it was also possible to recover a white powder essentially composed by pure silica. In a second, more forceful, approach a suspension of 100 mg of LSM in 15 mL of 1,4-dioxane was sonicated for 30 minutes. In this experiment the supernatant turned from clear to brown-coloured while remaining transparent, this was a clear indication that lignin was at least partially extracted from the material. However, the IR analysis of the solid residue showed the presence of residual lignin, even if the relative intensity of the corresponding signals was diminished (figure 64). In the light of the evidences obtained from this simple tests it was supposed that silica and lignin were at least partially interlocked at a microscopic level. On the other hand, the experiments permitted to recognise that a fraction of lignin was not tightly bound to the silica since it was released under the intense ultrasounds treatment.

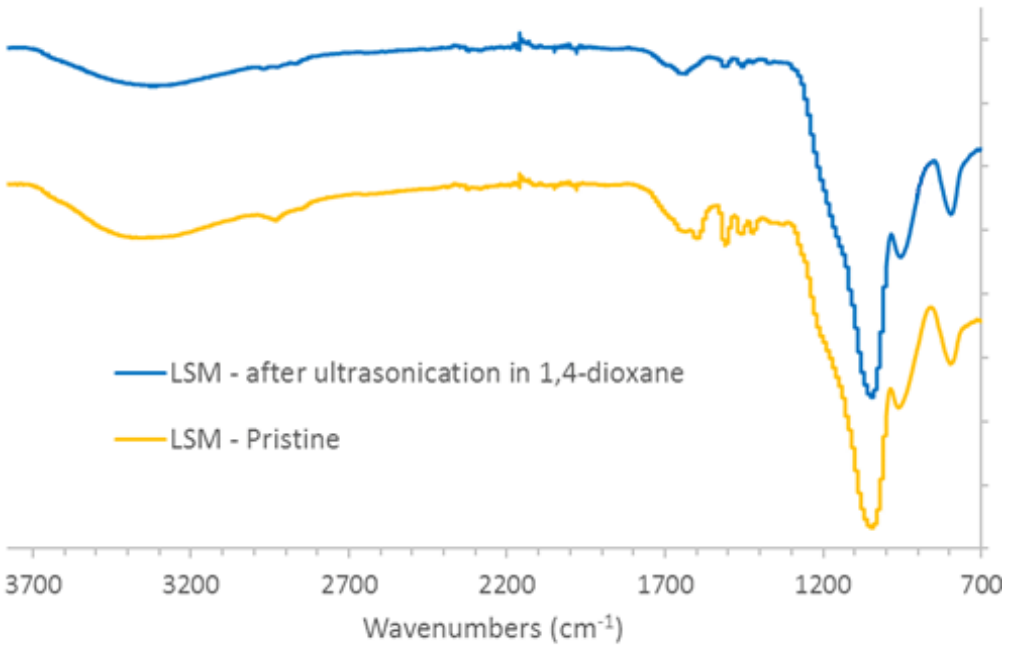

Figure 64 - FT-IR spectra of pristine LSM and after 30 minutes of ultrasonication in 1,4-dioxane.

5.7 Thermal stability of the products obtained from the biorefinery processes of rice husk.

The thermal stability of the organic bio-commodities produced from rice husk with the biorefinery processes was tested via thermogravimetric analysis. This was not only done to further characterize the products, but also in the perspective to use the materials in elastomeric composites. In fact, it is important that the candidate materials can withstand the high temperatures reached during mixing and vulcanization stages. Typically, the most demanding step is curing, where rubber goods are exposed to 140-170 °C temperatures for 10-30 minutes. The method used to test the materials was set up to assess the thermal properties in a wide range of temperatures, from 20 °C to 800 °C with a rate of 10 °C/minute. Along the temperature ramp there are two isothermal conditioning periods, each one lasting 15 minutes. The stops were introduced to assess the water content and to evaluate the thermal stability at curing conditions. Cellulose nanocrystals displayed a low moisture content and a high thermal stability up to ~300 °C. The neat behaviour reflects the chemical and morphological uniformity of the sample. LSM had an increased water content (~5%), a comparable thermal stability (weight loss at 170°C < 1%) and a high solid residue due to the presence of the inorganic fraction. Lignin had the highest moisture content (~8%) and displayed an increased weight loss at 170 °C (~3%). It is probable that lignin begins to degrade at curing condition, although to a limited extent. On the contrary, at high temperature, lignin resulted more stable than cellulose. The stepped slope could be due to the greater heterogeneity of the material, different components might degrade through distinct mechanisms, that are activated at different temperatures. The decomposition is slower also at 800 °C degrees, also in the presence of oxygen. This behaviour could be ascribed to the formation of a lignin char during the heating under nitrogen. It is known that char formation can reduce the combustion rate and for this reason lignin can act as flame retardant.[20]

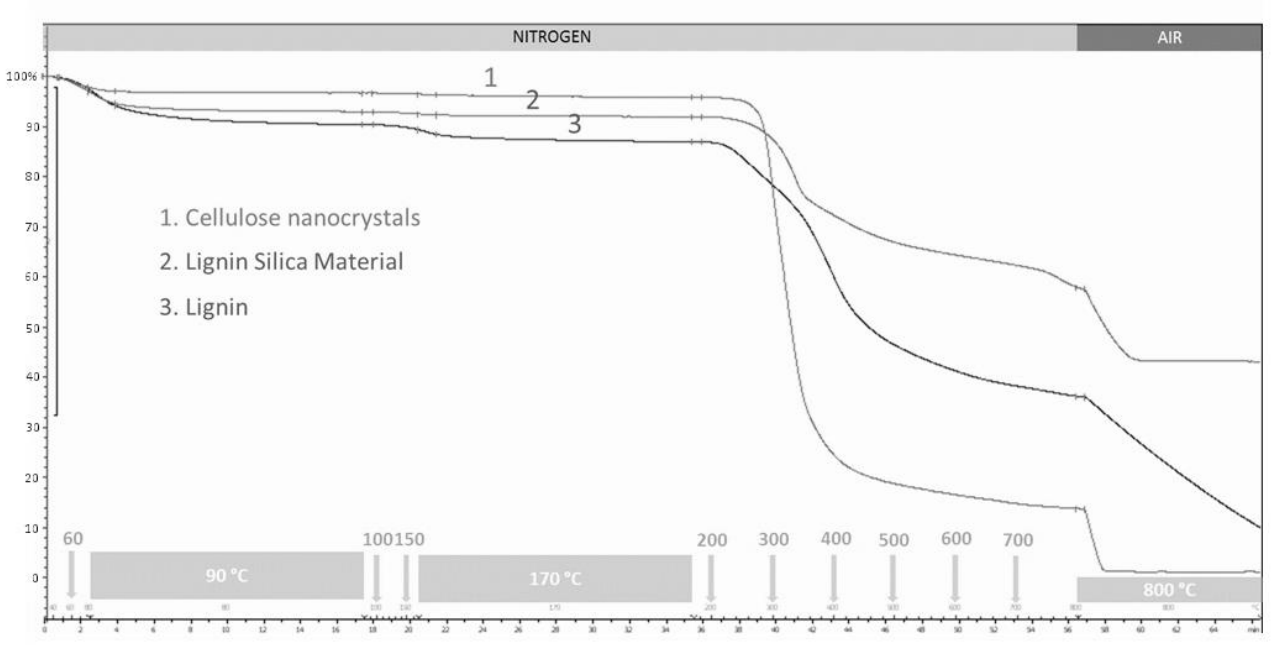

Figure 65 - TGA curves for the organic products obtained from the biorefinery of rice husk.

5.8 Assessment of the potential in model compounds with natural rubber

Rice husk is considered an alluring renewable source of bio-silica since a long time. In the last decades many efforts were made to produce activated silicas, micro-silicas, silica xerogels and silica nanoparticles from the ashes of the agricultural byproduct.[33–39] It was also proposed to use the silica obtained from the combustion of rice husk to produce silica fillers for rubber reinforcement.[40–42] Recently, major tyre manufacturers like Goodyear and Pirelli developed the technology to produce silica-based active fillers from rice husk on an industrial scale.[43,44] In these processes rice husk is incinerated to produce heat (converted into electricity at full scale) and ashes that are particularly rich in silicon dioxide. On the contrary, with the biorefinery process proposed in this chapter it was possible to effectively recover silica avoiding incineration, while cogenerating three additional products: lignin, LSM and CNCs. In the work reported in this section the possibility to use all the fractions as fillers for natural rubber was explored. Silica, lignin and CNCs from RH were tested in simple natural rubber compounds to assess the possibility to prepare greener elastomeric composites.

Experimental

Compounding - The model compounds were prepared according to the procedure number 1 reported in the experimental chapter (chapter 4 > 4.2 Rubber compounding), and the formulations summarized in table 17. Natural rubber was coagulated from natural rubber latex for all the specimens. The tentative fillers were used as recovered from the biorefinery process. Silica, SLM and CNCs powders were mixed directly in the Brabender internal chamber mixer (dry-mixing). Lignin was pre-blended with natural rubber latex using the coprecipitation technique. A total of four compounds, one for each tentative filler were prepared (Lignin RH; Silica RH; CNCs RH; LSM RH). In addition, other four compounds were prepared as references. One reference was prepared with only natural rubber to assess the behaviour of the unfilled polymer (NR ref), two references were prepared with commercially available fillers used in tyre manufacturing: carbon black N375 and silica Zeosil 1165 MP (CB ref and Silica ref), finally one reference was prepared using a commercial lignin: Protobind 1000 (Lignin ref).

Characterization – the mechanical properties of the rubber compounds were characterized performing tensile tests (stress-strain curves) and dynamic-mechanical analysis. Strain-sweep tests and vulcanization curves were recorded with the RPA. The detailed methodology is described in chapter 4.

Results and discussion

As it is possible to observe in table 17, the formulations of the rubber compounds are extremely simple. Stabilizers and processing aids were not introduced in the compounds and the curing was performed with a single component system. The properties of such simple model compounds might not be interesting in terms of absolute values, anyway the objective of this study was to assess the specific and peculiar properties of the innovative fillers, how they affected the properties of natural rubber, and finally, how they perform in comparison with commercial references. At first 5 g of green compounds were analysed at the RPA in strain-

	NR ref	*CB ref*	*Lignin ref*	*Silica ref*	*Lignin RH*	*Silica RH*	*CNCs RH*	*LSM RH*
Natural rubber	100	100	100	100	100	100	100	100
Carbon black (N375)		15						
Lignin (Protobind 1000)			15					
Silica (Zeosil 1165 MP)				15				
Lignin from rice husk					15			
Silica from rice husk						15		
Cellulose nanocrystals from rice husk							15	
Lignin-Silica Material from rice husk								15
Dicumyl peroxide	3	3	3	3	3	3	3	3

Table 17 – Formulations in PHR for rubber model compounds filled with the products obtained from rice husk (RH) and reference compounds (ref) prepared with commercially available fillers, used as references.

sweep tests. Subsequently the test was repeated on vulcanized compounds, curing was also monitored analysing the evolution of torque (S') over time. The results are reported in figure 66 (strain-sweeps) and 16 (curing). Unvulcanised rubbers possess a low elastic modulus and high hysteresis. In this scenario, a filler that forms a strong network can increase the stiffness of the material, at least when the amplitude of the applied periodical strain is low. SLM, silica (RH) and lignin (RH) enhanced the stiffness of natural rubber, increasing the storage modulus. CNCs on the other hand dramatically reduced G' and greatly improved the hysteresis. The extension of the filler-filler interactions can be quantified in terms of Payne effect ($G_0 - G_\infty = \Delta G$). For this set it was calculated as the difference between the value G' at 1% strain and the value at 70% strain according to the formula: [$\Delta G = \Delta G_{sample} - \Delta G_{NR(ref)}$]. As qualitatively observable in the plot, silica (ref) displayed high networking capability (ΔG = 91 KPa). The great extension of the filler-filler interactions correlates well with the known characteristics of the reference material: low particle size, high surface area, and the possibility to form strong hydrogen bonds between particles. The second reference – CB (ref) – also displayed a noticeable Payne effect (ΔG = 63 KPa), but lower than silica. The lignin-silica material (SLM) had a similar overall extension of the networking phenomena (ΔG = 65 KPa). The filler network of CB is built upon Van der Waals interactions, and, as expected, it broke down over a wide range of strain amplitudes. For CB reference, G' dropped linearly from 0 to 30% strain, afterwards decreased faster due to the simultaneous loss in the polymer. On the contrary, for LSM networking mechanism seemed to be very different. The G' of LSM remained constant until 10-15% strain and then dropped sharply. This could be explained with the formation of stronger interparticle interactions, that are compatible with aggregates breaking down at higher strains. This interpretation is also in good agreement with the trend of tan δ, in fact hysteresis is reduced at low-medium strains, meaning that at low strains there is no energy dissipation due to the periodical disruption of the network. Once again, the capability to form strong interactions can be accounted to the presence of polar hydroxyl groups on both silica and lignin. In addition, lignin can interact through other

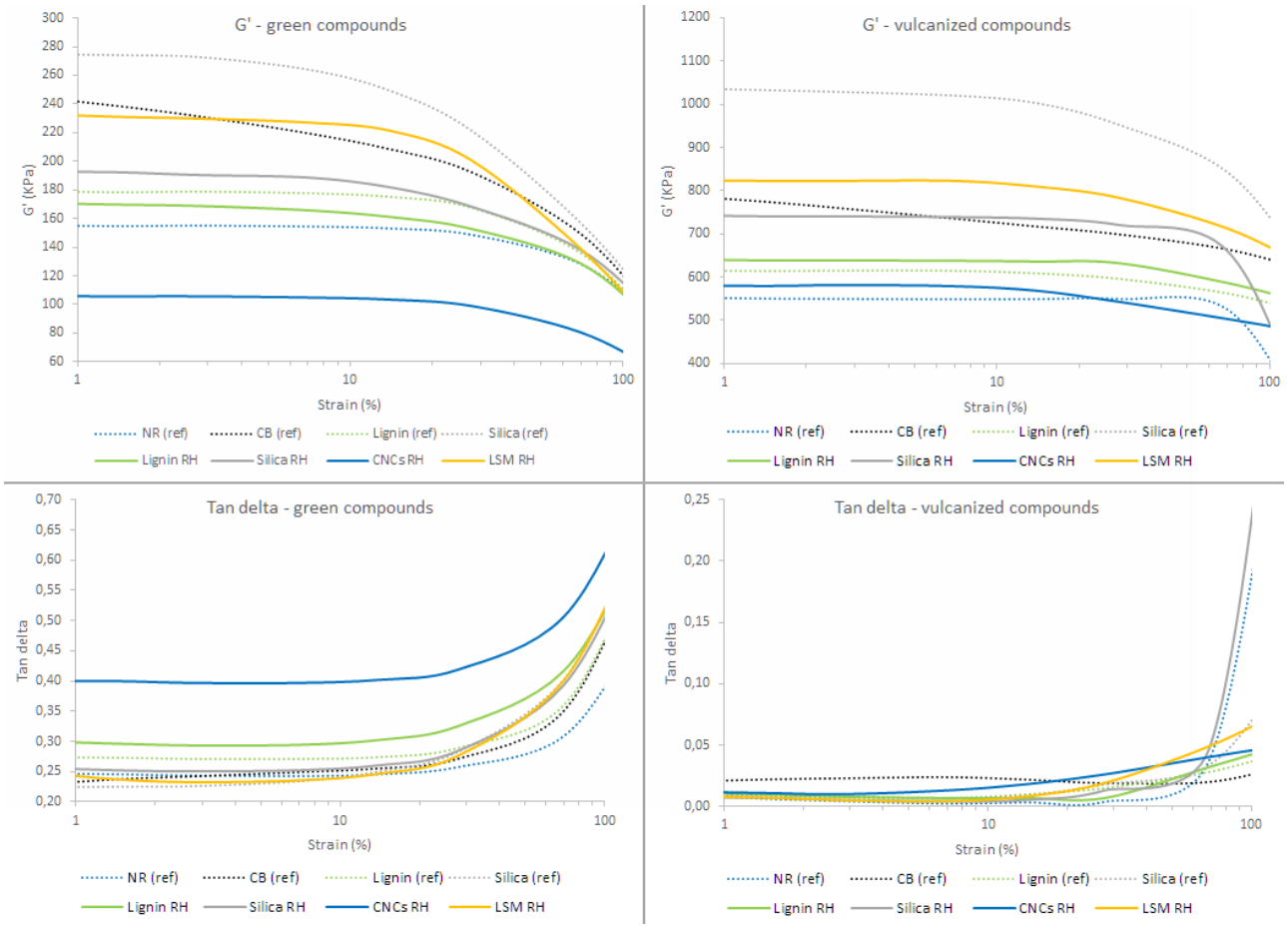

Figure 66 - Storage modulus (G') and tan delta values measured at increasing dynamic strains for green and vulcanized compounds filled with the materials obtained from rice husk (RH) and commercial references (ref).

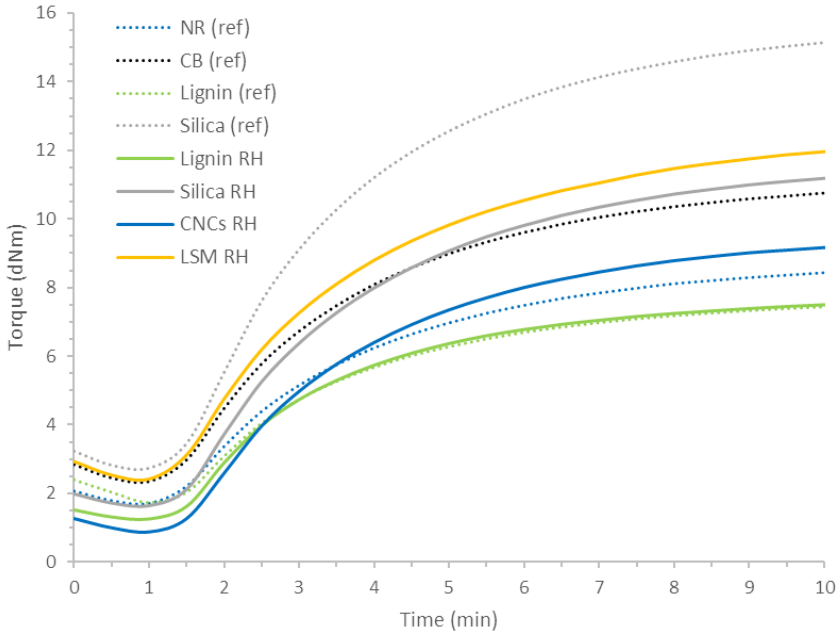

Figure 67 - Vulcanization curves (170 °C).

intermolecular forces as π-π stacking.[45] This characteristic of LSM is interesting, in fact, it was demonstrated that elastomeric compounds with lower energy dissipation (tan δ) under small oscillatory strains can be used to build tyres with lower rolling resistance.[46] On the other hand, at high strains, the G' curve of LSM (RH) falls below CB (ref). This behaviour could be attributed to a lesser compatibility between the filler and the polymeric matrix. The low compatibility between unfunctionalized silica and rubber is well recognised. Lignin as well is supposed to have a lower compatibility with rubber when compared with carbon black due to the presence of numerous polar functionalities. Silica extracted from rice husk displayed a lower Payne effect (ΔG = 28) with respect to the fillers discussed so far. It is probable that the average particle seize is larger than that of the reference silica as partially confirmed by SEM images (figure 57). The commercial silica (ref) is produced with an optimized process and every step is carefully controlled. In the case of the silica from RH the precipitation process aimed at the maximization of the yield but there was no control on the morphological properties of the particles. Furthermore, resistant aggregates might have formed during the drying stage and were not broken down during mixing. Lignin (RH) and lignin (ref) had the lowest Payne effects (ΔG = 15 and 16 respectively). Since lignin cohesive energy is high, the low extent of the filler network must be accounted to the lack of contact area between the particles. This could be explained by a better dispersion that is probably achieved through coprecipitation, but, on the other hand, could also be the consequence of a larger average particle size. Lignin (ref) built a stronger network than lignin (RH), revealed by a higher G' at low strains that is also constant over a wider range of amplitudes. This is in good agreement with the different molecular structure of the two lignins. Protobind 1000 has a higher concentration of hydroxyl groups than rice husk lignin (detailed characterization of lignins is reported in chapter 7); polar groups enhance filler-filler interactions, enabling the formation of a hydrogen bonding network, while reducing the compatibility between filler and rubber.

During vulcanization, the compounds filled with silica – Silica (RH), silica (ref) and SLM (RH) – had a greater change in torque (MH-ML). Probably this is due to a partial flocculation of the fillers. At high temperature, the enhanced mobility and the low compatibility with rubber promotes the migration of the fillers that tent to rearrange in larger clusters. Carbon black shows the same behaviour but to a lesser extent, in line with its higher compatibility. Lignins, on the contrary, clearly hindered vulcanization. There is the possibility that lignins interfered with the action of Dicumyl peroxide, stabilizing the radicals, and limiting the crosslinking between the chains of natural polyisoprene. In fact, Protobind 1000 lignin limited the curing to a greater extent than rice husk lignin. This matches well with the higher content of phenolic moieties that are acknowledged to play a pivotal role in the radical scavenging capability of lignins.[20] Most of the considerations made for the green compounds were confirmed by the strain-sweep tests on vulcanized compounds. The relative order of reinforcement is essentially the same and the small differences can be attributed to the considerations done for the vulcanization. The largest different was in the behaviour of the compound filled with CNCs that after vulcanization had a G' slightly higher than natural rubber, but lower than all other fillers.

One possibility is that the hydrophilic surface of CNCs promotes the slippage of the hydrophobic polymer chains and, in the green compounds, dynamic modulus and hysteresis are greatly affected. In the vulcanizates, on the other hand, chains are chemically linked to each other and the CNCs are probably physically locked into the polymeric network, this results in a limited reinforcing behaviour. Lastly, the rubber compounds were subjected to tensile test to analyse the stress-strains curves, with the aim to better comprehend the effect of the different fillers on the mechanical properties. Samples with silica and lignin from rice husk were not prepared due to an insufficient amount of material to make enough rubber compound and prepare the dumbbell shaped specimens. The silica recovered from the biorefinery process is not particularly interesting in terms of mechanical properties in rubber compounds because size and morphology were not controlled. However, the well-known precipitation processes that are used to prepare commercial silicas can be applied to the solution of soluble silicates extracted from rice husk to obtain a high performing silica. Hence, it is reasonable to believe that a silica filler produced from rice husk through an optimized procedure can reach properties in line with those of the commercial silica reference. Likewise, lignin from rice husk was represented by the commercially available reference. However, in this case, the dynamic mechanical properties were similar and the qualitative behaviour is not expected to differ greatly also in static tensile tests. It is worth noticing that the concentration of the fillers is 15 PHR, which corres-

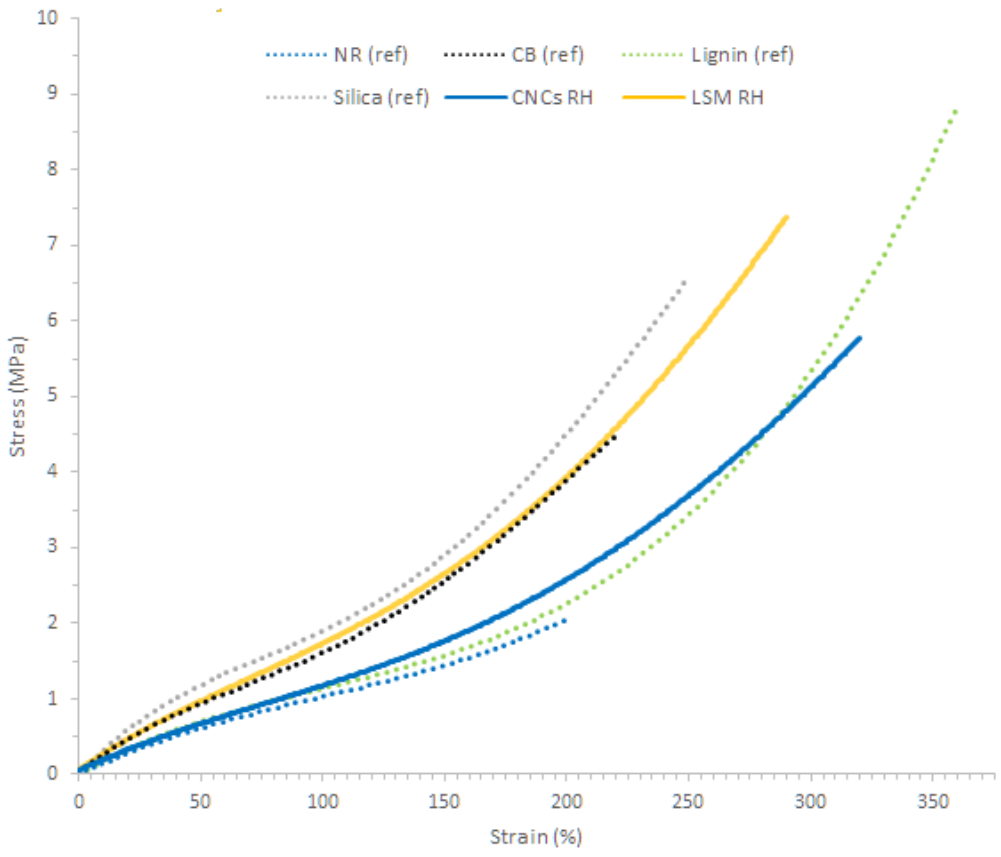

Figure 68 – Tensile tests on dumbbell shaped specimens.

ponds to 13 % in weight. At this loading conventional nanofillers are below percolation threshold, nonetheless the reinforcing effect is clearly visible. Only cellulose nanocrystals due to the high aspect ratio should be above percolation threshold and display enhanced mechanical properties.[47] However, the reinforcing effect is limited even if there is an approachable increase in the properties at break. For this reason, it was assumed that most CNCs rearranged in larger aggregates that offered little contact area and scares compatibility with rubber, ultimately resulting in modest mechanical properties. The highest modulus was observed in the compound reinforced with silica. The higher reinforcement with respect to carbon black can be justified by the lower particle size of silica that had a surface area (140-160 m^2/g) larger than that of carbon black (85-100 m^2/g). LSM gave interesting results, with a modulus essentially in line with carbon black, but increased properties at break. The macroscopic behaviour could be a combination of effects: the high surface area (~270 m^2/g), the reinforcing capability of silica and the peculiar properties of lignin. The reinforcement at moderate strains could be addressed to the presence of silica, the enhanced properties at break might be a consequence of the presence of lignin. In fact, the compound filled with lignin displayed only a modest increase in stiffness, but the highest properties at break among all the samples. It must be noted that natural rubber is sensitive towards thermal aging. In addition, stabilizers that are usually employed in technical formulations were not introduced in the basic rubber model compounds prepared in this study. Thus, the extent of oxidation is well reflected in the reduced properties at break observed in the reference prepared with unfilled natural rubber – NR (ref). Lignin's antioxidant properties are well recognized,[17,20] hence, it is possible that lignin protected natural rubber from thermal aging, preserving the good qualities of the polymer.

5.8 Conclusions

The biorefinery process here reported represents a viable method to fractionate lignocellulosic biomasses into lignin, hemicelluloses, silica and CNCs for the preparation of high-value products. The major appeal of the proposed process lies in the relative simplicity of the refining procedures that still enable to simultaneously recover several potentially valuable products with high purity and a valid overall yield. When compared to already reported methods, the presented process emerges for the relatively mild conditions applied and the use of inexpensive, largely available, environmentally secure reactants. In addition, all the subsequent procedures are designed to use exclusively water as solvent at atmospheric pressure. In the prospective of industrial scalability, this allows to avoid expensive and energy consuming machineries and a simplified safety management. The process focuses on the simultaneous recovery of three major fractions of the selected lignocellulosic biomasses: lignin, hemicellulose for *Arundo donax*, and silica from rice husk, avoiding combustion and simultaneously embodying the production of CNCs. The introduction of a coprecipitation step in the biorefinery processing of rice husk allowed to produce an organic/inorganic

material composed by lignin and silica and characterized by a high surface area, possibly constituted by nanometric particles. The properties of the materials produced from rice husk were tested in model compounds with natural rubber. The preliminary tests with the tentative fillers, although based on simple model compounds, highlighted interesting features: silica is already largely employed in tyre manufacturing and its qualities are well recognized, lignin displayed some unique features, with the capability to greatly improve the ultimate properties, and finally the LSM seemed to bring together the qualities of silica and lignin in a synergetic manner.

References

(1) FAO Rice Market Monitor (RMM) http://www.fao.org/economic/est/publications/rice-publications/rice-market-monitor-rmm/en/.

(2) Mor V, D. R. Utilization of Rice Husk and Their Ash: A Review. *RJCES* **2013**, *1* (5).

(3) Angelini, L. G.; Ceccarini, L.; Nassi o Di Nasso, N.; Bonari, E. Comparison of Arundo donax L. and Miscanthus x giganteus in a long-term field experiment in Central Italy: Analysis of productive characteristics and energy balance. *Biomass and Bioenergy* **2009**, *33* (4), 635–643.

(4) Ting-Feng Yeh; Tatsuhiko Yamada; Ewellyn Capanema; Hou-Min Chang; Vincent Chiang, and; John F. Kadla. Rapid Screening of Wood Chemical Component Variations Using Transmittance Near-Infrared Spectroscopy. **2005**.

(5) Komolwanich, T.; Tatijarern, P.; Prasertwasu, S.; Khumsupan, D.; Chaisuwan, T.; Luengnaruemitchai, A.; Wongkasemjit, S. Comparative potentiality of Kans grass (Saccharum spontaneum) and Giant reed (Arundo donax) as lignocellulosic feedstocks for the release of monomeric sugars by microwave/chemical pretreatment. *Cellulose* **2014**, *21* (3), 1327–1340.

(6) You, T.-T.; Mao, J.-Z.; Yuan, T.-Q.; Wen, J.-L.; Xu, F. Structural Elucidation of the Lignins from Stems and Foliage of Arundo donax Linn. *J. Agric. Food Chem.* **2013**, *61* (22), 5361–5370.

(7) Neto, C. P.; Seca, A.; Nunes, A. M.; Coimbra, M. A.; Domingues, F.; Evtuguin, D.; Silvestre, A.; Cavaleiro, J. A. S. Variations in chemical composition and structure of macromolecular components in different morphological regions and maturity stages of Arundo donax. *Ind. Crops Prod.* **1997**, *6* (1), 51–58.

(8) Savy, D.; Piccolo, A. Physical–chemical characteristics of lignins separated from biomasses for second-generation ethanol. *Biomass and Bioenergy* **2014**, *62*, 58–67.

(9) Abbas, A.; Ansumali, S. Global Potential of Rice Husk as a Renewable Feedstock for Ethanol Biofuel Production. *BioEnergy Res.* **2010**, *3* (4), 328–334.

(10) Kuznetsov, B. N.; Sudakova, I. G.; Garyntseva, N. V.; Djakovitch, L.; Pinel, C. Kinetic study of aspen-wood sawdust delignification by H2O2 with sulfuric acid catalyst under mild conditions. *React. Kinet. Mech. Catal.* **2013**, *110* (2), 271–280.

(11) Carmen Canevali; Marco Orlandi; Luca Zoia; Roberto Scotti; Eeva-Liisa Tolppa; Jussi Sipila; Francesca Agnoli and Franca Morazzoni. Radicalization of Lignocellulosic Fibers, Related Structural and Morphological Changes. **2005**.

(12) Singh, D. P.; Trivedi, R. K. Acid and alkaline pretreatment of lignocellulosic biomass to produce ethanol as biofuel. *Int. J. ChemTech Res.* **2013**, *5* (2), 727–734.

(13) Kim, S.; Park, J. M.; Seo, J. W.; Kim, C. H. Sequential acid-/alkali-pretreatment of empty palm fruit bunch fiber. *Bioresour. Technol.* **2012**, *109*, 229–233.

(14) Guo, B.; Zhang, Y.; Yu, G.; Lee, W. H.; Jin, Y. S.; Morgenroth, E. Two-stage acidic-alkaline hydrothermal pretreatment of lignocellulose for the high recovery of cellulose and hemicellulose sugars. *Appl. Biochem. Biotechnol.* **2013**, *169* (4), 1069–1087.

(15) Wan, C.; Zhou, Y.; Li, Y. Liquid hot water and alkaline pretreatment of soybean straw for improving cellulose digestibility. *Bioresour. Technol.* **2011**, *102* (10), 6254–6259.

(16) Salanti, A.; Zoia, L.; Frigerio, P.; Orlandi, M. Influence of acidic and alkaline aqueous regeneration on enzymatic digestibility of the cellulose fraction recovered from [amim]Cl-treated rice husk. *Bioresour. Technol.* **2013**, *128*, 330–336.

(17) Salanti, A.; Zoia, L.; Orlandi, M.; Zanini, F.; Elegir, G. Structural Characterization and Antioxidant Activity Evaluation of Lignins from Rice Husk. *J. Agric. Food Chem.* **2010**, *58* (18), 10049–10055.

(18) Salanti, A.; Zoia, L.; Tolppa, E.-L.; Orlandi, M. Chromatographic Detection of Lignin–Carbohydrate Complexes in Annual Plants by Derivatization in Ionic Liquid. *Biomacromolecules* **2012**, *13* (2), 445–454.

(19) Bertini, F.; Canetti, M.; Cacciamani, A.; Elegir, G.; Orlandi, M.; Zoia, L. Effect of ligno-derivatives on thermal properties and degradation behavior of poly(3-hydroxybutyrate)-based biocomposites. *Polym. Degrad. Stab.* **2012**, *97* (10), 1979–1987.

(20) Sadeghifar, H.; Argyropoulos, D. S. Correlations of the Antioxidant Properties of Softwood Kraft Lignin Fractions with the Thermal Stability of Its Blends with Polyethylene. *ACS Sustain. Chem. Eng.* **2015**, *3* (2), 349–356.

(21) Frigerio, P.; Zoia, L.; Orlandi, M.; Hanel, T.; Castellani, L. Application of sulphur-free lignins as a filler for elastomers: Effect of hexamethylenetetramine treatment. *BioResources* **2014**, *9* (1), 1387–1400.

(22) Barana, D.; Ali, S. D.; Salanti, A.; Orlandi, M.; Castellani, L.; Hanel, T.; Zoia, L. Influence of Lignin Features on Thermal Stability and Mechanical Properties of Natural Rubber Compounds. *ACS Sustain. Chem. Eng.* **2016**, *4* (10), 5258–5267.

(23) Kačuráková, M.; Capek, P.; Sasinková, V.; Wellner, N.; Ebringerová, A. FT-IR study of plant cell wall model compounds: pectic polysaccharides and hemicelluloses. *Carbohydr. Polym.* **2000**, *43* (2), 195–203.

(24) Zhuravlev, L. T. The surface chemistry of amorphous silica. Zhuravlev model. *Colloids Surfaces A Physicochem. Eng. Asp.* **2000**, *173*, 1–38.

(25) Castellano, M.; Turturro, A.; Marsano, E.; Conzatti, L.; Vicini, S. Hydrophobation of silica surface by silylation with new organo-silanes bearing a polybutadiene oligomer tail. *Polym. Compos.* **2014**, *35* (8), 1603–1613.

(26) Brinke, J. W. te.; Debnath, S. C.; Reuvekamp, L. A. E. M.; Noordermeer, J. W. M. Mechanistic aspects of the role of coupling agents in silica–rubber composites. *Compos. Sci. Technol.* **2003**, *63* (8), 1165–1174.

(27) Rosa, S. M. L.; Rehman, N.; de Miranda, M. I. G.; Nachtigall, S. M. B.; Bica, C. I. D. Chlorine-free extraction of cellulose from rice husk and whisker isolation. *Carbohydr. Polym.* **2012**, *87* (2), 1131–1138.

(28) Johar, N.; Ahmad, I.; Dufresne, A. Extraction, preparation and characterization of cellulose fibres and nanocrystals from rice husk. *Ind. Crops Prod.* **2012**, *37* (1), 93–99.

(29) PIRELLI - Tyre Glossary https://www.pirelli.com/corporate/en/deepen/glossary/tyre_r.html.

(30) Lemons e Silva, C. F.; Schirmer, M. A.; Maeda, R. N.; Barcelos, C. A.; Pereira, N. Potential of giant reed (Arundo donax L.) for second generation ethanol production. *Electron. J. Biotechnol.* **2015**, *18* (1), 10–15.

(31) Shatalov, A. A.; Pereira, H. High-grade sulfur-free cellulose fibers by pre-hydrolysis and ethanol-alkali delignification of giant reed (Arundo donax L.) stems. *Ind. Crops Prod.* **2013**, *43*, 623–630.

(32) S Argyropoulos, D. The Emerging Bio-Refinery Industry Needs to Refine Lignin Prior to Use. *J. Biotechnol. Biomater.* **2012**, *S6* (1).

(33) Yalçin, N.; Sevinç, V. Studies on silica obtained from rice husk. *Ceram. Int.* **2001**, *27* (2), 219–224.

(34) James, J.; Rao, M. S. Silica from rice husk through thermal decomposition. *Thermochim. Acta* **1986**, *97*, 329–336.

(35) Della, V. .; Kühn, I.; Hotza, D. *Rice husk ash as an alternate source for active silica production*; 2002; Vol. 57.

(36) Chandrasekhar, S.; Satyanarayana, K. G.; Pramada, P. N.; Raghavan, P.; Gupta, T. N. Review Processing, properties and applications of reactive silica from rice husk—an overview. *J. Mater. Sci.* **2003**, *38* (15), 3159–3168.

(37) Liou, T.-H. Preparation and characterization of nano-structured silica from rice husk. *Mater. Sci. Eng.*

A **2004**, *364* (1), 313–323.

(38) Real, C.; Alcala, M. D.; Criado, J. M. Preparation of Silica from Rice Husks. *J. Am. Ceram. Soc.* **1996**, *79* (8), 2012–2016.

(39) Kalapathy, U.; Proctor, A.; Shultz, J. A simple method for production of pure silica from rice hull ash. *Bioresour. Technol.* **2000**, *73* (3), 257–262.

(40) Chuayjuljit, S.; Eiumnoh, S.; Potiyaraj, P.; Pranut Potiyaraj, and. Using Silica from Rice Husk as a Reinforcing Filler in Natural Rubber. *J. Sci. Res. Chula. Univ. J. Sci. Res. Chula. Univ* **2001**, *26* (2).

(41) Sae-Oui, P.; Rakdee, C.; Thanmathorn, P. Use of rice husk ash as filler in natural rubber vulcanizates: In comparison with other commercial fillers. *J. Appl. Polym. Sci.* **2002**, *83* (11), 2485–2493.

(42) Fernandes, M. R. S.; Furtado, C. R. G.; de Sousa, A. M. F. Evaluation of rice husk ash as filler in tread compounds. In *AIP Conference Proceedings*; American Institute of PhysicsAIP, 2014; pp 512–515.

(43) Goodyear Turning Ash Into Silica for Tire Production - Tire Review Magazine http://www.tirereview.com/goodyear-turning-ash-silica-tire-production/ (accessed Dec 20, 2016).

(44) Hysterectomy: Silica extracted from rice husks makes for greener tyres | The Economist http://www.economist.com/news/science-and-technology/21569013-silica-extracted-rice-husks-makes-greener-tyres-hysterectomy (accessed Dec 20, 2016).

(45) Deng, Y.; Feng, X.; Yang, D.; Yi, C.; Qiu, X. π–π STACKING OF THE AROMATIC GROUPS IN LIGNOSULFONATES. *BioResources* **2012**, *7* (1), 1145–1156.

(46) LR, E.; WH, W. ULTRA-HIGH REINFORCING PRECIPITATED SILICA FOR TIRE AND RUBBER APPLICATIONS. *Kautschuk Gummi Kunststoffe* **1995**, *48* (10), 718–723.

(47) Siqueira, G.; Bras, J.; Dufresne, A. Cellulosic bionanocomposites: A review of preparation, properties and applications. *Polymers (Basel).* **2010**, *2* (4), 728–765.

CHAPTER 6

Lignin-silica materials (LSMs) as biofillers for elastomers reinforcement

In the previous chapter, a modification in the biorefinery process of rice husk introduced an alternative product, an organic-inorganic material constituted by lignin and silica, where the two components were conceivably combined at the microscopic level. The possibility to incorporate lignin and silica in a unique material, arose directly from the fact that the two substances were recovered simultaneously during the biorefinery processing of rice husk, indeed the outcome of the alkaline extraction was a solution of lignin and soluble silicates. In the first mechanical tests reported in chapter five, based on extremely simple model compounds, the lignin-silica material (LSM) displayed interesting properties, that seemed to be the outcome of the synergetic contribution of the two components. In fact, natural rubber was efficiently reinforced, probably due to the presence of silica; at the same time, the tensile tests showed that the LSM-filled compound possessed also enhanced ultimate properties, which were supposed to be linked to the protective effect of lignin. Based on these introductive considerations, the green organic/inorganic material was considered promising; hence a more exhaustive investigation was devoted to better assess its potential as a reinforcing filler.

6.1 Background

Recently, the preparation of lignin-silica materials through different approaches, was reported by several researchers. These materials are generating a growing interest, especially for their environmental friendliness and the raising necessity to sustain the industrial processes with renewable commodities. Lignin-silica materials were obtained starting from agricultural side-products that are naturally rich in both components: rice husk,[1,2] rice straw,[3] wheat husk,[4] or alternatively from silica/silicate-solutions and the largely available technical lignins.[5–9] The strategies selected to produce the materials are different: co-precipitation, sol-gel, mechanical mixing, and several chemical modifications are reported; the proposed applications are diversified as well: agents for the decontamination of different environments, metal adsorbents and multipurpose micro and nanoparticles promising for application in many areas of science and industry.

A facile method to synthetize lignin-silica nanoparticles from rice husk was proposed by Qu et al.[1] The authors performed a partial optimization of the preparation, investigating the effect of the most influent reaction

conditions (time, temperature and pH) on the final lignin/silica ratio, as well as the effect of the pH on the surface area of the obtained materials. The aim of the work reported in this thesis was to produce an appropriate amount of lignin-silica material (LSM) to prepare filled rubber compounds and further investigate the mechanical properties of the elastomeric composites with natural rubber. In the first place a study of the effect of the parameters of the process on the characteristics of the material was reiterated, to determine the yields of the synthesis, and to better understand the mechanism of formation. Furthermore, it was also considered plausible that the characteristics of the raw material (RH) differed from source to source, affecting the properties of LSM. Afterwards, the properties of the LSM prepared with the optimized conditions, were tested to in different rubber compounds to evaluate its potential as an alternative reinforcing filler for tyres. Ultimately, a similar LSM was prepared from alternative stock materials (precipitated silica, industrially produced from rice husk and Kraft lignin) to produce a larger amount of the filler, needed to prepare several rubber compounds with the same filler.

6.2 Materials

A local farm kindly provided the rice husk. The details regarding the standard ingredients used to prepare the rubber compounds can be found in chapter four. All the other reagents and solvents (ACS grade) were purchased from Sigma-Aldrich and used as received without further purification.

6.3 LSM preparation and characterization

Experimental

LSM preparation. A solution of silica and lignin was prepared from 50 g of RH with the same procedure used in the biorefinery process (acid leaching with 500 mL of HCl 0,1 M / 2h + alkaline extraction with 500 mL of NaOH 0,5 M / 4h, both at 100 °C). The alkaline solution obtained at the end of the extraction was divided in ten identical aliquots. Every sample was brought to the desired pH (2,3,4,5 or 6) slowly adding 2M sulfuric acid under constant magnetic stirring. The solutions were prepared in 250 mL round bottom flasks, then equipped with a condenser and were reacted at 90 °C for the desired time (1,2,3,4,5,6 or 12 hours), always under vigorous magnetic stirring. At the end of the reactions the products were recovered and purified through several centrifugation cycles. The precipitates were air-dried overnight, the drying was completed in the oven at 40 °C under vacuum.

Organic and inorganic content determination. The amount of organic matter (lignin) and inorganic (silica) was determined gravimetrically weighting the samples before and after a thermal treatment (3h in air at 550 °C). The amount of lignin was calculated from the equation: $\text{lignin}\ (\%) = \frac{\text{initial weight} - \text{final weight}}{\text{initial weight}} \times 100$, and silica from: $\text{silica}\ (\%) = 100 - \text{lignin}\ (\%)$.

Results and discussion

The investigation on the relationships between the parameters used for the preparation of the LSMs and their characteristics demonstrated that both studied parameters, pH, and reaction time, considerably affected the products in terms of overall yields, lignin/silica ratio and surface area. The effect of the pH was assessed in the 2 – 6 range, keeping temperature and reaction time fixed at 90 °C and 6 hours respectively. The characteristics depicted from the characterization of the LSMs are summarized in figure 69. At pH =2, the LSM did not contain a significant quantity of silica and the product was essentially constituted by lignin (~98%). At pH = 3, a sudden change was detected, the amount of silica increased dramatically and the LSM was almost equally composed by both fractions. The changes observed at higher values of pH followed a trend characterized by a nearly constant amount of silica and a decreasing lignin content. The trend of the lignin/silica ratios was qualitatively in good agreement with the values reported in the literature,[1] with the exception of the sample prepared at pH = 2. However, a comparable behavior, typified by a maximum of lignin content at pH = 2, was already observed in another work, where a similar material was synthetized from wheat husk.[4] The surface area of the sample prepared at pH 2 was not detectable, probably because it was too low. At pH values ≥ 3 the surface area increased rapidly with the relative amount of silica, reached a maximum for pH 4 and remained relatively constant at in the samples prepared at higher values of pH (5 and 6). It is worth mentioning that drastic changes in lignin content did not significantly affect the total surface area of the material. The results were rationalized considering the pH-responsiveness of lignin and silica. In the initial alkaline solution (pH ≥ 12) both substances are solubilized. In fact, most of the lignin's hydroxyl groups (carboxylic and phenolic) are in the dissociated form when pH is 12, greatly increasing the solubility in water and hindering aggregation. Carboxylic acids in lignin have pKa values around 4-5 and the different

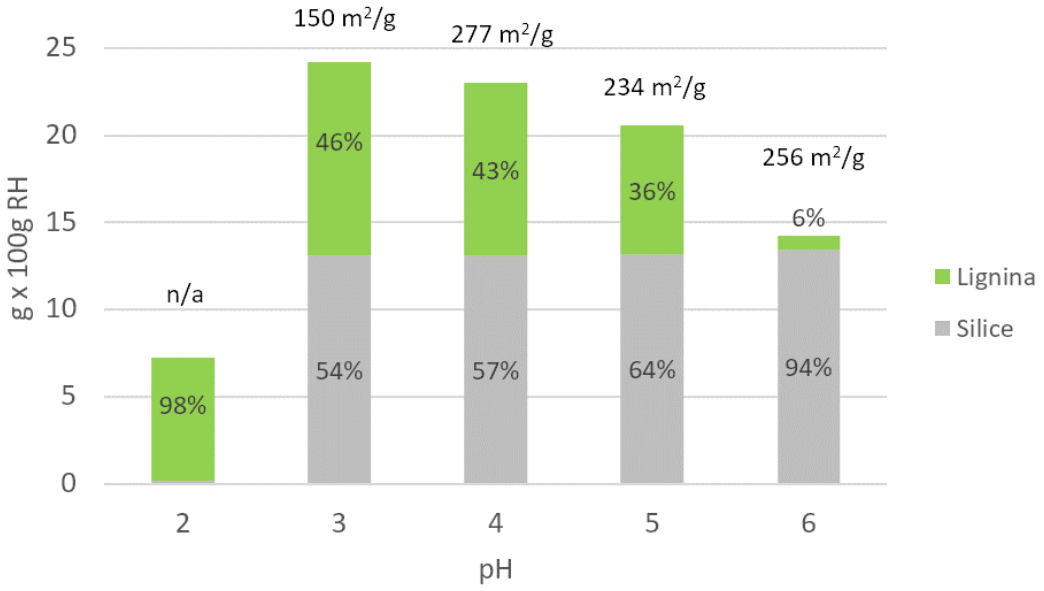

Figure 69 – Investigated characteristics of LSM obtained at different pH values (6 h / 90 °C).

phenolic groups in the range 6-10.[10] Silicates, above pH 10.5 are increasingly less stable and are also dissolved in aqueous solution.[11] When the pH decreases, the different hydroxyl groups of lignin are progressively protonated and the intermolecular forces start to prevail on the electrostatic repulsion generated by the fewer charges and the polymer begins to aggregate and flocculate. The pH also affects the charges on silica, however in the silica condensation reaction the condensation rate increases with the negatively charged silicates because of the favored nucleophilic attack:

The condensation rate shows parallel pH behavior as charge density for pH $\leq$ 7.5. The rate is minimum at pH = 2, in correspondence of the isoelectric point of silica, and increases gradually at higher pH values. However, the condensation rate reaches a maximum and decreases for pH $\geq$ 7.5 because of the increasing instability of silicates.[11] Silica polymerization and silica nanoparticle formation follows a 3-stage process. In the first stage (i) silica monomers polymerize via dimers, trimers, etc. to cyclic oligomers which then form three-dimensional internally condensed spherical nanoparticle. In the second stage (ii) particles grow by further accretion of silica oligomers and/or by Ostwald ripening. Finally, in the third stage (iii) colloidal silica particles start to aggregate.[12] The behavior qualitatively described is supported by the quantitative information presented in figure 70, where the z-potential of lignin and silica is plotted for a wide range of pH values (reproduced from reference,[8] silica was a commercial product, Syloid®244, and lignin was obtained from the Kraft process). The trend is similar for lignin and silica, and accounts for the comparable behavior. In fact,

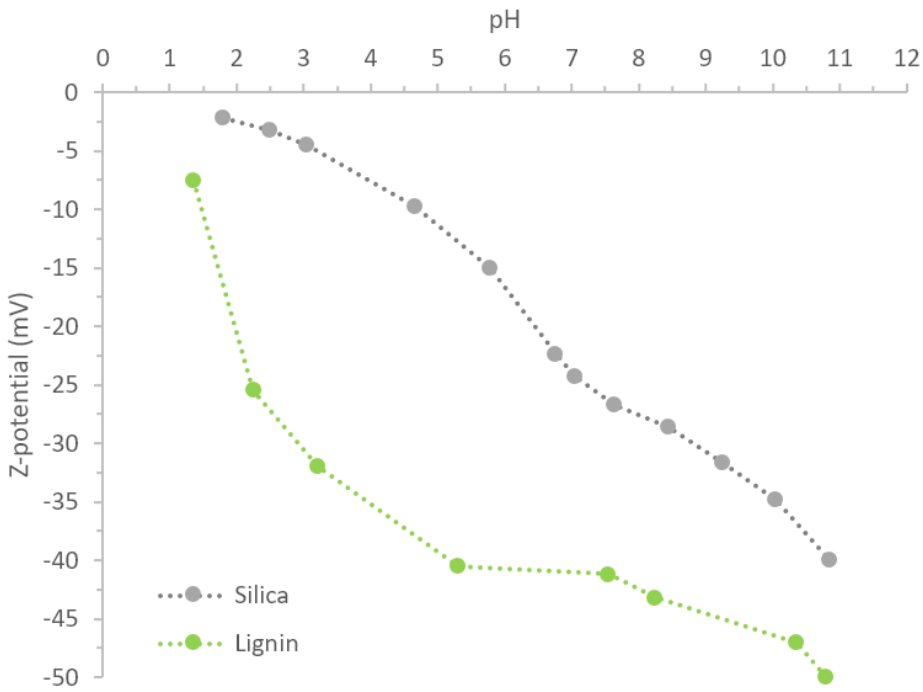

Figure 70 – z-potential of lignin and silica at different pH values (redrawn from reference).[8]

both substances are solubilized in the alkaline solution and precipitate when the environment becomes acidic, even if through different mechanisms. The fact that condensation of silica is much slower near the isoelectric point explained the peculiar composition of the sample prepared at pH = 2, almost exclusively composed by lignin. In the z-potential curve of lignin it is possible to observe a two-step increment; a first increase from -5 mV to -40 mV, between pH 2 and 5, associable to the deprotonation of the different phenolic moieties, and a secondary increase from -40 mV to -50 mV between pH 7 and 12, attributable to the progressive deprotonation of the phenolic moieties. The relationship between the z-potential and pH reflects also the increasing solubility of lignin, connected to the declining presence of the biopolymer in the LSM samples prepared at higher pH values.

The effect of the reaction time on the properties of the LSM was investigated preparing the material at pH = 4 and 90 °C for different periods (from 1 to 12 hours), the results are summarized in figure 71. At the beginning, during the first two hours, the amount of LSM recovered is low and the material is prevalently constituted by lignin. It is worth noticing that when the silica from rice husk was precipitated in similar condition, but without lignin, precipitated almost completely within one hour. Hence, the presence of a delay in silica precipitation suggested the instauration of interactions with lignin. At three hours, the yield and the composition of the LSM changed considerably, the amount of recovered lignin was doubled and the amount of silica increased 25 times. For longer periods the amount of silica steadily increased, whereas that of lignin began to decrease, probably in consequence of the resolubilization promoted by the high temperature and the precipitation of silica. The maximum yield was registered at 6 hours, at 12 hours the amount of silica was almost unchanged, whereas the yield of lignin slightly dropped. During the first three hours, the surface area

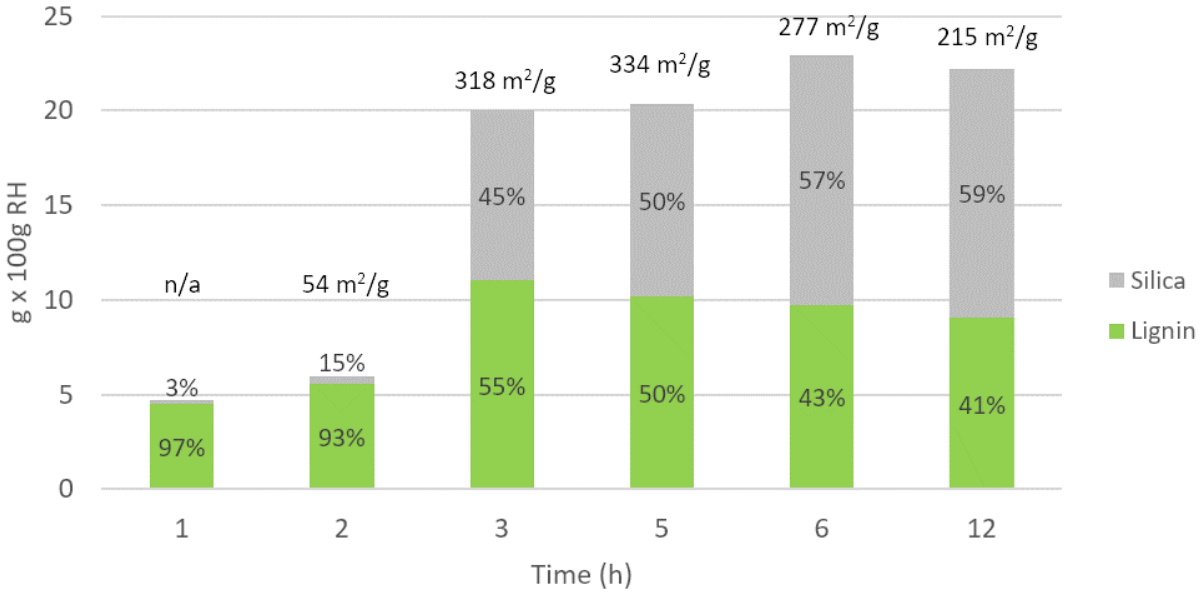

Figure 71 – Investigated characteristics of LSM prepared with different reaction p (pH = 4 / 90 °C).

raised rapidly while more silica was recovered, then slowly decreased for longer reaction periods. Only the effect of pH and time were investigated, whereas all the other parameters were kept as constant as possible, and temperature was selected on the basis of the partial optimization done by Qu et al.[1] Afterwards all the LSMs were prepared using the following conditions: pH = 4, temperature = 90 °C and reaction time = 6 hours. The conditions were selected because offered the best compromise between yield and high surface area. However, in the effort to improve the efficiency of the procedure, more concentrated solutions were employed. The yield per 100 g of RH was essentially unaffected by the initial concentration of lignin and silica; hence, the possibility to prepare more material in the same volumes was gradually explored, however the concentration of the precursors exerted a strong influence on the surface area of the LSMs, as illustrated in figure 72.

The morphology of the LSM was inspected via electron microscopy (FESEM), the analyses were effectuated on the pristine material (freeze-dried) and on after calcination (in air at 550 °C for 3 hours). The images are visible in figure 73 and 74. The morphology of the particles was irregular and the size was approximately 500-1000 nm. However, it was possible to detect structures characterized by a well-defined spherical morphology and a diameter of ~200 nm, partially embedded in the irregular particles. The spherical objects were supposed to be lignin particles, in fact it was not possible to detect them after calcination. In addition, the size matched with the data obtained with the DLS, analyzing the average size of rice husk lignin particles in diluted aqueous solutions, over a range of pH values. The results of the DLS analyses are displayed reported in figure 75. At pH 12 the average diameter of lignin particles was slightly above 200 nm, the average size gradually decreased reaching a minimum value of ~150 nm at pH 7 and then abruptly increased between pH 7 and 5 conceivably because of particle aggregation. After calcination, the material was clearly different, in

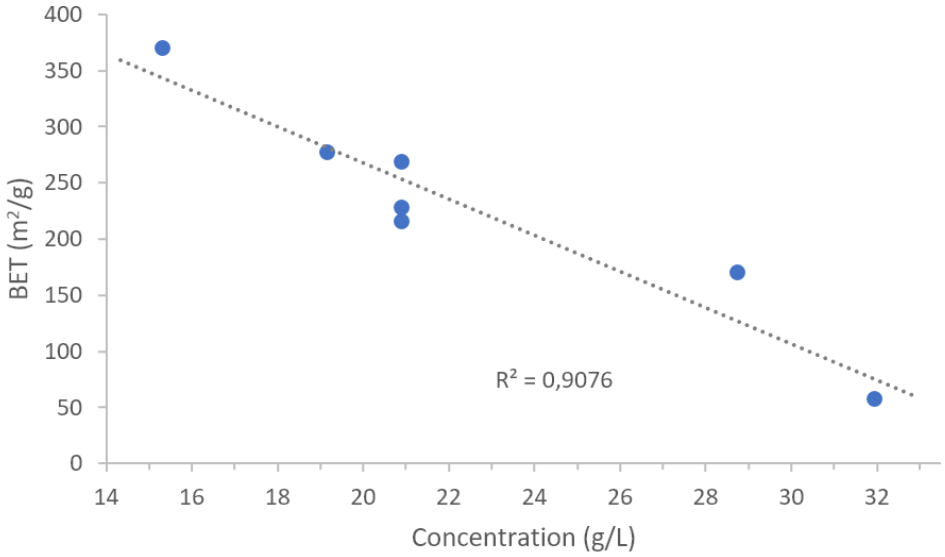

Figure 72 – Effect of the initial concentration (g of lignin + g of silica) on the surface area of the LSMs. (the other conditions were fixed: pH = 4, temperature = 90 °C, reaction time = 6 hours)

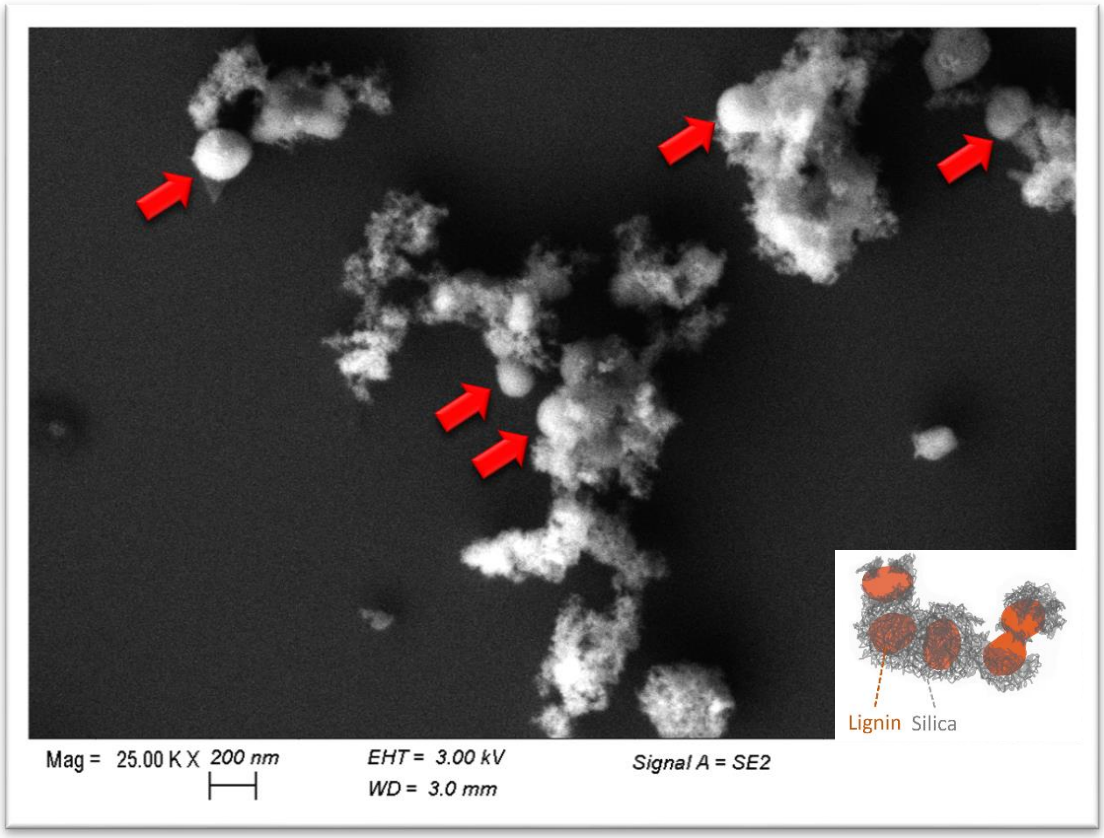

Figure 73 – FESEM image of the LSM and hypothetical schematic representation of the material.

550 °C

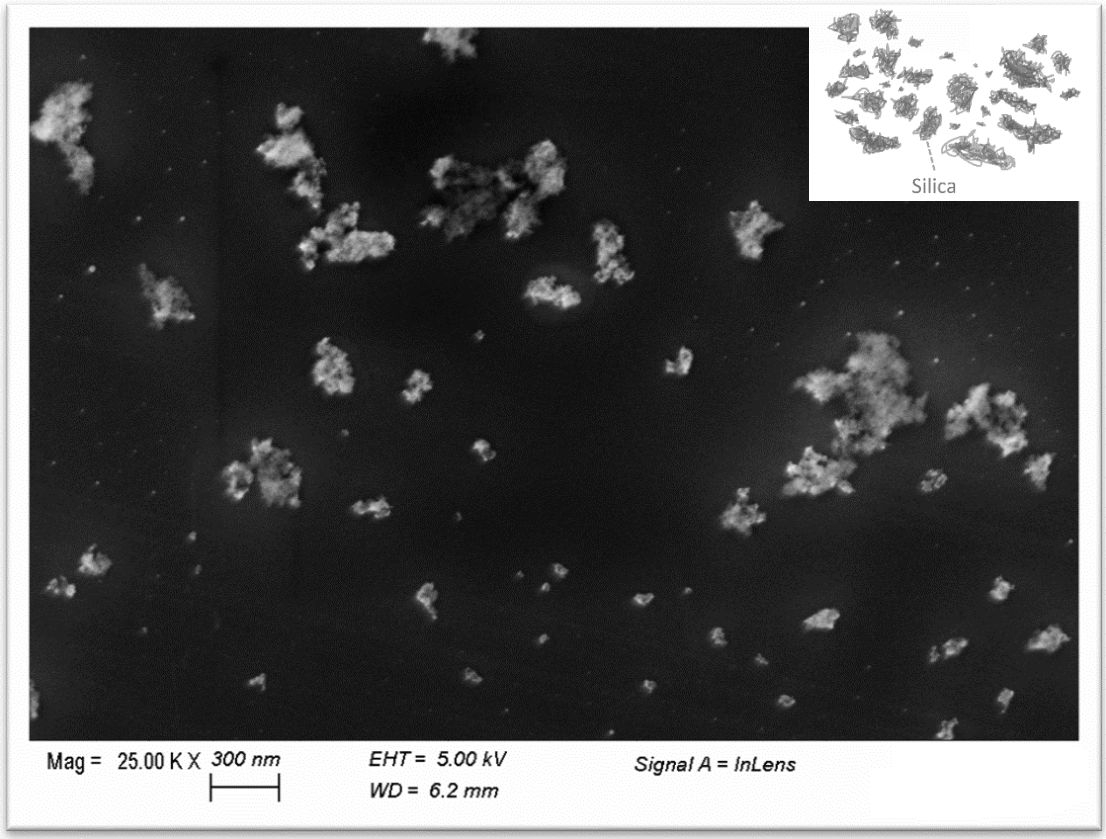

Figure 74 – FESEM image of the SLM after calcination (3 hours at 550 °C) and a plausible sketch.

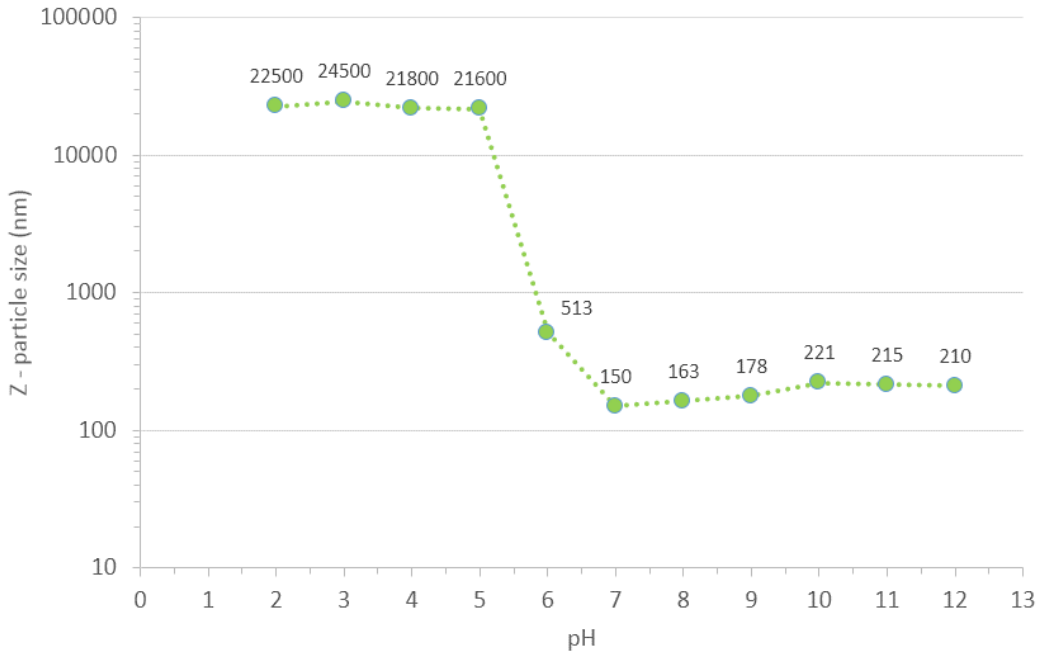

Figure 75 – Average particle diameter of RH lignin vs pH measured with DLS.

fact, it was constituted by smaller siliceous particles with sizes ranging from few tens of nanometers to several hundred nanometers. It was supposed that a core of lignin held together several smaller fragments of silica, forming larger particles, and that upon lignin removal the fragments were eventually released.

^{29}Si CP/MAS NMR was used to investigate the structure of silica and to detect eventual changes due to the presence of lignin (figure 76). The spectra revealed resonances at approx. -90, -100 and -110 ppm, owing to different chemical environments for the silicon atoms (Q2, Q3 and Q4). Cabrera and colleagues,[13] studied lignin-silica coprecipitates with ^{29}Si-NMR and found that lignin is capable of inducing substitution pattern changes on the surface of silica particles, likely due to hydrogen bonding interactions. They detected more Q2 and Q3 structures in lignin-silica coprecipitates, indicating the presence of more silanols. In our case the spectra were dominated by the peak attributable to Q3 species and a showed a low number of Q4 structures. The presence of lignin did not significantly change the structure of silica; however, it was possible to detect a limited increase in the relative intensity of the Q1 peak and a slight change in its shape, possibly due to small structural adjustments at the interface with lignin.

Beside the surface area (BET), also the pore size distribution was determined from the absorption isotherms using the BJH method. As observable in figure 77, the isotherm of the LSM material is similar to that of silica, both are type V isotherms, indicating that both materials are mesoporous (a,b). However, the shape of the hysteresis loop is slightly different, in relation to the different pore size distributions. While the distribution of silica is centered at around 30-40 nm, the pore distribution in the LSM is centered at ~15 nm, and the left tail approaches the region of the micropores. A high surface area is usually a good parameter for fillers, because it is usually associated with a reduced particle size. However, the presence of very small pores can

be a drawback because they are not accessible to rubber, but can withdraw other additives, such as vulcanizers and antioxidants.

The density of the LSM was also analyzed, determining the specific volume with a gas pycnometer. The LSM under investigation had a density of 1,75 g/cm^3. The density of the LSM was found to be lower than that of a typical silica used in tyres, ultrasil VN3, that was found to have a density of 2,05 g/cm^3.

Based on the collected evidences it was possible to identify a plausible mechanism for the formation of the LSM and to depict its final structure. As soon as the solution is acidified, lignin primary particles that are 150-200 nm in size start to flocculate. If the stirring is vigorous enough, it might disrupt particle association, limiting flocculation. Lignin particles/aggregates could behave as nucleating points for the oligomeric

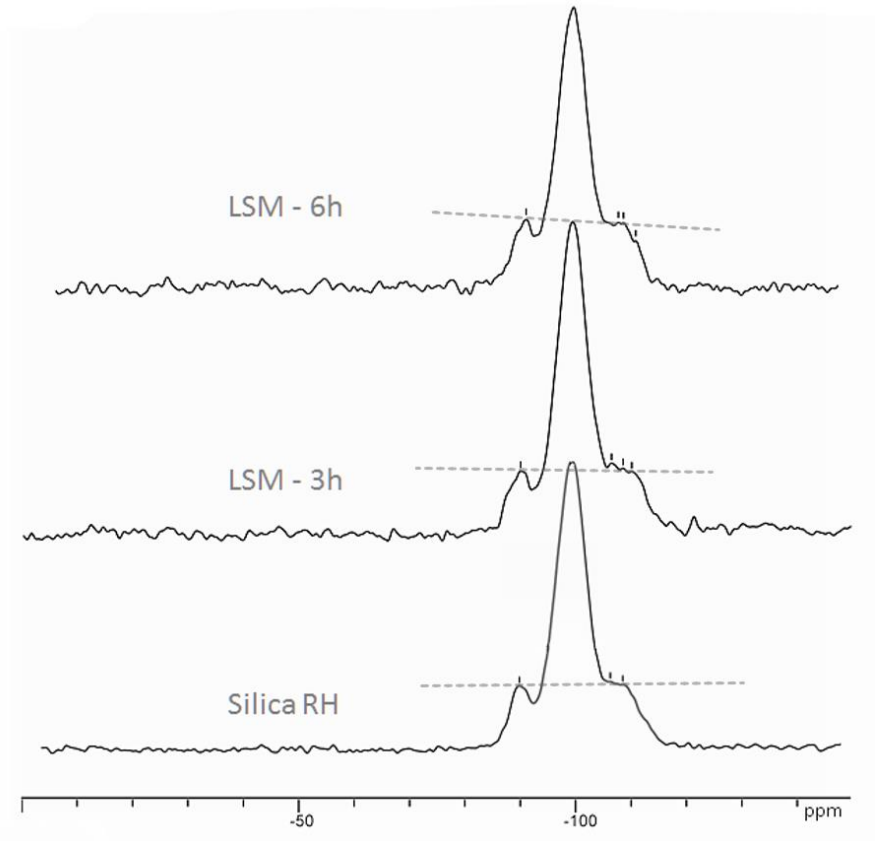

Figure 76 – ^{29}Si-NMR of silica from the biorefinery process of RH (pH 4, 4 h, 90 °C) and LSM (pH 4, 3 and 6 h, 90 °C).

silicates. Subsequently the silicates would continue to grow randomly by successive condensations, eventually surrounding the globular particle of lignin. At the end, the morphology and the dimension of the particles are not well defined and more lignin particles seem to be often entrapped in larger aggregates cemented by silica. It is plausible that a deeper investigation regarding the effect of the conditions of the coprecipitation process (concentration, temperature, ionic strength, mixing shear, etc.) on the morphology of the particles would permit to synthetize a more homogeneous material with improved properties.

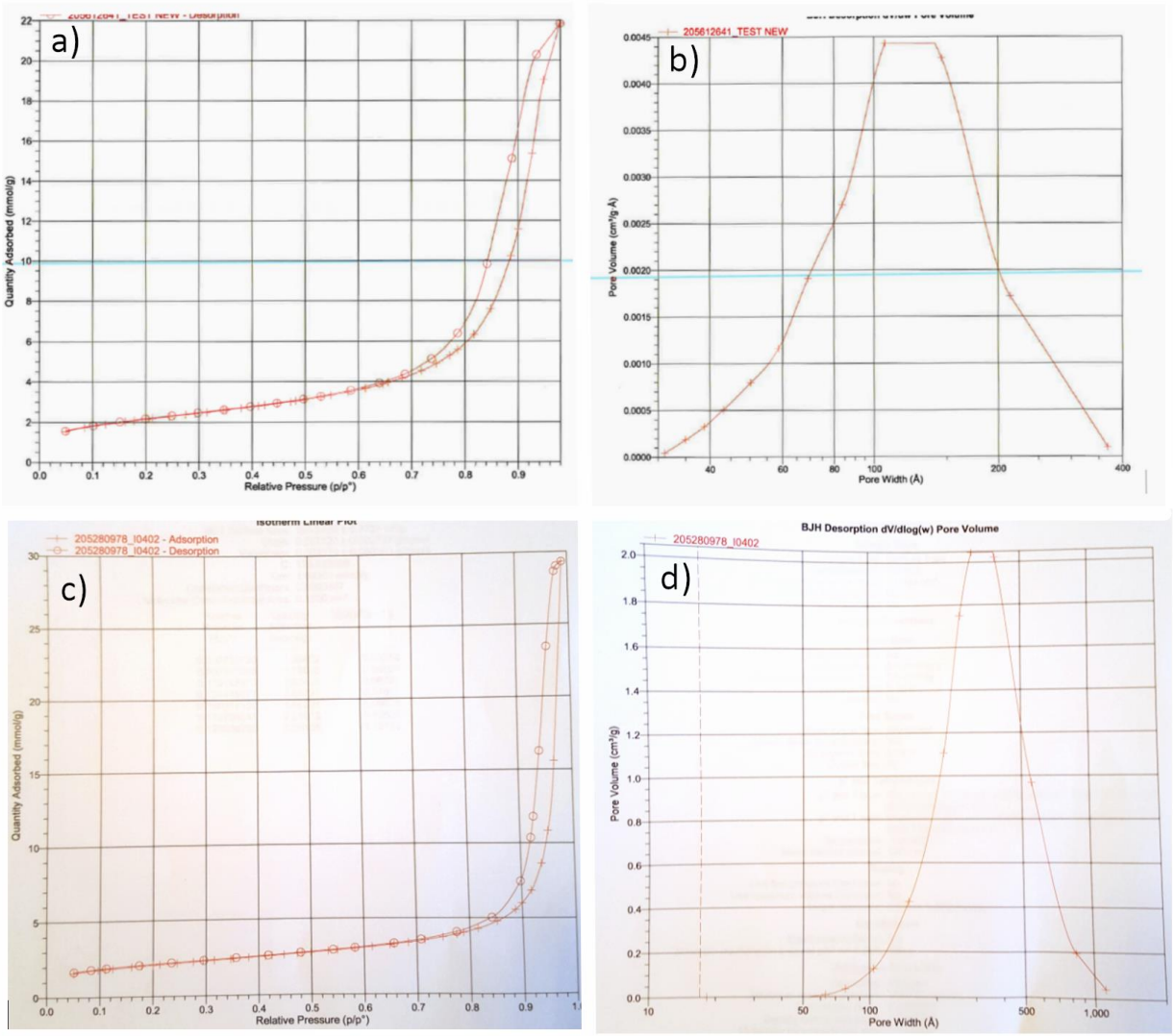

Figure 77 - Absorption isotherms and pore size distribution for LSM (a,b) and silica VN3 (c,d).

6.4 Rubber compounding with LSMs

In chapter 5, the LSM was blended with natural rubber to produce very simple rubber compounds. This section deals with a deeper analysis of the properties of different natural rubber composites prepared with LSM. At first small rubber compounds were prepared with the brabender mixer to investigate the effect of the coupling agent and the behavior at different loadings. Silanes like TESPT are fundamental in silica technology, they reduce the polarity and improve the filler-rubber interactions through chemisorption of rubber. In a second experiment, a larger amount of the composite was prepared at the Haake to have enough material to perform a broader assessment of the mechanical properties.

Experimental

LSM preparation. The LSM was prepared from 100 g of rice husk. After leaching (in 1L of 0,1M HCl, 2h at 100 °C) silica and lignin were extracted (with 1L of 0,5 M NaOH solution 4 h, 100 °C) and the dark solution was separated from the solid residue by filtration. The LSM was then prepared from the filtrate using the optimized conditions (temperature = 90 °C, reaction time = 6 h and pH = 4). The reaction was performed in a 2L round bottom flask equipped with a mechanical stirrer. At the end of the six hours the flask was left to cool off for one hour, afterwards the product was recovered through vacuum assisted filtration and was washed several times on the filter with a large amount of demineralized water. The wet powder was transferred in several petri dishes and freeze-dried. The procedure was repeated three times to obtain a suitable amount of LSM, the three fractions were collected together in a unique batch. The LSM composition was 59 % silica and 41 % lignin, and the material was characterized by a surface area (BET) of 216 m^2/g.

Rubber compounding. The rubber compounds were prepared with the formulation that are reported in each paragraph in the discussion. A first set of rubber compounds were prepared with the brabender, whereas the second set was prepared at the Haake to perform a more exhaustive characterization of the mechanical properties. The rubber compounds prepared without silane (TESPT) were prepared with the procedure number 2, the compounds with silane with procedure number 3; the procedures are described in chapter 4.

Rubber compounds characterization. The rubber compounds were investigated with different techniques: RPA, DMA, tensile tests, swelling measurements, and electron microscopy.

Figure 78 – Scale up of LSM preparation.

Results and discussion

At first small rubber compounds were prepared with the Brabender mixer, according to the formulations reported in table 18. The SLM was incorporated in rubber compounds at two different concentrations, 10 and 40 phr. The compounds at 10 phr were prepared with and without silane coupling agent (TESPT); in this first approach the amount of silane was not dosed according to the surface area of the filler, but was used in a fixed ratio with the phr of the fillers (SA - 180 m^2/g for silica and 215 m^2/g for LSM). The behavior of the LSM-filled rubber compounds was evaluated in comparison with the behavior of compounds filled with silica. Other compounds (with neat NR and CB) were also prepared to have additional references that might helped to better evaluate the effects of the LSM. The strain-sweep tests performed with the rubber process analyzer (RPA) gave useful information regarding the effectiveness of the coupling agent on the LSM. In silica, the effect of the coupling agent is clearly visible in the graph relative to the strain-sweeps on green compounds (top left in figure 79). The silane covered the silanols on the surface of silica particles, hydrophobilizing the material and hindering the otherwise strong filler-filler interactions; thus, the storage modulus (G') at low strains is reduced. The same behavior was observable for the compounds filled with the LSM, indicating that the coupling agent effectively covered the surface of the biofiller, increasing the compatibility with rubber and suppressing the association among particles; an indirect evidence that the surface of the particles was largely covered by silica. Besides it was also noticed that the Payne effect of the unmodified LSM was lower than that of the unmodified silica, presumably the presence of lignin slightly hindered filler aggregation and moderately enhanced the compatibility with rubber. However, after compatibilization with the silane the opposite was observed. At low loadings, the properties of silica and LSM were comparable, but at higher loadings, presumably above the percolation threshold of both fillers, it was possible to better appreciate the differences, and after compatibilization the SLM formed a stronger filler network than silica. The stronger filler-filler interactions formed in the LSM-filled compound were also detectable in the first part of the

	NR	CB 10	SLM 10	SLM S 10	Silica 10	Silica S 10	SLM S 40	Silica 40	Silica S 40
Natural rubber (SIR20)	100	100	100	100	100	100	100	100	100
Carbon black (N375)		10							
Silica (Ultrasil VN3)					10	10		40	40
SLM (215 m^2/g)			10	10			40		
Silane (TESPT)				1,2		1,2	4,8		4,8
Antioxidant (6PPD)	1	1	1	1	1	1	1	1	1
Soluble sulfur	2	2	2	2	2	2	2	2	2
Zinc oxide	5	5	5	5	5	5	5	5	5
Stearic acid	2	2	2	2	2	2	2	2	2
Accelerator (CBS)	2	2	2	2	2	2	2	2	2

Table 18 – Formulation in PHR for SLM filled rubber compounds with and without silane (TESPT), plus suitable references: neat natural rubber, carbon black, and silica.

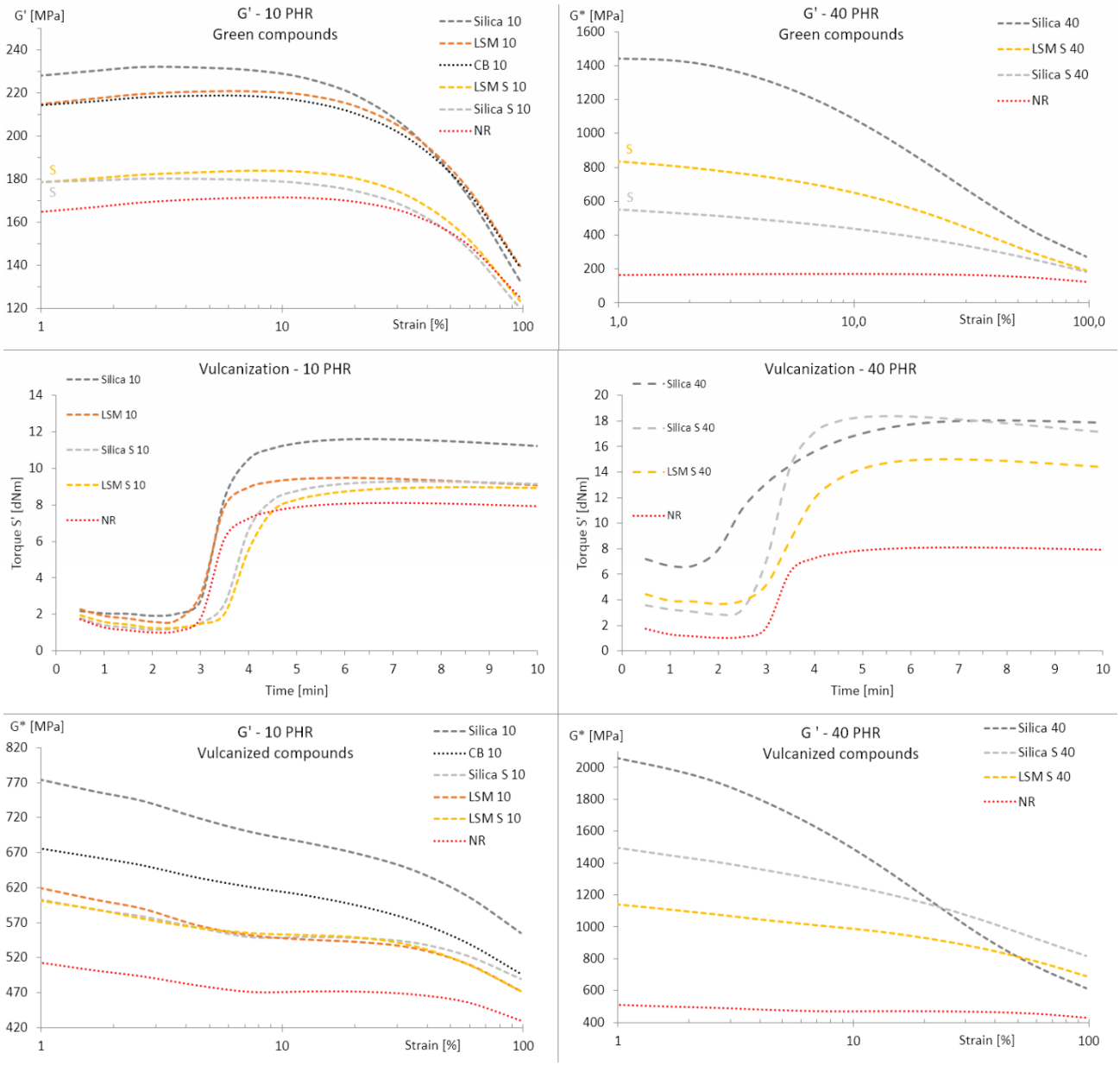

Figure 79 – Strain sweeps on green compounds, vulcanization curves (170 °C), and strain sweeps on vulcanized compounds. LSM at different loadings, with (S) and without coupling agent (TESPT), and suitable references.

vulcanization curves, in fact, before the beginning of curing the viscosity (ML) of the relative compound was higher. Successively, the LSM possibly hindered vulcanization, slowing the curing rate, and limiting vulcanization as evidenced by the limited change in torque (MH-ML). It must be pointed out that the difference between maximum and minimum torque is not only due to the crosslinking of the system but can also be influenced by other factors as the flocculation of the fillers. This event was particularly pronounced in the compound filled with 40 phr of unfunctionalized silica. At this regard, it was also noticed that unfunctionalized LSM seemed to have a lesser tendency for aggregation. In vulcanized compounds, in the samples prepared at 10 phr, both functionalized and unfunctionalized LSMs conferred properties that were like those conferred by the functionalized silica. However, a lower storage modulus at 100% deformation was

NR	CB 10	SLM 10	SLM S 10	Silica 10	Silica S 10	SLM S 40	Silica 40	Silica S 40
0	96	64	46	136	31	367	1365	598

Table 19 – Payne effect measured on vulcanized compounds ($\Delta G = G_0 - G_\infty$ | MPa).

	NR	CB 10	SLM 10	SLM S 10	Silica 10	Silica S 10	SLM S 40	Silica S 40
Bound rubber (%)	0	15,5	12,4	22,3	36,6	44,5	49,6	78,9
Crosslink density (mmol/g)	0,19	0,22	0,19	0,18	0,23	0,20	0,23	0,26

Table 20 - Bound rubber (%) and crosslink density (mmol/g) determined by means of toluene swellings.

interpreted as a possible indication of a lower interaction with the rubber. At 40 phr, the LSM clearly reinforced the elastomer, but to a lesser extent than the reference silica. The curve of LM-S-40 had the same shape of Silica-S-40 and it seemed to be shifted downwards. For this reason, it was supposed that the lower modulus was caused by a strain-independent contribution, and based on the vulcanization curves the hypothesis was that a non-optimal curing could have shrunk the contribution of the polymer. To verify the hypotheses the rubber compounds were furtherly tested with toluene swelling experiments, to determine the effective crosslinking density and the filler-polymer interactions (bound rubber). The bound rubber is the fraction of the polymer that is not removed by a good solvent, and is hence entrapped by the filler. The results (table 20) demonstrated that the filler-polymer interactions with the LSM are lower than with the traditional filler, but are not too far from carbon black. It must be noted that lignin has a good affinity for the solvent as well, and this could have influenced the test. However, it was also observed that compatibilization with the silane was effective also on the LSM, enhancing the bounded fraction at every phr. The suppositions made observing the vulcanization curves were confirmed by the analysis of the crosslinking densities. The crosslinking densities of the functionalized LSMs were found to be ~10% lower than those of the respective functionalized silicas. Hence it was supposed that a combination of high surface area and the presence of lignin could promote the interference with the vulcanizing system, possibly adsorbing sulfur, or other reactants. Finally it is worth highlighting that despite the lower value of G', the vulcanized LSM-S-40 displayed a tan Delta in line with that of silica, due to a lower viscous component of the modulus (G''). With a temperature sweep, it was observed that at higher

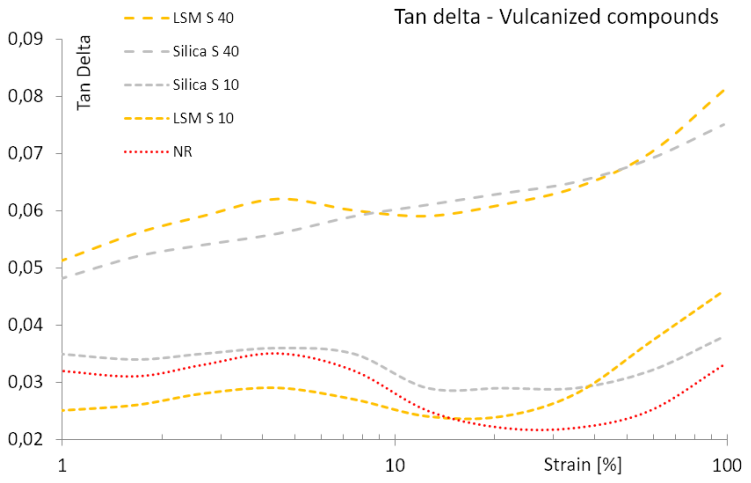

Figure 80 – Tan Delta measure during the strain sweep on the vulcanized compounds

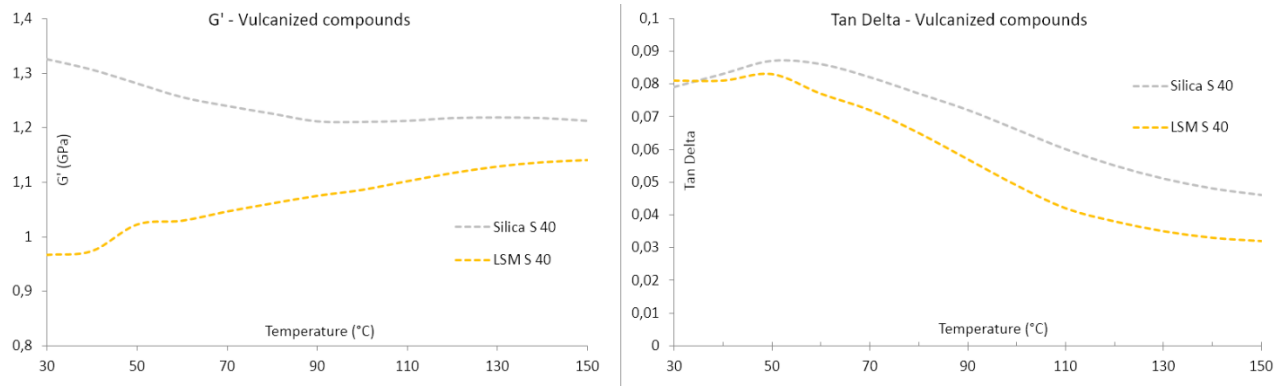

Figure 81 - Temperature sweep on vulcanized compounds (strain 5% - frequency 5 Hz).

temperatures the LSM improved the stiffness of the rubber compounds, whereas the compounds filled with silica tended to became softer. This behavior could be interesting since a low hysteresis is usually associated with a lower rolling resistance in tyres.[14]

Successively, larger amounts of the elastomeric composites were prepared at the Haake mixer, to perform a more detailed characterization of the mechanical properties. The formulations and the results of the various characterizations are summarized in table 21. The rubber compound filled with LSM was prepared at 15 phr, neat natural rubber and natural rubber filled with 15 phr of silica were also prepared as references. The dispersion of the filler was assessed with scanning electron microscopy, analyzing cut surfaces of the material sputtered with a thin layer of gold (figure 82). The filler was dispersed rather homogeneously through the polymeric matrix, with the presence of sporadic clusters and few areas with a lower density of particles. The filler didn't have a specific morphology, possessed a low structure and the dimensions of the particles ranged between 200 nm and 1 μm. At the selected concentration -15 phr - which is relatively low, the LSM didn't interfered with vulcanization and the values of ML, MH and the optimum vulcanization time (T95) are essentially in line with those of the silica-filled compound. The dynamic-mechanical properties (DMA) were considered interesting. The compound filled with the LSM had higher dynamic moduli (E') in the whole range of conditions (10-70 °C / 10-100 Hz), and identical values of tan Delta in comparison with the reference filled with silica. The mechanical properties were also evaluated at higher elongations via static tensile testing, the analyses were repeated after thermally aging the samples, exposing them to a temperature of 70 °C in air for one week. At low strain the tests essentially confirmed the results of the dynamic analyses. In fact, until 150% elongation the moduli of the LSM compound were virtually in line with that of the silica compound. The LSM effectively reinforced natural rubber, at 300% elongation the modulus was 78% higher than in the neat natural rubber reference, however, the effect was lower than in the silica-filled compound, where the modulus increased by +111%. The ultimate properties were also greatly improved by the LSM, as observed in the specimens prepared from rubber composites with lignin.

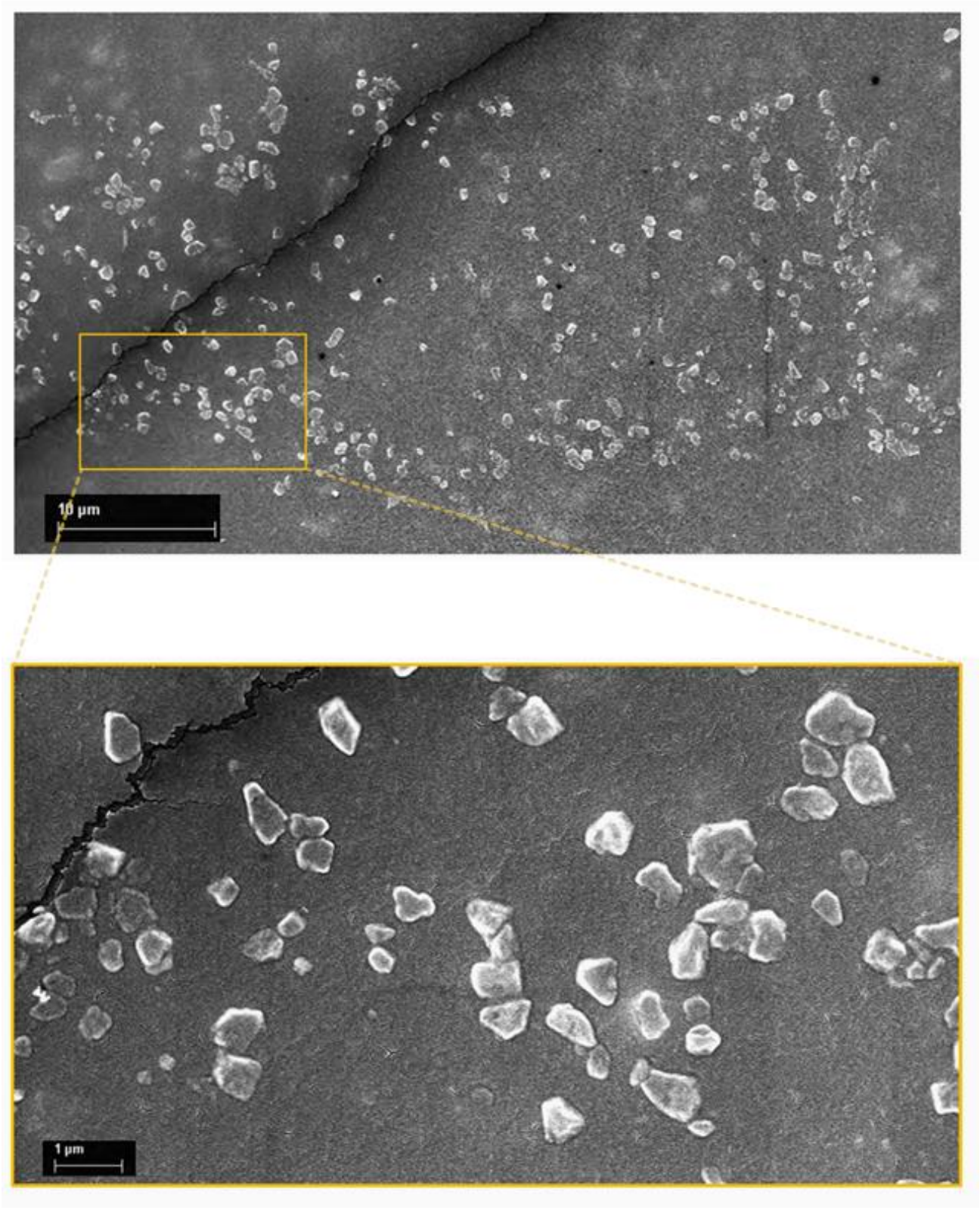

Figure 82 – SEM image of a rubber compound filled with 15 phr of SLM.

		NR	Silica	SLM
Formulations				
Natural rubber (SIR 20)		100	100	100
Silica (Ultrasil VN3)			15	
SLM (with SA = 215 m2/g)				15
Silane (TESPT)			1,2	1,2
Antioxidant (6PPD)		1	1	1
Soluble sulfur		2	2	2
Zinc oxide		5	5	5
Stearic acid		2	2	2
Accelerator (CBS)		2	2	2
Theoretical density		0,970	1,033	1,024
Vulcanization properties (10 min – 170 °C)				
ML [dN m]		0,9	1,45	1,39
MH [dN m]		9,32	11,57	11,58
T95 [min]		14,75	15,43	15,35
Dynamic-mechanical properties (DMA)				
10 °C 10Hz 7.5% -20%	E' [Mpa]	2,17	2,85	3,08
	Tan Delta	0,02	0,04	0,04
10 °C 100Hz 7.5% -20%	E' [Mpa]	2,24	3,02	3,27
	Tan Delta	0,10	0,12	0,12
23 °C 10Hz 7.5% -20%	E' [Mpa]	2,22	2,90	3,13
	Tan Delta	0,01	0,03	0,03
23 °C 100Hz 7.5% -20%	E' [Mpa]	2,24	2,99	3,24
	Tan Delta	0,05	0,07	0,07
70 °C 10Hz 7.5% -20%	E' [Mpa]	2,33	2,98	3,20
	Tan Delta	0,01	0,02	0,02
70 °C 100Hz 7.5% -20%	E' [Mpa]	2,35	3,03	3,30
	Tan Delta	0,04	0,05	0,05
Mechanical properties (tensile testing)				
Stress 10% [MPa]		0,27	0,33	0,32
Stress 50% [MPa]		0,69	0,86	0,82
Stress 100% [MPa]		1,05	1,40	1,33
Stress 300% [MPa]		2,90	6,13	5,16
Ultimate strength [MPa]		6,16	16,97	14,70
Ultimate elongation [%]		417	453	490
ENERGY [J/cm3]		9,18	24,65	23,92
Reinforcement index		2,8	4,4	3,9
Mechanical properties after thermal aging (70 °C, 168 h)				
Stress 10% [MPa]		0,27 (-)	0,32 (-3%)	0,31 (-3%)
Stress 50% [MPa]		0,7 (+1%)	0,87 (+1%)	0,85 (+4%)
Stress 100% [MPa]		1,08 (+3%)	1,44 (+3%)	1,43 (+8%)
Stress 300% [MPa]		-	-	5,55 (+8%)
Ultimate strength [MPa]		3,51 (-43%)	6,97 (-59%)	6,54 (-56%)
Ultimate elongation [%]		281 (-33%)	283 (-37%)	326 (-33%)
ENERGY [J/cm3]		4,82 (-47%)	8,95 (-64%)	9,55 (-60%)

Table 21 – Formulations, curing and mechanical properties of the natural rubber compounds.

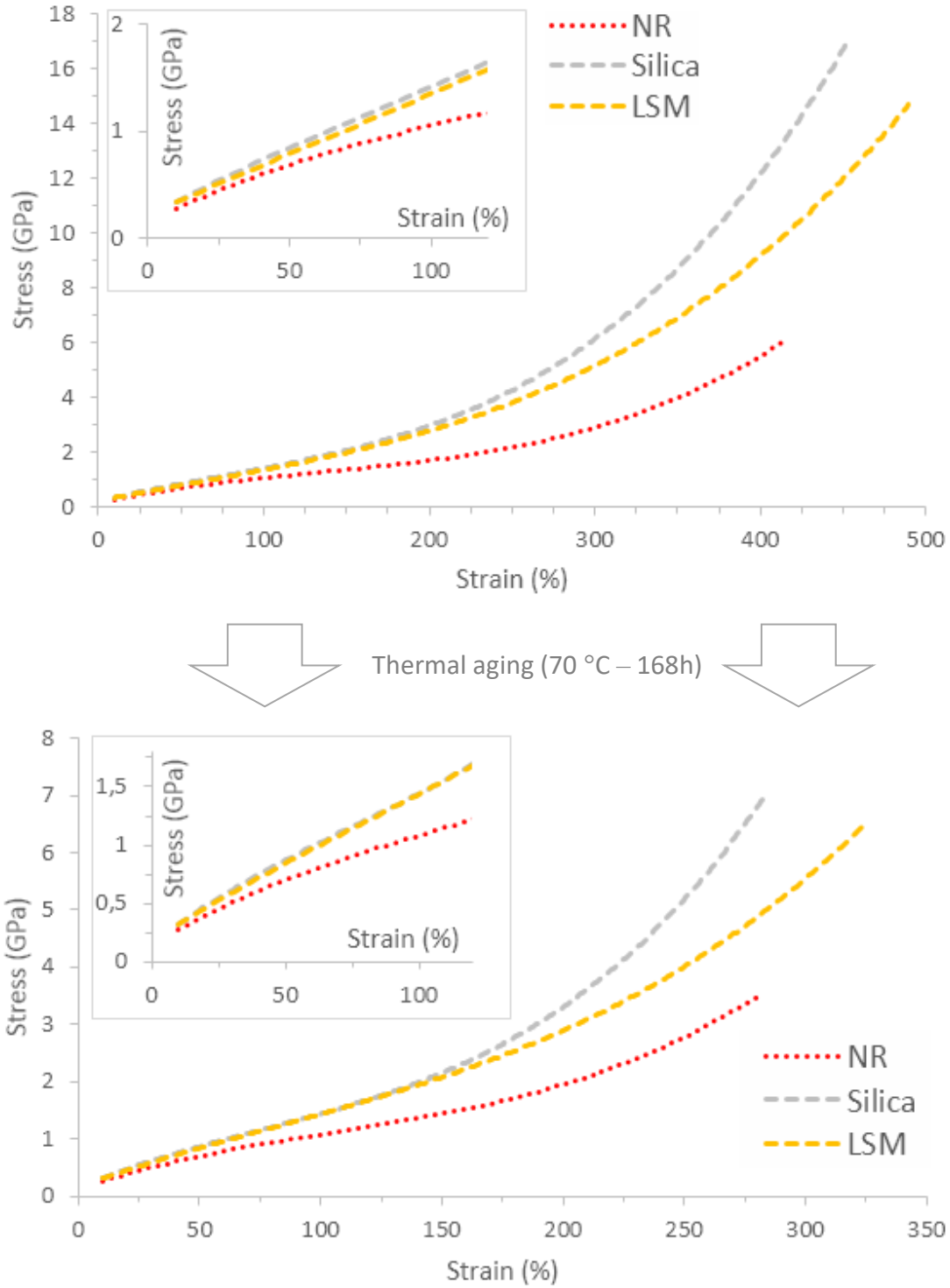

Figure 83 - Stress/strain curves on NR vulcanizates before and after thermal aging.

However, lignin was not capable to produce much stiffer compounds and that was hence connected to the presence of silica. The mechanical properties of all rubber compounds (NR, Silica and LSM) were clearly deteriorated in consequence to the thermal aging. The LSM seemed to limit the damage caused by oxidation and the properties of the relative compound improved in had a ultimate strength lower than silica, but an

improved ultimate elongation. This behavior might derived from the compresence of silica and lignin, in fact the improvement of the elongation at break was already comparison to silica after the treatment, as highlighted by the relative changes reported in the brackets (±%) in table 21.

6.5 Conclusions

A new organic/inorganic biofiller for rubber reinforcement was produced from a low-cost, renewable resource. The ligno-siliceous material was synthetized taking advantage of the peculiar composition of rice husk that often is considered a limit for possible applications. The two components of the material, lignin and silica, were supposed to mutually interact during the coprecipitation process. The responsiveness of the two substances to several factors (pH, temperature, concentration, ionic strength, etc.) can be used to tune the properties of the final material, however the sensitivity towards many parameters can also complicate the preparation and makes the scaling-up more difficult. The collected evidences allowed to hypothesize that the material was composed of spherical particles of lignin with an average diameter of few hundred nanometers, and randomly covered by silica. The tentative biofiller effectively reinforced natural rubber, even though to a somewhat lesser extent than commercial silica. The difference in the reinforcement was partially accounted to the relatively large average particle size, promoted by the fusion of several lignin and silica particles into larger aggregates and partially to the interference with vulcanization possibly caused by the presence of lignin and small mesopores. Overall, the material showed interesting properties, connected to the simultaneous presence of lignin and silica: reinforcement, protection, lower density than silica. In the end, it is plausible that through a better control over the parameters that govern the process and perhaps through their modulation over time it is possible to improve the microscopic characteristic of the LSM and enhance the overall properties conferred to elastomeric composites.

References

(1) Qu, Y.; Tian, Y.; Zou, B.; Zhang, J.; Zheng, Y.; Wang, L.; Li, Y.; Rong, C.; Wang, Z. A novel mesoporous lignin/silica hybrid from rice husk produced by a sol-gel method. *Bioresour. Technol.* **2010**, *101* (21), 8402–8405.

(2) Shweta, K.; Jha, H. Rice husk extracted lignin–TEOS biocomposites: Effects of acetylation and silane surface treatments for application in nickel removal. *Biotechnol. Reports* **2015**, *7*, 95–106.

(3) Zhang, X.; Zhao, Z.; Ran, G.; Liu, Y.; Liu, S.; Zhou, B.; Wang, Z. Synthesis of lignin-modified silica nanoparticles from black liquor of rice straw pulping. *Powder Technol.* **2013**, *246*, 664–668.

(4) Cui, J.; Sun, H.; Wang, X.; Sun, J.; Niu, M.; Wen, Z. Preparation of siliceous lignin microparticles from wheat husks with a facile method. *Ind. Crop. Prod.* **2015**, *74*, 689–696.

(5) Xiong, W.; Yang, D.; Zhong, R.; Li, Y.; Zhou, H.; Qiu, X. Preparation of lignin-based silica composite submicron particles from alkali lignin and sodium silicate in aqueous solution using a direct precipitation method. *Ind. Crop. Prod.* **2015**, *74*, 285–292.

(6) Jesionowski, T.; Klapiszewski, Ł.; Milczarek, G. Kraft lignin and silica as precursors of advanced composite materials and electroactive blends. *J. Mater. Sci.* **2014**, *49* (3), 1376–1385.

(7) Klapiszewski, Ł.; Nowacka, M.; Milczarek, G.; Jesionowski, T. Physicochemical and electrokinetic properties of silica/lignin biocomposites. *Carbohydr. Polym.* **2013**, *94* (1), 345–355.

(8) Klapiszewski, Ł.; Bartczak, P.; Wysokowski, M.; Jankowska, M.; Kabat, K.; Jesionowski, T. Silica conjugated with kraft lignin and its use as a novel “green” sorbent for hazardous metal ions removal. *Chem. Eng. J.* **2015**, *260*, 684–693.

(9) Klapiszewski, L.; Nowacka, M.; Szwarc-Rzepka, K.; Jesionowski, T. Advanced biocomposites based on silica and lignin precursors. *Physicochem. Probl. Miner. Process.* **2013**, *49* (2), 497–509.

(10) Ragnar, M.; Lindgren, C. T.; Nilvebrant, N.-O. Proposed pK a -values in water at 25 °C of guaiacyl and syringyl phenols related to lignin.

(11) Si-Han Wu, a C.-Y. M. and H.-P. L. Synthesis of mesoporous silica nanoparticles. *Chem. Soc. Rev.* **2013**, *42* (9), 3862.

(12) Tobler, D. J.; Shaw, S.; Benning, L. G. Quantification of initial steps of nucleation and growth of silica nanoparticles: An in-situ SAXS and DLS study. *Geochim. Cosmochim. Acta* **2009**, *73* (18), 5377–5393.

(13) Cabrera, Y.; Cabrera, A.; Larsen, F. H.; Felby, C. Solid-state 29Si NMR and FTIR analyses of lignin-silica coprecipitates. *Holzforschung* **2016**, *70* (8), 709–718.

(14) Zhang, P.; Morris, M.; Doshi, D. Materials Development for Lowering Rolling Resistance of Tires. *Rubber Chem. Technol.* **2016**, *89* (1), 79–116.

(15) Schön, F.; Gronski, W. Filler networking of silica and organoclay in rubber composites: Reinforcement and dynamic-mechanical properties. *KGK-Kautschuk und Gummi Kunststoffe* **2003**, *56* (4), 166–171.

CHAPTER 7 - Relationships between lignin molecular structure and the properties of its composites with natural rubber

From the results of the experiments reported in chapter 5 it was observed that when lignin from rice husk was blended with natural rubber via coprecipitation technique it improved the mechanical properties of the elastomeric composites, especially at high elongations. However, as deeply discussed in chapter 2, lignin is a complex material and its properties can greatly differ according to the botanical origin of the biopolymer and the isolation process employed for its recovery. In this study five lignins obtained from different sources and through different extraction processes were characterized in terms of purity, sulfur content, molecular weight distribution, and functional group distribution. Afterwards the lignins were blended with natural rubber using dry-mixing and coprecipitation techniques. Finally, thermal and mechanical properties of the composites were analyzed to understand their dependence from several characteristics of lignins.

7.1 Background

Lignin is considered an interesting candidate for the substitution of fossil-derived materials due to its high abundance, large annual renewability, low average molecular weight, environmental friendliness, and CO_2 neutrality.[1] Furthermore it was demonstrated that lignin can behave as an antimicrobial, antifungal, antioxidant, flame retardant and can absorb UV radiation.[2–4] Due to these characteristics, lignins were used in combination with natural and synthetic polymers for the production of thermosets, thermoplastics, elastomers, resins, and foams and many applications are reported in literature.[1,5–8] The first attempts to use lignin in composites with rubbers date back to 1950s.[9] However, when lignin was used as a replacement for carbon black and functionalized silica a loss of mechanical properties was observed. This is believed to be a consequence of the lower compatibility and larger particle size of lignin.[10–12] At the same time, the use of lignin was found appealing for the possibility to protect rubber from thermo-oxidative degradation.[10,13,14] Despite the large number of works that are available in literature, in each study typically only one kind of lignin is considered and the critical differences that can exist between the structures of different lignins are often underestimated. In this work the importance of lignin's heterogeneity was taken into account analyzing the properties of rubber compounds prepared with five different lignins. The selected lignins were obtained from different lignocellulosic feedstocks and via different industrial and laboratory scale processes to have a good variety of structural features.

7.2 Materials

Soda Grass lignin (SG) lignin is a lignin commercialized by Green Value under the trade name of Protobind 1000. It is obtained from annual plants using a process based on soda pulping. **Softwood Kraft lignin (SWK)** and **Hardwood Kraft lignin (HWK)** are a side products of the Kraft process, used for the production of the cellulose pulp in paper industry. HWK lignin was the only product to be subjected to purification due to its extremely high ash content. It was purified via dissolution in a NaOH solution at pH 13 and reprecipitation by addition of sulfuric acid 98% until pH 1. Afterwards it was purified through several centrifugation cycles and freeze-dried. **Wheat Straw lignin (WS)** was purchased from Chemtex srl. It is a byproduct generated during the production of bioethanol from lignocellulosic biomasses that are pretreated with steam-explosion. **Rice Husk lignin (RH)** was extracted from rice husk using the biorefinery process presented in chapter 5. The details of the materials used for rubber compounding are reported in the related section of chapter 4. All the other reagents and solvents (ACS grade) were purchased from Sigma-Aldrich and used as received without further purification.

7.3 Characterization of lignins

Experimental

Lignin Content. The amount of total lignin (purity degree) was calculated as the sum of the acid-insoluble (Klason lignin) and acid soluble lignin content.[15] The values reported are the average of three analyses (±1.0%).

Ash Content. Accurately weighed and dried samples (around 100 mg) were put in tared, well-desiccated porcelain crucibles, and placed in a muffle furnace set at 550 °C for 3 h. The crucibles were then stored in a desiccator until room temperature was reached. The ash content was determined gravimetrically. The values reported are the average of three analyses (±0.1%).

Chemical functionalities. The presence of different chemical groups was assessed qualitatively with FT-IR spectroscopy and quantitatively with ^{31}P-NMR.

Molecular weight distribution. The molecular weight distribution was determined for each lignin analyzing acetylated samples with GPC.

Sulphur content. Sulfur content was assessed using a Leco SC632 sulfur and carbon analyzer. The instrument uses an ASTM-approved technique to determine the amount of sulfur contained in different materials. The method refers to sulfur determination according to ASTM D6741-10, ASTM D1619-11 (Method A), and ASTM D7679-13 (Method A).

Results and discussion

Before assessing the properties conferred to rubber compounds, the five lignins were preliminarily characterized by gravimetric, spectroscopic, and chromatographic techniques. At first the biopolymers were investigated with FT-IR spectroscopy. It is a fast and convenient technique, however it can provide a fair amount of information, since the absorption spectra are influenced by the structural features of lignin but also by the presence of contaminants. The IR spectra obtained from the analysis of the five specimens are reported in figure 84 (full range 800-3800 cm^{-1} and fingerprint region 800-1800 cm^{-1}). The assignments were made referring to published data available in literature, a correlation table with the characteristic bands of lignin and the other components of lignocellulosic materials is available in chapter 4. At first sight it is possible to recognize many similarities in the five spectra, as every sample displays the characteristic peaks that correspond to the fundamental architecture of lignin. At the same time, it is also possible to spot considerable differences, especially in the relative intensity of the absorption bands in the fingerprint region. This is a first evidence of the heterogeneity of the selected lignins. Every sample displayed a broad and irregular peak in the 3200-3500 cm^{-1} range. This absorption band is common in all the main components of lignocellulosic materials and is related to the presence of many aliphatic and phenolic hydroxyl groups and eventually also to the presence of moisture. In the region dominated by the stretching of the C-H groups every lignin specimen had two peaks centered at 2934 and 2846 cm^{-1}. Afterwards, from 2800 to roughly 1800 cm^{-1} in all the spectra is not possible to observe meaningful peaks. Only RH lignin possess a positive peak in this interval, but it is probably due to the contamination of the atmosphere with a small amount of CO_2 during the acquisition of the background. The first peak that is possible to identify in the fingerprint region, at around 1700 cm^{-1}, is attributable to the unconjugated stretching of C=O in carbonyl and carboxylic groups. In WS and RH samples it might overlaps to another band caused by the presence of adsorbed water. Subsequently, bands associated with aromatic skeletal vibrations are clearly visible at 1595 and 1509 cm^{-1}, while peaks connected to C–H deformation in methyl or methylene groups and aromatic ring stretching are found at 1453 and 1426 cm^{-1}, respectively, in all samples. At 1319 cm^{-1} a weak band is present in all the samples but not in SWK lignin. The band can be attributed to the C–O stretching of the syringyl (S) units that in fact, are particularly scarce in softwoods. On the other hand, a peak at 1265 cm^{-1}, associable to the C–O stretching of guaiacyl (G) units can be found in all the spectra. At 1215 cm^{-1} every sample shows a band associable with the C–O stretching of phenolic functionalities and aromatic ethers. Peaks related to C–H in-plane deformations of guaiacyl (G) and syringyl (S) units are found at 1147 and 1114 cm^{-1}, respectively. As before SWK lignin doesn't present the signal relative to the S units. The same peak is shifted at higher wavenumbers for RH lignin, this is might due to the overlapping with other absorptions signals caused by the presence of residual polysaccharides that usually display increased IR activity at these wavelengths. The signal centered around 1024 cm^{-1} is connected to aliphatic hydroxyls and esters, and also this peak is enhanced by the resence of saccharide residues. Only in certain samples it was possible to finally identify two weak peaks at

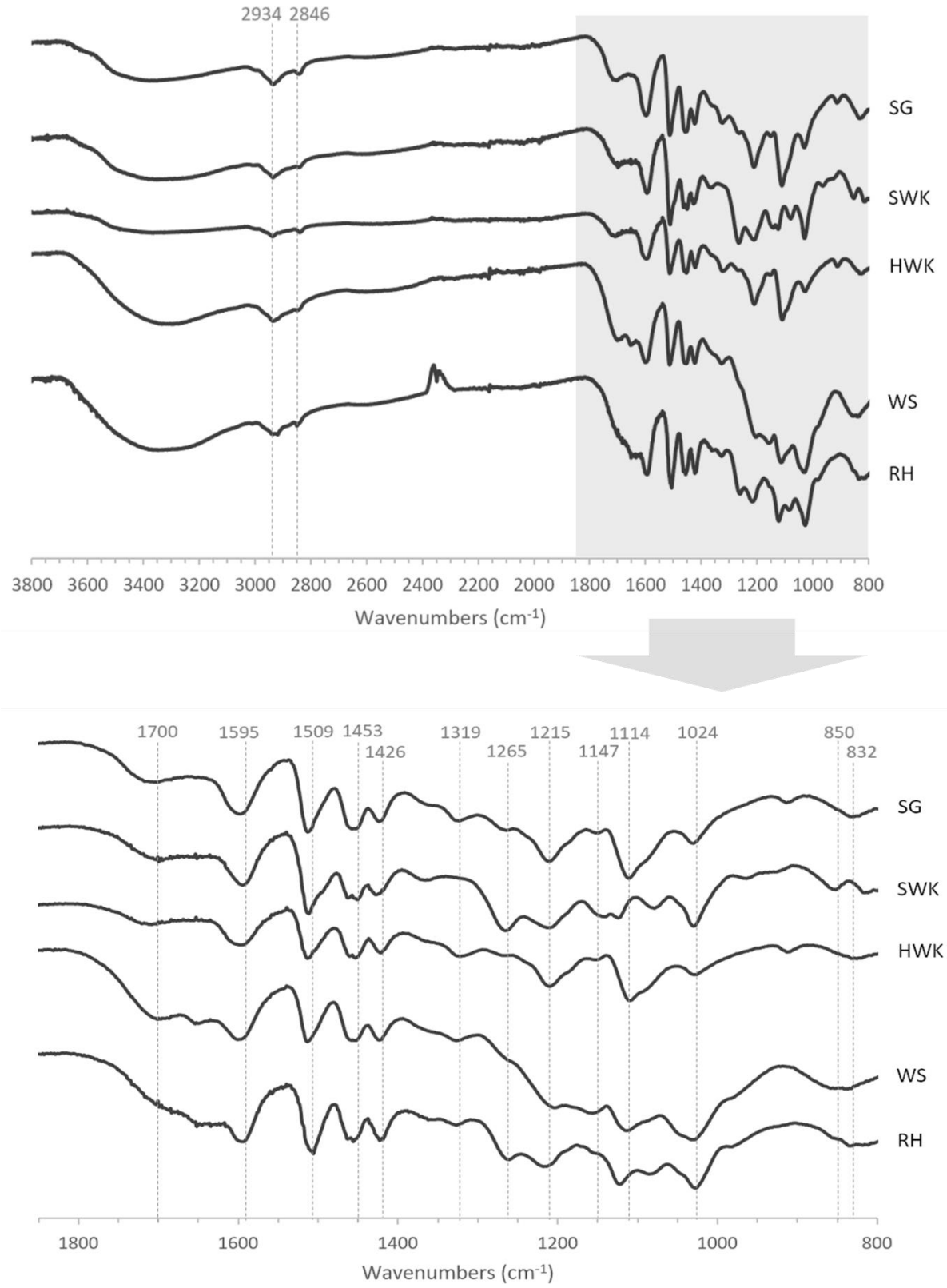

Figure 84 - FT-IR spectra of the five lignins under investigation.

850 and 832 cm^{-1} allegedly ascribable to the bending of C-H groups in guaiacyl (G) and syringyl (S) units respectively. As previously introduced, the variability in the intensities of the characteristic absorption bands clearly revealed structural heterogeneity among the different lignin specimens, especially in the 1400−1000 cm^{-1} range, where the signals are influenced by the divergences in the relative amount of p-hydroxycumaryl (H), guaiacyl (G), and syringyl (S) units.

The quantitative analysis of the distribution of different hydroxyls functionalities into lignin macromolecule was achieved by ^{31}P NMR analysis, the spectra are displayed in figure 85, while the quantitative results obtained from the integration of the peaks are recapitulated in table 22. The total amount of aliphatic hydroxyl groups wasn't found to differ greatly among the five lignins. It increased smoothly: HWK < SG < WS < RH < SWK, with SWK lignin having roughly 50% more aliphatic -OH than HWK lignin. Also the number of carboxylic acids was found to be well aligned in all lignin samples with the exception of SG lignin that was found to have almost a double amount of such functionalities. On the contrary, the absolute amount phenolic hydroxyls and the relative abundancy of H, G and S/condensed phenolic moieties varied greatly. The concentration of phenolic moieties decreased in the order: SWK > HWK > SG > WS > RH, ranging from ~1 mmol/g in RH lignin to ~5 mmol/g in SWK lignin. As expected, in herbaceous lignins all the three monomeric constituents were well represented, on the other hand, Kraft lignins had a greater amount of S-type and condensed phenols. However, considering that native lignin in softwoods has a low amount of S units,[16] it is possible to assume that SWK lignin is particularly rich in condensed structures.

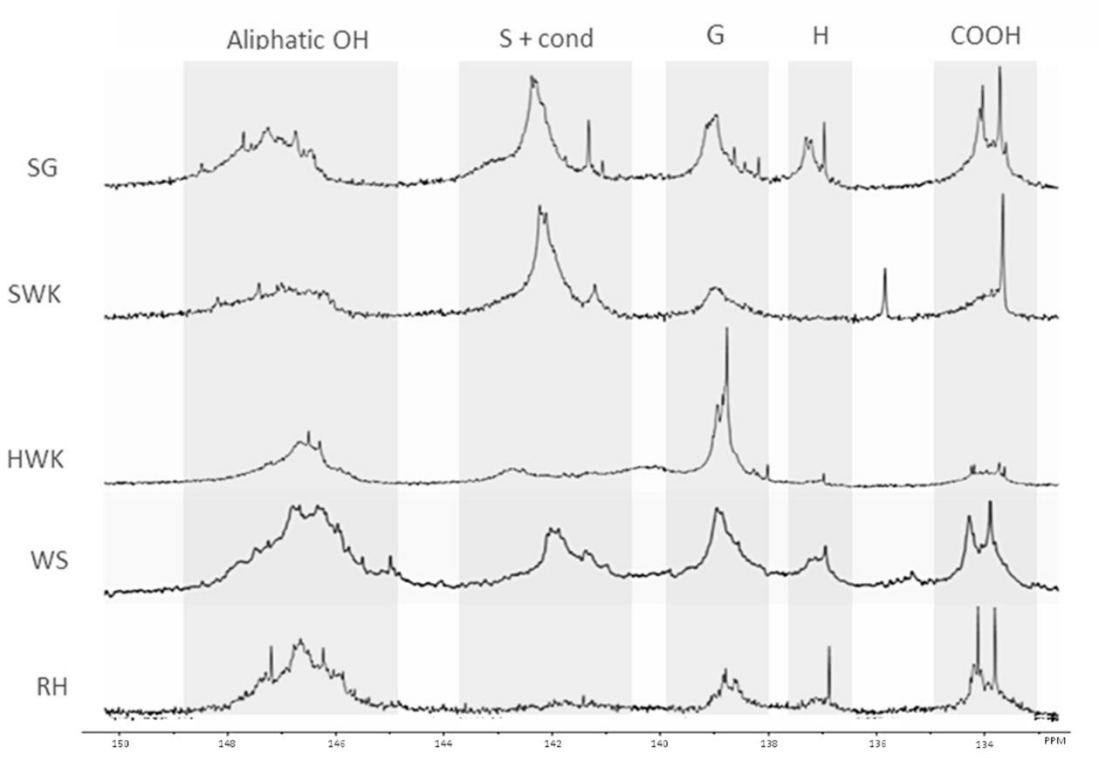

Figure 85 - ^{31}P-NMR spectra of the five investigated lignins.

This also agrees with the harsh conditions used to separate the lignin from the pulp and the documented observation that the Kraft process induces substantial modifications in the structure of lignin enhancing condensation.[17] Besides, SWK lignin also displayed an increased concentration of G type phenolic moieties, more than double of the amount present in the other lignins rich in phenolic groups, such as HWK and SG. The absolute amount of p-hydroxyphenyls was low in all the samples and was found to be negligible in HWK lignin. The contribution of H-type phenols to the total concentration of phenolic moieties was also generally very low, but not in RH lignin where roughly one in three phenolic moieties was a p-hydroxyphenyl.

In polymers, also the average size of the macromolecules is an important feature. It plays a major role in the definition of the macroscopic qualities of the materials and can have a noticeable effect on the mechanical properties. The molecular weights distributions were assessed via GPC on small acetylated samples. The results of the analysis are presented graphically in figure 86, while the Number-average molecular weight, Weight-average molecular weight and Peak-average molecular weight (Mn, Mw and Mp) and the polydispersity index (PDI) are summarized in table 22. In line with the observations made during the discussion of the spectroscopic analysis, also the molecular weight distributions revealed a great heterogeneity among the studied lignins. Once more it was possible to confirm that the characteristics of lignin are dramatically affected by the botanical source and the extraction process. SG lignin had the lowest average molecular weight, with a narrow distribution characterized by a conspicuous number of oligomeric

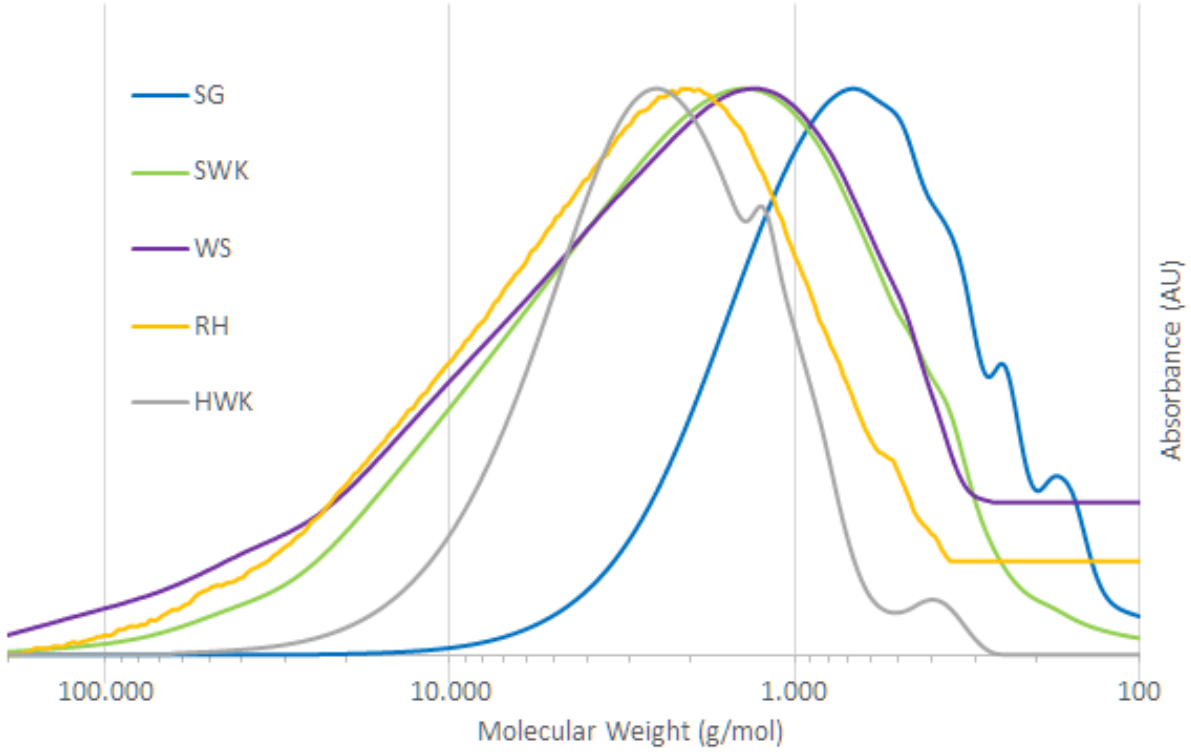

Figure 86 - Molecular weight distributions obtained from the GPC analysis of acetylated samples of the five lignins.

compounds. All the other lignins were constituted by larger molecules, with peak-average molecular weight that were roughly two times (SWK and WS) and three times (HWK and RH) greater than that of SG lignin. The chromatograms of WS, RH, and SWK lignins exhibited a shoulder at high molecular weights which greatly affected the values of the mass-average molecular weights (Mw). Although the purity of all the lignin samples is above 94%, residual saccharides covalently linked to lignin can significantly alter this large molecule-sensitive index. Also the ^{31}P-NMR data agree with a hypothetical correlation between the retention of some LCC and the presence of fractions with high molecular weights. In fact, the content of aliphatic hydroxyls increased in WS, RH and SWK lignins. Another aspect that was assessed was the content of Sulphur. In fact, it is acknowledged that Kraft lignins contains about 1.5–3% sulfur, even though its nature has not been completely established yet. Nevertheless, the presence of Sulphur, also if modest, could play an important role in the definition of the mechanical properties in vulcanized compounds. In literature, it is reported that sulfur may be present in lignin as organically bound sulfur, sulfate ions, elemental sulfur, and adsorbed polysulfide forms. Additionally, it was also mentioned that the influence of the sulfuric acid used for lignin precipitation on the sulfur content is negligible (up to 0.2%) and that consequently the sulfur content in lignin samples is mainly derived from the cooking process.[18] For instance, thiol groups are introduced in the structure of lignin during the Kraft process.[19] As expected, the sulfur content was found to be higher in Kraft lignins, with total concentrations in line with the values already reported.[20] However, SG and WS lignins had more Sulphur than expected in agreement with the previous considerations. It is probable that, contrary to the kraft process, the Sulphur was originated from the sulphuric acid used in lignin precipitation. This hypothesis and the amount of Sulphur are in good agreement with the results of more recent studies that dealt with the characterization of technical lignins.[21]

	SG	SWK	HWK	WS	RH
Purity (%)	94,3	96,7	99,2	94,1	95,0
Ashes (%)	2,5	1,7	0,6	0,2	1,0
Sulphur (%)	0,7	2,4	2,3	1,5	0,1
31P-NMR (mmol/g)					
carboxylic acids	1,07	0,59	0,63	0,51	0,52
aliphatic -OH	1,69	2,23	1,46	1,84	1,95
phenolic -OH	3,62	4,83	4,08	1,80	0,95
S + condensed -OH	2,02	2,13	3,07	0,82	0,27
G -OH	1,12	2,36	1,01	0,74	0,36
H -OH	0,48	0,34	nd	0,24	0,32
GPC (g/mol)					
Mn	1000	4700	4400	4900	5500
Mw	2400	27500	7800	41000	19500
Mp	700	1450	2550	1300	2200
PDI	2,4	5,9	1,8	11,1	3,5

Table 22 - Purity degree, ash content, Sulphur content, functional group quantification (^{31}P-NMR) and molecular weight distribution (GPC) for the five investigated lignins.

7.4 Preparation of lignin/natural rubber composites

After the characterization, the objective was to evaluate the effect of the different lignin structures on the thermal properties of natural rubber compounds. Lignin/natural rubber masterbatches were prepared using the coprecipitation technique to obtain an improved dispersion. Subsequently, the thermal stability of the masterbatches was evaluated measuring the oxygen induction time (OIT) and compared with a reference of neat natural rubber prepared form the same latex.

Experimental

Lignin/natural rubber composites. All the masterbatches were obtained adding the solubilized lignins to natural rubber latex, following the coprecipitation procedure described in chapter 4. The reference of neat natural rubber was prepared coagulating the same latex used for the masterbatches. The dry-mixing references were obtained blending dry SG and SWK lignin powders with solid natural rubber coagulated from the same latex in the brabender mixer.

Dispersion. The dispersion of soda grass (SG) lignin was assessed by SEM, analyzing cut surfaces of samples prepared with dry-mixing and coprecipitation.

Results and discussion

The aromatic backbone of lignin contains a plethora of polar functional groups, for this reason it has a relatively scarce interaction with rubber that is more hydrophobic. During mechanical mixing, the suboptimal interactions between the two components doesn't favor the dispersion of lignin that remains aggregated in particles that are rather large for active fillers. As highlighted in chapter 3, particle size is one of the prominent features of the fillers for rubber reinforcing. Lignin particle size greatly affects the final mechanical properties of the compounds and an insufficient filler dispersion can compromise its antioxidant and reinforcing capability and undermine the overall properties of the compounds. It was already demonstrated that the dispersion into rubber is enhanced when lignin is purified, however, it was not possible to obtain an optimal dispersion with unmodified lignin.[22] Chemical modifications of lignin such as acetylation of hydroxyl groups are reported to improve the compatibility with the polymeric matrix and to promote a better dispersion.[8] Unfortunately, while on one side the chemical modification of the phenolic hydroxyls can enhance the compatibility with rubber, promoting better filler-polymer interactions and increased dispersion, on the other hand the loss of phenolic groups results in the inhibition of antioxidant properties of lignin.[23] Hence there is a tradeoff between compatibilization and retention of the antioxidant capability. As anticipated mixing lignin powder with rubber directly in the mixer (dry-mixing) doesn't produce compounds with enhanced mechanical properties.[22] However it is possible to improve the dispersion of unmodified lignin using the coprecipitation technique (described in detail in chapter 4). Coprecipitation takes advantage of the akin pH-responsiveness of natural rubber latex and lignin. Natural rubber latex is a dispersion of polymer

microparticles, the presence of proteins and phospholipids assures stability in the alkaline environment. Ammonia is added to the latex to prevent premature coagulation; in fact, by neutralizing the activity of micro-organisms it hinders acidification and ensures long-term preservation. Phenolic hydroxyl and carboxylic groups confer to lignin the ability to dissolve in alkaline solutions, at lower pH values, on the contrary, the (re)protonation of the dissociated functionalities induces the precipitation of the biopolymer. This implies that an alkaline solution containing lignin can be added to natural rubber latex without compromising its stability. Subsequently lignin and rubber can be simultaneously coprecipitated adding an acidic solution. In this way, lignin is incorporated in the coagulating rubber, and the outcome is a composite material where smaller particles of lignin are more homogeneously dispersed in the rubber matrix. Accordingly lignin/natural rubber compounds prepared through coprecipitation reportedly displayed increased mechanical properties.[24,25] The quality of the dispersions was qualitatively assessed analyzing SEM images of cut surfaces. In figure 87 it is possible to observe a comparison between two composites prepared with natural rubber and 15 PHR of SG lignin, using dry-mixing (a) and coprecipitation (b). The enhancement in the dispersion achieved with coprecipitation is clear. The sample prepared with dry-mixing was characterized by particles with diameters up to few tens of microns, using coprecipitation, on the other hand, the particle size was limited and lignin was dispersed more homogeneously. In dry-mixing the cohesion of lignin is strong and the shear forces produced in the mixer are not capable to disrupt also relatively large particles, in the final composite it is possible to spot particles and aggregates with irregular shapes and sizes in the 1–20 μm range. The low dispersion of lignin in the dry-mixing approach is due to the strong intermolecular interactions (hydrogen bonds and π–π stacking) that hold together lignin particles, preventing adequate dispersion. Large particles not only hinder the reinforcing effect of fillers, but they could also behave as macroscopic defects, favoring crack propagation and premature failure of the materials. In coprecipitation, on the other hand, lignin is initially molecularly dispersed in the alkaline solution. During the acidification, the solubility of lignin drops and the polymer tents to flocculate forming larger aggregates. However, at the same time also the

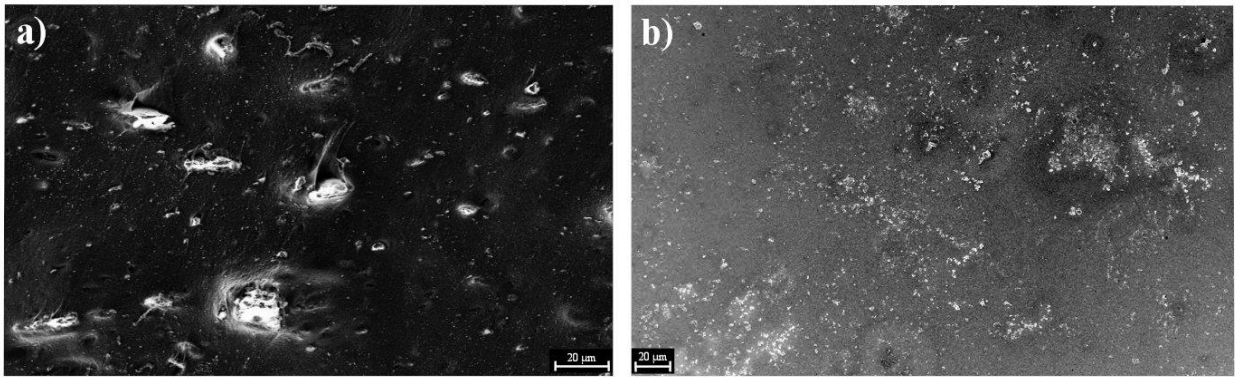

Figure 87 - SEM images of SG lignin incorporated in NR by dry-mixing (a) and coprecipitation (b).

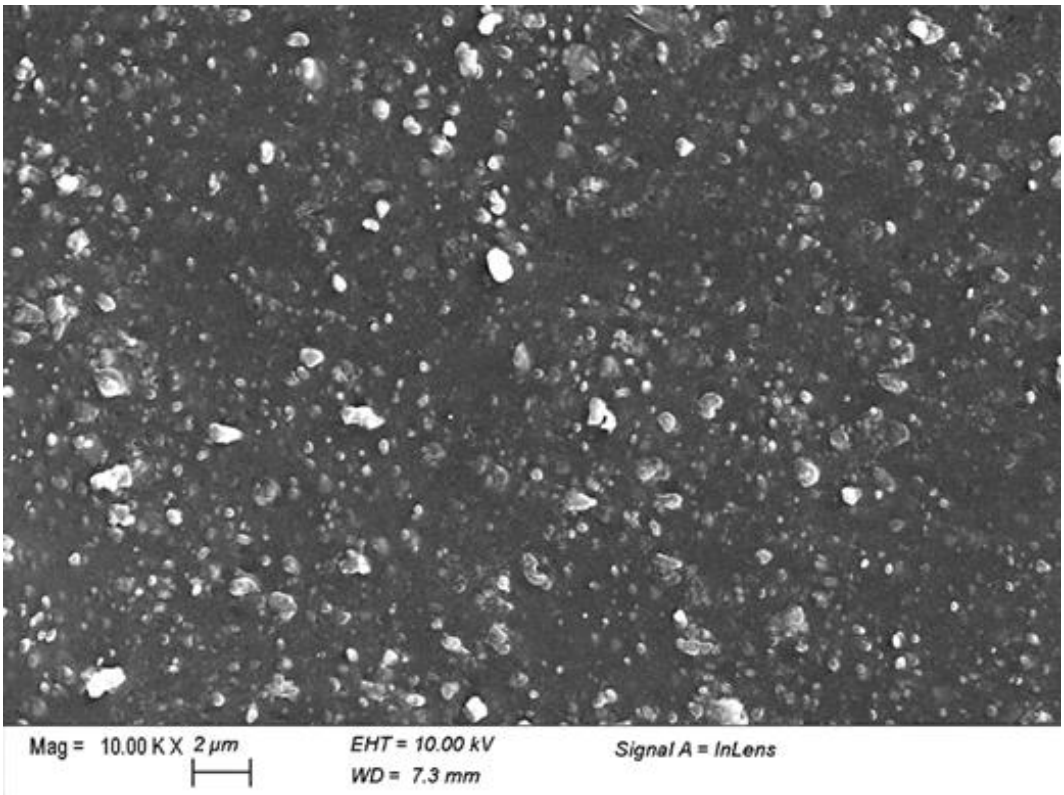

Figure 88 – FESEM image of a SWK-lignin/NR masterbatch prepared via coprecipitation.

latex starts to flocculate, and lignin remains entangled in the coagulating matrix, retaining a higher dispersion. The quality of the dispersion achievable using coprecipitation can be better observed in figure 88. The FESEM image is obtained analyzing a masterbatch prepared coprecipitating 15 PHR of SWK lignin with natural rubber latex. Most of the particles seemed to be sub-micrometric, with larger particles measuring up to a couple of microns. The average particle size is very important, as it constitutes one of the main parameters affecting mechanical properties of rubber composites. As discussed in chapter 3, the filler particle size determines the effective contact area between the filler and polymeric matrix: in term of mechanical properties, fillers with particle size larger than 10 μm do not have reinforcement capabilities or have a negative impact. Fillers with particle size between 1 and 10 μm are inert fillers and are used as diluents. Finally, semi-reinforcing fillers have primary particles ranging from 100 to 1000 nm.[26] Moreover, the particle size, by affecting the filler exposed surface probably also influences the antioxidant capability. When lignin is poorly dispersed also the concentration of the active chemical functionalities such as phenolic hydroxyl groups is reduced and the antioxidant activity is undermined. With the coprecipitation technique it is possible to achieve increased dispersions without compromising the peculiar structure of lignin, retaining the desirable characteristics, and avoiding costly modifications. Based on these results, coprecipitation was selected as the standard procedure for the preparation of the lignin/natural rubber masterbatches that were used to evaluate the thermal stability and mechanical properties conferred by different lignins to NR.

7.5 Thermal stability

As discussed in chapter 3, unsaturated elastomers are particularly susceptible to thermal degradation and the addition of synthetic anti-degradants in the compounds to protect rubber is mandatory to maintain the initial properties and to prevent the embrittlement of the products. In this scenario, the magnification of the protective behavior of lignin is particularly interesting because it could bring a technological advantage. In this work, the influence of lignin structure on the thermal stability of natural rubber was evaluated measuring the time intercurred before the beginning of the oxidation in neat natural rubber and in masterbatches prepared with the five different lignins.

Experimental

Thermal stability. The ability to preserve rubber from oxidation was assessed measuring the oxygen induction time (OIT) in air at 170°C. The detailed procedure is described in chapter 4, in the paragraph dedicated to the differential scanning calorimetry (DSC).

Results and discussion

The main objective of this effort was to investigate the influence of lignin structure and composition on the thermal stability of natural rubber. The stabilizing effect of antioxidants on rubbers can be assessed using the DSC, measuring the oxygen induction time (OIT) in isothermal conditions.[27] In this tests a small sample is heated under inert atmosphere and afterwards oxygen is introduced into the environment. The OIT is the delay, measured in minutes, that intercurred between the exposure to oxidative conditions and the onset time of the first exothermic peak. The protection time was assumed to be the difference between each sample OIT and the corresponding OIT of the blank reference constituted by neat natural rubber. Induction time and protection time are influenced by the specific antioxidant activity of each substance and also by the loading. The oxygen induction time was measured for each masterbatch prepared coprecipitating natural rubber latex with 15 PHR of each lignin. The results are summarized in table 23. The first thing that was noted is that the differences among the lignins dramatically affect the protection time, from the lower value of the RH lignin/NR masterbatch (2.7 min) to the higher value of the masterbatch loaded with SG lignin (54.6 min).

	Oxygen Induction Time (min)	Protection time (min)
SG – 15 PHR	55,6	54,6
SWK – 15 PHR	44,2	42,4
HWK – 15 PHR	23,6	21,7
WS – 15 PHR	18,5	16,6
RH – 15 PHR	4,5	2,7
Neat NR – 0 PHR	1,9	-

Table 23 - OIT and Protection Times for Lignin/NR masterbatches at lignin loadings of 15 PHR and neat NR reference.

Rice husk lignin offers almost no additional protection to the rubber while SG lignin extends the induction time from ~2 to ~55 minutes, greatly improving the resistance towards oxidative conditions. At first glance, the data seemed to confirm the pivotal role of the phenolic moiety, with the lignins rich in phenolics conferring higher protection times. However, a consistent linear correlation between protection time and the concentration of phenolic hydroxyl groups concentration was not found. Higher phenolic contents in lignin (total phenolic content: SWK > HWK > SG > WS > RH) did not necessarily produce a more effective protection against NR degradation, nevertheless, their abundance seems to be clearly related to the OITs. Hence, other characteristics of lignin must influence its antioxidant properties in rubber compounds. Regarding synthetic antioxidants, it is known that also the solubility and the mobility in the specific elastomeric matrix affect the effectiveness.[28] Furthermore, studies on the antioxidant properties of lignin in polypropylene found that high molecular weights were detrimental and the behavior was correlated with the limited solubility of the heavier fractions.[29] In these works the solubility of lignin was reported to play a major role, and it was found that higher phenolic concentrations could also induce a negative effect on antioxidant properties reducing the compatibility with the polymeric matrix. The considerations can probably be also applied to the behavior of lignin in rubbers. However, it was demonstrated that the issue of the poor dispersion of lignin in the masterbatches was mitigated using coprecipitation. Assuming a satisfactory dispersion of lignin, it was thought that the mobility of lignin in the rubber phase could have played a primary role. In fact, the ability to migrate through the rubber is a desirable characteristic of antioxidants, in this way the active species can move from the bulk of the sample toward the surface, where they are effectively depleted. For conventional antioxidant the rate of diffusion is inversely proportional to the molecular weight.[30] In the light of these consideration, it was possible to rationalize the behavior of the investigated materials. For instance, SG lignin was the most effective and is characterized by a considerably lower average molecular weight. When also the molecular weight was considered (as Mp: SG < WS < SWK < RH < HWK) it was possible to find a positive correlation between the oxygen induction time and the concentration of phenolic groups. A good linear correlation was found between the OIT and the ratio [PhOH]/Mp indicating that, when dispersion is not a limiting factor, the thermal stabilization of lignin on rubber is proportional to the concentration of the species that are effectively exerting the antioxidant activity (phenolic -OH) and to their ability to migrate through the polymeric matrix that is well described by the molecular weight of the more abundant fractions. It is possible to conclude that lignins with higher molecular weights have a lower diffusion rate in the rubber phase, and the result is a decreased activity. It is worth noticing the correlation was found for lignins obtained from different botanical origins and production processes, increasing the validity of the correlation. In addition, it was observed that other characteristics, such as concentration of aliphatic hydroxyls and carboxylic acids or the amount of Sulphur and ashes did not affect the antioxidant properties of the investigated lignins. For SWK lignin also the effect of the lignin concentration on the protection time was investigated. It is worth noticing that at low concentrations (up to 15 PHR) the

relationship between protection time and lignin concentration is essentially linear. This behavior is in good agreement with that observed for completely soluble antioxidants.[27]

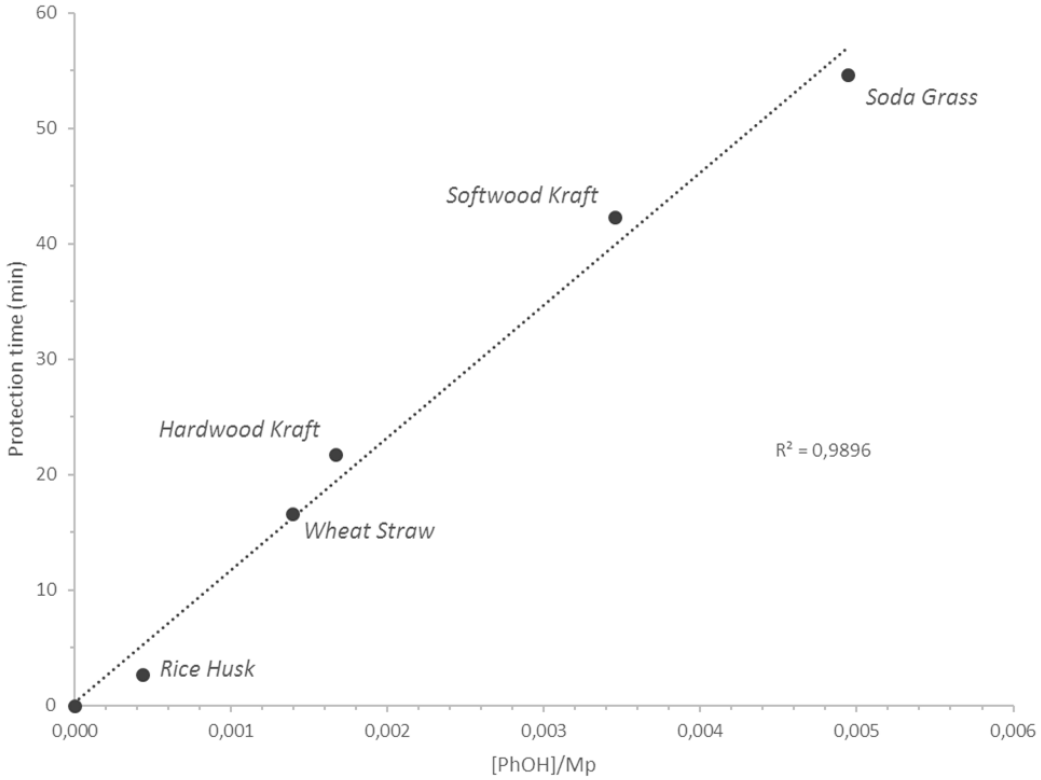

Figure 89 - Influence of the concentration of phenolic hydroxyls and the Mp on the protection time.

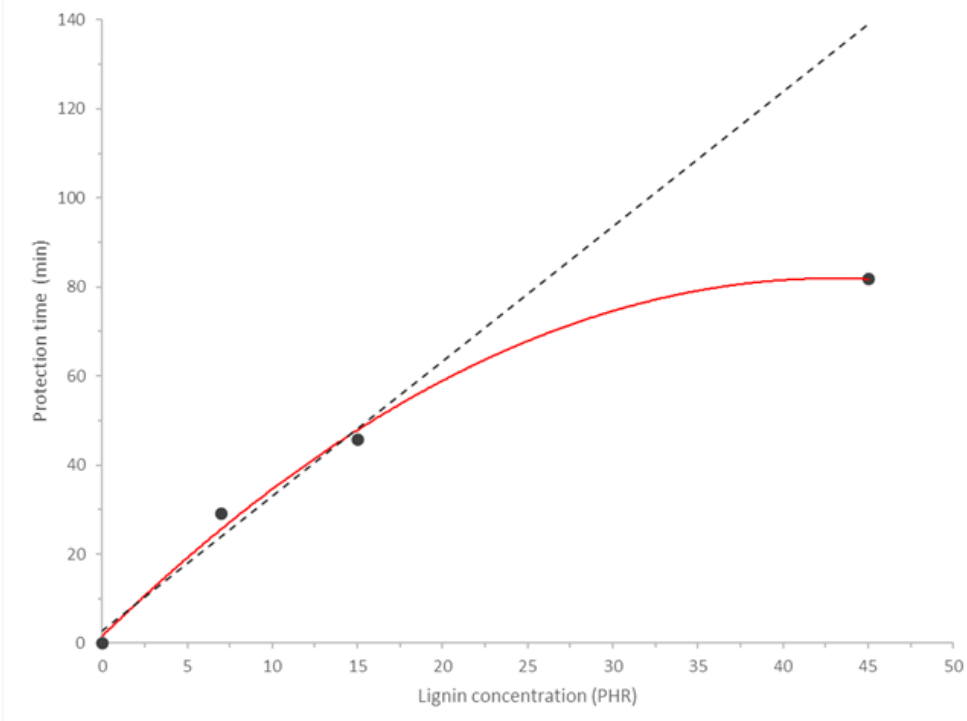

Figure 90 - Influence of the loading of SWK lignin (0, 7, 15 and 45 PHR) on the protection time.

Conversely, at higher concentrations (45 PHR) a saturation effect was noticed. Above a certain concentration threshold lignin probably forms a percolation network, forming strong intermolecular interactions through hydrogen bonding and $\pi-\pi$ stacking. The instauration of a strong lignin network was supposed to prevent also smaller molecules from migrating across the sample. When the mobility is hindered it is likely that the thermal degradation starts in those areas where the initial amount of antioxidant is rapidly consumed.[25] Additionally, at high concentrations, the fractions with high and low molecular weight might compete for solubility. According to the consideration made so far, if the solubility of the smaller fractions is hindered, also the antioxidant capability is affected, explaining the non-linear behavior at higher concentrations.

7.6 Mechanical properties

In the previous section, it was demonstrated that certain kinds of lignin are more effective in preventing the loss of the mechanical properties caused by the oxidative degradation of natural rubber. The protective aspect is very interesting, in fact during the manufacturing process the polymers are exposed to mechanical and thermal stresses, especially during mixing and vulcanization. However, this compelling characteristic can become a technological advantage only if also the initial mechanical properties of the compounds are in line or better than those of natural rubber. For this reason, model rubber compounds were prepared adding vulcanizing agents to neat natural rubber and lignin/natural rubber masterbatches in order to assess the mechanical properties conferred by the different lignins to the rubber composites.

Experimental

Rubber compounding. The vulcanizers were added to neat natural rubber and lignin/natural rubber masterbatches to prepare rubber compounds using the brabender mixer and the procedure number 2 reported in chapter 4.

Mechanical properties. The mechanical properties of the rubber compounds filled with different lignins and the suitable references were assessed performing tensile tests on dumbbell shaped specimens.

Results and discussion

To evaluate the mechanical behavior of natural rubber compounds filled with different lignin specimens, several model compounds were prepared according to the formulations reported in table 24. The mechanical properties were evaluated performing tensile tests on vulcanized specimens. A reference compound (NR) was prepared using neat natural rubber in place of the lignin/rubber masterbatches. Additionally, a second reference (SWKDM) was prepared adding dry SWK lignin powder to coagulated natural rubber directly in

	NR	SWKDM	SG	SWK	HWK	WS	RH
Natural rubber*	100	100					
Lignin powder (SWK)		15					
Lignin/NR masterbatch			115	115	115	115	115
Soluble Sulphur	2	2	2	2	2	2	2
Zinc Oxide	5	5	5	5	5	5	5
Stearic Acid	2	2	2	2	2	2	2
CBS	2	2	2	2	2	2	2

*coagulated from the same latex used for the preparation of the masterbatches

Table 24 - Formulations in PHR used to assess the mechanical properties of the composites prepared with the five lignins, a reference of neat natural rubber and a reference prepared adding SWK lignin to NR via dry-mixing.

the mixer to evaluate the effect of the enhanced dispersion achieved with coprecipitation on the mechanical properties of the composites. The results of the tensile tests are listed in figure 91 and table 25. It is interesting to analyze the behavior of the SWKDM specimen. With electron microscopy, it was observed that when lignin is compounded directly in the mixer with natural rubber the outcome is a poor dispersion, with many particles having diameters of 10 μm or larger. Fillers having particles of such dimensions are categorized at best as inert fillers. The results of the tensile tests are in line with previous considerations, in fact the mechanical properties of the SWKDM sample are very close to those of the NR reference. A small increase in Young's modulus was detected at low strains (< 50 %), however it could be attributed to dilution effects, and the properties at high strains, the tensile strength and the elongation at break are deteriorated by the presence of the lignin. The data essentially confirmed the considerations made during the discussion of the dispersion and indicated that with the dry-mixing technique lignin is not effectively incorporated in the rubber matrix. Large particles affected negatively the mechanical properties and the antioxidant activity was hindered by the poor dispersion. On the other hand, when SWK lignin was incorporated through coprecipitation the outcome was different and an overall improvement in the mechanical properties was observed. The well dispersed SWK lignin increased the Young's modulus of the material in the whole range of deformations without compromising elongation at break. The increase in the modulus at low strains was supposed to be connected to the reinforcing behavior of SWK lignin, in fact, because of coprecipitation, the stiffer biopolymer was well dispersed in the matrix of natural rubber in the form of submicrometric particles. Interestingly the ultimate elongation (or elongation at break) was unaffected by lignin, and at the same time the tensile strength was greatly enhanced. This behavior was supposed to be also connected to the protection of natural rubber from the degradative processes that was granted by the presence of lignin. In fact, during mixing and vulcanization rubber is exposed to mechanical and thermo-oxidative stresses, and because of the chain scissions the mechanical properties deteriorate. The behavior of the rubber compounds filled with the other four lignin types supported this interpretation. In fact, the compounds filled with the lignins that showed better antioxidant properties in the OIT tests (SG > SWK > HWK) also exhibited overall

better performances in the mechanical tests (SWK > HWK > SG). The compounds containing SWK, HWK, and SG lignin displayed greater values of the Young modulus especially at high strain and superior elongation at break, whereas compounds filled with WS and RH lignin had comparable modulus at low deformations but lower values of tensile strength and elongation at break. Additional evidence supporting the close relationship between the antioxidant capability of lignin and the mechanical performances at high strains was obtained preparing the rubber compound with different mixing temperatures (60 °C vs 90 °C).

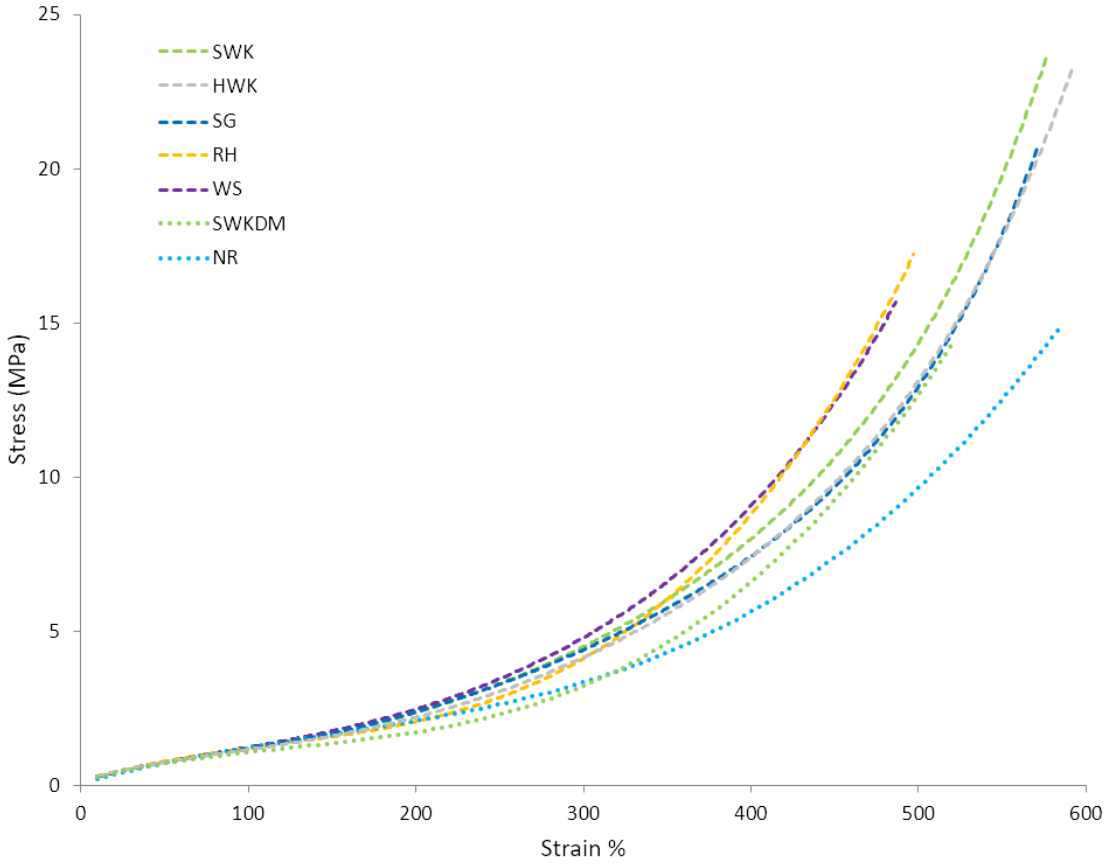

Figure 91 – Stress/strain curves obtained from the tensile tests on the natural rubber compounds prepared from the masterbatches with the five different lignins and the reference compounds.

Stress at progressive elongations (MPa)

Elongation (%)	SWK	HWK	SG	RH	WS	NR	SWKDM
10	0,29	0,30	0,28	0,29	0,29	0,23	0,27
50	0,75	0,75	0,75	0,75	0,76	0,68	0,72
100	2,36	1,16	2,38	1,16	1,24	1,07	1,08
300	4,55	4,15	4,40	4,07	4,79	3,25	3,23
Ultimate	23,76	23,25	20,78	17,21	15,67	15,02	14,39

Ultimate elongations (%)

SWK	HWK	SG	RH	WS	NR	SWKDM
578	592	572	497	487	586	521

Table 25 – Numerical values obtained from the tensile tests.

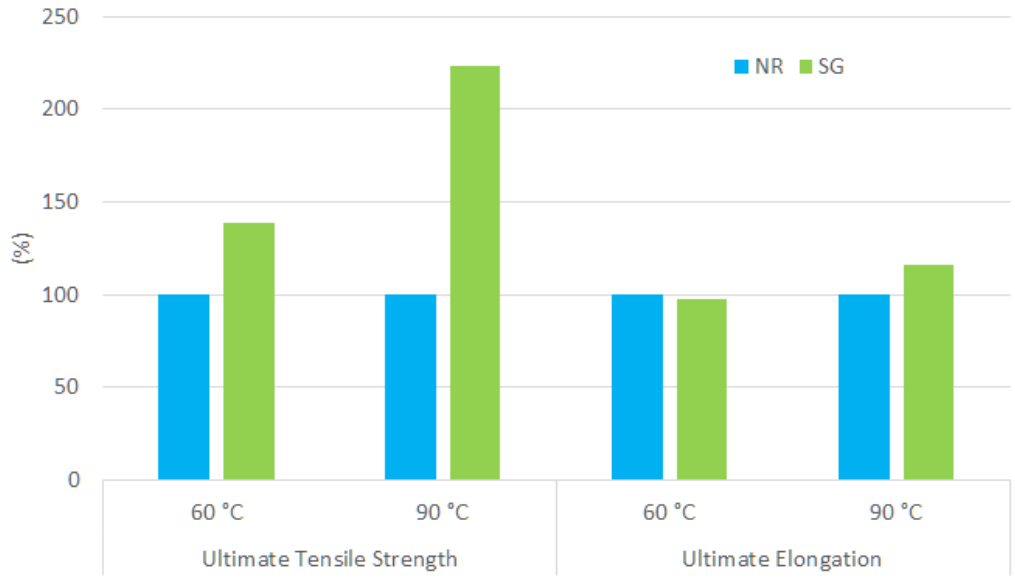

Figure 92 - Tensile strength and elongation at break of SG lignin filled NR compounds (15 PHR) for different processing temperatures (60 and 90°C). Values are expressed as a percent relative to the values of neat NR references.

In figure 92 it is possible to observe the change in the ultimate properties for different mixing temperatures, the values are expressed in percent relatively to the neat NR reference. At high temperature (90 °C) the ultimate tensile strength and the ultimate elongation of the sample filled with SG lignin are higher respect to that of the sample processed at lower temperature (60 °C). This indicates that when natural rubber is exposed to mechanical and thermos-oxidative stresses the protective effect of lignin exerts a decisive role in the in the definition of the mechanical properties. The microscopic mechanisms accountable for the changes observed in the macroscopic properties of lignin filled natural rubber compounds are not simple to rationalize. Many evidences indicated that the protective behavior exerted by the phenolic moieties of lignins played a decisive role, especially at high temperatures, on the properties at high elongations. However, it seems reasonable that beside the protection against degradative, other characteristics of lignin can influence the overall mechanical properties of the composites. In fact, despite the highest protection time in the OIT test was scored by SG lignin, the best mechanical properties, including ultimate properties, were achieved with Kraft lignins. It was hence hypothesized that the extractive process had a predominant role in the definition of the structural features that promoted the reinforcement, in fact since both lignin showed similar properties it seemed that the botanical origin of the lignin exerted only a minor effect. As previously observed in chapter 2, in the Kraft process lignins tent to react forming more condensed structures and to incorporate sulfur. The higher amount of condensed structures might improve the stiffness of the filler providing an increased resistance against deformation. If this was the case, it might also explain the higher performances obtained with SWK, in fact, softwood lignins have a higher amount of G units if compared with hardwood lignins that are enriched in S units. Hence, softwood lignin has more positions where the 5-5’

condensation can occur, this determines the possibility to have more crosslinking and increased structural strength. Another possibility is that the organic sulfur introduced in the structure of lignin during the extraction process reacted during vulcanization. In fact, the presence of thiol groups in the structure of Kraft lignins is well recognized as well as the capability of mercaptans to react during the vulcanization creating new carbon–sulfur covalent bonds with the unsaturated chains of the polymeric matrix. This rationalization could explain also the high modulus at 300% elongation measured for the compound filled with WS lignin. In fact, the Sulphur content in WS lignin is second only to Kraft lignins. Additionally, it was also speculated that Kraft lignins could react through another peculiar mechanism forbid to other lignins. In native lignin, primary benzyl alcohol functions are absent, anyway Kraft lignin is a modified lignin, and some primary benzyl alcohol functionalities are formed during the pulping process. It was demonstrated that, in the presence of a catalytic amount of acid, Kraft lignins can react via a mechanism that involves the benzylic carbon giving polymerization.[31] It absolutely possible that traces of sulphuric acid were still present in the masterbatches, as a consequence of coprecipitation. Hence, kraft lignin might have undergone additional condensation through the mechanism involving the benzylic carbon, or more remotely, it could also have been reacting with rubber during vulcanization, through a mechanism involving directly the rubber chains (tentatively proposed in figure 93), or mediated by the Sulphur. What is more plausible is that the generation of lignin-rubber chemical bonds explains the stiffening behavior, in fact strong rubber–filler interactions are at the base of the reinforcing mechanism of particulate fillers.[32] However, it is difficult to understand the interconnectivity among the different components in the materials after vulcanization and a comprehensive

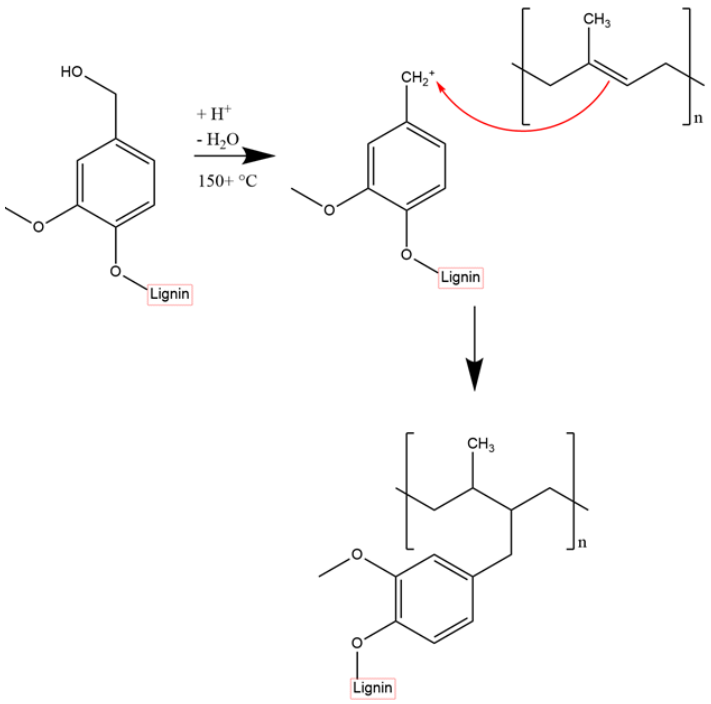

Figure 93 – Hypothetical reactivity between Kraft lignins and natural rubber.

study of the lignin reinforcement mechanism lied outside the aim of this work. In a second moment, SWK lignin was selected for the investigation of the effect of lignin concentration on the mechanical properties of the composite elastomeric materials. At first an improvement in the mechanical properties was observed when the loading was increased from 7 to 15 PHR. However, ad high loadings (45 PHR) the mechanical properties didn't improve as expected. At low strains, it was possible to observe a moderate improvement of the elastic modulus, however it was not proportional to the amount of lignin added. The behavior was rationalized analyzing the vulcanization curves. In fact, it was found that introducing high amounts of lignin in the compounds strongly hindered vulcanization. In literature, it was found that that lignin can actually take part in the vulcanization process, and was already reported that lignin can have a deleterious on the technical properties of natural rubber vulcanizates due to the decreased final crosslink density.[33] It is possible that lignin interacts with the radicals formed during vulcanization, influencing the crosslinking mechanism, however it is also plausible that some vulcanizing agents are adsorbed on the surface of lignin and are not anymore available in the bulk of the polymer for the vulcanization. This hypothesis might seems more convincing if it is taken into account that efficient vulcanization was found to be less hindered by the presence of lignin,[33] supporting the idea that the greater limit is the adsorption of the accelerator. However, a moderate impairment of the crosslinking was observed also in the experiments reported in chapter 5, when the vulcanizing agent was constituted by a single element, Dicumyl peroxide.

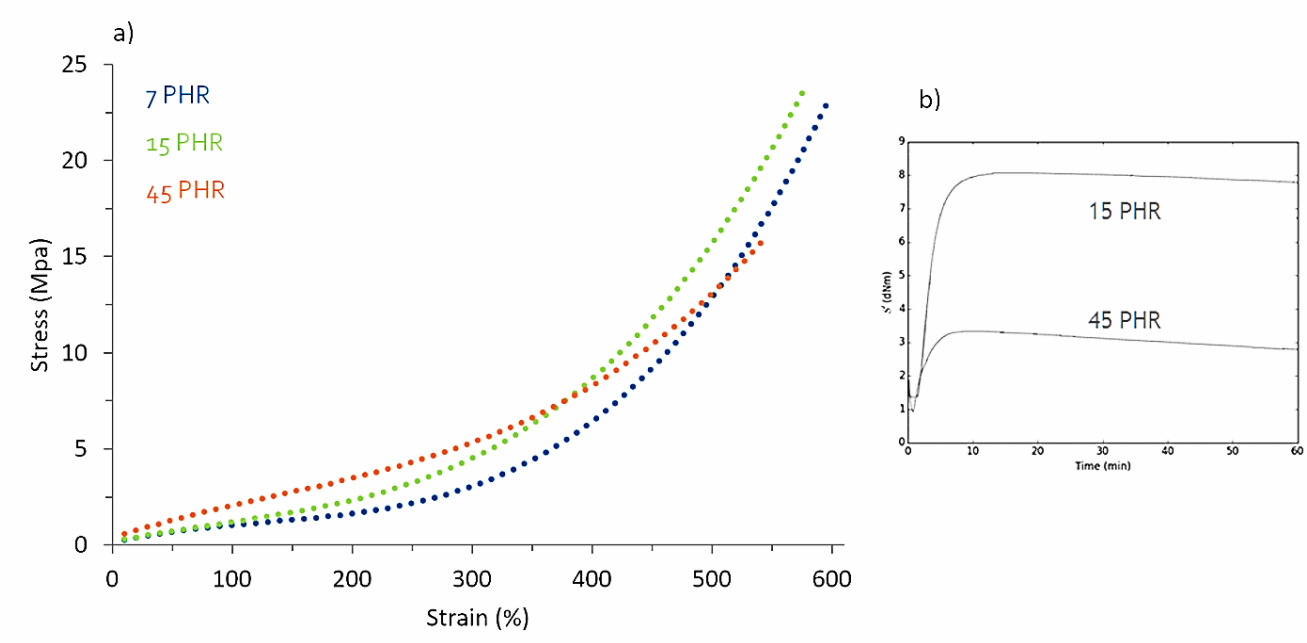

Figure 94 - Stress/strain curves obtained from the tensile tests on the natural rubber compounds prepared from the masterbatches loaded with different amounts of SWK lignin (a) vulcanization curves (b).

7.7 Applicability in technical compounds

Through the chapter, it was verified that when a proper amount of lignin is well dispersed in the polymeric matrix, and presents a suitable structure, it can improve the properties of natural rubber, enhancing the thermal stability and the mechanical properties. The simple model compounds were a useful tool to isolate the influence of lignin on the properties of natural rubber. However, the actual rubber compounds are much more complex and the interesting properties observed in model rubber compounds are not always transferable due to the interference with other ingredients. In this study, a limited amount of lignin was introduced in technical compounds, in partial substitution to carbon black. To assess the applicability of lignin in real systems, the biopolymer was pre-dispersed through coprecipitation, to prepare a masterbatch that was then added to the mixer, instead of natural rubber and carbon black powder. The formulations are reported in table 26, but only the ingredients that are useful to this discussion are reported. REF1 is the original technical compound. In REF 2 6 phr of carbon black were removed. In LIGNIN1 6 phr of carbon black were replaced by 6 phr of pre-dispersed softwood Kraft lignin. LIGNIN 2 is similar to LIGNIN1, but 60% of the antioxidants were removed. During vulcanization, lignin didn't affect significantly the processability of the rubber compounds. The main effect of lignin was raising the initial viscosity (ML), but the other parameters were more influenced by the removal of the CB and the antioxidants. The presence of lignin exerted a positive effect on the dynamic properties. The storage modulus slightly decreased, but was always closer to that of REF1 than REF2. At the same time the hysteresis (TanD) was significantly improved, a lower damping is important because it is connected to the rolling resistance of tyres and hence to the fuel economy of the vehicles.[34] The tensile tests also showed few interesting outcomes. The presence of lignin reduced the stiffness of the compound (LIGNIN1), especially at higher strains. However, the loss towards carbon black (REF1) was limited and lignin sensibly improved the properties if confronted with the blank (REF2), effectively reinforcing rubber. The partial removal of the synthetic antioxidants (LIGNIN2) produced a double advantage. In fact the biggest disadvantage of 6PPD is its partial decomposition during the vulcanization leading to the formation of toxic amines,[35] its replacement with the cheaper, safer and renewable lignin also reduces the plasticizing effect, further improving the mechanical characteristics. The protection conferred by lignin seemed to be sufficient for rubber to withstand the thermos-oxidative stresses during the regular processing (mixing and vulcanization). At the same time, some issues could arise on the long period, hence the compounds were tested again after artificial aging. The aging was achieved exposing the specimens at 70 °C in air, for one week. The difference between LIGNIN1 and LIGNIN2 was slightly reduced after the treatment, indicating that lignin is not exactly as effective as the combination of 6PPD and TMQ in protecting the rubber, however the presence of lignin was still positive and the final mechanical properties were found to be rather good, and a moderate loss in the elastic moduli was observed only for strains greater than 150%. Overall the results are satisfactory and demonstrated that the abundant technical lignins represent an important asset with the capability to replace high-tech materials when their intrinsic characteristics are properly exploited.

		REF 1	REF 2	LIGNIN 1	LIGNIN 2
Formulations					
Natural Rubber		40	40	-	-
Lignin Masterbatch (13%)		-	-	46	46
Carbon Black		17	11	11	11
Antioxidant 1 (6PPD)		1	1	1	0,5
Antioxidant 2 (TMQ)		1,5	1,5	1,5	0,5
Vulcanization (10 min - 170 °C)					
ML [dN m]		2,33	2,13	2,60	2,64
MH [dN m]		23,2	21,2	22,3	23,0
T90 [min]		1,88	2,00	1,99	1,81
TS2 [min]		0,74	0,79	0,78	0,79
Dynamic-mechanical properties (DMA)					
23 °C 1Hz 3.5% -25%	E'[%]	100,0	89,2	96,2	98,0
	TanD[%]	100,0	89,6	92,2	90,9
23 °C 10Hz 3.5% -25%	E'[%]	100,0	89,2	95,9	97,6
	TanD[%]	100,0	92,1	93,3	92,1
23 °C 100Hz 3.5% -25%	E'[%]	100,0	89,1	95,4	97,0
	TanD[%]	100,0	93,7	94,6	93,7
70 °C 1Hz 3.5% -25%	E'[%]	100,0	89,6	95,6	97,5
	TanD[%]	100,0	87,7	93,0	93,0
70 °C 10Hz 3.5% -25%	E'[%]	100,0	89,5	95,4	97,2
	TanD[%]	100,0	89,1	92,2	90,6
70 °C 100Hz 3.5% -25%	E'[%]	100,0	89,3	95,1	96,8
	TanD[%]	100,0	90,9	92,2	90,9
Mechanical properties (tensile testing)					
Stress 10% [MPa]		0,62	0,56	0,62	0,65
Stress 50% [MPa]		1,80	1,56	1,71	1,87
Stress 100% [MPa]		3,63	2,95	3,35	3,76
Stress 300% [MPa]		-	13,5	-	-
Ultimate strength [MPa]		13,0	13,6	13,4	14,7
Ultimate elongation [%]		253	300	275	269
ENERGY [J/cm3]		14,6	18,0	16,3	17,6
Mechanical properties after thermal aging (70 °C, 168 h)					
Stress 10% [MPa]		0,73	0,66	0,70	0,74
Stress 50% [MPa]		2,12	1,89	1,98	2,14
Stress 100% [MPa]		4,44	3,85	4,04	4,48
Ultimate strength [MPa]		12,4	11,4	12,2	12,2
Ultimate elongation [%]		204	219	219	213
ENERGY [J/cm3]		10,2	10,8	11,4	11,3
Aging indicators					
Δ Stress at 50% after aging [%]		17,7	21,1	15,7	14,4
Δ Ult.elong. after aging [%]		-19,4	-27,0	-20,0	-20,8

Table 26 - Formulations, curing and mechanical properties of lignin-filled technical compounds.

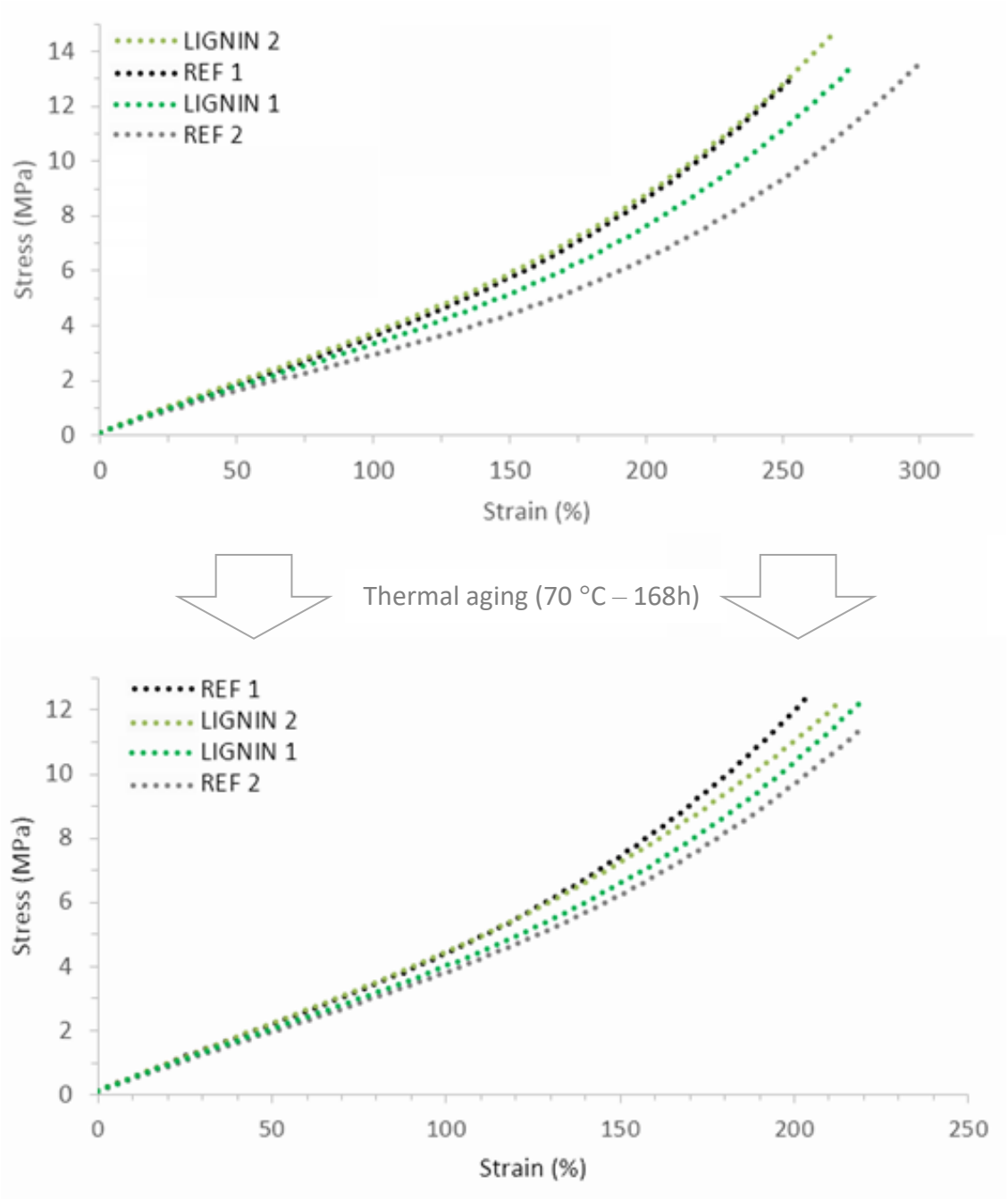

Figure 95 - Stress/strain curves on technical compounds before and after thermal aging.

7.8 Conclusions

Analyzing the thermal and mechanical behavior of lignin/natural rubber compounds prepared with different lignin types, it was confirmed that the chemical and morphological structure of lignin exerts a strong influence on the properties of natural rubber compounds. The antioxidant capability in natural rubber blends was found to vary remarkably among the different lignin specimens. The thermal stabilization mechanism was rationalized relating its effectiveness to the concentration of the active antioxidant species and their ability to migrate through the polymeric matrix. It was also assessed that the antioxidant effect of lignin results in improved mechanical properties of natural rubber compounds also before aging, especially at high strains. In addition, it was noted that various structural features of lignin, unrelated to antioxidant capability and molecular weight, could also affect the tensile strength of the lignin filled compounds. In the light of the collected evidence, it was possible to assert that the abundant and low-priced technical lignins are suitable for an effective utilization in natural rubber compounds and that they can improve the thermal stability and the mechanical properties. The results could represent a useful basis for the implementation of future strategies, aimed at the improvement of the performances of lignin/rubber compounds, such as purification, fractionations and modification steps.

References

(1) Thakur, V. K.; Thakur, M. K.; Raghavan, P.; Kessler, M. R. Progress in green polymer composites from lignin for multifunctional applications: A review. *ACS Sustain. Chem. Eng.* **2014**, *2* (5), 1072–1092.

(2) Kai, D.; Tan, M. J.; Chee, P. L.; Chua, Y. K.; Yap, Y. L.; Loh, X. J. Towards lignin-based functional materials in a sustainable world. *Green Chem.* **2016**, *18* (5), 1175–1200.

(3) Zimniewska, M.; Kozłowski, R.; Batog, J. Nanolignin Modified Linen Fabric as a Multifunctional Product. *Mol. Cryst. Liq. Cryst.* **2008**, *484* (1), 43/[409]-50/[416].

(4) Liu, X.; Wang, J.; Li, S.; Zhuang, X.; Xu, Y.; Wang, C.; Chu, F. Preparation and properties of UV-absorbent lignin graft copolymer films from lignocellulosic butanol residue. *Ind. Crops Prod.* **2014**, *52*, 633–641.

(5) Lyubeshkina, E. G. et al. Lignins as Components of Polymeric Composite Materials. *Russ. Chem. Rev.* **1983**, *52* (7), 675–692.

(6) Feldman, D.; Lacasse, M.; Beznaczuk, L. M. Lignin-polymer systems and some applications. *Prog. Polym. Sci.* **1986**, *12* (4), 271–299.

(7) Thielemans, W.; Can, E.; Morye, S. S.; Wool, R. P. Novel applications of lignin in composite materials. *J. Appl. Polym. Sci.* **2002**, *83* (2), 323–331.

(8) Bertini, F.; Canetti, M.; Cacciamani, A.; Elegir, G.; Orlandi, M.; Zoia, L. Effect of ligno-derivatives on thermal properties and degradation behavior of poly(3-hydroxybutyrate)-based biocomposites. *Polym. Degrad. Stab.* **2012**, *97* (10), 1979–1987.

(9) Keilen, J. J.; Pollak, A. Lignin for Reinforcing Rubber. *Ind. Eng. Chem.* **1947**, *39* (4), 480–483.

(10) Bahl, K.; Miyoshi, T.; Jana, S. C. Hybrid fillers of lignin and carbon black for lowering of viscoelastic loss in rubber compounds. *Polymer (Guildf).* **2014**, *55* (16), 3825–3835.

(11) Frigerio, P.; Zoia, L.; Orlandi, M.; Hanel, T.; Castellani, L. Application of sulphur-free lignins as a filler for elastomers: Effect of hexamethylenetetramine treatment. *BioResources* **2014**, *9* (1), 1387–1400.

(12) Yu, P.; He, H.; Jia, Y.; Tian, S.; Chen, J.; Jia, D.; Luo, Y. A comprehensive study on lignin as a green alternative of silica in natural rubber composites. *Polym. Test.* **2016**, *54*, 176–185.

(13) Košíková, B.; Gregorová, A.; Osvald, A.; Krajčovičová, J. Role of lignin filler in stabilization of natural rubber–based composites. *J. Appl. Polym. Sci.* **2007**, *103* (2), 1226–1231.

(14) Gregorová, A.; Košíková, B.; Moravčík, R. Stabilization effect of lignin in natural rubber. *Polym. Degrad. Stab.* **2006**, *91* (2), 229–233.

(15) Ting-Feng Yeh; Tatsuhiko Yamada; Ewellyn Capanema; Hou-Min Chang; Vincent Chiang and John F. Kadla. Rapid Screening of Wood Chemical Component Variations Using Transmittance Near-Infrared Spectroscopy. **2005**.

(16) Wagner, A.; Tobimatsu, Y.; Phillips, L.; Flint, H.; Geddes, B.; Lu, F. Syringyl lignin production in conifers : Proof of concept in a Pine tracheary element system. **2015**, *112* (19), 2–7.

(17) Chakar, F. S.; Ragauskas, A. J. Review of current and future softwood kraft lignin process chemistry. *Ind. Crops Prod.* **2004**, *20* (2), 131–141.

(18) Alekhina, M.; Erdmann, J.; Ebert, A.; Stepan, A. M.; Sixta, H. Physico-chemical properties of fractionated softwood kraft lignin and its potential use as a bio-based component in blends with polyethylene. *J. Mater. Sci.* **2015**, *50* (19), 6395–6406.

(19) Zakzeski, J.; Bruijnincx, P. C. A.; Jongerius, A. L.; Weckhuysen, B. M. The Catalytic Valorization of

Ligning for the Production of Renewable Chemicals. *Chem. Rev.* **2010**, *110*, 3552–3599.

(20) Svensson, S. Minimizing the sulphur content in Kraft lignin. **2008**.

(21) Constant, S.; Wienk, H. L. J.; Frissen, A. E.; Peinder, P. de; Boelens, R.; van Es, D. S.; Grisel, R. J. H.; Weckhuysen, B. M.; Huijgen, W. J. J.; Gosselink, R. J. A.; et al. New insights into the structure and composition of technical lignins: a comparative characterisation study. *Green Chem.* **2016**, *18* (9), 2651–2665.

(22) Frigerio, P.; Zoia, L.; Orlandi, M.; Hanel, T.; Castellani, L. Application of Sulphur-Free Lignins as a Filler for Elastomers: Effect of Hexamethylenetetramine Treatment. *BioResources* **2014**, *9* (1), 1387–1400.

(23) Sadeghifar, H.; Argyropoulos, D. S. Correlations of the Antioxidant Properties of Softwood Kraft Lignin Fractions with the Thermal Stability of Its Blends with Polyethylene. *ACS Sustain. Chem. Eng.* **2015**, *3* (2), 349–356.

(24) Asrul, M.; Othman, M.; Zakaria, M.; Fauzi; 4. Lignin Filled UnvulcanisedNatural Rubber Latex: Effectsof Lignin on Oil Resistance, Tensile Strength and Morphology of Rubber Films. *Int. J. Eng. Sci. Invent. ISSN (Online* **2013**, 2319–6734.

(25) Jiang, C.; He, H.; Jiang, H.; Ma, L.; Jia, D. M.; Srisuwan, L.; Jarukumjorn, K.; Suppakarn, N.; Xiao, S.; Feng, J.; et al. Nano-lignin filled natural rubber composites: Preparation and characterization. *Express Polym. Lett.* **2013**, *7* (5), 480–493.

(26) Edwards, D. C. Polymer-filler interactions in rubber reinforcement. *J. Mater. Sci.* **1990**, *25* (10), 4175–4185.

(27) Goh, S. H. Thermoanalytical studies of rubber oxidation: Prediction of isothermal induction time. *Thermochim. Acta* **1984**, *75* (3), 323–328.

(28) Narathichat, M.; Sahakaro, K.; Nakason, C. Assessment degradation of natural rubber by moving die processability test and FTIR spectroscopy. *J. Appl. Polym. Sci.* **2010**, *115* (3), 1702–1709.

(29) Pouteau, C.; Dole, P.; Cathala, B.; Averous, L.; Boquillon, N. Antioxidant properties of lignin in polypropylene. *Polym. Degrad. Stab.* **2003**, *81* (1), 9–18.

(30) Ignatz-Hoover, F.; To, B. H.; Datta, R. N.; De Hoog, A. J.; Huntink, N. M.; Talma, A. G. Chemical Additives Migration in Rubber. *Rubber Chem. Technol.* **2003**, *76* (3), 747–768.

(31) Pouteau, C.; Cathala, B.; Dole, P.; Kurek, B.; Monties, B. Structural modification of Kraft lignin after acid treatment: characterisation of the apolar extracts and influence on the antioxidant properties in polypropylene. *Ind. Crops Prod.* **2005**, *21* (1), 101–108.

(32) Ge, X.; Li, M. C.; Cho, U. R. Novel one-step synthesis of acrylonitrile butadiene rubber/bentonite nanocomposites with (3-Mercaptopropyl)trimethoxysilane as a compatilizer. *Polym. Compos.* **2015**, *36* (9), 1693–1702.

(33) Nando, G. B.; De, S. K. Effect of lignin on the network structure and properties of natural rubber mixes vulcanized by conventional, semiefficient and efficient vulcanization systems. *J. Appl. Polym. Sci.* **1980**, *25* (6), 1249–1252.

(34) Zhang, P.; Morris, M.; Doshi, D. Materials Development for Lowering Rolling Resistance of Tires. *Rubber Chem. Technol.* **2016**, *89* (1), 79–116.

(35) Kruger, R. H.; Boissiere, C.; Klein-Hartwig, K.; Kretzschmar, H.-J. New phenylenediamine antiozonants for commodities based on natural and synthetic rubber. *Food Addit. Contam.* **2005**, *22* (10), 968–974.

CHAPTER 8 - Lignin modification and behavior of modified lignins in rubber model compounds

The possibility to use lignin to manufacture natural rubber composite was explored in the previous chapters. It was confirmed that the addition of pristine lignin directly in the mixer produces composites with poor mechanical properties due to the non-optimal compatibility between the two polymers that leads to poor dispersion and large particle size. At the same time, it was demonstrated that when lignin is well dispersed it improves the mechanical properties of natural rubber hypothetically through a tandem mechanism of protection and reinforcement. It was also observed that lignins with specific molecular structures can produce composite materials with higher mechanical properties. However, despite lignin offers many advantages, its reinforcing potential is limited and cannot reach the effectiveness of carbon black and silica. This behavior was supposed to be mainly a consequence of the weak interactions taking place at the interface between lignin and rubber. Secondly it was also found that lignin can interfere with vulcanization, this aspect can be neglected when lignin is used at low concentrations, however applications involving high loadings are precluded. The work reported in this chapter deals with the modification of lignin. Different strategies were perused to overcome the issues mentioned above and to produce lignins with an enhanced affinity for rubber, suitable for the preparation of green elastomeric composites with different or superior properties.

8.1 Background

In tire industry, there is an increasing interest in the use of materials produced from renewable resources to replace fossil counterparts. Carbon black is one of the main components in the average tire; it can constitute one third of the total weight. Carbon black is produced from partial combustion of the heavy fraction of petroleum or other fossil resources and is therefore intrinsically non-renewable. Reinforcing fillers are added to elastomeric compounds mainly to dramatically improve tensile strength and abrasion resistance of rubbers. Lignocellulosic biomass is a promising source of renewable resources as it represents the most abundant biomaterial produced on a global scale, furthermore it is low cost and often is readily available as it is generated as a side product by agricultural and forestry industries. While the polysaccharide fractions are already successfully processed to produce fuels and chemicals, lignin, the second most abundant components of lignocellulosics, only has limited uses. For these reasons, the possibility of replacing carbon

black with lignin is particularly alluring. Yet lignin, besides being low coast and eco-friendly, brings along other interesting features, as its antioxidant capability. However, the mechanical properties conferred by lignin to the elastomeric composites don't match with the required performances, that are currently obtained using carbon black. The purpose of the work presented in this chapter was to improve the effectiveness of lignin when it is used as a reinforcing filler in rubber compounds. In this view, three different strategy were pursued to obtain modified lignins, namely: fractionation, thermal conditioning, and chemical modification. The work started with the identification of potentially suitable modification of lignin based on the available literature, hence it continued with the setup and the optimization of the modification procedures, followed by the characterization of the products. Finally, the modified lignins were tested in rubber compounds to assess the reinforcing potential.

8.2 Materials

The lignin that gave the best results in the mechanical tests of chapter 6 was used as starting material for the modifications (SWK lignin). It is a technical lignin produced in large amounts from softwoods by the paper industry using the Kraft process. The details regarding the materials used for rubber compounding are reported in the related section of chapter 4. All the other reagents and solvents (ACS grade) were purchased from Sigma-Aldrich and used as received without further purification.

8.3 Fractionation

The first technique used to produce lignins with different properties was fractionation. In literature, it is possible to find different approaches that permit to separate lignin into different fractions according to specific characteristics. In fact, one of the challenges of operating with lignins is their inherent heterogeneity; fractionation techniques were often developed to overcame the issues connected to the variable nature of lignins, and a refinement of technical lignins seems to be unavoidable to use the large streams as a renewable substitute of petrol in most applications.[1] There is substantially a double advantage arising from fractionation. The first is an increase in purity, the second is the generation of products with well-defined properties. To select a fraction with specific characteristics it is possible to take advantage of essentially two attributes: solubility and molecular weight.[2] Molecules with similar structures can be isolated by selective extraction in different solvents,[3] or with alkaline solutions.[4] Alternatively also by fractional precipitation, adding increasing amounts of a non-polar solvent to a polar solution,[1] or gradually lowering the pH of a aqueous solution.[5] On the other hand it is possible to separate lignin in different fractions with a specific molecular weight using ultrafiltration, selecting ceramic membranes with different cut-offs (eg. 5, 10 and 15 kDa).[6] When differential precipitation is achieved controlling the pH it is not possible to have a good control

on the characteristic of the fractions and the presence of residual lignin–carbohydrate complex (LCC) was observed. Ultrafiltration gives better results in terms of purity and allows for enhanced control over the molecular weight distribution, however it is a technique that needs specific equipment and can be energy consuming.[2] On the other hand, it was reported that via fractionation with solvents of different polarity it is possible to obtain homogeneous lignin products, characterized by with differentiated properties.[7] The objective at the base of the present work was to obtain different lignin fractions with higher purity and different affinity for rubber. Hence it was decided to fractionate lignin via consecutive extraction with organic solvents having increasing polarity.

Experimental

Lignin fractionation. Lignin was fractionated by successive extractions with methyl ethyl ketone (MEK) and methanol (MeOH). Lignin (250 g) was suspended in 1000 mL of the respective solvent and continuously stirred at room temperature for 2 h. The undissolved material was filtered and re-suspended for a second identical extraction. Afterward the solubilized fractions from both steps were recovered evaporating the solvent. The residue that was not soluble in both solvents was also recovered and dried.

Lignin characterization. Lignin fractions were qualitatively analyzed in terms of chemical groups with FT-IR spectroscopy and quantitatively with 31P-NMR. The molecular weight distribution was determined via SEC (Alkaline Size Exclusion Chromatography) for each lignin fraction analyzing unmodified samples using a 0.5M NaOH aqueous solution as mobile phase.

Rubber compounding. Fillers, vulcanizing agents, and antioxidants were added to neat natural rubber and lignin/natural rubber masterbatches to prepare rubber compounds using the Haake internal chamber mixer, with the formulations of table 3 and the procedure number 4 reported in chapter 4.

Characterization of rubber compounds. The mechanical properties of the rubber compounds filled with different lignins and the suitable references were assessed performing tensile tests on dumbbell shaped specimens.

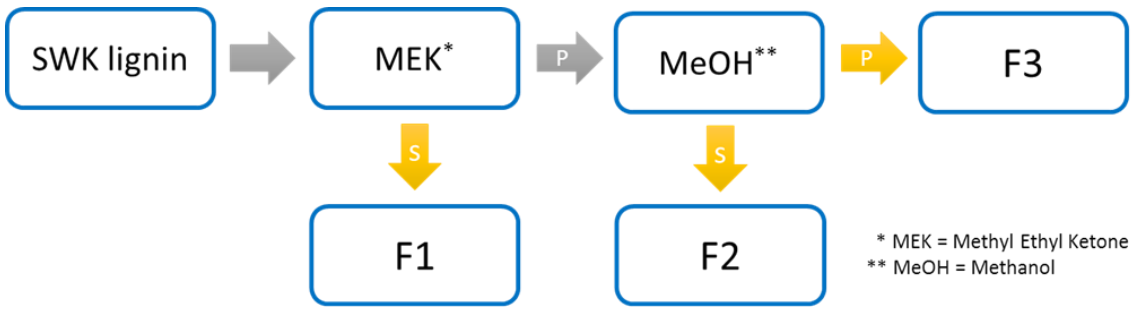

Figure 96 - Flow diagram for the fractionation of SWK lignin with solvents of increasing polarity.

Results and discussion

Characterization of the recovered fractions

With the selected solvents, it was possible to separate the original SWK lignin in three fractions: F1 is the fraction that was solubilized in methyl ethyl ketone (MEK), F2 was solubilized in methanol (MeOH) and finally, F3 is the residual fraction that was not soluble in both solvents. SWK lignin was extracted twice with each solvent, F1a is the fraction recovered after the first extraction with MEK and F1b the fraction recovered with the second extraction with MEK. The same was done with methanol. The solids obtained from the evaporation of the solvent were analyzed with FTIR, afterwards F1a and F1b were united in a unique fraction F1 and in the same way the union of F2a and F2b gave the fraction F2. The data relative to the yields of the recovered fractions are available in table 27. More than half of SWK lignin was readily solubilized in MEK and another 11% was recovered with the second extraction. Roughly one third of the remaining lignin, 10% of the initial mass, was extracted by methanol. With both solvents, the second extraction increased the yield of the recovered products by an additional 20%. Finally, approximately 1/5 of the lignin was found to be not soluble in both solvents. The spectra in figure 97 were obtained from the FTIR analysis of the starting lignin and the recovered fractions. The spectra were found to be very similar, with the same characteristic peaks and only small differences in the relative intensities. Between 3200 and 3600 cm^{-1} it was possible to recognize the broad peak due to hydroxyl groups. The shape of the peak was very similar in all samples with small differences in the spectra of F3. The characteristic bands associable to the vibrations of the CH groups are also similar. At 1700 cm^{-1} the fraction extracted with methyl ethyl ketone presented a strong band that involves the presence of unconjugated C=O and COOH groups and was probably due to the persistence of a small amount of solvent. The peaks associated with aromatic skeletal vibrations are clearly visible at 1595, 1508 and 1425 cm^{-1}, whereas the signals attributable to CH_2 and CH_3 groups are clearly distinguishable at 1463 and 1452 cm^{-1}. At 1367 cm^{-1} there is a peak that is not much pronounced with the exception of the F1 fraction where is more clearly detectable. This could be attributed at an increased number of phenolic hydroxyl groups but also to the methyl group, hence it could have been influenced by the traces of MEK. In F1a and F1b the peaks relative to the CO stretching of guayacil units (1265 cm^{-1}), phenolics and aromatic ethers (1213 cm^{-1}) are more intense than the peaks of CH in guyacils (1147 cm^{-1}) and aliphatic OH groups (1078 and 1030 cm^{-1}). The situation gradually change for F2 fractions and is completely reversed for the F3 sample, indicating that the first fraction is richer in phenolic moieties while the fractions obtained succes-

Starting	MEK extracted (F1)		MeOH extracted (F2)		Residual (F3)
SWK	F1a	F1b	F2a	F2b	F3
250g	138g	28g	26g	6g	52g
	55%	11%	10%	2%	21%
	166g - (66%)		32g - (13%)		52g - (21%)

Table 27 - Yields obtained from the consecutive extractions of SWK lignin with organic solvents.

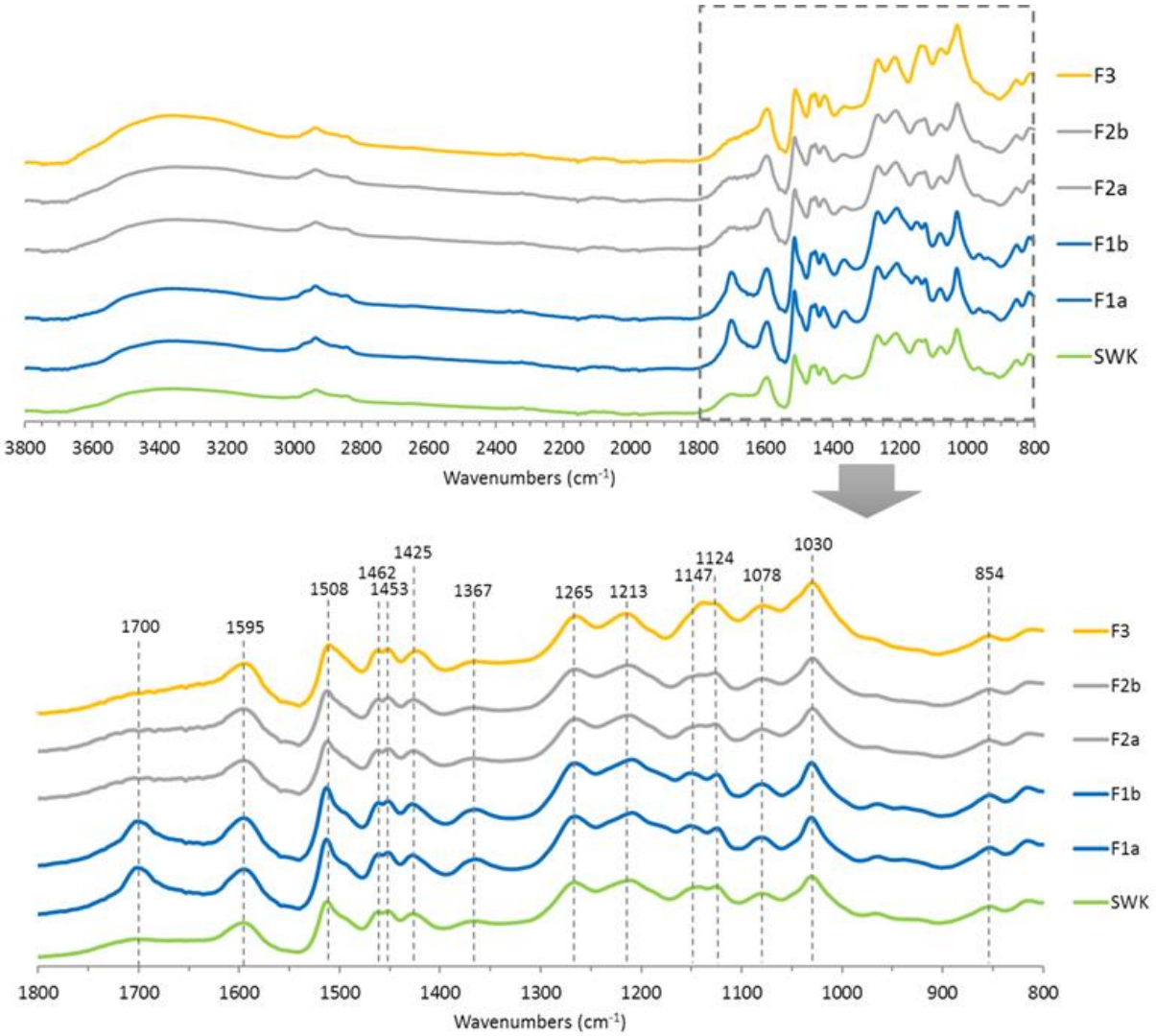

Figure 97 – FTIR spectra of the starting SWK lignin and the products generated by the successive extractions.

sively had progressively more aliphatic hydroxyls. This indicative trend, observed qualitatively in the results of the FTIR analysis was more accurately detected with ^{31}P-NMR. At last, it was possible to attest that the products extracted in two steps with the same solvent had extremely similar spectra, for this reason they were successively reunited and further characterized as a unique sample. As anticipated there is a clear trend in the concentrations of the different hydroxyls. The MEK soluble fraction, F1 was enriched in phenolic hydro-

	Aliphatic OH	Aromatic OH	Cond.	Syringyl	Guaiacyl	p-Hydroxyl	Carboxyl COOH
SWK	1,97	4,78	1,71	0,45	2,15	0,33	0,52
F1	1,42 ↓	4,94 ↑	1,77	0,47	2,39	0,31	0,55 ↑
F2	2,18 ↑	4,01 ↓	1,5	0,39	1,91	0,21	0,30 ↓
F3	2,76 ↑	3,34 ↓	1,41	0,36	1,41	0,15	0,15 ↓

Figure 98 – Quantitative determination of the different OH groups with ^{31}P-NMR.

xyls and carboxylic acids, contrarily the concentration of aliphatic hydroxyls was found to be inferior in comparison with the starting lignin and also the overall concentration of hydroxyls was found to be reduced. (F1 = 6,91 mmol/g, SWK = 7,27 mmol/g). The second product, the fraction that was solubilized by methanol but not by MEK (F2), displayed an opposite trend. The number of phenolic and carboxyl groups decreased, while the concentration of aliphatic hydroxyls increased, with a total concentration of hydroxyls of 6,49 mmol/g. The concentration of aliphatic OH was found to be furtherly increased in the insoluble fraction (F3), on the other hand, following the trend already observed for F2, the concentration of phenolic and carboxylic groups and the total concentration of hydroxyls (6,25 mmol/g) were lower. The distribution of the molecular weights was also investigated to better understand the nature of the products obtained from the fractionation of SWK lignin. The results obtained from size exclusion chromatography are graphically presented in figure 99, whereas molecular weights and polydispersity indexes are summarized in table 28. Also in the mass distributions, it was possible to observe a trend. The fraction F1 was the smallest, followed by F2 and F3. When compared to the original lignin (SWK), F1 is clearly smaller, as highlighted simultaneously by all three molecular weights (Mn, Mw and Mp) and more homogeneous as evidenced by the reduction of

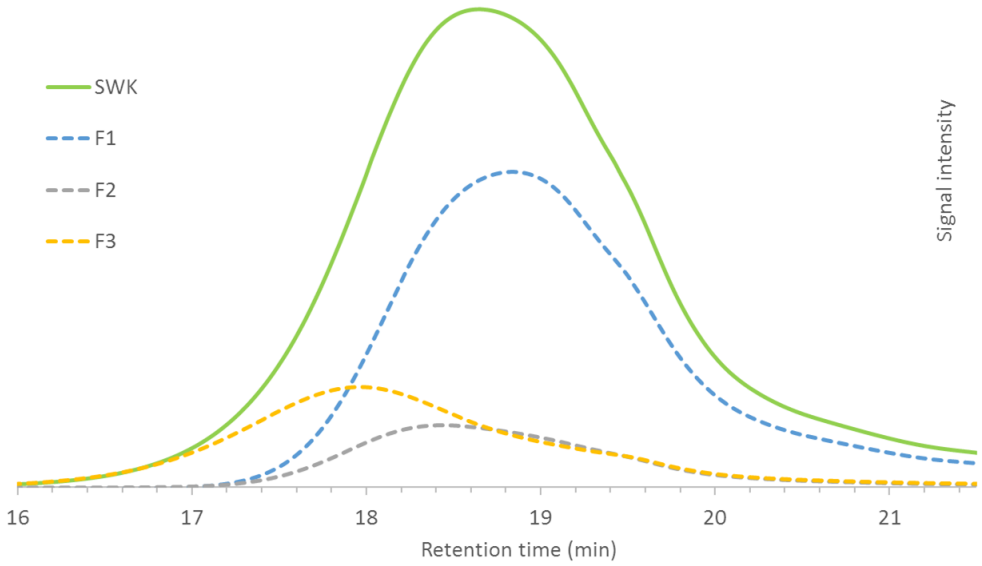

Figure 99 - Chromatograms obtained with SEC for the starting lignin (SWK) and its fractions (F1, F2 and F3). The normalized signal intensity of the fractions was multiplied for their relative abundancies.

	Mn	Mw	MP	PDI
SWK	700	3300	2000	4,6
F1	600	1900	1500	3,2
F2	800	2800	2750	3,5
F3	1300	9000	5900	7,0

Table 28 – Average molecular weights and polydispersity index for the starting lignin and the fractionated products.

the polydispersity index. The fraction F2, on the other hand, had a distribution of molecular weights not too dissimilar from that of the starting lignin, but a reduced dispersity. It is worth noticing that the chromatogram of F2 follows that of F3 at lower molecular weights (higher retention times) and the chromatogram of F1 at higher molecular weights (lower retention times). It is probable that the molecular weight played a decisive role on the solubility of the molecules, in fact it seemed that below a certain molecular weight, corresponding to a retention time of approximately 20 minutes, most molecules were soluble in MEK, whereas above another threshold, corresponding to a retention time of approximately 17 minutes, everything showed a dramatically reduced solubility. Finally, F3 was constituted by the larger macromolecules and had the highest polydispersity index among all the samples. From all the characterization techniques emerged a clear trend in the observed features. This could be partially since molecular weight and chemical functionalities are not completely independent, but are somewhat correlated. This correlation might not exist in native lignin, but during the extraction from wood lignin's chains are often cleaved and new functionalities are formed. The most abundant and labile linkages, β-O-4, are disrupted generating more phenolic hydroxyls; at the same time condensation reactions generate new bonds, forming structures that are impoverished in phenolic hydroxyls. In second place, the fractionation process serves also as a purification process, and all the insoluble fractions (eg. polysaccharides) end up in the insoluble fraction (F3), additionally increasing the amount of aliphatic hydroxyls at the expense of the phenolic ones. The fractions solubilized in the organic solvents should be characterized by a higher purity, nevertheless it is possible that small fragments having a low molecular weight such as extractives, fatty acids, and resinous plant material are also solubilized and recovered in the first fractions.[8] Eventually three fractions with narrower characteristic were prepared from the starting lignin. The concentration of phenolic hydroxyls increased in the order F1 > F2 > F3, the number of aliphatic hydroxyls, on the other hand, followed the opposite trend F3 > F2 > F1 as well as the average molecular weight.

Properties in composites with natural rubber

Through fractionation with solvent of increasing polarity it was possible to produce lignin fractions with determined characteristics, a narrower molecular weight distribution and higher purity. Furthermore, it is reasonable that the fraction solubilized in the solvent with the lowest polarity has an increased affinity for natural rubber. It was supposed that the fraction F1 could have a better compatibility with rubber, in addition, according to the results reported in chapter 6, F1 should also possess an increased antioxidant activity, due to the higher concentration of phenolic hydroxyl groups and the lower average molecular weight. On the basis of these considerations, and the higher amount of fraction F1 available it was decided to test the properties in rubber adding directly the lignin powder in the mixer (dry-mixing), while the lesser amounts of the fractions F2 and F3 were preserved for the trials with coprecipitation. The influence of F1 on the mechanical properties of natural rubber was evaluated in relation to the properties of three references:

Ingredients	NR	CB	SWK	F1
Natural Rubber (SIR20)	100	100	100	100
Starting lignin (SWK)	0	0	15	0
Fractionated lignin (F1)	0	0	0	15
Carbon Black (N375)	0	15	0	0
Soluble sulfur	2	2	2	2
Zinc Oxide	5	5	5	5
Stearic acid	2	2	2	2
Accelerator (CBS)	2	2	2	2
Antioxidant 1 (6PPD)	1	1	1	1
Antioxidant 2 (TMQ)	1	1	1	1
PHR TOT	113.0	128.0	128.0	128.0
Density TOT	0.970	1.025	1.006	1.006

Table 29 - Formulations expressed in PHR for the compound prepared with the lignin fractionated in MEK (F1) and three references (Neat Natural Rubber - NR, Carbon Black - CB and Softwood Kraft lignin - SWK).

neat natural rubber (NR), natural rubber filled with unfractionated lignin (SWK) and natural rubber filled with a commercial filler - carbon black N375 (CB). Observing the vulcanization curves reported in figure 100, it was visible that lignins interfered with vulcanization, delaying the beginning of the crosslinking. In the region of the plateau it was also possible to observe that lignin increased the stiffness of the compounds but with lesser extent then carbon black. The compound filled with F1 had a lower modulus than the reference compound filled with SWK lignin, this was supposed to relate to an increased interference with vulcanization.

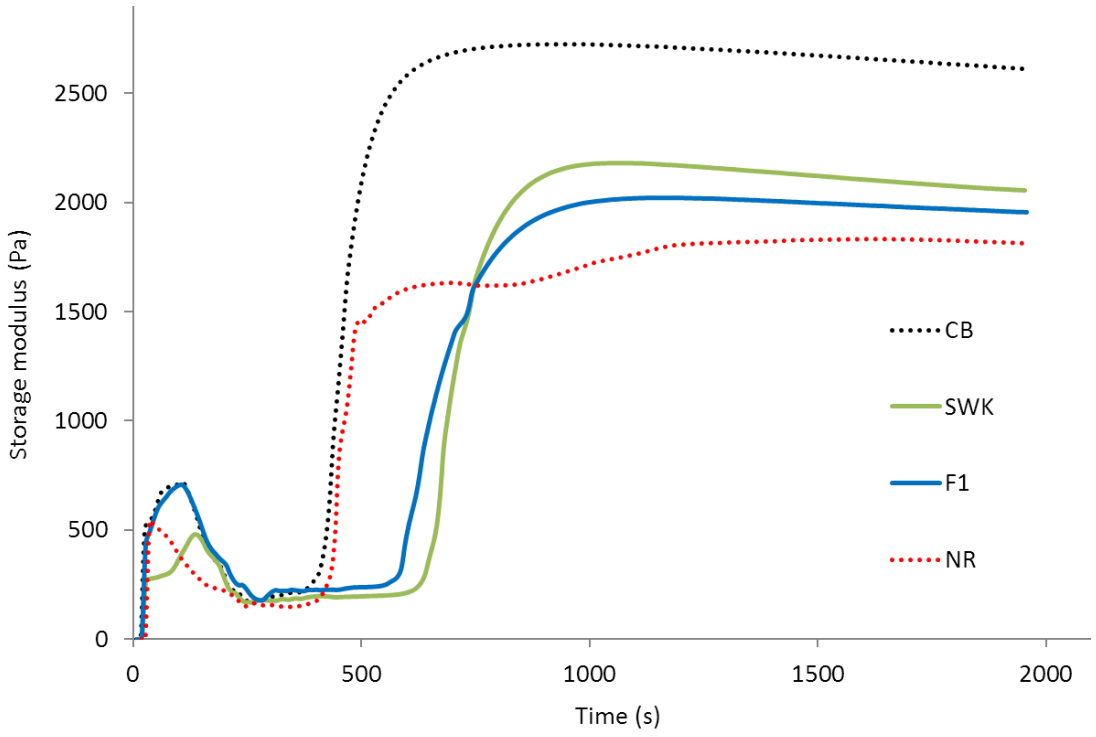

Figure 100 - Vulcanization curves registered at 150 °C for 30 minutes.

In fact, the fraction extracted in MEK should have possessed a higher compatibility with rubber and was presumably better dispersed, giving rise to a higher contact area between the two biopolymers. Secondly, F1 was also characterized by a greater content of acidic functions that are known to hinder vulcanization.[9] After vulcanization, the mechanical properties of the four samples were evaluated with tensile tests. The results of the experiments are reported graphically in figure 101 and the corresponding values are summarized in table 30. As already observed analyzing different systems in chapter 6, when the raw technical lignin (SWK) was added via dry-mixing there was no improvement of the mechanical properties, rather a moderate loss

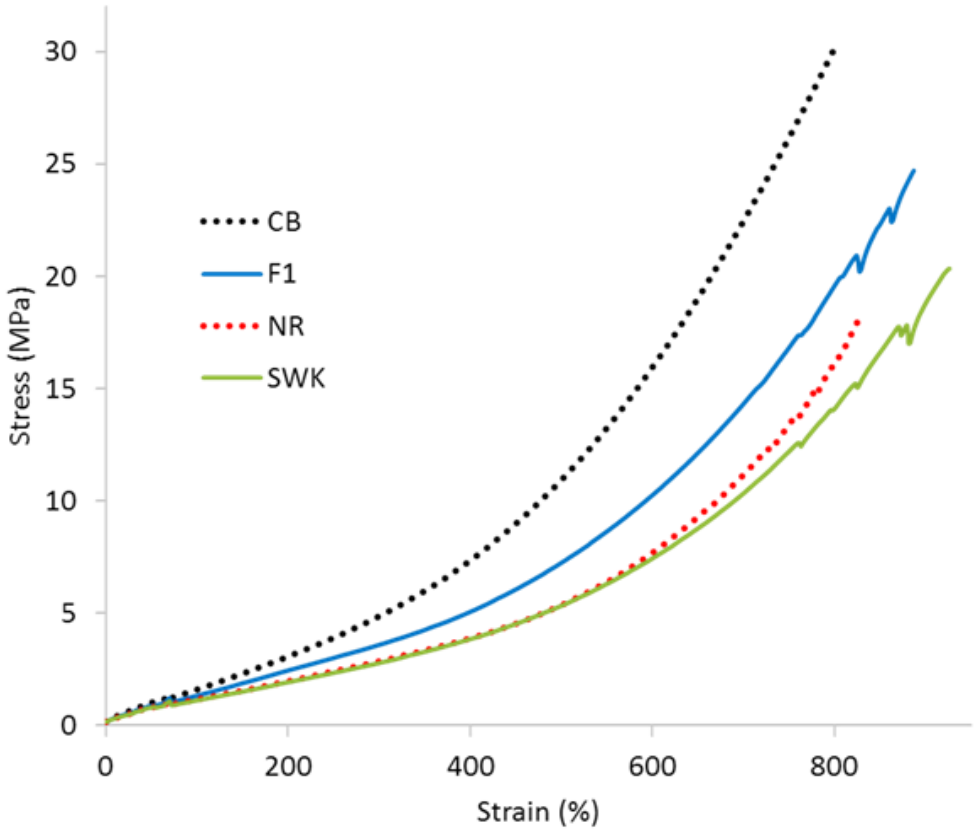

Figure 101 - Stress/strain curves measured on vulcanized dumbbell shaped specimens.

	NR	CB	SWK	F1
50 (%)	0,80	1,02	0,79	0,86
100 (%)	1,16	1,60	1,12	1,31
300 (%)	2,85	4,87	2,79	3,58
700 (%)	11,2	22,5	10,4	14,3
UTS (MPa)	18,2	30,3	20,3	24,7
UE (%)	828	801	926	888
RI	2,5	3,1	2,5	2,7

Table 30 - Numerical values relative to the tensile tests - Stress at progressive elongations, Ultimate Tensile Strength (UTS), Ultimate Elongation (UE) and Reinforcement Index (RI).

of stiffness at high deformation and a small improvement of the properties at break (Ultimate Tensile Strength – UTS and Ultimate Elongation – UE). The curve of SWK lignin was superimposed to that of the NR reference until ~550 % elongation, afterwards the presence of lignin reduced the modulus of the compound. Observing the characteristic curvature, it was supposed that lignin interfered with the strain crystallization of natural rubber. At the same time, there are few fluctuations that are visible at the right ending of the curves and were supposed to be caused by small rearrangements of the specimens inside the hydraulic clamps, in fact the samples filled with lignins sustained very high deformations and when the samples are so elongated the thickness is extremely reduced. When the smaller and purer fractionated lignin (F1) was used as a filler for natural rubber the behavior was different. The more hydrophobic lignin was supposedly better dispersed and capable to generate enhanced interactions with rubber. Thus, with the addition of F1, the mechanical properties were improved in the whole range of deformations. The results were considered positive despite the performances were not matching those of reinforcing grade of carbon black. Once more it was confirmed that to achieve specific properties and gain an elevated added value, technical lignins must be further refined. Fractionation was found to be a suitable technique to improve the purity degree of lignin and to enhance specific characteristics. For instance, the concentration of phenolic hydroxyls, connected to an improved antioxidant capability, and the compatibility with rubber, responsible for better dispersion and stronger polymer-filler interactions, that ultimately promoted a rise in the reinforcement. Moreover, fractionation opened the possibility to prepare rubber compounds filled with lignin and characterized by superior mechanical properties avoiding coprecipitation. This feature is particularly interesting in the view of an industrial application where the versatility and cost-effectiveness of dry-mixing can offer a substantial technological and economic advantage. It is also worth noticing that in the presence of lignin vulcanization was partially hindered, and the final crosslinking density was seemingly inferior in the compounds filled with lignins. Nevertheless, F1 lignin effectively reinforced rubber despite a suboptimal crosslinking density and lower performances of the polymeric matrix. It follows that if the issue can be fixed tuning the vulcanizing system, the properties of F1 filled compounds will presumably be enhanced and will get closer to those of carbon black.

In a second experiment lignins were added to natural rubber via coprecipitation, to improve dispersion and to reduce the average particle size. The compounds prepared from the NR/lignin masterbatches were examined in relation to new references obtained using natural rubber coagulated from the same latex employed for the coprecipitation. The related formulations are presented in table 31, whereas the data obtained from the tensile tests are reported in figure 102 and table 32. In the first place, it was possible to notice small discrepancies in the behavior of the reference constituted by neat natural rubber (NR), presumably due to differences in the average molecular weight, polydispersity, and in the content of proteins, impurities, and moisture. The rubber prepared through coagulation from the latex was slightly

stiffer than SIR 20 natural rubber up to 700% elongation, but suffered premature failure, showing lower properties at break. This beha-

	NR cop	CB cop	SWK cop	F1 cop	F2 cop	F3 cop
NR form latex (60%)	100	100	-	-	-	-
NR/lignin masterbatch (13%)	-	-	115	115	115	115
Carbon Black (N375)	-	15	-	-	-	-
Soluble sulfur	2	2	2	2	2	2
Zinc Oxide	5	5	5	5	5	5
Stearic acid	2	2	2	2	2	2
Accelerator (CBS)	2	2	2	2	2	2
Antioxidant 1 (6PPD)	1	1	1	1	1	1
Antioxidant 2 (TMQ)	1	1	1	1	1	1
PHR TOT	113.0	128.0	128.0	128.0	128.0	128.0

Table 31 - Formulations expressed in PHR for the compounds prepared from the masterbatches obtained coprecipitating the four lignins (SWK, F1, F2 and F3) and two references (Natural Rubber – NR and Carbon Black – CB).

viour could also be alleged to an increased sensitivity towards the mechanical and thermal stresses imparted during mixing and vulcanization. This hypothesis was supported by the fact that samples filled with lignin registered a noticeable increase in the properties at break. In fact, lignin was added through a cold process and was able to exert its protective activity from the early stages of mixing. It is also worth noticing that the specimens prepared from the NR/lignin masterbatches didn't come to a break but all five specimens slipped out of the clamps at very high elongations, hence the registered ultimate properties are somewhat underestimated. Nevertheless, all lignins, when added via coprecipitation, improved the mechanical properties of the natural rubber compounds over the full range of elongations, simultaneously enhancing the tensile modulus at low, medium, and high strains and the ultimate properties (UTS and UE). Among lignin fractions there is a clear trend in the mechanical properties conferred to the rubber compounds (F1 > F2 > F3), this trend reflected well the trends individuated in the molecular properties of the fractions. In fact, the fraction F1 was characterized by an improved compatibility with rubber that presumably promoted greater filler-rubber interactions and led to an enhanced solubility that, along with the lower molecular weight and the higher amount of hindered phenolic groups, also boosted the antioxidant capability. The sample filled with the mother lignin (SWK) showed properties that clearly arise from the sum of the contributions of the three fractions, in fact the relative curve falls between the curves of F1 and F2 at low strain, and between F2 and F3 at high strains. The properties of the lignin filled compounds were found to be closer to that of carbon black in this experiment, highlighting the fact that despite the better dispersability showed by F1 in the "dry-mixing" experiment, coprecipitation still improved dispersion and probably provided a smaller particle size distribution. The properties conferred by F1 were found to be particularly interesting at low strains and at break. At low strains (< 50 %), the tensile modulus of F1 cop was higher than that of CB cop and was still comparable at 100% elongation, however at higher elongation the reinforcing capability of carbon black was

still superior. This might indicate that in the initial state lignin had a satisfactory dispersion and was successfully bounding rubber, afterwards, when the local strain increased it is plausible that the interactions between filler and matrix were too weak and the rubber desorbed from the surface of the filler's particles. In the end, it was confirmed that the greater limit for the use of technical lignins in rubber compounds is the poor compatibility that precludes a good dispersion. The results showed that the fraction that is more soluble in solvents with lower polarity (F1) had a better compatibility with rubber and attained a better dispersion also when dry-mixed, consequently granting also enhanced mechanical properties to rubber compounds. However, despite some properties were found to be in line or even superior to those provided by carbon black, the reinforcing capability of lignin was found to be still undermined by the inability to form strong interactions with the elastomeric matrix.

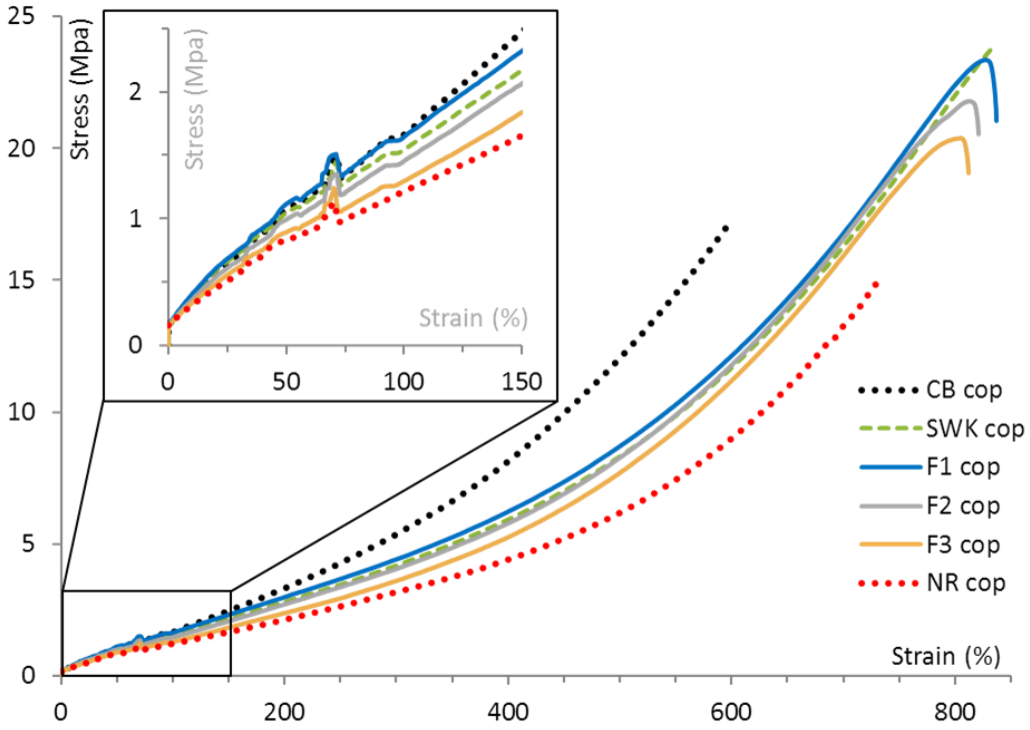

Figure 102 – Stress/strain curves obtained with tensile tests on dumbbell shaped specimens vulcanized for 30 minutes at 150 °C, filled with 15 PHR of fractionated lignin (F1, F2, F3) and references (NR, CB and SWK).

	NR cop	CB cop	SWK cop	F1 cop	F2 cop	F3 cop
50 (%)	0,83	1,08	1,06	1,13	1,00	0,90
100 (%)	1,22	1,75	1,63	1,73	1,52	1,36
300 (%)	3,19	5,53	4,29	4,51	4,14	3,69
500 (%)	6,20	12,38	8,52	8,89	8,44	7,86
700 (%)	13,29	-	16,63	17,15	16,9	16,29
UTS (MPa)	14,69	17,22	22,86	20,28	19,24	18,39
UE (%)	730	598	833	837	821	812

Table 32 - Numerical values relative to the tensile tests - Stress at progressive elongations (from 50% to 700%), Ultimate Tensile Strength (UTS) and Ultimate Elongation (UE).

8.4 Thermal conditioning

The work on the fractionation of lignin presented in the previous section demonstrated that exalting certain features of the polyphenolic biopolymers it is possible to improve the properties of lignin/natural rubber composites. Besides, the work also provided new insight regarding the relationship between the molecular characteristics of lignin and its performances in natural rubber compounds. However, the final mechanical properties, were not found to be in line with those provided by carbon black. Furthermore, it can be challenging to use organic solvents in an environmentally and economic compatible way on a large scale; and through fractionation only a part of the lignin is valorized, while another is converted into a lower value side-product. In the light of these consideration, the work proceeded with the research of alternative approaches with the constant objective to modify lignin in a way that was suitable to produce lignin/natural rubber composites with improved performances. In these section, are reported the results achieved modifying lignin with thermal treatments. Following the same outline used in the previous section, the characterization of the products is firstly proposed, followed by the assessment of the mechanical properties of the elastomeric composites prepared with the modified lignin products. The idea to modify lignin via thermal conditioning arose from an alluring potential opportunity, the possibility to convert the abundant technical lignins in value-added products controlling the chemical/structural characteristics with a convenient process, limiting the need of sophisticated equipment. Two different approaches were taken. The first treatment was envisaged on the basis of the limited available in literature that dealt with the chemical/structural modification of lignins using heat treatments under inert conditions.[10] It was reported that heating lignin in an inert atmosphere above 250 °C yielded different structural modifications: cleavage of some methoxy groups, cleavage of propane side chains, depolimerization caused breakdown of α-O-4 and β-O-4 linkages, re-condensation via free radical coupling, and H abstraction by neighboring radicals. A more condensed structure, a diminished overall content of oxygen and an increased number of double bonds characterized the heat-treated lignin. The weight-average molecular weight was found to be substantially unchanged, even if the increase in the polydispersity index might revealed the presence of larger structures. A plausible reconstruction of the modified structure is proposed in figure 103. The treatment seemed to somewhat modify the starting lignin into a substance that was more like carbon black, due to the presence of less oxygen and more carbonaceous, unsaturated, and condensed structures. For this reason, it was supposed that such substance could might have been a potential filler for rubber. Differently, the second approach was found on the results obtained with the fractionated lignin (F1). The idea was to partially depolymerize the starting lignin (SWK), to obtain a modified lignin, characterized by a structure that resembled the structure of F1, i.e. with a lower average molecular weight and an increased concentration of phenolic groups. In the last decade, many research groups focused on the depolimerization of lignin to produce chemicals, with a focus on aromatics.[11–15] The belief at the base of the experiment was that milder conditions might have resulted in a controlled

depolimerization, with the prominent cleavage of the aryl ethers, yielding a smaller lignin characterized by an increased content of phenolic hydroxyls.

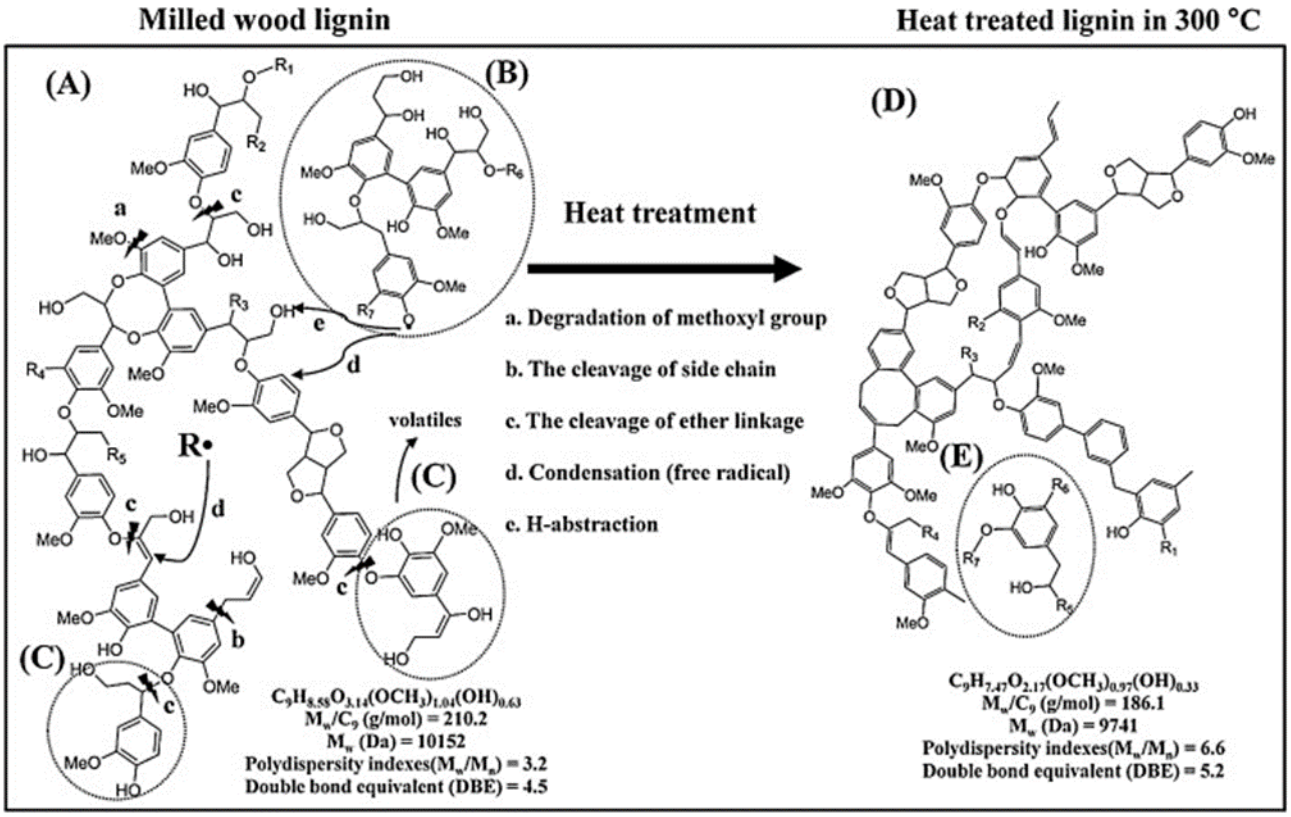

Figure 103 - Plausible scheme of the reactions occurring during heat treatment of milled poplar wood lignin under inert atmosphere (reproduced from reference).[10]

Experimental

Thermal conditioning method 1 - TC1. 20 g of SWK lignin were placed in the rotating chamber of a Kugelrohr reactor, the chamber was fluxed with N_2 to create an inert atmosphere and the temperature was raised until 300 °C. The sample was kept at isothermal conditions for 10 minutes; hence it was gradually cooled until room temperature avoiding exposure to oxygen. The experiment was repeated three times to accumulate enough material to prepare the rubber compounds.

Thermal conditioning method 2 - TC2. 35 g of lignin were dispersed in 350 mL of a propanol/water solution (1:1) and stirred at room temperature for 10 minutes. Afterwards the solution was transferred into a 500 mL Parr stirred reactor. The reactor was heated to 200 °C and the reaction was carried on for 2 hours at that temperature. After that time, the reactor was let to cool until room temperature over few hours. A fraction of the product precipitated (labelled TC2p), whereas another fraction was still solubilized in the supernatant and was recovered evaporating the solvents after separation by vacuum assisted filtration (labelled TC2s). The experiment was repeated twice to produce enough materials for the rubber compounding.

Lignin characterization. Thermally treated lignins were qualitatively analyzed with FT-IR spectroscopy. The molecular weight distribution was determined via SEC (Alkaline Size Exclusion Chromatography) for TC2 lignin, analyzing the unmodified sample after dispersion in an aqueous alkaline solution.

Rubber compounding. Fillers, vulcanizing agents, and antioxidants were added to neat natural rubber and lignin/natural rubber masterbatches to prepare rubber compounds using the Haake internal chamber mixer, with the formulations of table 108 and the procedure number 4 reported in chapter 4. TC1 was incorporated into natural rubber using dry-mixing, whereas TC2 through coprecipitation. The references were prepared accordingly, using sir 20 rubber and natural rubber coagulated from latex.

Characterization of rubber compounds. Vulcanization curves were recorded with the Ares rheometer at 150 °C for 30 minutes. The mechanical properties of the rubber compounds were assessed performing tensile tests on vulcanized dumbbell shaped specimens.

Results and discussion

During the thermal conditioning, it was possible to observe the sample turning from light brown to dark brown. At the end of the experiment the lignin powder condensed in a three-dimensional structure that expanded in the whole chamber of the reactor. A coarse powder was recovered with the spatula and was finely grinded in a mortar before any handling. About 15,9 g of solid product were recovered in both experiments, accounting for the 79,5% of the starting weight. The recovered product (TC1) was found to be insoluble in any organic solvent (THF, Acetone and 1,4-Dioxane), and neither in an aqueous alkaline solution

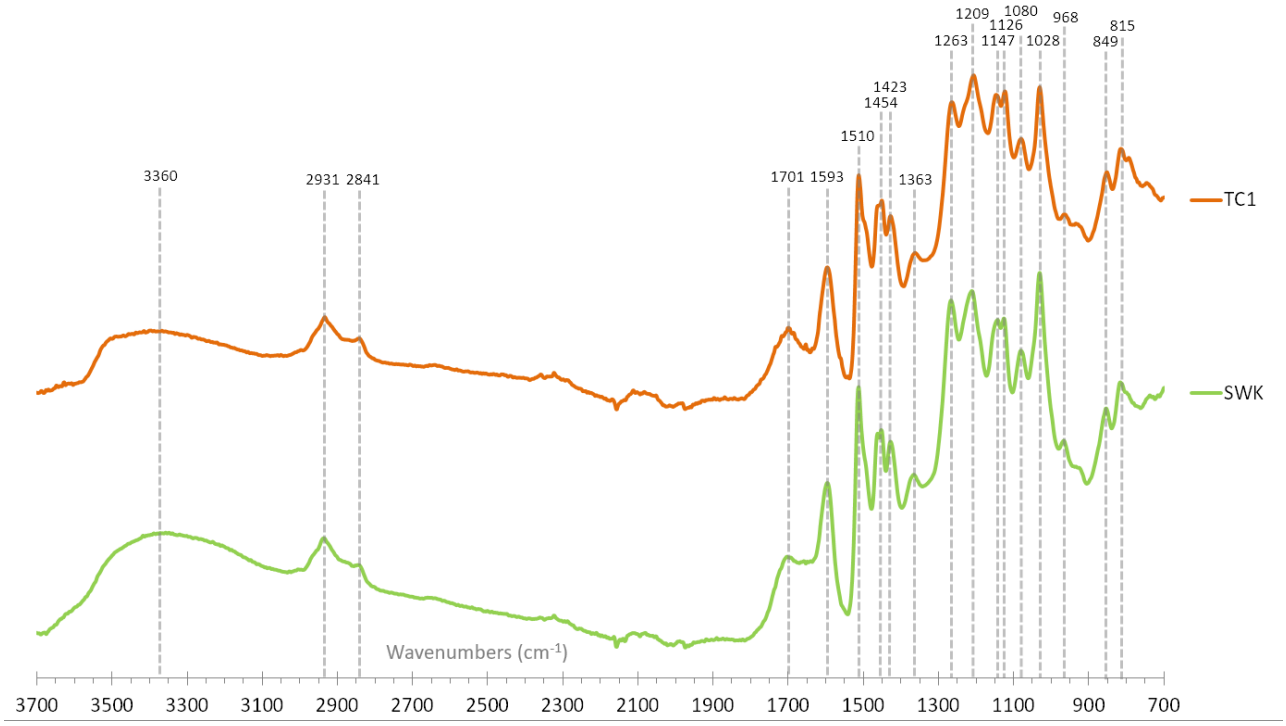

Figure 104 - FTIR spectra of the starting lignin (SWK) and the thermally conditioned lignin (TC1).

(NaOH 0,5M). This condition greatly limited the possibility to analyze the sample and the only available characterization technique was the FT-IR in ATR configuration. The spectra obtained from the spectroscopic analysis are shown in figure 104. Confronting the spectrum of the original lignin (SWK) with that of the thermally modified product (TC1) it is possible to notice that the broad absorption band centered at around 3360 cm^{-1}, owed to the presence of free and hydrogen bonded aliphatic and phenolic hydroxyls changed shape because of the thermal conditioning and the intensity decreased compatibly with a loss of OH functionalities. The peak at ~1700 cm^{-1} associated to the presence of unconjugated carbonyl and carboxyl groups slightly increased, whereas the bands attributed to the stretching in the CO of G units (1263 cm^{-1}) and to the primary aliphatic OH (1028 cm^{-1}) were found to be less intense. This changes and the formation of an insoluble matter are compatible with the changes observed by Chengzhong et al.[16] In the paper, the investigated softwood Kraft lignins showed thermal instability at relatively low temperatures, also before glass transition (T_g) which was reported at 153 °C. It was also found that heating lignins at only 20 °C above T_g for 20 minutes led to a 70-fold increase in the Mw and that after 30 minutes the material became highly crosslinked and could no longer be solubilized. Hence, the condensation reactions (illustrated in figure 105) supposedly prevailed on the chain scissions leading to an insoluble network characterized by an extremely high molecular weight. It is also possible that the loss of hydroxyl groups detected with the spectroscopic

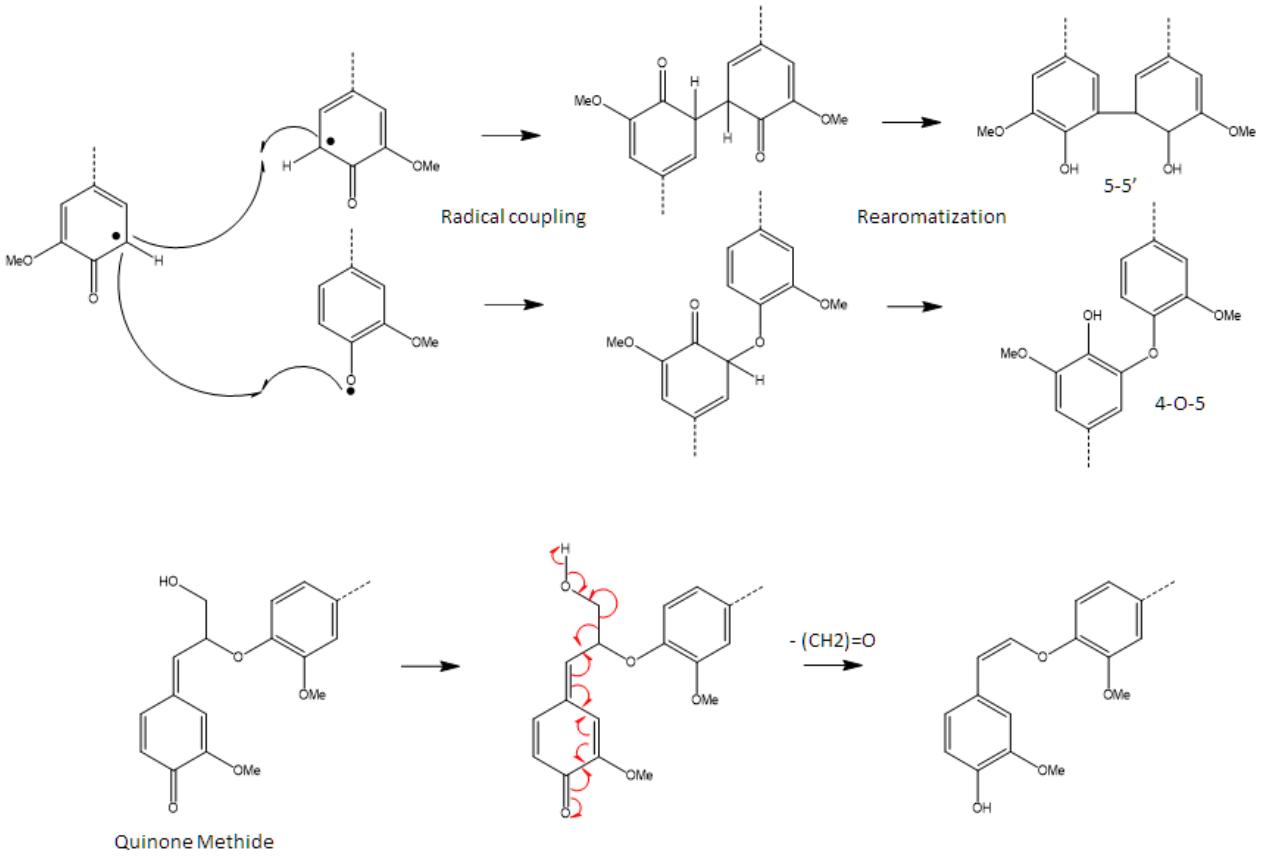

Figure 105 – Plausible thermally induced radical condensations and γ-elimination of the methylol group as formaldehyde within residual β-O-4 linkages (redrawn from reference).[16]

analysis was connected to the thermal decomposition of primary alcohols. The consecutive release of formaldehyde could have promoted additional condensation and might have contributed to the formation of the insoluble network. The differences observed in the behavior of the SWK lignin with respect to the behavior of the lignin obtained from poplar were supposed to arise from the different molecular structure of softwood and hardwood lignins. The preponderance of G units in softwood lignins provided more sites for condensation and presumably promoted the formation of an extended crosslinked network. The loss in weight is probably the result of the cleavage of several types of terminal phenolic groups attached by β-O-4 linkages, in fact they are easily exposed to heat and the β-O-4 linkage is thermally labile, a minor contribution might also arise from the cleavage propane side chain and functional groups as already observed by Kim et al.[10] Due to its marked insolubility, the modified lignin (TC1) was compounded with natural rubber and additives via dry-mixing to prepare the rubber model compounds. The results of the tensile tests are reported in figure 106. The addition of the tentative filler (TC1) to natural rubber degraded the properties of the elastomer. Despite a light stiffening detected at low strains, the overall mechanical characteristics were compromised as evidenced by the marked loss in the elastic modulus from mid to high strains. This behavior was imputed to a poor dispersion characterized by large particle size. The formation of resistant, macroscopic particles was observed during the trials done to test the solubility of TC1, as shown in figure 107. It was supposed that the condensation reactions occurred during the thermal treatment stiffened the structure of

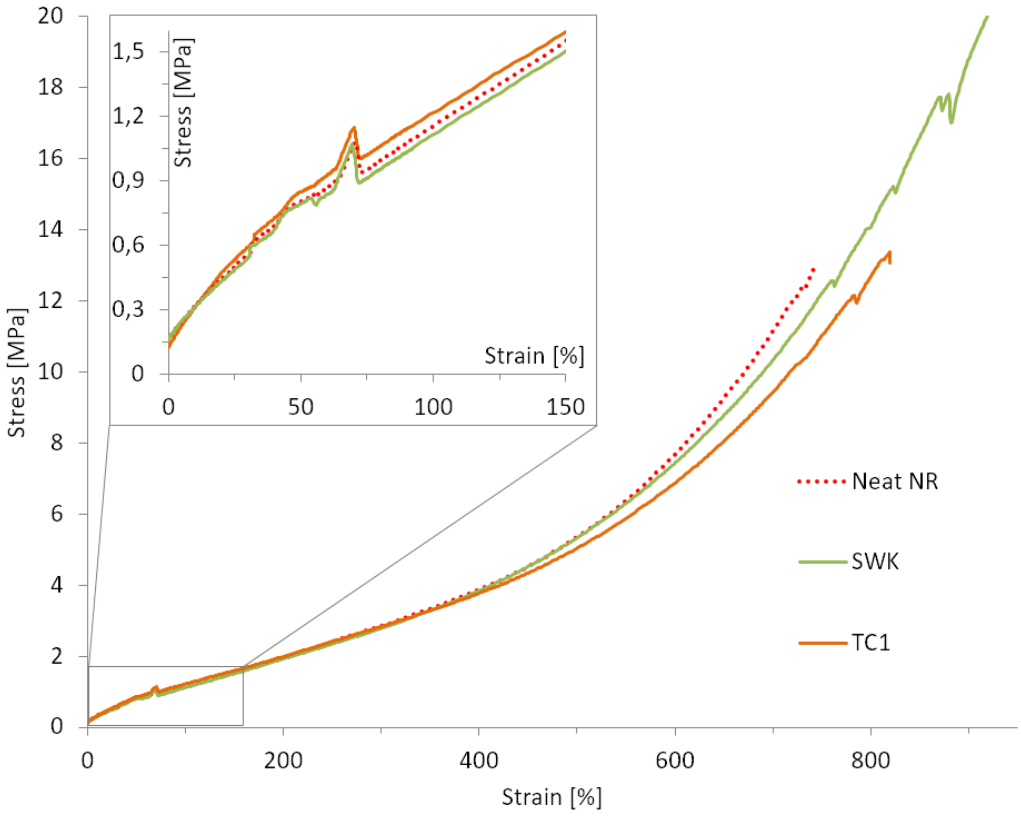

Figure 106 - Stress/strain curves obtained with tensile tests on dumbbell shaped specimens vulcanized for 30 minutes at 150 °C, filled with 15 PHR of thermally conditioned lignin (TC1) and references: SWK and Neat NR.

Figure 107 – Picture of a vial positioned in front of a light source containing a dispersion of TC1 modified lignin in a 0.5 M NaOH solution. The image was recorded with a digital camera.

the biopolymer, producing particles with improved mechanical resistance. The mechanical grinding and the shear forces generated in the internal chamber mixer, during the blending with rubber, were not able to disrupt the highly-crosslinked particles that persisted in the final rubber compounds, giving rise to a deterioration of the mechanical properties typically observed in the presence of large particles and aggregates. It is also worth noticing that the ultimate elongation and the ultimate tensile strength were found to be much closer to those of the unfilled rubber (NR) than to those of the reference filled with the softwood kraft lignin (SWK). This was saw as an indication that after the thermal conditioning, TC1 lignin was not exerting a significant antioxidant activity. This fact correlates well with the results obtained in chapter 6, and could be explained by the strong increase in the molecular weight and by the reduction in the number of phenolic hydroxyls. This kind of thermal conditioning negatively influenced the immediate applicability of softwood Kraft lignin in composites with natural rubber, mainly hindering dispersion by stiffening the rather

	NR	SWK	TC1	NR cop	CB cop	SWK cop	TC2 cop
Natural Rubber (Sir 20)	100	100	100	-	-	-	-
NR form latex (60%)	-	-	-	100	100	-	-
SWK lignin		15					
TC1 lignin	-	-	15	-	-	-	-
NR/lignin masterbatch (13%)	-	-	-	-	-	115	115
Carbon Black (N375)	-	-	-	-	15	-	-
Soluble sulfur	2	2	2	2	2	2	2
Zinc Oxide	5	5	5	5	5	5	5
Stearic acid	2	2	2	2	2	2	2
Accelerator (CBS)	2	2	2	2	2	2	2
Antioxidant 1 (6PPD)	1	1	1	1	1	1	1
Antioxidant 2 (TMQ)	1	1	1	1	1	1	1
PHR TOT	113.0	128.0	128.0	113.0	128.0	128.0	128.0

Figure 108 - Formulations expressed in PHR for the compounds prepared from

large particle that were already present in the starting lignin.[17] However this simple technique could be useful for the preparation of stiffer, lignin based fillers if applied on materials already displaying a suitable particle size distribution. The second approach was aimed at the controlled depolimerization of the starting lignin (SWK), targeting the aryl ethers, to produce a smaller lignin characterized by an increased content of phenolic hydroxyls, possibly resembling the structure of the F1 product obtained from the fractionation process described in the previous section of this chapter. At the end of the reaction two fractions were recovered, the fraction composed by the solubilized products was labelled TC2s and was separated by the precipitated material, that was found on the bottom of the parr reactor and was labelled TC2p. The fraction found in the supernatant (TC2s) accounted for almost 15 g and the precipitated matter (TC2p) for roughly 20 g. Almost the totality of the starting material was recovered beside small loss might occurred during the recovery of the materials (filtration). The analysis with the FT-IR provided little insight regarding the changes in the structure caused by the thermal treatment. The spectrum of TC2, reported in figure 109, presents the same peaks of the starting lignin, showing only a moderate increase in the relative intensity of the peaks attributable to the OH groups (3365 cm^{-1}) and in the band centered at 1215 cm^{-1} associable to the CO stretching of phenolic hydroxyls and aromatic ethers. Additionally, in the spectrum of TC2s it is possible to detect and increased intensity in the peaks falling at 2931, 1701 cm^{-1} and 966 cm^{-1}, respectively associated to the CH stretching of methyl and methylene groups, the stretching of C=O in unconjugated carbonyls and carboxylic acids and the stretching of CO stretching in the CH_2-O group. Further information for the comprehension of the structure of the conditioned products (TC2s and TC2p) was obtained analyzing the

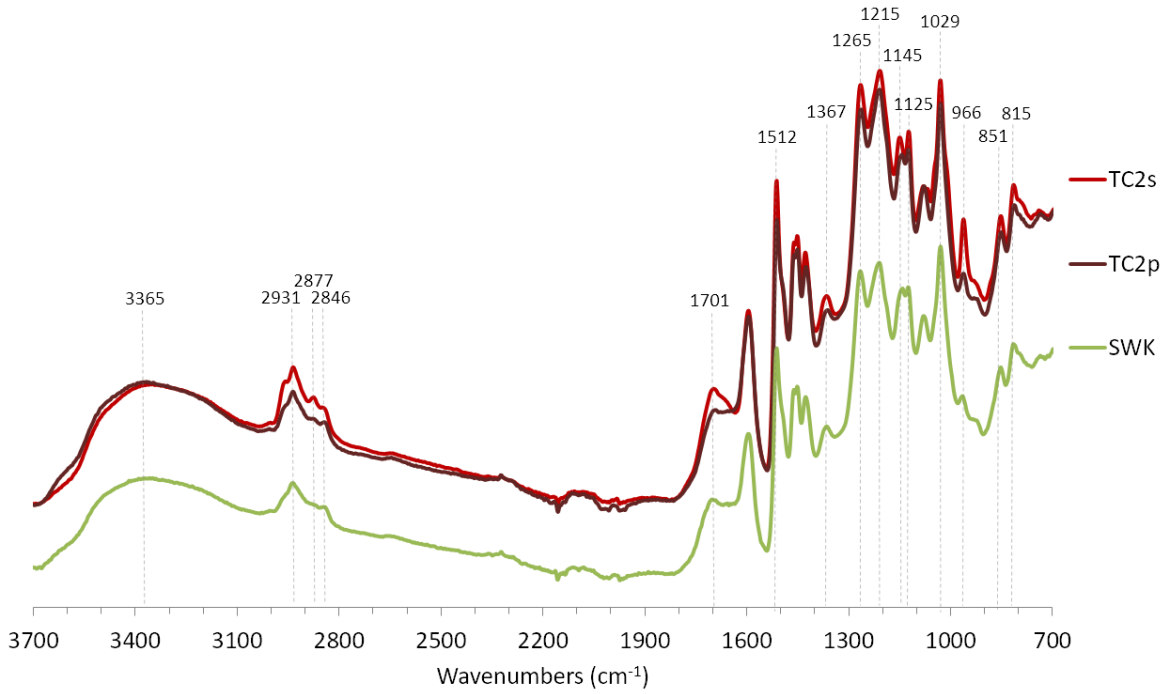

Figure 109 - FTIR spectra of the starting lignin (SWK) and the thermally conditioned lignin (TC2).

distribution of molecular weights of the polymer. For the soluble fraction – TC2s – the molecular average weight was successfully reduced and the distribution was found to be not too dissimilar from that of the targeted fraction (F1). Regarding TC2p, on the other hand, the treatment drastically increased the molecular weight. The trends were rationalized assuming that TC2s was the result of the cleavage of the aryl ethers. The liberated fragments were probably able to disperse in the solution avoiding the condensation reactions. On the other hand, in TC2p the reactions of radical coupling must have prevailed and the resulting materials was highly condensed. It is possible that the condensation could be hindered working with more diluted systems, however such systems would not be very energy efficient, hence not suitable for the production of large amounts of modified lignins. Since both products, TC2s and TC2p were still soluble aqueous alkaline solutions, the rubber compounds were prepared using coprecipitation technique, bypassing the issue connected with insufficient dispersion. Both products originated composites with better mechanical properties than natural rubber, however the performances were found to be lower than those obtainable using the unmodified technical lignin. TC2s didn't increase the stiffness of the compound at very low strains, but improved substantially the properties at high elongations. TC2p had an opposite trend, gave little reinforcement at low strain (higher elastic modulus) but less improvement in the ultimate properties. The results demonstrated that thermal treatments are not a suitable way to improve the reinforcing behavior of softwood Kraft lignin. The complex reactivity of these lignins is activated at relatively low temperatures and

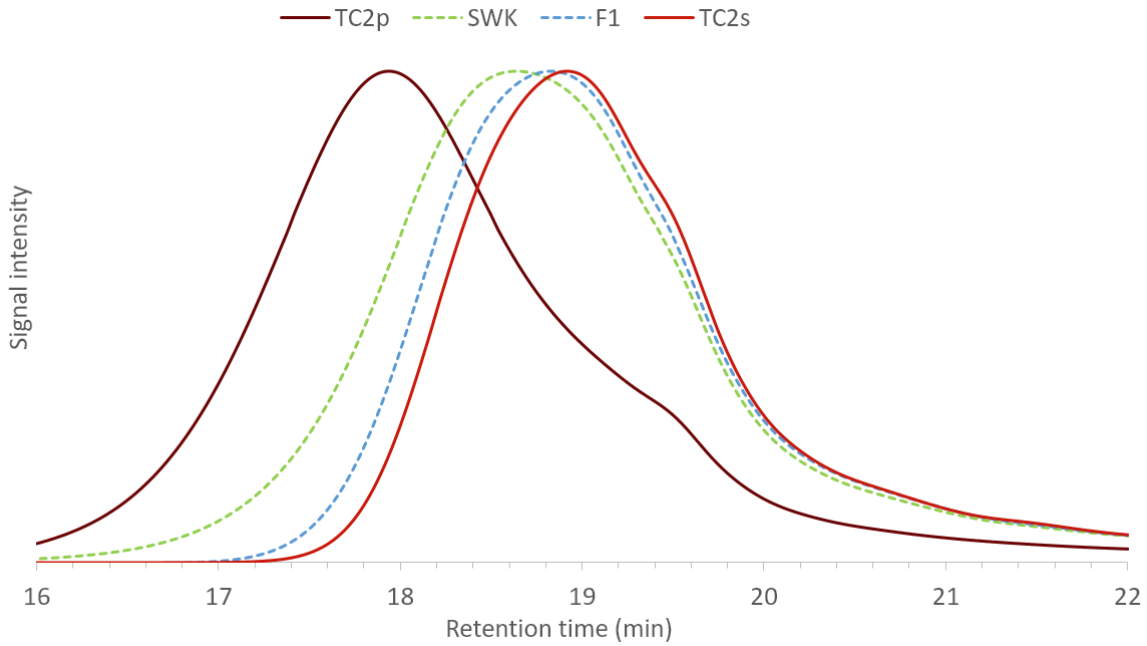

Figure 110 – SEC chromatograms for the starting lignin (SWK) and the thermally treated sample (TC2). (NB: TC2 was not completely soluble in the mobile phase)

changes in the structures seem to reduce the capability of lignin to positively interact with rubber, enhancing the mechanical properties of the lignin/natural rubber composite materials. Furthermore, also the protective effect of lignin seemed to be lowered by thermal conditionings, as highlighted by the reduced properties measured at high strains. On the basis of the peculiar thermal behavior of softwood Kraft lignin it is also possible to hypothesize that the thermally activated reactivity responsible for the self-condensation might also play a role in the improved performances of Kraft lignins (reported in chapter 6). In the previous chapter, the reinforcing behavior of Kraft lignins was tentatively explained as the consequence of many possible causes, among which the possibility to form chemical bonds with rubber through thiols and benzylic alcohols. With thermal conditioning, it was observed that after heating the capability of SWK lignin to interact with rubber is reduced. Hence, it was supposed that during the thermal treatments functionalities that can possibly react directly or through Sulphur with rubber, as thermally generated radicals or released formaldehyde, are cleaved or tent to react promoting self-condensation of lignin, and are not anymore available for rubber.

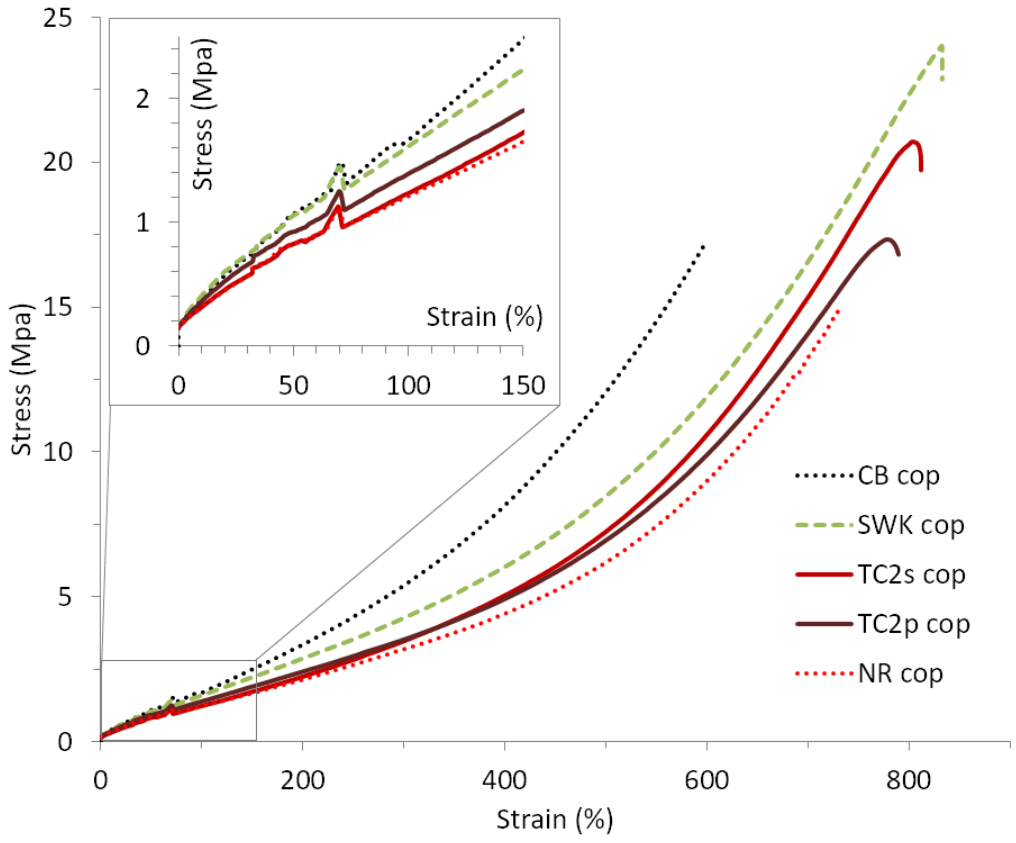

Figure 111 - Stress/strain curves obtained with tensile tests on dumbbell shaped specimens vulcanized for 30 minutes at 150 °C. Thermally treated lignins (TC2s and TC2p) vs references: CB, SWK lignin and Neat NR.

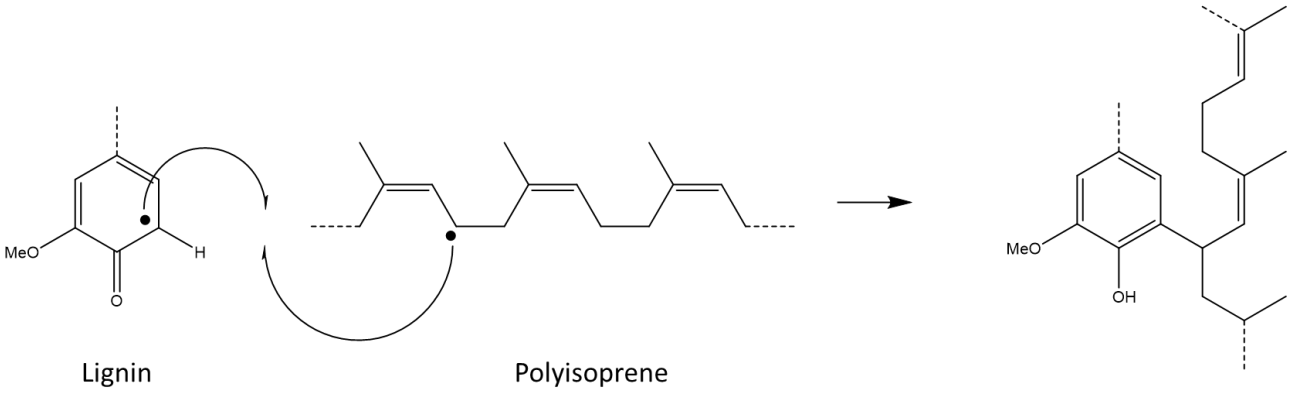

Figure 112 - Plausible reaction between lignin and natural rubber in presence of thermally generated free-radicals. (Adapted from reference)[18]

In a side experiment softwood Kraft lignin was heated in an oven at 170 °C, under vacuum. Small samples were withdrawn after different periods. The molecular weight distribution was analyzed on acetylated specimens with GPC. The results are reported in figure 113 and table 33. It is possible to see that at temperatures that are in the range typically used for vulcanization of rubber there is a substantial effect of condensation that dramatically affects the molecular weights of the starting softwood Kraft lignin.

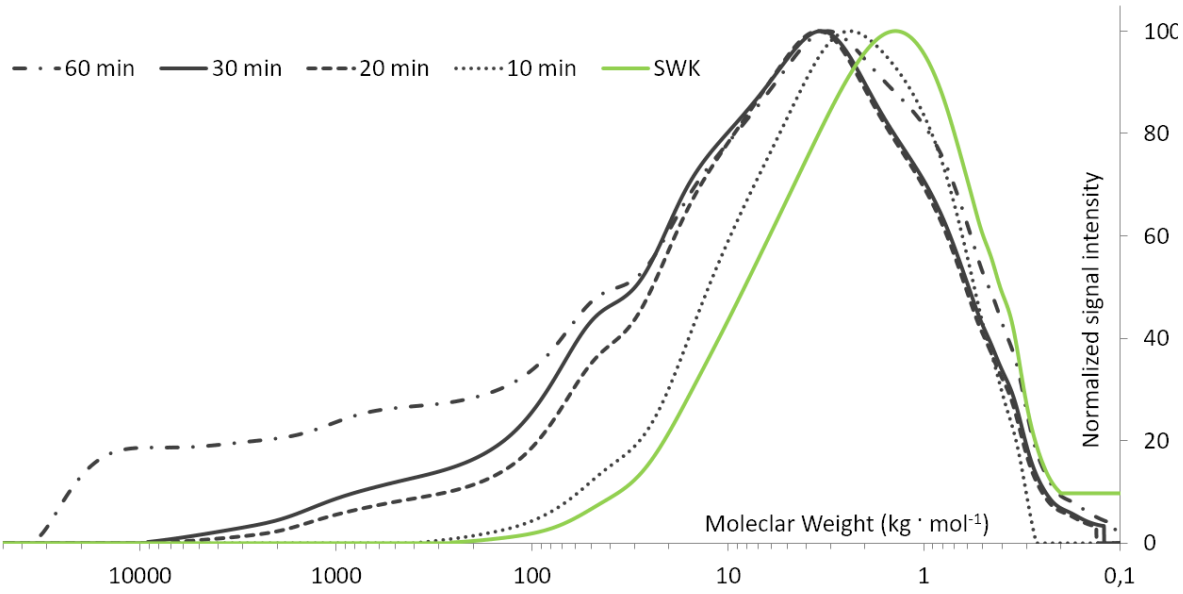

Figure 113 - Changes in the molecular weight distribution of SWK lignin with increasing heating periods. (from 10 to 60 minutes at 170 °C under vacuum)

	Mn	Mw	Mp	PDI	Mn	Mw
SWK	4 K	27 K	1450	6,0	n-fold increase	
10 min	7 K	45 K	2500	6,4	1,5	1,6
20 min	40 K	1,1 M	3500	29,4	9	43
30 min	63 K	1,8 M	3500	28,3	14	64
60 min	650 K	11 M	3500	18,5	138	429

Table 33 - Average molecular weights, polydispersity index and n-fold increase based on the starting (SWK) lignin.

8.5 Chemical modification

In the first two sections of this chapter, two strategies were tested to modify lignin and to improve the mechanical properties of lignin/natural rubber composite materials. It was found that a selected fraction of the biopolymer, characterized by a higher affinity towards organic solvents with medium polarity, was more easily dispersed and improved the mechanical properties of the rubber compounds also when directly blended in the mixer. On the contrary thermal conditioning was proven to promote self-condensation, probably trough a radical coupling mechanism. The properties of the composites were lowered when thermally conditioned lignins were used as a filler, possibly also because of a loss of reactivity in lignin. In this section the results of a third approach, that focused on several chemical modifications of lignin, are reported, and discussed. As considered in chapter 6, it was supposed that the main issue is related to the weak filler-rubber interactions that undermine the final mechanical properties of the composites. The poor affinity between lignin and rubber is supposed to limit the bonding of rubber and to hinder the dispersion of the lignin, which is also hampered by the strong intermolecular bonding that occur within the biopolymer. Regarding this aspect, it was demonstrated that when lignin is mixed with rubbers with increased polarity it is possible to obtain a better dispersions and consequently to produce composites with improved mechanical properties.[19] Chau and coworkers blended softwood lignin with copolymers of butadiene and acrylonitrile at different acrylonitrile contents (33% - 41% - 51%). Their results indicated that softwood lignin and NBR-33 were rather immiscible, whereas lignin and NBR-41 were more compatible, and the formation of a nearly miscible single-phase was observed with NBR-51. The increase in miscibility improved the dispersion of lignin and produced a significant increase in the stiffness of the composites. The behavior was rationalized analyzing the differences between the cohesive energy density or solubility parameter (δ) of lignin and the different rubbers. The solubility parameter of softwood lignin was assumed to be 24.6 $MPa^{1/2}$ from literature[20]. BR and SBR have δ values of 14.7–17.6 and 16.4–17.8 $MPa^{1/2}$ respectively, and formed highly immiscible polyblends with lignin. The dispersion of lignin improved with NBR-33 that has a δ in the range of 19.2–20.3 $MPa^{1/2}$. Even more polar rubbers like NBR-41 (δ = 21.0 $MPa^{1/2}$) and NBR-51 (δ = 21–23 $MPa^{1/2}$) had higher compatibility/miscibility with lignin and were found suitable to produce composites with greatly improved mechanical properties.[19] The results of the cited work indicated that when the difference between the solubility parameters of lignin and rubber ($\Delta\delta = \delta_{lignin} - \delta_{rubber}$) is greater than 7.5 $MPa^{1/2}$, as for lignin and butadiene rubber, the dispersion is poor and the resulting composite has limited mechanical properties. Further, it was observed that when $\Delta\delta$ approached ~4.5, as in the case of NBR-31, lignin was dispersed in smaller domains and the composite had improved characteristics. Finally, when $\Delta\delta$ fell in the 1.5 - 3.5 range, as with NBR-51, the dispersion was excellent, giving rise to superior properties. The differences between solubility parameters were also successfully used to explain the solubility of different lignin fraction obtained by selective extraction with green organic solvents.[3] Boeriu et al. demonstrated that the obtained fractions were characterized by a narrow molecular weight distribution and a defined functional group content

Figure 114 – Differences between cohesive energy density or solubility parameter (δt) for lignin and different rubbers.

resulting in different solubility parameters. Analyzing the solubility factor of the fractions in various solvent, it was found that solubility is a function of the difference between the average solubility parameter of lignins and the solubility parameter of each solvent tested (Δδ). The solubility was maximum when the difference between the solubility parameter of lignin was less than two ($-2 < \Delta\delta < +2$), whereas for most lignins the solubility was still appreciable (solubility index > 0.8) when the difference between the solubility parameters was lower than 4 ($-4 < \Delta\delta < +4$]). These considerations also help to better understand the good properties obtained with the fraction F1 (discussed in the first section of the chapter). It is probable that F1 had an average solubility parameter closer to that of the rubber than the starting lignin (SWK), justifying the improvements in compatibility, dispersion, and mechanical properties.

The solubility parameter of lignins is high, falling between 24.6 and 31.0 according to different references,[20–22] while the solubility parameter of natural rubber is lower, 17.5 – 18.2,[23,24] with a minimum Δδ of 7.1. The large gap in the solubility parameters explains why it is difficult to disperse lignin in natural rubber. To improve the compatibility between lignin and natural rubber, and consequently the dispersion of the filler and the adhesion of rubber, the Δδ must be decreased in the $\Delta\delta < 4$ range, or preferably in the $\Delta\delta < 2$ range. The functionalization of hydroxyl groups opens a wide range of possibilities for lignin modification.[25] In this work we chose to modify lignin via esterification. Esterification with anhydrides can be achieved easily and the solubility of lignin in nonpolar solvents can be optimized selecting carbon chains on the ester group of different lengths. Furthermore the reaction yields a low amount of waste products, can be performed also without solvent, at low temperatures and can be readily scaled up.[20] Recently esterification with different anhydrides was used to successfully improve the compatibility of lignin with different thermoplastics, as polyethylene (PE) and polylactic acid (PLA).[26,27] Five anhydrides were selected to study the effect of different side chains on the properties of modified-lignin/natural rubber composites. To complete the investigation lignin was also reacted with dimethyl carbonate, a green alternative for lignin methylation.[28] The strategies selected for the chemical modification of lignin are schematically summarized in figure 116. The Hansen Solubility Parameters (HSP) of lignin and modified lignins were predicted with the new group-contribution method for organic compounds developed by Stefanis and Panayiotou.[29,30] The results were used to evaluate

the changes in the compatibility of modified lignin with natural rubber and to rationalize the variations in the behavior of modified-lignin/natural rubber composites.

Experimental

Lignin esterification. The chemical modification was performed following the method proposed by Thielemans and Wool[20] with some marginal adjustments. 30 g of SWK lignin were dispersed in a 250 mL round bottom flask containing 90 mL of 1,4-Dioxane. 40 g of the corresponding anhydride were added to the solution and the air was purged with nitrogen. 0,6 mL of 1-methylimidazole (1MIM) were added after stabilizing the temperature at 50 °C and the reaction was carried on for 3 hours at the same temperature, applying vigorous magnetic stirring. The reaction was quenched in 500 mL of demineralized water, briefly stirred, and equally divided in 6 - 250 mL plastic bottles for centrifugation (10 min – 5000 rpm). After the first centrifugation, the clear supernatant was disposed and fresh demineralized water was added to re-

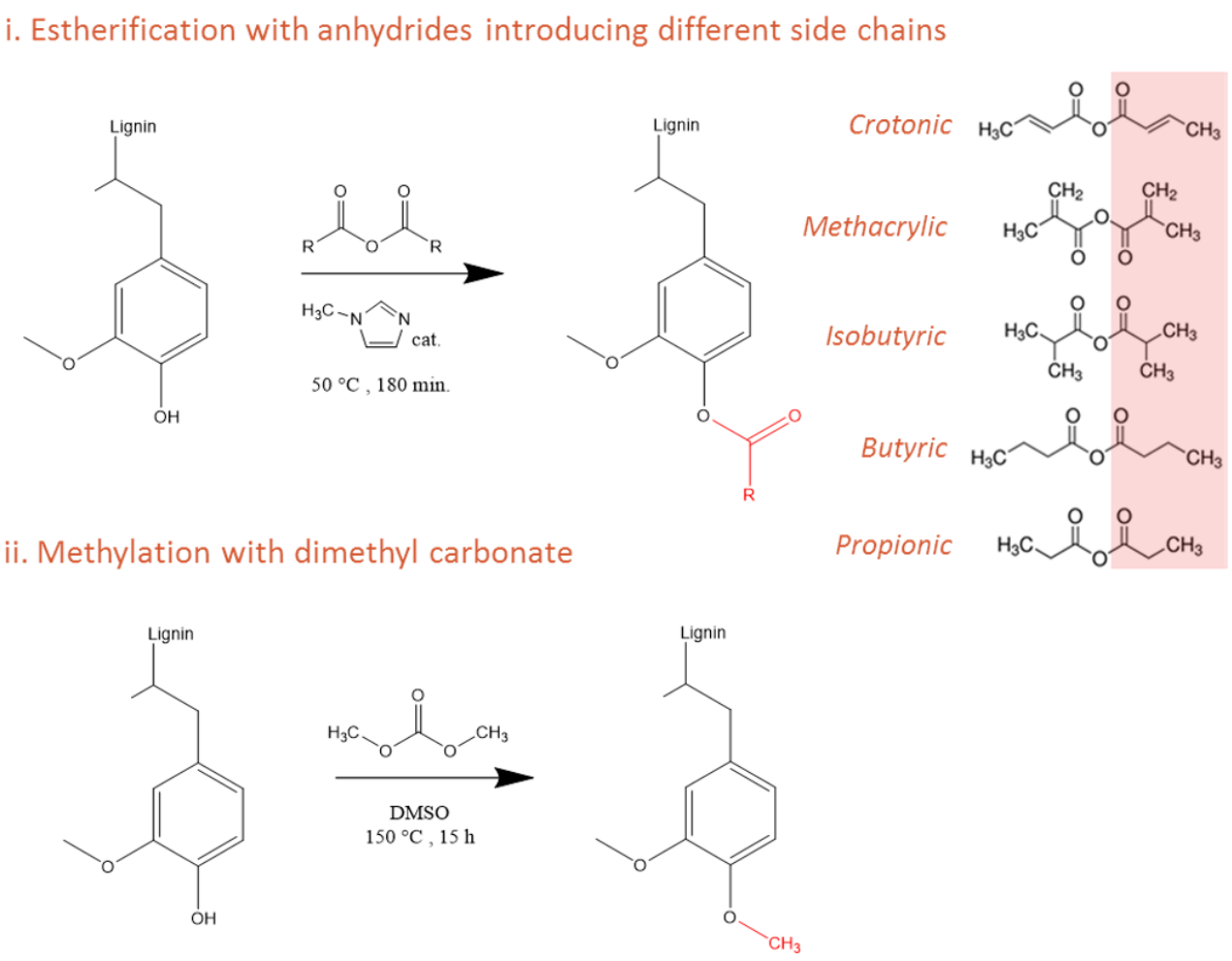

Figure 115 – Strategies selected for the chemical modification of lignin.

suspend the precipitate; then the dispersion was centrifuged again and finally the precipitate was transferred in several wide aluminium pans with the help of a small amount of acetone. The clear supernatant in excess was drained and the products were left to dry under the fume hood for several days, until constant weight.

Lignin methylation. The procedure was developed following the alternative method for lignin methylation optimized by Sen et al.[28] 30 g of SWK lignin were pre-dispersed into a 500 mL round bottom flask containing 200 mL of dimethyl sulfoxide (DMSO) and 9,6 g of NaOH (2 eq. to the phenolic hydroxyl group). 60 g of dimethyl carbonate (DMC, 2 eq.) were added and after few minutes of magnetic stirring the solution was transferred in a 600 mL parr reactor. The system, provided with mechanical stirring, was heated at 150 °C and the reaction was protracted for 15h. After the completion of the reaction, the sealed reactor was cooled to room temperature. The product was precipitated acidifying the solution with 2 N HCl and washed with a large excess of demineralized water to restore a neutral pH and remove salts and other impurities. Finally, the solids were transferred in several aluminium pan and air dried.

Products characterization. The solid products were investigated with FT-IR spectroscopy to assess the effectiveness of the modifications. Before the analysis, the samples were oven dried at 40 °C for few hours.

Rubber compounding. Modified lignins, vulcanizing agents, and antioxidants were added to natural rubber sir 20 and compounds using the Haake internal chamber mixer, with the formulations of table 37 and the procedure number 4 reported in chapter 4. All the compounds were prepared via dry-mixing.

Solubility Modeling. The Stefanis-Panayiotou model was used to predict the HSP of polyisoprene, lignin and chemically modified lignins. A brief description of the model and the method used to predict the individual solubility parameters are reported in chapter 4.

Results and discussion

The esterification was relatively easy to perform also on 30g scale. The reactions gave good overall yields even if with some differences between the various products. It must be noted that after the modification some lignins were easily separated from the supernatant, whereas other suffered minor material loss during the purification step since it was preferred to obtain purer substrates than maximizing the yield at all costs. However, the yield of the lignin modified with crotonic anhydride was significantly lower, far beyond what

	Start (g)	Theoretical (g)	Effective (g)	Yield (%)
Propionated	30	36,7	35,1	96
Butyrated	30	38,4	34,2	89
Isobutyrated	30	38,3	35	91
Crotonated	30	38,2	30,4	80
Methacrylated	30	38,3	37,6	98
Methylated	30	31,7	26,5	84

Table 34 - Yields of the reactions of esterification and methylation of SWK lignin.

can be justified by errors due to the operational procedures. The results are summarized in table 34, where it can also be noted that the yield of the methylation reaction was also somewhat lower. In both reactions, esterification and methylation, the reactants were in excess with respect to the stochiometric amount required to functionalize every hydroxyl groups of lignin, hence the biopolymer was supposed to be completely modified. However, esterification with crotonic was already reported to leave 25% of the aliphatic hydroxyls and 22% of phenolic hydroxyls unmodified, while in the same conditions butyric and isobutyric anhydrides were reported to give essentially complete modification.[26] Moreover, using the same conditions selected in this work it was reported that methylation with dimethyl carbonate successfully modified 91% of the phenolic hydroxyls and 60% of the aliphatics.[28] In the present study, the outcome of the modifications was assessed via IR spectroscopy. Between 3200 and 3600 cm^{-1} it is possible to see how the peak typically associated to the stretching of the different hydroxyl groups disappears in the samples modified with propionic, butyric and isobutyric anhydrides, indicating that modification was virtually complete. A residual number of hydroxyl functionalities is clearly observable in methylated and crotonated lignins, in agreement with the observations already made by other researchers, just outlined above. A lesser absorption is also detectable in the methacrylated sample, despite the high yield. At lower wavenumbers, 2800-3000 cm^{-1}, the CH stretching of methyl and methylene groups dominates the spectra. In the esterified specimens, the intensity of these bands increases with chain length and chain saturation. In the methylated specimen, the same trend is detectable confirming the effectiveness of the methoxylation, as highlighted by the higher intensity of the peak at 2830 cm^{-1} ascribed to the stretching of the methoxy group. Between 1700 and 1800 cm^{-1} esterified lignins display strong peaks attributed to the stretching of conjugated and unconjugated

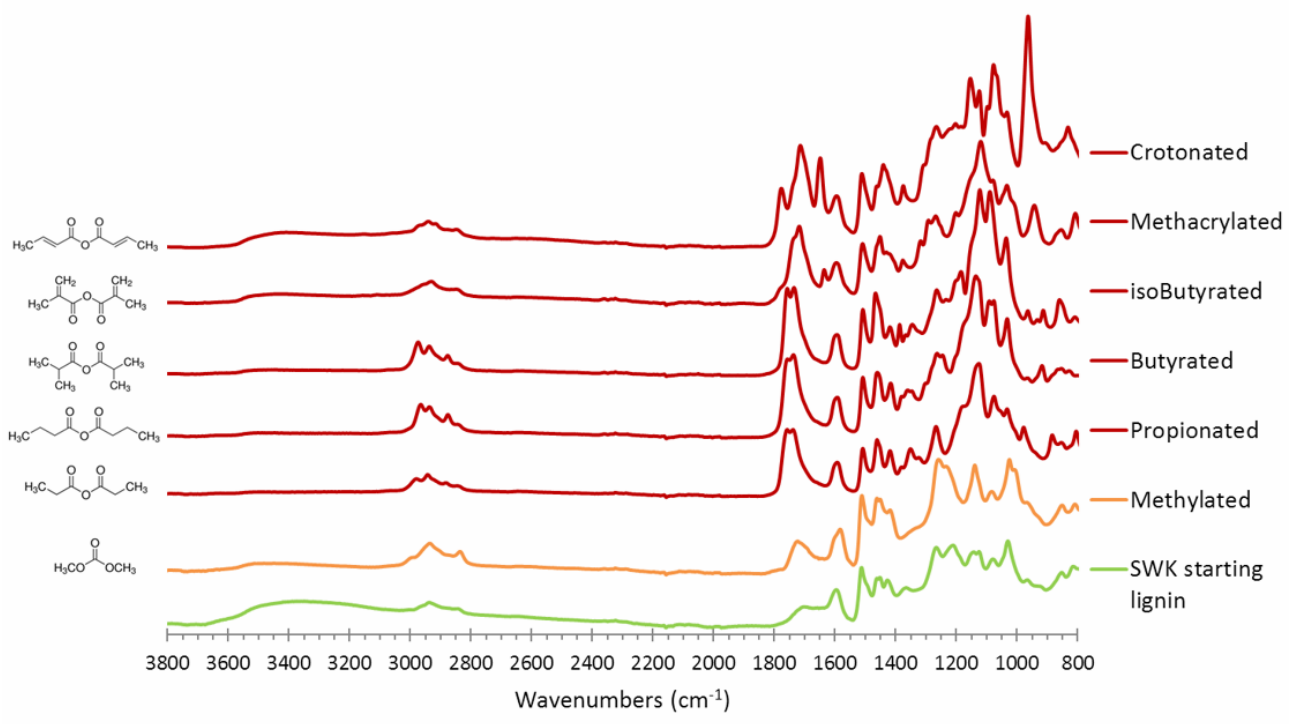

Figure 116 - Overlaid FT-IR spectra of starting SWK lignin and chemically modified lignins.

Figure 117 – Modified lignins after drying. From top left to bottom right: crotonated, methylated, methacrylated, isobutyrated, butyrated and propionated.

carbonyl groups. A minor increase in the absorbance in this region was also detected for the methylated lignin. This might be associated with a moderate degradation of the substrate, as already observed in the thermal conditioning of lignin (TC2s), that could be promoted by the higher temperature needed by the reaction (150 °C). For crotonated and methacrylated lignins a new peak appeared at ~1650 cm^{-1} identifying the presence of the C=C double bond. In the crotonated sample also a strong peak at 960 cm^{-1} highlights the presence of the alkene (CH out of plane deformation for a trans alkene). Finally, increased absorption was detected in the 1000-1200 cm^{-1} region, in agreement with the formation of the ester bonds. In figure 118 it is possible to observe that the modified lignins were also characterized by different colors.

In table 35, are summarized the predictions for the solubility parameters of natural rubber (polyisoprene), starting lignin (SWK) and chemically modified lignins. The predictions for the total (Hildebrand) solubility parameters were found to be in good agreement with the values obtained by Thielemans and Wool using the Hoy model (e.g. propionated 22.1, butyrated 21.9, methacrylated 21.8).[20] What it is possible to observe

	δ_d	δ_p	δ_h	δ_{Total}	$\Delta\delta_{Total}$	R_o	R_a	RED
Polyisoprene	15,7	4,2	5,2	17,1		7,3[24]		
SWK Lignin	19,4	8,1	14,5	25,6	8,5		12,5	1,72
SWK Propionated	18,4	8,9	6,0	21,3	4,2		7,2	0,98
SWK Butyrated	18,4	8,5	5,6	20,8	3,7		6,9	0,95
SWK Isobutyrated	18,1	8,0	5,3	20,5	3,4		6,0	0,82
SWK Crotonated	18,7	8,6	6,4	21,5	4,4		7,4	1,01
SWK Methacrylated	18,2	8,1	5,6	20,7	3,6		6,2	0,85
SWK Methylated	18,6	7,1	6,3	20,9	3,8		6,6	0,90

Table 35 - Hansen solubility parameters (δ_d, δ_p, δ_h) $MPa^{1/2}$, total or Hildebrand solubility parameter (δ_T) $MPa^{1/2}$, interaction radius (R_0), HSP distance (R_a) and relative energy difference (RED = R_a/R_o) for polyisoprene, starting lignin and modified lignins.

is the reduction of the total solubility parameter (δ_{Total}) that became closer to that of rubber for all modifications. The difference between the solubility parameters of the modified lignins and rubber ($\Delta\delta_{Total}$) was roughly halved for all the modified specimens, decreasing in the order: crotonated > propionated > methylated > butyrated > methacrylated > isobutyrated. More insight can be obtained from the Hansen solubility parameters (HSP) where δ_{Total} is split into dispersion (δ_d), polar (δ_p) and hydrogen bonding (δ_h) terms. The greater contribution derived from the hydrogen bonding term that was reduced with all modifications. A smaller contribution came from the dispersion term, while the polar parameter was slightly affected only in the case of methylation. The predicted parameters are in good agreement with the results qualitatively expected from the functionalization. Two graphical representations of the Hansen solubility parameter are proposed in figure 119 and 120 (made with freeware app).[31] In figure 119, it is possible to observe that, in the Hansen space, modified lignins are closer to polyisoprene than the original lignin, qualitatively indicating increased affinity. The quantification of the HSP distances (R_a) are summarized in table 35, their ratio with the solubility radius of polyisoprene (R_0) determines the relative energy difference (RED = Ra/Ro).

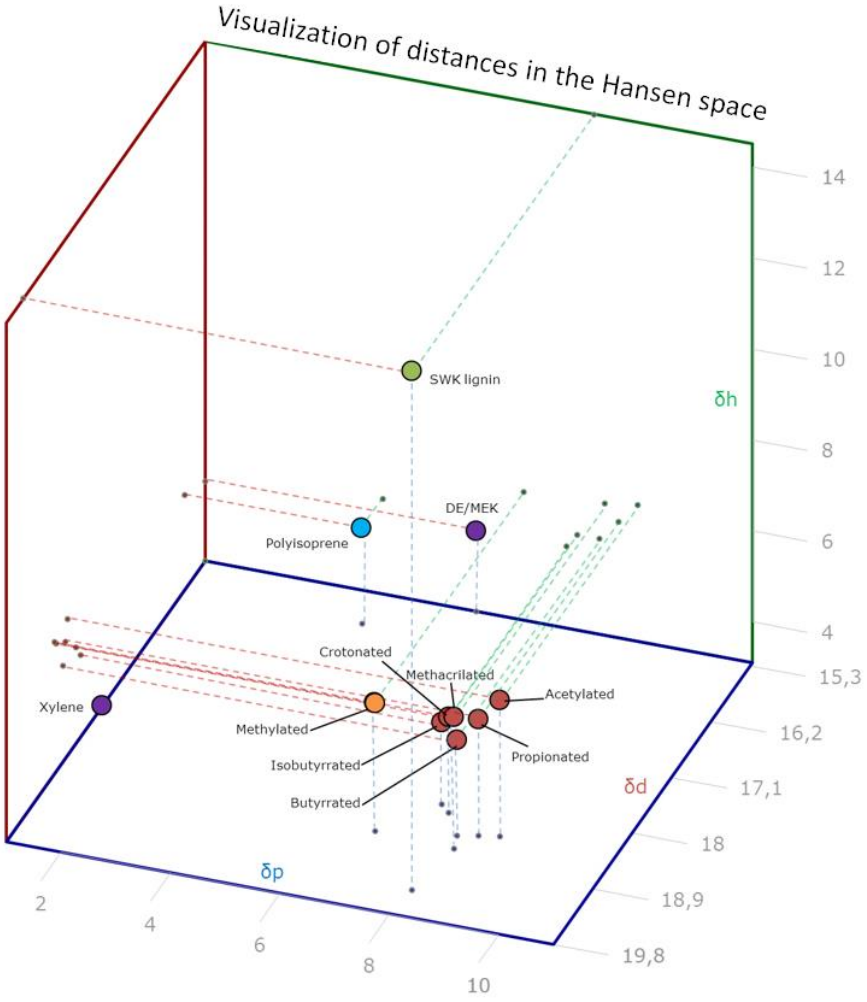

Figure 118 – Representation of the Hansen space positions for starting lignin (SWK), modified lignins and polyisoprene. (Xylene, DE/MEK 1:1 solution and acetylated lignin are also presented as additional references)

If the RED > 1 the two substances don't mix, if RED < 1 the two substances are miscible, when RED = 1 there is partial miscibility. R_0 is measured empirically evaluating the solubility of the substance in different solvents.[24] According to the predicted HSP, the starting lignin is clearly not miscible with polyisoprene and the prediction matches well with the empirical evidence. On the contrary, all modified lignins were at least partially miscible with polyisoprene, with the compatibility increasing in the order: crotonated < propionated < butyrated < methylated < methacrylated < isobutyrated. Another perspective is given by the triangular graph (figure 120). In these graphs, the position of a substance is defined by the contribution of the three components (δ_d, δ_p and δ_h) to the total intermolecular bonding. Substances of the same class are close and the position shift towards the bottom-right corner as the molecular weight increases (as shown in the smaller graph).[32] The starting lignin is positioned in the region between alcohols and esters, while polyisoprene sits among long chained esters and hydrocarbons. Modified lignins are positioned much closer to polyisoprene, displaying a greater affinity. In this perspective methylation seemed to be more promising than the esterifications, displaying a higher possibility to fall in the solubility range of polyisoprene (solubility range must be determined empirically, in the plot it is only qualitatively represented by the dotted circles). To quickly evaluate the results obtained from the modelling, small samples of unmodified and chemically

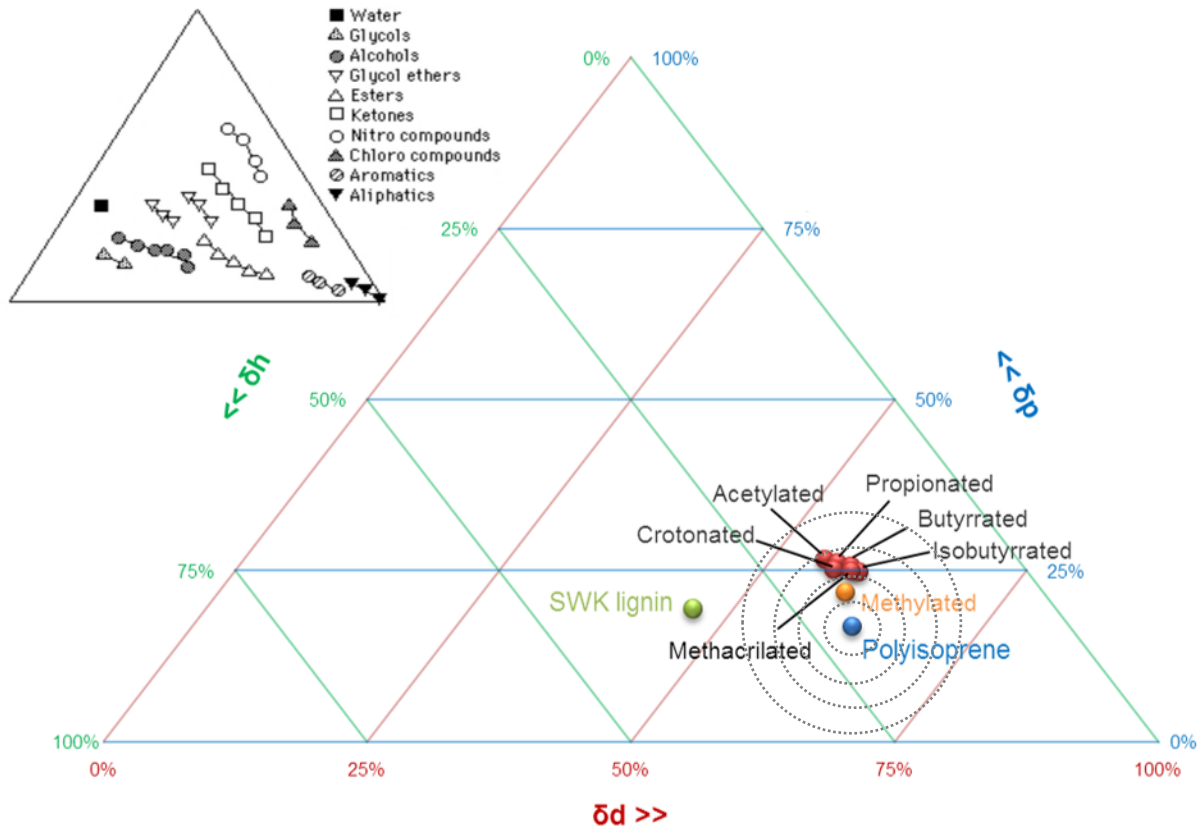

Figure 119 – Triangular graph visualizing the contributions of the dispersive, polar and hydrogen bonding interactions to the total solubility parameter. The sum of the three coordinates is always 100%. (acetylated lignin was not featured in this work)

modified lignins were dispersed in a 1:1 solution of diethyl ether and methyl ethyl ketone (DE/MEK), as well as in xylene. The solvents were selected among the available ones to approximatively represent rubber (the calculated total solubility parameters (δ_{Total}) for the solvents are: DE 15,8 / MEK 19,0 / Xylene 19,1). The starting lignin was almost completely insoluble in the DE/MEK solution, on the contrary, propionated, butyrated and isobutyrated lignins were completely solubilized, confirming the enhancement of compatibility with less-polar systems. Methylated lignin dissolved rapidly in the same solvent, but left an insoluble sediment, maybe a warning light indicating a partial condensation. The esterified lignins bearing an unsaturated side chain (crotonated and methacrylated) were only partially soluble in MEK, however were almost completely soluble in xylene, displaying better compatibility with the aromatic solvent. This quick test demonstrated the effective improvements in the solubility of modified lignins, but also highlighted that among the products there are important differences.

	DE/MEK	Xylene
SWK lignin	Mostly insoluble	n/a
Propionated	Complete	n/a
Butyrated	Complete	n/a
IsoButyrated	Complete	n/a
Crotonated	Partial	Almost complete
Methacrylated	Partial	Almost complete
Methylated	Mostly soluble	n/a

Table 36 – qualitative solubility of the modified lignins in different solvents evaluated by visual inspection.

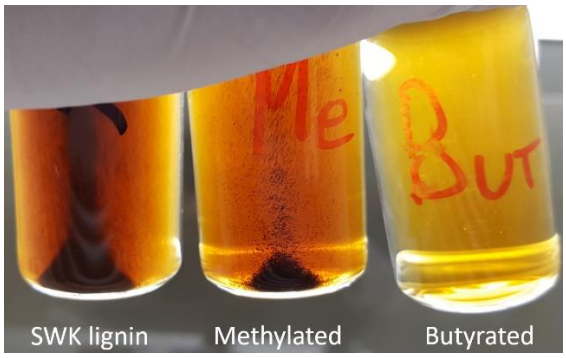

Figure 120 – Solubility of three samples in a 1:1 solution of methyl ethyl ketone and diethyl ether.

Eventually, the modified products were used as tentative fillers in model compounds prepared with natural rubber via dry-mixing, to assess the impact of the modified structures on the mechanical properties of the elastomeric composites. Despite most of the hydroxyl groups were covered with other functionalities, lignins still interfered with the curing mechanism as clearly highlighted in the vulcanization curves (figure 122). Two behaviors were detected, partially rationalizable according to the different chemical structures. Crotonic, methacrylic and methylated lignins delayed the beginning of the crosslinking comparably to SWK lignin. Propionated, butyrated and isobutyrated, affected vulcanization in a different way, producing a longer delay. The differences in curing seemed to clearly correlate to the structure of the side chains introduced on lignin, however it was difficult to understand the underlying mechanism. In fact, the Sulphur vulcanization process is rather complex and the fillers probably interact with more than one component of the system. It was also

	Neat	CB	SWK	SWK modified
Natural Rubber (SIR20)	100	100	100	100
SWK (unmodified)	0	0	15	0
SWK chemically modified	0	0	0	15
Carbon Black (N375)	0	15	0	0
Soluble sulfur	2	2	2	2
Zinc Oxide	5	5	5	5
Stearic acid	2	2	2	2
Accelerator (CBS)	2	2	2	2
Antioxidant 1 (6PPD)	1	1	1	1
Antioxidant 2 (TMQ)	1	1	1	1
Total PHR	113	128	128	128

Table 37 - Formulations in PHR for the rubber compounds under investigation. SWK modified stands for all the modified lignins: propionated, butyrated, isobutyrated, crotonated, methacrylated and methylated.

observed that the rubber compound filled with the unmodified lignin reached early the maximum torque and successively suffered reversion. The rehograms of the compounds filled with the modified lignins, on the contrary, never reached a maximum or the equilibrium, but were characterized by a marching modulus.

The mechanical properties of the rubber compounds, assessed through tensile tests, were also affected by the different modifications. In general, all the modified fillers reinforced natural rubber, producing stiffer

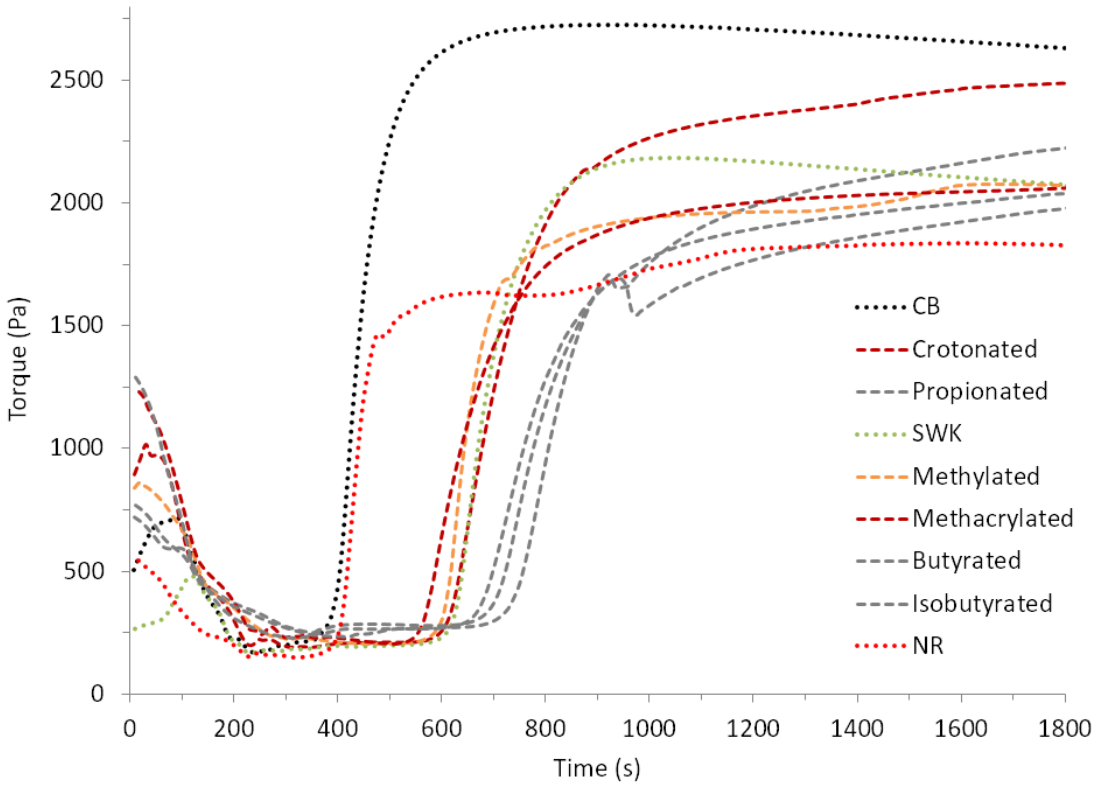

Figure 121 – Vulcanization curves 150 °C / 30 minutes.

materials. Hence, it was supposed that the increased miscibility with rubber and the reduction of the hydrogen networking between lignin molecules granted a better dispersion of the fillers in the rubbery matrix and improved the adhesion at the interfaces. However, it was not possible to find an absolute correlation between reinforcement and the miscibility predicted with the solubility parameters. It is also worth noticing that the ultimate properties, that were enhanced by the unmodified lignin and its fractions, were not particularly influenced by the functionalized biopolymers. The improvement of the properties at high elongations was previously correlated with the protective effect of lignin, exerted by its antioxidant properties which are in turn affected by the concentration of the sterically hindered phenolic hydroxyls. The

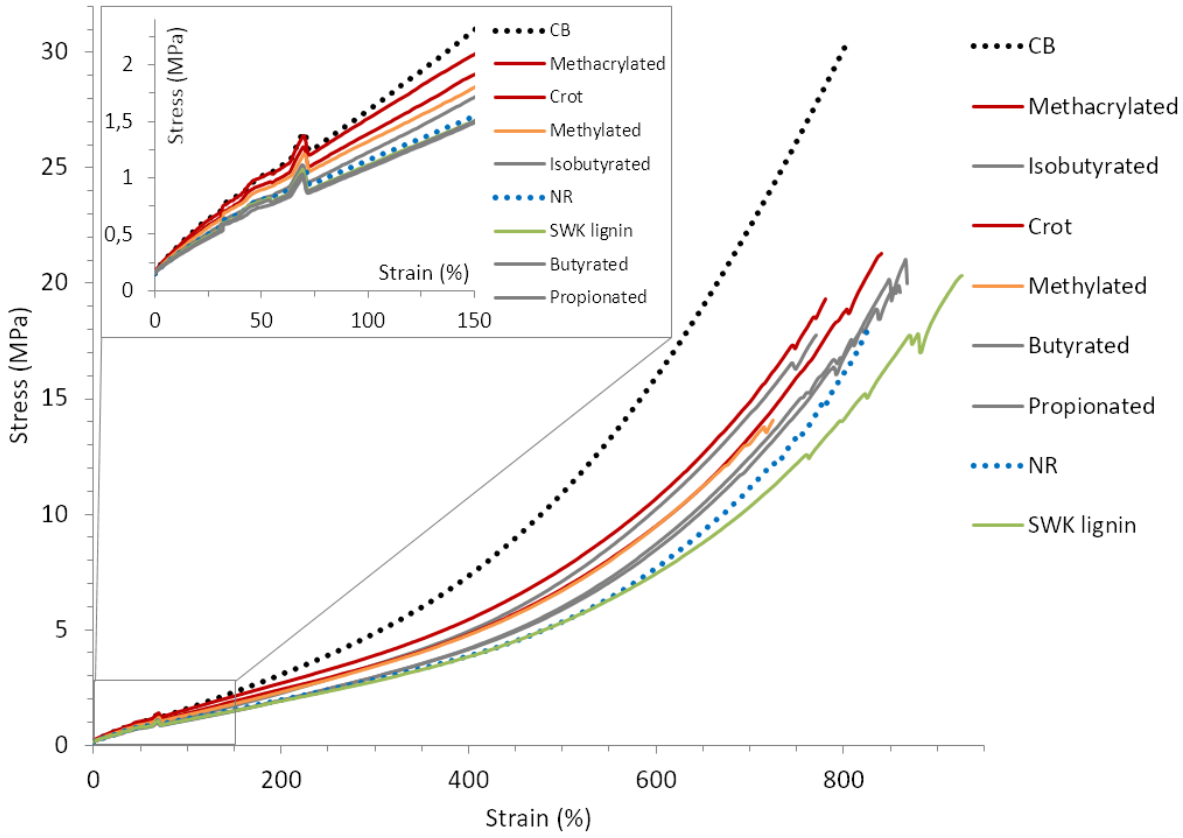

Figure 122 – Stress-strain curves measured on dumbbell shaped specimens.

	NR	CB	SWK	Prop	But	Isobut	Crot	Metha	Methyl
50 (%)	0,80	1,02	0,79	0,78	0,73	0,81	0,94	1,00	0,89
100 (%)	1,16	1,60	1,12	1,10	1,08	1,22	1,40	1,53	1,32
300 (%)	2,85	4,87	2,79	2,96	2,97	3,49	3,47	3,87	3,42
700 (%)	11,21	22,48	10,37	12,07	12,50	14,34	13,43	14,87	13,05
UTS (Mpa)	18,17	30,28	20,33	19,60	19,99	18,11	21,28	19,34	14,06
UE (%)	828	801	926	860	868	789	840	781	725

Figure 123 - Numerical values relative to the tensile tests - Stress at progressive elongations, Ultimate Tensile Strength (UTS), and Ultimate Elongation (UE).

fact that when the phenolic moieties were masked through chemical modification the mechanical properties at break were no longer significantly enhanced represented an additional indirect evidence of the active effect of the functional groups and its relation with such properties. Finally, it was possible to rationalize the behavior in relation to the molecular structure of the materials when the possible effects of vulcanization were considered. In fact, when the compatibility of the various fillers predicted with the solubility parameters was compared with the reinforcing effect, quantified as the increase in stiffness at 300% elongation, it was possible to envisage a certain relationship. However, the methacrylated and the crotonated samples conferred higher reinforcement than expected, whereas the effect of the other modified lignins seemed to be directly correlated with the predictions of miscibility. From the observed behavior, schematically summarized in table 38, it was possible to hypothesize that the presence of the unsaturated bonds on the side chains of the methacrylated and the crotonated lignins activated the fillers during vulcanization, promoting chemisorption and enhancing the adhesion between the polymer matrix and the fillers' particles.

Compatibility	Isobut	Metha	Methyl	But	Prop	Croton	SWK
(RED)	0,82	0,85	0,90	0,95	0,98	1,01	1,72
Reinforcement	Metha	Isobut	Croton	Methyl	But	Prop	SWK
(Stress at 300%)	3,87	3,49	3,47	3,42	2,97	2,96	2,79

Table 38 – Fillers ranked per the predicted compatibility (top) and the reinforcing capability (bottom).

8.6 Conclusions

Three main strategies were explored with the intent to improve the mechanical properties of lignin/natural rubber composite elastomeric materials. The main cause of the limited reinforcing capability of the unmodified lignin was accounted to the non-optimal compatibility with the rubbery matrix and the resulting inadequate dispersion and large particle size. The first approach focused on fractionation through successive extractions with organic solvents. It was demonstrated that the smaller, purer, and probably more hydrophobic fraction (F1) can improve the properties of natural rubber also when mechanically mixed. The enhanced performances possibly arose from the combined effect of the higher compatibility and the increased protective potential. Thermal conditioning treatments hindered the applicability of lignin, however the results helped to strengthen the comprehension of the reinforcing mechanism of softwood Kraft lignin and to expose the sources of potential issues that could limit the exploitation of lignin in rubber compounds. Finally, chemical modifications demonstrated that it is possible to tune lignin's behavior in natural rubber by rationally modifying its chemical structure. The solubility of modified lignins was modelled using the solubility parameters, which offered a powerful tool to better understand the interaction

with rubber and the resulting macroscopic properties. The reinforcing potential of the modified lignins was linked to the miscibility with rubber and to the presence of functionalities that are active during vulcanization, hence to the improvements in the physio- and chemi-sorption of rubber. All in all, two of the three approaches were successful in producing modified lignins that offered significant improvements to the mechanical properties of the composites, with the great advantage brought by the possibility to bypass coprecipitation. The experimental fillers didn't match the effectiveness of the commercial reference (carbon black N375). However, based on the results of the present work it will be possible to envisage improved strategies to further enhance the desired properties.

References

(1) Cui, C.; Sun, R.; Argyropoulos, D. S. Fractional Precipitation of Softwood Kraft Lignin: Isolation of Narrow Fractions Common to a Variety of Lignins. *ACS Sustain. Chem. Eng.* **2014**, *2* (4), 959–968.

(2) Toledano, A.; Serrano, L.; Garcia, A.; Mondragon, I.; Labidi, J. Comparative study of lignin fractionation by ultrafiltration and selective precipitation. *Chem. Eng. J.* **2010**, *157* (1), 93–99.

(3) Boeriu, C. G.; Fiţigău, F. I.; Gosselink, R. J. A.; Frissen, A. E.; Stoutjesdijk, J.; Peter, F. Fractionation of five technical lignins by selective extraction in green solvents and characterisation of isolated fractions. *Ind. Crops Prod.* **2014**, *62*, 481–490.

(4) Leskinen, T.; Kelley, S. S.; Argyropoulos, D. S. Refining of Ethanol Biorefinery Residues to Isolate Value Added Lignins. *ACS Sustain. Chem. Eng.* **2015**, *3* (7), 1632–1641.

(5) García, A.; Toledano, A.; Serrano, L.; Egüés, I.; González, M.; Marín, F.; Labidi, J. Characterization of lignins obtained by selective precipitation. *Sep. Purif. Technol.* **2009**, *68* (2), 193–198.

(6) Toledano, A.; García, A.; Mondragon, I.; Labidi, J. Lignin separation and fractionation by ultrafiltration. *Sep. Purif. Technol.* **2010**, *71* (1), 38–43.

(7) Arshanitsa, A.; Ponomarenko, J.; Dizhbite, T.; Andersone, A.; Gosselink, R. J. A.; van der Putten, J.; Lauberts, M.; Telysheva, G. Fractionation of technical lignins as a tool for improvement of their antioxidant properties. *J. Anal. Appl. Pyrolysis* **2013**, *103*, 78–85.

(8) Gosselink, R. J. A.; van Dam, J. E. G.; de Jong, E.; Scott, E. L.; Sanders, J. P. M.; Li, J.; Gellerstedt, G. Fractionation, analysis, and PCA modeling of properties of four technical lignins for prediction of their application potential in binders. *Holzforschung* **2010**, *64* (2), 193–200.

(9) Coran, A. Y. Chemistry of the vulcanization and protection of elastomers: A review of the achievements. *J. Appl. Polym. Sci.* **2003**, *87* (1 SPEC.), 24–30.

(10) Kim, J.-Y.; Hwang, H.; Oh, S.; Kim, Y.-S.; Kim, U.-J.; Choi, J. W. Investigation of structural modification and thermal characteristics of lignin after heat treatment. *Int. J. Biol. Macromol.* **2014**, *66*, 57–65.

(11) Brodin, I.; Sjöholm, E.; Gellerstedt, G. The behavior of kraft lignin during thermal treatment. *J. Anal. Appl. Pyrolysis* **2010**, *87* (1), 70–77.

(12) Miller, J. .; Evans, L.; Littlewolf, A.; Trudell, D. . *Batch microreactor studies of lignin and lignin model compound depolymerization by bases in alcohol solvents*; 1999; Vol. 78.

(13) Roberts, V. M.; Stein, V.; Reiner, T.; Lemonidou , A.; Li, X.; Lercher, J. A. Towards Quantitative Catalytic Lignin Depolymerization. *Chem. - A Eur. J.* **2011**, *17* (21), 5939–5948.

(14) Pandey, M. P.; Kim, C. S. Lignin Depolymerization and Conversion: A Review of Thermochemical Methods. *Chem. Eng. Technol.* **2011**, *34* (1), 29–41.

(15) Gosselink, R. J. A.; Teunissen, W.; van Dam, J. E. G.; de Jong, E.; Gellerstedt, G.; Scott, E. L.; Sanders, J. P. M. *Lignin depolymerisation in supercritical carbon dioxide/acetone/water fluid for the production of aromatic chemicals*; 2012; Vol. 106.

(16) Cui, C.; Sadeghifar, H.; Sen, S.; Argyropoulos, D. S. Toward Thermoplastic Lignin Polymers; Part II: Thermal & Polymer Characteristics of Kraft Lignin & Derivatives. *BioResources* **2013**, *8* (1), 864–886.

(17) Fierro, V.; Torné-Fernández, V.; Celzard, A. Kraft lignin as a precursor for microporous activated carbons prepared by impregnation with ortho-phosphoric acid: Synthesis and textural characterisation. *Microporous Mesoporous Mater.* **2006**, *92* (1), 243–250.

(18) Bova, T.; Tran, C. D.; Balakshin, M. Y.; Chen, J.; Capanema, E. A.; Naskar, A. K. An approach towards tailoring interfacial structures and properties of multiphase renewable thermoplastics from lignin–nitrile rubber. *Green Chem.* **2016**, *18* (20), 5423–5437.

(19) Tran, C. D.; Chen, J.; Keum, J. K.; Naskar, A. K. A New Class of Renewable Thermoplastics with Extraordinary Performance from Nanostructured Lignin-Elastomers. *Adv. Funct. Mater.* **2016**, *26* (16), 2677–2685.

(20) and, W. T.; Wool*, R. P. Lignin Esters for Use in Unsaturated Thermosets: Lignin Modification and Solubility Modeling. **2005**.

(21) Hansen, C. M. M.; Björkman, a.; Bjorkman, A. The Ultrastructure of Wood from a Solubility Parameter Point of View. *Holzforschung* **1998**, *52* (4), 335–344.

(22) Hansen, C. M. Polymer additives and solubility parameters. *Prog. Org. Coatings* **2004**, *51* (2), 109–112.

(23) Zellers, E. T.; Anna, D. H.; Sulewski, R.; Wei, X. Improved methods for the determination of Hansen's solubility parameters and the estimation of solvent uptake for lightly crosslinked polymers. *J. Appl. Polym. Sci.* **1996**, *62* (12), 2081–2096.

(24) Hansen, C. M. *Hansen Solubility Parameters: A User's Handbook*, Second.; Group, T. & F., Ed.; 2000.

(25) Laurichesse, S.; Avérous, L. Chemical modification of lignins: Towards biobased polymers. *Prog. Polym. Sci.* **2014**, *39* (7), 1266–1290.

(26) Vila, C.; Santos, V.; Saake, B.; Parajó, J. C. Manufacture, Characterization, and Properties of Poly-(lactic acid) and its Blends with Esterified Pine Lignin. *BioResources* **2016**, *11* (2), 5322–5332.

(27) Dehne, L.; Vila Babarro, C.; Saake, B.; Schwarz, K. U. Influence of lignin source and esterification on properties of lignin-polyethylene blends. *Ind. Crops Prod.* **2016**, *86*, 320–328.

(28) Sen, S.; Patil, S.; Argyropoulos, D. S. Methylation of softwood kraft lignin with dimethyl carbonate. *Green Chem.* **2015**, *17*, 1077–1087.

(29) Stefanis, E.; Panayiotou, C. Prediction of hansen solubility parameters with a new group-contribution method. *Int. J. Thermophys.* **2008**, *29* (2), 568–585.

(30) Stefanis, E.; Panayiotou, C. A new expanded solubility parameter approach. *Int. J. Pharm.* **2012**, *426* (1–2), 29–43.

(31) fernando cinquegrani, pagine personali, office http://www.prodomosua.it/ppage02.html (accessed Jan 7, 2017).

(32) Burke, J. Solubility Parameters: Theory and Application. **1984**.

CHAPTER 9 - Conclusive remarks

The research activity dealt with the development of greener elastomeric materials for tyre manufacturing. The objective was to produce alternative materials from renewable resources to substitute the fossil counterparts that are still extensively used despite the growing concern regarding their impact on the environment and future sustainability. The possibility to produce different materials from lignocellulosic biomasses was explored. Two agricultural by-products, rice husk and *Arundo donax* were selected as sources of raw materials, representing the typical example of abundant and low-cost biomass. The first challenge, in the valorization of the lignocellulosic biomasses is the separation of the main fraction that constitute the materials: cellulose, lignin, hemicellulose, extractive and inorganics. The separation process must be sustainable from the economic and environmental point of view, and at the same time it must effectively fractionate the biomass, possibly delivering high yields of pure materials. The biorefinery process proposed in this work was relatively simple, was characterized by rather mild conditions and was based on inexpensive technologies. At the same time, the lignocellulosics were effectively fractionated, yielding several different products characterized by a high purity and with reasonable overall yields. Among the products, nanocrystalline cellulose, silica and lignin were tested in elastomeric model compounds based on natural rubber. Silica and cellulose nanocrystals could be used in many application, they possess a high potential and in prospective they could be easily converted into a high-added value. Lignin, on the other hand, is often considered a by-product, since due to the intrinsic characteristics it is difficult to convert the biopolymer in high-added value products. At the same time, the valorization of lignin often plays a crucial role in the feasibility of a biorefinery process; transforming lignin into a valuable product could greatly impact the remunerability of the process, making it economically viable. In this scenario, the focus shifted on lignin, and different approaches were followed to find suitable applications in elastomeric materials for tyres. Lignin was used in combination with silica, generating a new organic/inorganic filler, exclusively produced from renewable resources through an integrated process, possibly capable to introduce different desirable characteristics in the elastomeric composites. The ligno-siliceous biofiller improved the properties of natural rubber, effectively reinforcing the compounds. However, in absolute terms the mechanical properties were not yet in line with those of the traditional reinforcing fillers, in this case represented by commercial silica (VN3). The behavior was connected to specific morphological features of the material, and it was supposed that with a finer tuning of the several parameters that influence the formation process, the lignin-silica

material (LSM) could be further improved. The potential of lignin as a stand-alone component was also additionally explored investigating the relationships between lignin molecular structure and the properties of its composites with natural rubber. It was discovered that the structure of lignin, which can greatly differ among various botanical sources and is altered by the diverse extractive processes, exerts a strong influence on the properties of natural rubber compounds. Certain lignins, characterized by specific structural features, demonstrated a much higher antioxidant capability and were particularly effective in protecting natural rubber from the thermo-oxidative stresses. The thermal stabilization mechanism was rationalized correlating the effectiveness of lignin to the concentration of the active antioxidant species (i.e. hindered phenolic functionalities) and their ability to migrate through the polymeric matrix, which is inversely proportional to the molecular weight. It was also found that Kraft lignins are more effective as reinforcing fillers and several hypotheses were proposed to explain the behavior in relation to the molecular features. Thanks to the information gathered on the thermal/mechanical behavior of different lignins in model compounds it was possible to successfully employ a specific lignin in a technical formulation, partially replacing carbon black, demonstrating the possibility to use the cheap and abundant technical lignins in high-tech applications when their peculiar characteristics are properly exploited. However, the compatibility between lignin and rubber is not optimal and thus lignin must be introduced through special techniques into the rubber to achieve a good dispersion (coprecipitation) and the reinforcement is still limited. Different strategies were explored to assess the possibility to reduce the hydrophilicity of lignin and improve processability and reinforcement. The first approach aimed to fractionate lignin. Through successive extractions with organic solvents, a technical lignin was separated into three fractions that were characterized by different molecular weight distributions and distinct concentrations of the functional groups. The smaller, purer, and more hydrophobic fraction (F1) was found to additionally improve the properties of natural rubber and was effective also when mechanically blended with rubber. The second approach, based on thermal treatments, didn't produce any practical advantage, however, the results provided several hints that could help to better understand the reinforcing mechanism of softwood Kraft lignin and to expose potential issues that could arise during processing. At last, lignin was chemically modified, masking the hydroxyl groups with different substituents. The solubility of the modified lignins was predicted using the solubility parameters. The results offered a powerful tool to rationalize the behavior of lignin based on the miscibility with rubber. The capability of lignin to reinforce rubber was found to be determined by two factors: i) the compatibility, which rules dispersion and the physisorption of rubber, and ii) the presence of reactive functional groups that can promote the chemisorption of the polymer during vulcanization.

List of publications

1. Barana, D., Salanti, A., Orlandi, M., Ali, D. S., & Zoia, L. (2016). Biorefinery process for the simultaneous recovery of lignin, hemicelluloses, cellulose nanocrystals, and silica from rice husk and Arundo donax. *Industrial Crops and Products*, *86*, 31-39.

2. Barana, D., Ali, S. D., Salanti, A., Orlandi, M., Castellani, L., Hanel, T., & Zoia, L. (2016). Influence of lignin features on thermal stability and mechanical properties of natural rubber compounds. ACS Sustainable Chemistry & Engineering, 4(10), 5258-5267.

3. Pantent Application

- Title: Pneumatico per ruote di veicoli
- Inventors: Barana Davide, Castellani Luca, Hanel Thomas, Olandi Marco and Zoia Luca
- Application number: 102015000087513
- Filing date: 23 Dec 2015
- Publication date: 24 Jun 2017

Acknowledgments

I would like to express my deep appreciation to the university of Milano Bicocca and Pirelli Tyre for creating the exceptional opportunity presented by this Industrial PhD course. From my point of view the collaboration was extremely positive and fruitful, I'm convinced that the simultaneous interaction with industry and academia created a unique set of opportunities for professional and personal growth. I want to thank my mentor, professor Marco Orlandi for giving me the possibility to work on this amazing topic and for the uninterrupted support through the whole journey. Some very special thanks go to Dr. Luca Zoia for the guidance, the encouragement, the patience, the funny moments and above all for the massive amount of time that he dedicated to me. I would also like to thank my company supervisor, dott. Luca Castellani, for being always present and helpful, with a great attitude, even in his busiest days. I was very fortunate for working in an awesome group at the university that provided an enjoyable and stimulating environment, thank you Anika, Francesco, Eva Lisa and Danish. It was also a great pleasure to have the opportunity to work together with many professionals in the staff of Pirelli. I have always felt welcome and I have always found a great spirit of collaboration, also when I was approaching with eccentric requests and ideas. My sincere thanks also go to the members of the FBR institute of Wageningen where I had the chance to spend a terrific period of six months, in particular to ir. Christiaan Bolck and Dr. ing. Richard Gosselink for arranging the stay and for helping me through and after it *(dankuwel)*. Last but not the least, I would like to thank my family: my parents Mara and Danilo, my brother Riccardo, my girlfriend Anja and all my friends for supporting me throughout this awesome but still challenging experience.